Defence and Response during Bacterial Warfare



Thomas A. Meiller-Legrand
Worcester College
University of Oxford

A thesis submitted for the degree of
Doctor of Philosophy
Michaelmas 2021

Abstract

At the heart of most microbial communities lie competitive interactions. These interactions are often mediated by a wide array of dedicated weapons that bacteria use to kill and inhibit competitors. In response, bacteria have therefore had to evolve ways to cope with these attacks. However, our understanding of how bacteria deal with such stresses is largely confined to the effects of clinical antibiotics. Here we argue that there is need for a dedicated focus on how bacteria respond and defend themselves against other bacterial competitors. In this thesis, we use lab-based experiments and agent-based modelling to investigate two different ways bacteria respond to assaults from competitors, filamentation and biofilm formation.

Under stress, many bacterial cells will elongate without dividing to generate long filaments. We found that DNase colicins, narrow-spectrum toxins of *E. coli*, trigger dramatic filamentation in susceptible conspecifics, which is associated with cells actively pushing themselves out from microcolonies. We explored whether this behaviour could be a strategy for escaping from toxins by deleting the gene reported to control filamentation. However, this locus and several others tested, failed to prevent inhibition meaning that tests of a dispersal benefit were inconclusive. However, with a second toxin that induces filamentation — the drug mitomycin C — I found evidence that filamentation does indeed provide a strong benefit by allowing cells to disperse better from growing colonies.

A second widespread response to toxins is for bacteria to increase biofilm formation. We explored the potential benefit of this response in competition with other bacteria using agent-based modelling. We found that making a thicker biofilm is a good way to compete even without the effects of toxins, because of the well-known benefits of reaching nutrients first. Moreover, when toxin competition occurs, we found that thick biofilms can serve to mop up toxins and help defend a strain against incoming attacks. Overall, the biofilm response can be clearly rationalised in the context of interbacterial warfare.

Finally, we present a review of the ecology and evolution of bacterial warfare, which includes an extensive survey of currently known bacterial weapons, and how and when they are used.

My thesis stresses the importance of toxin-mediated warfare for shaping the ecology and evolution of bacteria. But there is still much to learn about bacterial defences, and we argue that greater understanding will be needed if we are to effectively control bacterial communities for our own ends.

Acknowledgements

I am hugely thankful to a number of people for making this work possible. I hope many of these people already know how grateful I am to have worked and/or shared time with them. However, just to be sure and to tell the tale to those few lost souls who will wander an eye over the next few pages and wonder who made all of this possible (for better or for worse), I here list the culprits.

First of all, I am indebted to the EPSRC, the University of Oxford, the ERC and more generally all the taxpayers of both Great-Britain and the European Union for the financial support provided. This work and many others could not be possible without the trust and support of public funding and institutions.

I would like to thank Kevin for his supervision, patience, lightning-fast feedback on things I have written here and elsewhere and all climbing-related advice and gifts. Thank you for putting up with me! I would also like to thank Will for his supervision on the biofilm project, for (foolishly) trying to teach me how to model and for what seemed like an almost infinite amount of patience. I have learnt a great deal from you.

I would like to thank all the Foster lab members. In particular, Daniel who helped me to get started in the lab and whom I was always happy to see in the lab. Ravinash who included me in his projects and supported me in mine. Elisa for being a driving force in getting the review done. Jake and Olivier who always seemed interested in what I was doing and took the time to chat with me about things work- and non-work related. Jamie, whose wisdom sadly did not manage to rub off on me.

Of course, these acknowledgements would be incomplete without mentioning my DPhil companions. Kate, who was so fun to hang out with and so easy to talk to. Signe, for all the kindness, becoming my friend and always being there for me. Frances for all the nice breaks, tennis matches, and foolishly occasionally seeking my advice and help which made me feel useful when most other things were going wrong. You guys have been great and some of the most meaningful relationships I have had these past few years. Without all your attentions and support, I don't know what would have become

of me. I am incredibly thankful that you were a part of this journey.

I would also like to mention Valentin and Koyel who have been great friends. I am glad I've had you around during my DPhil.

I would like to especially thank Laura for her blind love and unwavering support. You have fed, lodged, listened to and supported me in more ways than I have space for here. You have been a great source of comfort and I don't think I can thank you enough for it.

Finally, I would like to thank my creator, maman, and my sisters. They are the lighthouses of my life. Their support from literally day 0 (well, not quite for my little sister who was a bit late to the party) means the world to me.

Publications and Contributions

The following published papers have arisen from this thesis, and are presented in Chapter 4 and Appendix D.

- **Chapter 4**: Granato, E.T.*, **Meiller-Legrand, T.A.*** & Foster, K.R. (2019) The Evolution and Ecology of Bacterial Warfare. *Current Biology 29(11)*, R521-R537. *These authors are joint first authors.

- **Appendix D**: Krishna Kumar, R, **Meiller-Legrand, T.A.**, Alcinesio, A., Gonzalez, D., Mavridou, D.A.I., Meacock, O.J., Smith, W.P.J., Zhou, L., Kim, W., Pulcu, G.S., Bayley, H. & Foster, K.R. (2021) Droplet printing reveals the importance of micron-scale structure for bacterial ecology. *Nature Communications 12, 857*

This thesis has been a collaborative effort although the majority of the work is my own. The contributions for each chapter are as follows:

- **Chapter 2**: Ravinash Krishna Kumar, Kevin R. Foster and I conceived the project. I performed all experiments and analysis. Ravinash Krishna Kumar gave feedback and Kevin R. Foster supervised. I wrote the first draft of this chapter. I wrote the final version of this chapter with feedback from Ravinash Krishna Kumar and Kevin R. Foster.

- **Chapter 3**: William P.J. Smith, Kevin R. Foster and I conceived the project. William P.J. Smith and I created the model. I performed all the experiments and analysis. I wrote the first draft of this chapter. William P.J. Smith and Kevin R. Foster supervised. I wrote the final version of this chapter with feedback from Kevin R. Foster and William P. J. Smith.

- **Chapter 4**: Elisa T. Granato and I conceived the manuscript and wrote the first draft. I carried out the literature review for the data in figures 1, 2, 3 and S1 and

designed these figures. Elisa T. Granato, Kevin R. Foster and I contributed to the final manuscript.

- **Appendix D**: I performed some of the experiments and contributed to the analysis for supplementary figures 3 and 6.

Contents

	Page
List of Figures	**viii**
List of Tables	**xi**
1 Introduction	**1**
2 Filamentation as an escape strategy in *Escherichia coli*	**33**
3 Biofilm formation as a response to bacterial warfare	**78**
4 The Evolution and Ecology of Bacterial Warfare	**117**
5 Conclusion and Discussion	**135**
A Supplementary information for Chapter 2: "Filamentation as an escape strategy in *Escherichia coli*"	**149**
B Supplementary information for Chapter 3: "Biofilm formation as a response to bacterial warfare"	**157**
C Supplementary information for Chapter 4: "The Evolution and Ecology of Bacterial Warfare"	**185**
D Droplet Printing Reveals the Importance of Micron-Scale Structure for Bacterial Ecology	**204**

List of Figures

1.1 Examples of bacteriocins and their targets 4

1.2 Danger sensing 9

1.3 Filamentation as a survival strategy 13

2.1 SulA prevents division by sequestering FtsZ 36

2.2 Schematic of cells embedded in an agarose droplet 43

2.3 Colony expansion assay 45

2.4 Filamentation of susceptible cells in response to DNase colicin E2 in agarose droplets 51

2.5 Filamentation of susceptible cells in response to DNase colicin E2 on agar plates 52

2.6 Deleting *sulA* does not abolish filamentation in response to colicins 53

2.7 Deleting *sulA* reduces but does not abolish filamentation in response to colicins in the droplet assay 55

2.8 Competition between WT, SulA$^-$ and a colicin producer E2 strain in a droplet 56

2.9 Competition between WT and SulA$^-$ on agar containing the supernatant of either a colicin producer (E2) or a non-producer (WT) 57

2.10 Mutants of genes involved in inhibiting division can still filament in response to colicin E2 60

2.11 Deleting *btuB* abolishes filamentation in response to colicins 62

2.12 Competition between WT and BtuB$^-$ in a colony growing next to a colicin E2 producer or a non-producer WT strain 63
2.13 Competition between WT, BtuB$^-$ and a colicin producer E2 strain in a droplet 64
2.14 Deleting *sulA* reduces filamentation in response to mitomycin C 65
2.15 Susceptible cells stressed with mitomycin C gain preferential access to the edge of the colony 66
2.16 Filamentous cells fluxing out of an agarose droplet 69

3.1 Geometry of the virtual cells and environment 83
3.2 Detachment Rules 84
3.3 Single strain fitness optimum — Nutrient-rich conditions 89
3.4 Single strain fitness optimum — Nutrient-limited conditions 90
3.5 Optimal detachment height in 2-strain exploitative competition in nutrient-rich conditions 92
3.6 Optimal detachment height in 2-strain exploitative competition in nutrient-limited conditions 94
3.7 Optimal detachment height in a 2-strain exploitative competition as a function of patch life-span 95
3.8 Optimal strategy for a toxin producer in competition with a sensitive strain — nutrient-limited conditions 98
3.9 Optimal biofilm height for a sensitive strain in competition with a toxin producer — nutrient-limited conditions & low toxin production 100
3.10 Optimal biofilm height for a sensitive strain in competition with a toxin producer — nutrient-limited conditions & high toxin production 102
3.11 Optimal biofilm height for two toxin-producing strains competition — nutrient-limited conditions & low toxin production 104
3.12 Optimal biofilm height for two toxin-producing strains competition — nutrient-limited conditions & high toxin production 105

A.1 Time lapse of sensitive cells filamenting out of a droplet containing a strain producing a colicin (E2) . . . 149
A.2 Droplets treated with Propidium Iodide . . . 150
A.3 Susceptible cells do not filament in response to pore-forming colicins . . . 151
A.4 Distribution of the length of filaments in a culture exposed to either E2 or WT supernatant . . . 152
A.5 Competition with colicin-resistant strains . . . 153
A.6 Competition between WT and BtuB$^-$ on agar 1.5% containing the supernatant of an E2 colicin producer . . . 154
A.7 CFU of WT and SulA$^-$ colonies alone grown on mitomycin C . . . 155

B.1 Geometry of the virtual cells and environment . . . 159
B.2 Detachment Rules . . . 162
B.3 Group formation illustrated . . . 171
B.4 Single strain fitness optimum — volume weighted by growth rate . . . 179
B.5 Snapshots of competition where strains reach different heights but have the same growth rate . . . 180
B.6 ESS in nutrient-rich conditions depending on initial density — side by side configuration . . . 181
B.7 ESS in nutrient-rich conditions depending on the initial configuration of cells . . . 182
B.8 Optimal detachment height in a 2-strain exploitative competition as a function of patch life-span — random initial configuration . . . 183
B.9 Optimal strategy for a toxin producer in competition with a sensitive strain — nutrient-limited conditions & high toxin production . . . 184

List of Tables

2.1 Bacterial strains used in this study 38

2.2 Antibiotics used in this study 38

2.3 FAST parameters used for the segmentation of cells 49

2.4 Loci screened for absence of filamentation 59

A.1 Output of the Kruskal-Wallis test comparing the proportion of WT between all treatments 156

A.2 Output of the *post hoc* Steel-Dwass-Critchlow-Fligner test comparing the proportion of WT between all treatments 156

B.1 State variables 160

B.2 Parameters used in this study 174

Chapter 1

Introduction

In a world out of sight, ruthless battles rage involving billions of individuals. This is the world of microorganism where competition appears to be the most common interaction (Chassaing and Cascales, 2018; García-Bayona and Comstock, 2018; Parijs and Steenackers, 2018). From the discovery of the first bacteriocins in 1925 (Gratia, 1925) to the wide array of weapons we now know bacteria possess (Zhang et al., 2012; Chassaing and Cascales, 2018; Granato et al., 2019; Klein et al., 2020), bacterial killing systems have revolutionised medicine (especially thanks to the discovery of antibiotics). Not only has this arsenal been instrumental in medicine but it also has completely transformed our understanding of the microbial world and how bacteria interact with one another (Kommineni et al., 2015; Chassaing and Cascales, 2018; Coyte and Rakoff-Nahoum, 2019; Heilbronner et al., 2021).

The past hundred years have brought a wealth of knowledge about bacterial weapon systems. A myriad of toxic effectors have been identified both experimentally and bioinformatically (Zhang et al., 2012; Coulthurst, 2019; Ruhe et al., 2020). The nature of these toxins and how they are synthesised by cells is increasingly clear. New and amazing means of delivering these toxins have been and are still being unraveled (Klein et al., 2020). The ubiquity of war amongst bacteria must then have strongly driven the evolution of defensive tools and measures in these populations. Yet, how bacteria respond when they are under attack remains relatively unexplored. Most of the work done on

defensive responses in bacteria concerns how they respond and resist antibiotic treatments in a clinical setting. This work has led to important discoveries but there is growing concern that this understanding is now reaching its limit with antibiotic resistant microorganisms still on the rise worldwide. Death caused by drug-resistant diseases (including bacterial infections) already total over 700000 per year and the *Ad hoc* Interagency Coordination Group on Antimicrobial Resistance convened by the UN estimates that this number could reach 10 million by 2050 (NoT, 2019). Understanding the defence mechanisms used during interbacterial competition, therefore, also has the potential to shed new light on the problem of antimicrobial resistant pathogens. Bacteria have been locked in conflicts with other bacteria for billions of years, and studying these conflicts can help us to understand how pathogens succeed, or fail, during infections.

My thesis is focussed on the question of how bacteria respond when faced with aggressive behaviours from competitors. We consider two different responses, filamentation and biofilm formation. To do this we employ two different approaches, experiments and agent-based modelling respectively. In both cases, our goal is to understand why bacteria engage in these responses and the benefits they receive from doing so during competition. We then zoom out and consider bacterial warfare as a whole and review the threats that bacteria experience from other bacteria and provide the context in which these defences evolved.

1.1 Dog eat dog

Like all organisms, bacteria have to compete for resources in order to survive. Their success depends on their ability to obtain nutrients and a key competitive strategy is to harvest nutrients more effectively than competitors (exploitative competition) (Hibbing et al., 2010; Ghoul and Mitri, 2016). This can, for example, be achieved by consuming nutrients faster than their competitors or producing public goods used in nutrient acquisition only when surrounded by clonemates (Hibbing et al., 2010; Nadell et al., 2016). However, it appears that bacteria also commonly directly interfere with one another (Ghoul and Mitri, 2016). A striking form of such interference competition is the use of

toxins, sometimes delivered using elaborate mechanisms, to kill and inhibit competing bacteria (Granato et al., 2019). These toxins include the antibiotics, which form the cornerstone of modern medicine and often derive from bacteria (Hutchings et al., 2019). In the genus *Streptomyces*, which provides many clinically-used antibiotics (Embley and Stackebrandt, 1994), antibiotics have for example been shown to inhibit other species and lead to a competitive advantage. This competitive advantage manifested itself by preventing invasion of competitors in established populations (Wiener, 1996). Moreover, co-culture of *Streptomyces tenjimariensis* with 53 marine bacteria isolates revealed that about 20% induced antibiotic up-regulation in *S. tenjimariensis* and all of these exhibited sensitivity to the antibiotic produced. Again, these results point to antibiotics being used to ward off invaders (Slattery et al., 2001).

However the total number of studies dedicated to understanding the role of antibiotics in their natural environment remains relatively low. Better understood in this context are bacteriocins. This broad category of toxins is generally defined as proteinaceous molecules that have bactericidal or bacteriostatic properties. Bacteriocins are hailed by some as viable alternatives to currently used antibiotics because of their inhibitory properties (Cotter et al., 2013; Behrens et al., 2017; Soltani et al., 2021). There has long been clear evidence that these toxins mediate interbacterial warfare *in vitro* (Fredericq and Levine, 1947; Prinsloo, 1966; McCurdy and MacRae, 1974; De Lorenzo et al., 1984; Paz-Yepes et al., 2013; Mavridou et al., 2018; Gonzalez et al., 2018). In recent years, it has also become increasingly clear that bacteriocins have an important role *in vivo* (Corr et al., 2007; Nedialkova et al., 2014; Kommineni et al., 2015; Sassone-Corsi et al., 2016; Roelofs et al., 2016; Wholey et al., 2016; Hertzog et al., 2018; Heilbronner et al., 2021). Like all toxins, bacteriocins interfere with essential cellular functions, such as replication, transcription, translation and cell wall synthesis, either by inhibiting enzymes involved in these processes or by degrading the molecules they rely on (Figure 1.1) (Michel-Briand and Baysse, 2002; Cascales et al., 2007; Cotter et al., 2013; Soltani et al., 2021).

The most well studied and understood bacteriocins are that of *Escherichia coli* (Cascales et al., 2007). These bacteriocins encompass colicins and microcins. Colicins were

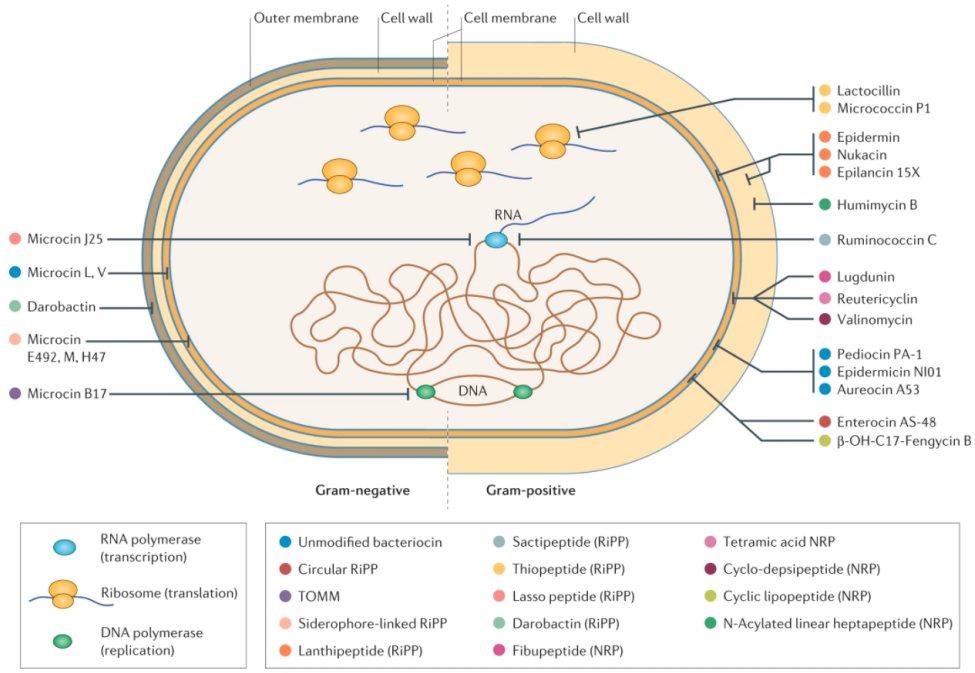

Figure 1.1: Examples of bacteriocins and their targets. Common targets of bacteriocins are the DNA replication, transcription and translations machinery and the cell envelope. Reproduced with permission from Heilbronner et al. (2021)

in fact the first examples of interference competition ever observed in bacteria (Gratia, 1925). They are quite unusual compared to other bacteriocins in that they are relatively large and require lysis to be released. Nonetheless, colicins have been a model system to study competitive interactions in microbes (Chao and Levin, 1981; Riley and Gordon, 1999; Gordon and Riley, 1999; Kerr et al., 2002; Hol et al., 2014). Despite having been studied for decades in the lab, the role colicins play in the healthy gut is still unclear (Samuels et al., 2020). There is some evidence, though, that they are important in the inflamed gut (Nedialkova et al., 2014). Similarly, microcins have also been shown to be involved in mediating competition in the inflamed gut (Sassone-Corsi et al., 2016).

Beyond *E. coli*, many other bacteria produce bacteriocins. Lactic acid bacteria are, for example, prolific bacteriocin producers (Klaenhammer, 1988; Soltani et al., 2021). The classification of their bacteriocins (and more broadly those of gram-positive bacteria) is still a topic of discussion as they are a very diverse group of antimicrobial molecules (Heng and Tagg, 2006; Soltani et al., 2021). But their potential use in probotics and as

food preserving agents made them an intensely studied class of antimicrobials. A class of lactic acid bacteria bacteriocins are the lantibiotics. These are small peptides (up to 38 amino-acids) that are heavily post-translationally modified. They take their name from the lanthionine residues, created by such post-translational modifications, often observed in this class of peptides. Nisin, the only bacteriocin used in the food industry and the best characterized lantibiotic, is produced by *Lactococcus lactis*. This drug acts by creating pores in the membrane of the target cells (Willey and van der Donk, 2007). However, when and how *Lactococcus lactis* uses nisin in its original context is still unknown. In fact, most studies on bacteriocins are carried out in a biotechnological context and few studies report on the ecological relevance of these toxins. Corr et al. (2007) showed that a bacteriocin produced by *Lactobacillus salivarius* UCC118 allows protection against *Listeria monocytogenes* infections in mice, but such studies are few.

Antibiotics and bacteriocins are usually released to diffuse in the environment to reach their target. But many more strategies to deliver toxins exist. An exciting development in the past two decades is the discovery that bacteria also deliver toxins using contact-dependent mechanisms (Hayes et al., 2014; Willett et al., 2015; Klein et al., 2020).

One of the most intricate machinery that bacteria use to directly intoxicate neighbours is the type VI secretion system (T6SS) (Pukatzki et al., 2006, 2007). This contractile molecular machine allows bacteria to stab and directly translocate toxic effectors into neighbouring cells (Basler and Mekalanos, 2012; Basler et al., 2012; Basler, 2015). This delivery mode is capable of targeting a wide range of organisms because it does not rely on its victim's receptors and transporters. The T6SS was, in fact, first discovered in the context of bacteria translocating effectors in eukaryotic cells during infections (Pukatzki et al., 2007; Basler, 2015). Its primary function is now thought to be the delivery of toxins directly into competing bacteria and evidence suggest it is a key factor in shaping microbial communities (Hood et al., 2017; Steele et al., 2017; Bernal et al., 2018; Speare et al., 2018; García-Bayona and Comstock, 2018). The T6SS is present in as many as 25% of sequenced bacteria (Bingle et al., 2008) and is mostly found in Proteobacteria.

The deadly cargos delivered by the T6SS range from nucleases to toxins attacking the cell envelope and metabolism (Russell et al., 2011; Whitney et al., 2013; Russell et al., 2013; Ma et al., 2014; Alcoforado Diniz et al., 2015; Whitney et al., 2015; Flaugnatti et al., 2016; Tang et al., 2018; Coulthurst, 2019; Mariano et al., 2019), with many of the toxins delivered serving to ensure efficient lysis of receiving cells (Smith et al., 2020).

While the T6SS is restricted to gram-negative bacteria, gram-positive bacteria have also evolved a contact-dependent mechanism of killing, the type VII secretion system (T7SS) (Cao et al., 2017). Like the T6SS, it was first described in an infective context in Mycobacteria. However, it quickly appeared that this secretion system was present in other phyla (Unnikrishnan et al., 2017). It was only recently experimentally demonstrated to be involved in interbacterial antagonism (Cao et al., 2017). However, there is increasing evidence that this still mysterious apparatus is used to secrete toxins in a variety of Firmicutes and might be an important way to mediate competitive interactions in gram positive bacteria (Whitney et al., 2017; Tassinari et al., 2020; Chatterjee et al., 2021; Bowran and Palmer, 2021; Kobayashi, 2021).

Another contact-dependent mechanism used by bacteria to kill their competitors is the Contact-Dependent Inhibition (CDI) system (Aoki, 2005; Hayes et al., 2014). When a bacteria equipped with CDI recognises a closely related competitor in the vicinity, a poisoned tip is deployed and directly delivers toxic effectors using its victims' receptors (Ruhe et al., 2018). This two-protein system is generally deployed against closely-related bacteria, although recent research shows that some have cross-species capabilities (Virtanen et al., 2019). Other contact-dependent mechanisms, such as the T4SS (Souza et al., 2015; Bayer-Santos et al., 2019), Cdz (T1SS-dependent) (García-Bayona et al., 2017), membrane exchange (Dey et al., 2016; Vassallo et al., 2017) and nanotubes (Stempler et al., 2017) have also been shown to be involved in interbacterial antagonism.

In summary, bacteria have evolved many different ways to directly inhibit or kill neighbouring cells, suggesting that strong interference competition is an important process in microbial communities. This conclusion is further supported by a growing number of studies that show how bacterial weapons are central to the outcome of competition in

bacterial communities (García-Bayona and Comstock, 2018; Heilbronner et al., 2021). These observations suggest that bacteria must be under strong natural selection to evolve responses that allow them to cope with these conditions.

1.2 Sensing and regulating responses to aggression

Bacterial cells exposed to noxious substances, such as antibiotics, often exhibit widespread gene expression changes (Goh et al., 2002; Walker et al., 2004; Delhaye et al., 2019). These changes allow bacterial cells to deploy defences to cope and potentially respond to the threat they are facing. Many of these responses, such as the oxidative stress response, the SOS response and envelope stress responses, have been studied in the context of how microbes respond to antibiotic treatments (Poole, 2012). However how these responses come into play during stress caused by competitors has received little attention. Competition can manifest itself in two ways. Either cells can sense nutrient-deprivation, which might be indicative of a competitor consuming common resources, or they can sense direct attacks from competing cells. Cornforth and Foster (2013) argued that some of the stress responses bacteria have developed to cope with stress have evolved, at least in part, in response to ecological competition, a concept they named competition-sensing. In the case of direct interference competition, damage to DNA, the cell envelope and other essential structures and functions, which are often the targets of the many toxins bacteria produce, can thus be indicative of the presence of nearby competitors.

One of the best characterised stress responses, which is activated by many bacterial toxins, is the SOS response (Walker et al., 2004; Jana et al., 2019; Baharoglu and Mazel, 2014; Pissaridou et al., 2018). Diverse toxins targeting DNA, such as nucleases and inhibitors of DNA replication, can create breaks in the DNA of their targets (Kohanski et al., 2010; Baharoglu and Mazel, 2014). In *E. coli*, RecA, a nucleoprotein, is, as a result, recruited at the site of the lesions. DNA-bound RecA can cleave LexA, a repressor of a set of genes involved in dealing with the damage to the DNA (cell division arrest and production of the machinery that will repair the DNA). The activation of these genes

(and of the genes they might in turn activate or repress) constitute the SOS response (D'Ari, 1985; Simmons et al., 2008).

The activation of the SOS response is often important for the ability of cells challenged with genotoxic substances to compete successfully. Indeed, the activation of the SOS response often leads to the up-regulation of genes involved in toxin production (Michel-Briand and Baysse, 2002; Gillor et al., 2008) which can be key for the success of competing strains (Majeed et al., 2011; Granato and Foster, 2020; Krishna Kumar et al., 2021).

Another major target of bacterial toxins is the cell envelope. The cell wall and membrane(s) are critical for the integrity of cells. Some β-lactam antibiotics, which target enzymes involved in cell wall synthesis and remodelling, have also been shown to trigger the SOS response (Miller et al., 2004). But there are also specific stress responses that help cells to deal with the various stresses the cell envelope undergoes. These can rely on phosphorelays, such as Cpx and Rcs in *E. coli* or LiaRS in *Bacillus subtilis* or sigma factors (σ^{E} in *E. coli*, σ^{W} in *B. subtilis*) or other mechanisms (Jordan et al., 2008; Mitchell and Silhavy, 2019; Delhaye et al., 2019). These pathways can be activated when antibiotics target the cell envelope and disrupt its integrity. Cefsulodin and mecillinam, antibiotics targeting penicillin-binding proteins (PBP), have for example been shown to induce the Rcs system in *E. coli* (Laubacher and Ades, 2008). Moreover, this system also seems to be involved in providing immunity to T6SS attacks (Hersch et al., 2020). These systems activate a variety of processes aimed at stabilising the targeted structure, producing a capsule or even triggering biofilm formation (Mitchell and Silhavy, 2019).

The role of envelope stress responses in bacterial warfare is currently under intense investigation in the context of T6SS attacks. A model system for this type of studies is *Pseudomonas aeruginosa*, which can fire its T6SS upon being first provoked, clearly illustrating that bacteria can sense and respond to aggressions (Basler and Mekalanos, 2012; Basler et al., 2013). This tit-for-tat behaviour has interestingly been shown to rely on the presence of phospholipase effectors and not on the physical puncture the T6SS performs when delivering its toxic cargo (Kamal et al., 2020). In fact, other tox-

ins attacking the membrane, such as polymyxin B, have been shown to elicit a samilar behaviour (Ho et al., 2013; Storey et al., 2020). Stolle et al. (2021) recently proposed a model of how these various membrane stress signals are integrated but the nature of these signals remain elusive. This retaliatory behaviour does not seem to be limited to *P. aeruginosa*. For example, *Klebsiella pneumoniae* also fires its T6SS in response to membrane perturbations (although it has not been demonstrated whether this response occurs at the site of the damage as is the case in *P. aeruginosa*) (Storey et al., 2020; Hersch et al., 2020). The T7SS has also recently been shown to be triggered by such membrane disturbances in gram positive bacteria. Indeed, Chatterjee et al. (2021) showed that phage attacks and daptomycin, a membrane targeting antibiotic, trigger the activation of T7SS while cell wall targeting antibiotics did not.

Cell damage caused by toxins is not the only cue that cells can use to infer the presence of competitors (Cornforth and Foster, 2013). LeRoux et al. (2015) put forth the idea of "danger sensing" whereby cells can use indirect cues to detect and respond to threats (Figure 1.2). For example, *P. aeruginosa* cells can activate a response called PARA (*Pseudomonas aeruginosa* Response to Antagonism) when they sense molecules released by lysed kin cells (LeRoux et al., 2015). Some species can also eavesdrop on competitors by monitoring the level of quorum-sensing (QS) molecules their opponents are producing (Durán et al., 2016). Since QS molecules are often used to trigger the production of antimicrobial molecules, eavesdropping on these signals can allow bacteria to spy on their competitors and know when to up-regulate their own toxin production in response (Chandler et al., 2012).

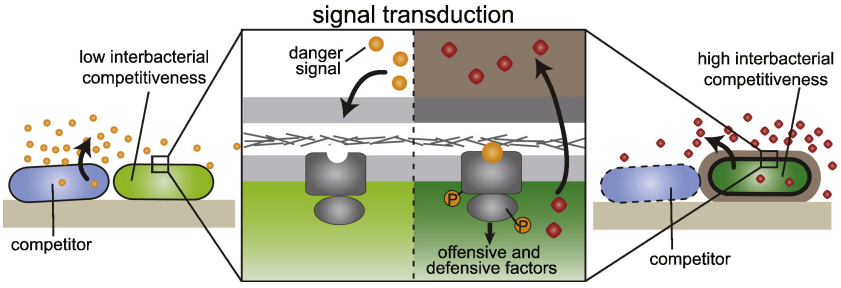

Figure 1.2: Danger sensing. Cells are able to sense competition using cues from competitors (and kin neighbouring cells) and activate defences in response. Reproduced with permission from LeRoux et al. (2015)

The multiplicity of the cues bacteria receive begs the question of how bacteria know when to turn on which defences in response to which cues? Westhoff et al. (2017) suggested that the responses to danger cues and signals are loosely distance-dependent. For example, they argue that T6SS clearly indicates an imminent threat because of the contact-dependent nature of the weapon, which can elicit immediate responses such as retaliation. At the other end of the spectrum, volatile organic compounds (VOCs) can travel large distances and will trigger general defences, such as increased antibiotic resistance and biofilm formation. Diffusible toxins cannot travel as far as VOCs because of their larger size, which impedes their progression. They might then indicate an intermediate level of danger, where competitors are in the vicinity but not in contact and therefore triggers all types of defence mechanisms. These predictions need testing but they give one way to help organise the many signals and cues that bacteria can perceive to respond to aggression.

Bacteria, therefore, have evolved many mechanisms to monitor and sense harmful competitors. How then do they use these cues and what defence mechanisms then do they activate?

1.3 Defence mechanisms

Responding appropriately to an incoming toxin or warning sign has the potential for strong fitness benefits. Indeed, failing to do so can mean death. The result is an impressive array of defensive mechanisms to help cells cope with the insults they face, which range from the molecular to the multicellular scale (Justice et al., 2014; Flemming et al., 2016; Hersch et al., 2020).

Bacteria can act at the molecular level to degrade or modify toxins that threaten them. β-lactamases, for example, are enzymes able to degrade β-lactam antibiotics, which protects their producers from the effect of this class of antibiotics (Tooke et al., 2019). β-lactamases were first observed in 1940 in *E. coli* cultures, well before the use of β-lactam in the clinic (Abraham and Chain, 1940). While these enzymes are most discussed in the context of antibiotic resistance, β-lactamases (and other antibiotic

resistance enzymes) have been identified in bacteria frozen in ice cores around 30000 years ago and phylogenetic analysis even date the evolution of metallo-β-lactamases to at least 2 billion years ago (D'Costa et al., 2011; Hall et al., 2004). Other enzymes will modify their targets to render them inactive. For example, aminoglycoside modifying enzymes add hydroxyl or amino groups to these molecules, making them inactive (Munita and Arias, 2016).

Another defence mechanism acting at the molecular level is the production of immunity proteins that bind and sequester the toxic effectors. Usually produced at the same time as the toxins they confer immunity to, these proteins protect the aggressor against self-intoxication or intoxication by clonemates (Cascales et al., 2007; Hersch et al., 2020). However, there is increasing evidence that orphan immunity genes can be acquired horizontally independently from the toxin genes suggesting that susceptible cells can acquire immunity (Ross et al., 2019).

Bacteria also use cellular phenotypes to cope with toxins. Again coming from the study of antibiotic resistance is the discovery of efflux pumps. These transporters are able to pump out noxious compounds out of the cells and therefore avoid intoxication (Munita and Arias, 2016). Arguably better than pumping toxins out of the cell is preventing them from getting in in the first place. Bacteria possess elaborate armours that protect them from the external world, the cell envelope. There are two main types of bacterial cell envelope. Gram-positive bacteria's envelope is constituted of a cell membrane and a thick cell wall while gram-negative bacteria have an inner membrane, a thin cell wall and an outer membrane. The outer membrane of the gram-negative cell presents a second barrier to antimicrobial molecules. The effectiveness of this second membrane as a barrier can be modulated by adjustments in the lipid composition and the porins that offer a route for some antimicrobials to enter the cell (Delcour, 2009). Moreover, the outer membrane is often decorated with lipopolysaccharide which can help to decrease the likelihood of toxins reaching the membrane (van der Ley et al., 1986; Sharp et al., 2019). Some bacteria can also produce a capsule that acts as an additional layer of protection. This capsule has for example been shown to render *K.*

pneumoniae resistant to polymyxin B (van der Ley et al., 1986). The role that capsules, S-layers and other polymeric layers surrounding some bacteria, play in interbacterial warfare has not yet been fully determined. However, Toska et al. (2018) showed that exopolysaccharide (EPS) secreted by *Vibrio cholerae* does act as an armour against T6SS attacks. Moreover Flaugnatti et al. (2021) showed that *K. pneumoniae* could withstand T6SS assaults thanks to its capsule. There is, therefore, growing evidence that these types of layer may play an important defensive role. Beyond altering or reinforcing the boundary that separate them from the outside world (i.e. the cell envelope), bacteria also have the potential to drastically alter their morphologies (Justice et al., 2008). In *E. coli*, filamentation has been shown to be a defence mechanism in response to immune system attacks (Justice et al., 2006) where long filamentous cells are better able than normal cells at escaping the immune system cells. The authors showed *in vitro* that these long filamentous cells did not resist phagocytosis by macrophages better than normal cells. Yet, *in vivo*, this filamentous phenotype was key to the uropathogenic *E. coli*'s survival. The authors concluded that filamentation allowed cells to evade the immune system, by a mechanism they did not determine (Figure 1.3). This raises the possibility that such escape phenotypes could also play a role in interbacterial warfare. In support of this, there is some evidence suggesting that filamentation allows cells to colonise new grounds more quickly when challenged with antibiotics (Möller et al., 2013; Phan et al., 2018; Frost et al., 2018). In Chapter 2, we ask whether this phenotype can serve as an escape mechanism in response to bacterial competition.

In addition to defences, some bacteria will fight back with the very weapons that are being used against them. A key example of this, as just discussed, is the tit-for-tat response of *P. aeruginosa* (Basler and Mekalanos, 2012; Basler et al., 2013). Upon being attacked, *P. aeruginosa* deploys its own T6SS in retaliation. It was recently shown that cells mount a disproportionate response, firing multiple times in response to an incoming attack in order to win using this strategy (Smith et al., 2020). Moreover, many bacteriocins are upregulated under DNA damage, which gives the capacity for reciprocation in the face of incoming attacks via DNA damaging agents (Mavridou et al.,

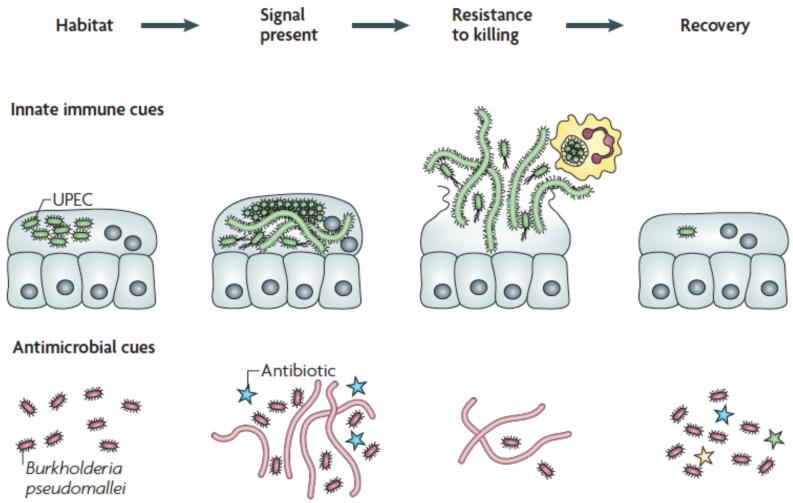

Figure 1.3: Filamentation as a survival strategy. Insults from the immune system or antibiotics can trigger filamentation, which can help bacteria cope with stress. Adapted with permission from Justice et al. (2008)

2018; Granato and Foster, 2020; Cascales et al., 2007; Michel-Briand and Baysse, 2002).

Finally, bacteria also use collective strategies to defend themselves. One such source of tolerance to toxins is heterogeneity in the population. This heterogeneity means that cells in different micro-environments and physiological states will not respond to adverse conditions in the same way. An extreme example of this phenomenon are persisters, dormant cells, which, although not genetically resistant to the stresses they encounter, manage to tolerate normally deadly concentrations of antibiotics (Harms et al., 2016).

The most prominent example of collective defence in bacteria is biofilms, polymicrobial populations of bacteria encased in an extracellular matrix (Flemming et al., 2016). These have been shown to exhibit increased tolerance and resistance to a wide range of antibiotics and other toxins. Many mechanisms contribute to this effect, including limited toxin diffusion, secreted toxin-degrading enzymes that protect the focal cell and its neighbours and the physiological state biofilm bacteria find themselves in (Fux et al., 2005; Pabst et al., 2016; Stewart and Franklin, 2008). While the vast majority of our understanding of how biofilms protect cells comes from antibiotic treatment, there is growing recognition that they are important for bacterial competition too (Nadell et al., 2016). A key observation in this regard is that biofilm formation can be induced during

interbacterial warfare (Oliveira et al., 2015; Lories et al., 2020). We explore this response as a possible adaptation to bacterial warfare in Chapter 3.

Defence mechanisms in bacteria, therefore, go hand-in-hand with offensive mechanisms. Indeed, almost as soon as bacteria are challenged by toxic substances produced by other bacteria one can often observe the emergence of cells capable of evading, at least partially, the deleterious effects of the insults they are facing (Gratia, 1925). However, the study of these defences has been dominated by the focus on resistance and tolerance to antibiotic treatment. There is a need to study these defences in the context that they originally evolved, which is often likely to be one of bacterial warfare. This need comes from both the value to better understand the function of these defences and their place in bacterial evolution, but also so that we can reflect back on the problem of antibiotic resistance with the hope of finding new ways to treat pathogens.

1.4 Thesis outline

My thesis studies how bacteria respond to incoming toxins from other strains, with a focus on two main phenotypes, filamentation and biofilm formation.

In Chapter 2, we study filamentation in response to toxins and ask whether this response can provide an escape benefit in *E. coli*. Filamentation in bacteria is often observed in response to antibiotic treatment (Suzuki et al., 1967; Frost et al., 2018). Moreover, filamentation is also observed in some infections and shown to be necessary for survival in this context (Justice et al., 2006). Taken together, these prior results suggest that filamentation, far from being an abnormal response, may serve as a bacterial defence strategy. We show that both narrow-spectrum bacteriocins and the broad-spectrum drug mitomycin C induce filamentation. Moreover, filamentation in response to mitomycin C allows cells to gain a competitive advantage in expanding population over cells less able to filament, which is consistent with an escape behaviour.

In chapter 3, we ask whether making a biofilm can help bacteria overcome competitors during bouts of warfare. The fact that biofilm formation is promoted in response to antibiotic treatment is well known and has been documented in diverse species. However,

there is good reason to believe that these responses predate the human use of antibiotics. Consistent with this, recent work has shown that biofilm formation is promoted by bacterial competition, as well as by antibiotic treatment (Oliveira et al., 2015; Lories et al., 2020). Using agent-based modelling, we explore the hypothesis that the biofilm response to toxins evolved to allow bacteria to better compete with other strains and species. Our work suggests that making thicker biofilms can help cells in both exploitative (space/nutrients) and interference competition with toxins. During toxin warfare, our models predict that thicker biofilms can allow cells to both defend themselves against toxins, and better deploy toxins against competitions. These findings provide an evolutionary rationale for the well-known biofilm response to antibiotics and other toxins.

In Chapter 4, we take a broader perspective and present a review and synthesis on the ecology and evolution of bacterial warfare. We performed a large literature search with the goal of collating all clear examples of bacterial warfare in order to assess how prevalent and important warfare is in bacteria. This analysis revealed that bacterial weapons are extremely widespread and appear to be reliably found when a species is well studied. We frame this literature with parallels from the animal world, for which theories of conflict and conflict resolution are better understood. Finally, we highlight where the differences lie and what still needs to be resolved to better understand how bacteria fight and defend.

Finally, in chapter 5, we summarise the results presented in chapter 2 and 3, and discuss directions for future work, both to better understand how bacteria cope with interference competition and how this knowledge might be used to circumvent these defences in the clinic.

1.5 Bibliography

(2019, April). No time to wait: Securing the future from drug-resistant infections. Technical report, Interagency Coordination Group on Antimicrobial Resistance.

Abraham, E. P. and E. Chain (1940, December). An Enzyme from Bacteria able to Destroy Penicillin. *Nature 3713*, 837.

Alcoforado Diniz, J., Y.-C. Liu, and S. J. Coulthurst (2015, December). Molecular weaponry: Diverse effectors delivered by the Type VI secretion system: Type VI secretion system effectors. *Cellular Microbiology 17*(12), 1742–1751.

Aoki, S. K. (2005, August). Contact-Dependent Inhibition of Growth in *Escherichia coli*. *Science 309*(5738), 1245–1248.

Baharoglu, Z. and D. Mazel (2014, November). SOS, the formidable strategy of bacteria against aggressions. *FEMS Microbiology Reviews 38*(6), 1126–1145.

Basler, M. (2015, October). Type VI secretion system: Secretion by a contractile nanomachine. *Philosophical Transactions of the Royal Society B: Biological Sciences 370*(1679), 20150021.

Basler, M., B. T. Ho, and J. J. Mekalanos (2013, February). Tit-for-Tat: Type VI Secretion System Counterattack during Bacterial Cell-Cell Interactions. *Cell 152*(4), 884–894.

Basler, M. and J. J. Mekalanos (2012, August). Type 6 Secretion Dynamics Within and Between Bacterial Cells. *Science 337*(6096), 815–815.

Basler, M., M. Pilhofer, G. P. Henderson, G. J. Jensen, and J. J. Mekalanos (2012, March). Type VI secretion requires a dynamic contractile phage tail-like structure. *Nature 483*(7388), 182–186.

Bayer-Santos, E., W. Cenens, B. Y. Matsuyama, G. U. Oka, G. Di Sessa, I. D. V. Mininel, T. L. Alves, and C. S. Farah (2019, September). The opportunistic pathogen

Stenotrophomonas maltophilia utilizes a type IV secretion system for interbacterial killing. *PLOS Pathogens 15*(9), e1007651.

Behrens, H. M., A. Six, D. Walker, and C. Kleanthous (2017, April). The therapeutic potential of bacteriocins as protein antibiotics. *Emerging Topics in Life Sciences 1*(1), 65–74.

Bernal, P., M. A. Llamas, and A. Filloux (2018, January). Type VI secretion systems in plant-associated bacteria: T6SS in phytobacteria. *Environmental Microbiology 20*(1), 1–15.

Bingle, L. E., C. M. Bailey, and M. J. Pallen (2008, February). Type VI secretion: A beginner's guide. *Current Opinion in Microbiology 11*(1), 3–8.

Bowran, K. and T. Palmer (2021, March). Extreme genetic diversity in the type VII secretion system of *Listeria monocytogenes* suggests a role in bacterial antagonism. *Microbiology 167*(3), 001034.

Cao, Z., M. G. Casabona, H. Kneuper, J. D. Chalmers, and T. Palmer (2017, January). The type VII secretion system of *Staphylococcus aureus* secretes a nuclease toxin that targets competitor bacteria. *Nature Microbiology 2*, 16183.

Cascales, E., S. K. Buchanan, D. Duche, C. Kleanthous, R. Lloubes, K. Postle, M. Riley, S. Slatin, and D. Cavard (2007, March). Colicin Biology. *Microbiology and Molecular Biology Reviews 71*(1), 158–229.

Chandler, J. R., S. Heilmann, J. E. Mittler, and E. P. Greenberg (2012, December). Acyl-homoserine lactone-dependent eavesdropping promotes competition in a laboratory co-culture model. *The ISME Journal 6*(12), 2219–2228.

Chao, L. and B. R. Levin (1981). Structured habitats and the evolution of anticompetitor toxins in bacteria. *Proceedings of the National Academy of Sciences 78*(10), 6324–6328.

Chassaing, B. and E. Cascales (2018, April). Antibacterial Weapons: Targeted Destruction in the Microbiota. *Trends in Microbiology 26*(4), 329–338.

Chatterjee, A., J. L. E. Willett, G. M. Dunny, and B. A. Duerkop (2021, January). Phage infection and sub-lethal antibiotic exposure mediate *Enterococcus faecalis* type VII secretion system dependent inhibition of bystander bacteria. *PLOS Genetics 17*(1), e1009204.

Cornforth, D. M. and K. R. Foster (2013, April). Competition sensing: The social side of bacterial stress responses. *Nature Reviews Microbiology 11*(4), 285–293.

Corr, S. C., Y. Li, C. U. Riedel, P. W. O'Toole, C. Hill, and C. G. M. Gahan (2007, May). Bacteriocin production as a mechanism for the antiinfective activity of *Lactobacillus salivarius* UCC118. *Proceedings of the National Academy of Sciences 104*(18), 7617–7621.

Cotter, P. D., R. P. Ross, and C. Hill (2013, February). Bacteriocins — a viable alternative to antibiotics? *Nature Reviews Microbiology 11*(2), 95–105.

Coulthurst, S. (2019, May). The Type VI secretion system: A versatile bacterial weapon. *Microbiology 165*(5), 503–515.

Coyte, K. Z. and S. Rakoff-Nahoum (2019, June). Understanding Competition and Cooperation within the Mammalian Gut Microbiome. *Current Biology 29*(11), R538–R544.

D'Ari, R. (1985). The SOS system. *Biochimie 67*, 343–347.

D'Costa, V. M., C. E. King, L. Kalan, M. Morar, W. W. L. Sung, C. Schwarz, D. Froese, G. Zazula, F. Calmels, R. Debruyne, G. B. Golding, H. N. Poinar, and G. D. Wright (2011, September). Antibiotic resistance is ancient. *Nature 477*(7365), 457–461.

De Lorenzo, V., J. L. Martínez, and C. Asensio (1984). Microcin-mediated interactions between *Klebsiella pneumoniae* and *Escherichia coli* strains. *Journal of General Microbiology 130*, 391–400.

Delcour, A. H. (2009, May). Outer membrane permeability and antibiotic resistance. *Biochimica et Biophysica Acta (BBA) - Proteins and Proteomics 1794*(5), 808–816.

Delhaye, A., J.-F. Collet, and G. Laloux (2019, November). A Fly on the Wall: How Stress Response Systems Can Sense and Respond to Damage to Peptidoglycan. *Frontiers in Cellular and Infection Microbiology 9*, 380.

Dey, A., C. N. Vassallo, A. C. Conklin, D. T. Pathak, V. Troselj, and D. Wall (2016, March). Sibling Rivalry in *Myxococcus xanthus* Is Mediated by Kin Recognition and a Polyploid Prophage. *Journal of Bacteriology 198*(6), 994–1004.

Durán, N., G. Z. Justo, M. Durán, M. Brocchi, L. Cordi, L. Tasic, G. R. Castro, and G. Nakazato (2016, September). Advances in *Chromobacterium violaceum* and properties of violacein - Its main secondary metabolite: A review. *Biotechnology Advances 34*(5), 1030–1045.

Embley, T. M. and E. Stackebrandt (1994, October). The Molecular Phylogeny and Systematics of the Actinomycetes. *Annual Review of Microbiology 48*(1), 257–289.

Flaugnatti, N., S. Isaac, L. F. Lemos Rocha, S. Stutzmann, O. Rendueles, C. Stoudmann, N. Vesel, M. Garcia-Garcera, A. Buffet, T. G. Sana, E. P. C. Rocha, and M. Blokesch (2021, December). Human commensal gut Proteobacteria withstand type VI secretion attacks through immunity protein-independent mechanisms. *Nature Communications 12*(1), 5751.

Flaugnatti, N., T. T. H. Le, S. Canaan, M.-S. Aschtgen, V. S. Nguyen, S. Blangy, C. Kellenberger, A. Roussel, C. Cambillau, E. Cascales, and L. Journet (2016, March). A phospholipase A_1 antibacterial Type VI secretion effector interacts directly with the C-terminal domain of the VgrG spike protein for delivery: Phospholipase A_1 antibacterial T6SS effector. *Molecular Microbiology 99*(6), 1099–1118.

Flemming, H.-C., J. Wingender, U. Szewzyk, P. Steinberg, S. A. Rice, and S. Kjelleberg (2016, September). Biofilms: An emergent form of bacterial life. *Nature Reviews Microbiology 14*(9), 563–575.

Fredericq, P. and M. Levine (1947, December). Antibiotic Interrelationships among the Enteric Group of Bacteria. *Journal of Bacteriology 54*(6), 785–792.

Frost, I., W. P. J. Smith, S. Mitri, A. S. Millan, Y. Davit, J. M. Osborne, J. M. Pitt-Francis, R. C. MacLean, and K. R. Foster (2018, June). Cooperation, competition and antibiotic resistance in bacterial colonies. *The ISME Journal 12*(6), 1582–1593.

Fux, C., J. Costerton, P. Stewart, and P. Stoodley (2005, January). Survival strategies of infectious biofilms. *Trends in Microbiology 13*(1), 34–40.

García-Bayona, L. and L. E. Comstock (2018, September). Bacterial antagonism in host-associated microbial communities. *Science 361*(6408), eaat2456.

García-Bayona, L., M. S. Guo, and M. T. Laub (2017, March). Contact-dependent killing by *Caulobacter crescentus* via cell surface-associated, glycine zipper proteins. *eLife 6*, 6:e24869.

Ghoul, M. and S. Mitri (2016, October). The Ecology and Evolution of Microbial Competition. *Trends in Microbiology 24*(10), 833–845.

Gillor, O., J. A. C. Vriezen, and M. A. Riley (2008, June). The role of SOS boxes in enteric bacteriocin regulation. *Microbiology 154*(6), 1783–1792.

Goh, E.-B., G. Yim, W. Tsui, J. McClure, M. G. Surette, and J. Davies (2002, December). Transcriptional modulation of bacterial gene expression by subinhibitory concentrations of antibiotics. *Proceedings of the National Academy of Sciences 99*(26), 17025–17030.

Gonzalez, D., A. Sabnis, K. R. Foster, and D. A. I. Mavridou (2018, July). Costs and benefits of provocation in bacterial warfare. *Proceedings of the National Academy of Sciences 115*(29), 7593–7598.

Gordon, D. M. and M. A. Riley (1999). A theoretical and empirical investigation of the invasion dynamics of colicinogeny. *Microbiology 145*(3), 655–661.

Granato, E. T. and K. R. Foster (2020, July). The Evolution of Mass Cell Suicide in Bacterial Warfare. *Current Biology 30*(14), 2836–2843.

Granato, E. T., T. A. Meiller-Legrand, and K. R. Foster (2019, June). The Evolution and Ecology of Bacterial Warfare. *Current Biology 29*(11), R521–R537.

Gratia, A. (1925). Sur un remarquable exemple d'antagonisme entre deux souches de colibacille. *Comptes Rendus des Séances de la Société de biologie et de ses filiales 93*, 1040–1041.

Hall, B. G., S. J. Salipante, and M. Barlow (2004, July). Independent Origins of Subgroup Bl+B2 and Subgroup B3 Metallo-β-Lactamases. *Journal of Molecular Evolution 59*, 133–141.

Harms, A., E. Maisonneuve, and K. Gerdes (2016, December). Mechanisms of bacterial persistence during stress and antibiotic exposure. *Science 354*(6318), aaf4268.

Hayes, C. S., S. Koskiniemi, Z. C. Ruhe, S. J. Poole, and D. A. Low (2014, February). Mechanisms and Biological Roles of Contact-Dependent Growth Inhibition Systems. *Cold Spring Harbor Perspectives in Medicine 4*(2), a010025.

Heilbronner, S., B. Krismer, H. Brötz-Oesterhelt, and A. Peschel (2021, November). The microbiome-shaping roles of bacteriocins. *Nature Reviews Microbiology 19*(11), 726–739.

Heng, N. C. K. and J. R. Tagg (2006, February). What's in a name? Class distinction for bacteriocins. *Nature Reviews Microbiology 4*(2), 160.

Hersch, S. J., K. Manera, and T. G. Dong (2020, October). Defending against the Type Six Secretion System: Beyond Immunity Genes. *Cell Reports 33*(2), 108259.

Hersch, S. J., N. Watanabe, M. S. Stietz, K. Manera, F. Kamal, B. Burkinshaw, L. Lam, A. Pun, M. Li, A. Savchenko, and T. G. Dong (2020, May). Envelope stress responses defend against type six secretion system attacks independently of immunity proteins. *Nature Microbiology 5*(5), 706–714.

Hertzog, B. B., Y. Kaufman, D. Biswas, M. Ravins, P. Ambalavanan, R. Wiener, V. Angeli, S. L. Chen, and E. Hanski (2018, March). A Sub-population of Group A *Strepto-*

coccus Elicits a Population-wide Production of Bacteriocins to Establish Dominance in the Host. *Cell Host & Microbe 23*(3), 312–323.e6.

Hibbing, M. E., C. Fuqua, M. R. Parsek, and S. B. Peterson (2010, January). Bacterial competition: Surviving and thriving in the microbial jungle. *Nature Reviews Microbiology 8*(1), 15–25.

Ho, B. T., M. Basler, and J. J. Mekalanos (2013, October). Type 6 Secretion System-Mediated Immunity to Type 4 Secretion System-Mediated Gene Transfer. *Science 342*(6155), 250–253.

Hol, F. J., M. J. Voges, C. Dekker, and J. E. Keymer (2014). Nutrient-responsive regulation determines biodiversity in a colicin-mediated bacterial community. *BMC Biol 12*(1), 68.

Hood, R. D., S. B. Peterson, and J. D. Mougous (2017, March). From Striking Out to Striking Gold: Discovering that Type VI Secretion Targets Bacteria. *Cell Host & Microbe 21*(3), 286–289.

Hutchings, M. I., A. W. Truman, and B. Wilkinson (2019, October). Antibiotics: Past, present and future. *Current Opinion in Microbiology 51*, 72–80.

Jana, B., C. M. Fridman, E. Bosis, and D. Salomon (2019, December). A modular effector with a DNase domain and a marker for T6SS substrates. *Nature Communications 10*(1), 3595.

Jordan, S., M. I. Hutchings, and T. Mascher (2008, January). Cell envelope stress response in Gram-positive bacteria. *FEMS Microbiology Reviews 32*(1), 107–146.

Justice, S. S., A. Harrison, B. Becknell, and K. M. Mason (2014, November). Bacterial differentiation, development, and disease: Mechanisms for survival. *FEMS Microbiology Letters 360*(1), 1–8.

Justice, S. S., D. A. Hunstad, L. Cegelski, and S. J. Hultgren (2008, February). Morpho-

logical plasticity as a bacterial survival strategy. *Nature Reviews Microbiology 6*(2), 162–168.

Justice, S. S., D. A. Hunstad, P. C. Seed, and S. J. Hultgren (2006, December). Filamentation by *Escherichia coli* subverts innate defenses during urinary tract infection. *Proceedings of the National Academy of Sciences 103*(52), 19884–19889.

Kamal, F., X. Liang, K. Manera, T.-T. Pei, H. Kim, L. G. Lam, A. Pun, S. J. Hersch, and T. G. Dong (2020, June). Differential Cellular Response to Translocated Toxic Effectors and Physical Penetration by the Type VI Secretion System. *Cell Reports 31*, 107766.

Kerr, B., M. A. Riley, M. W. Feldman, and B. J. M. Bohannan (2002, July). Local dispersal promotes biodiversity in a real-life game of rock–paper–scissors. *Nature 418*(6894), 171–174.

Klaenhammer, T. R. (1988). Bacteriocins of lactic acid bacteria. *Biochimie 70*, 337–349.

Klein, T. A., S. Ahmad, and J. C. Whitney (2020, May). Contact-Dependent Interbacterial Antagonism Mediated by Protein Secretion Machines. *Trends in Microbiology 28*(5), 387–400.

Kobayashi, K. (2021, July). Diverse LXG toxin and antitoxin systems specifically mediate intraspecies competition in *Bacillus subtilis* biofilms. *PLOS Genetics 17*(7), e1009682.

Kohanski, M. A., D. J. Dwyer, and J. J. Collins (2010, June). How antibiotics kill bacteria: From targets to networks. *Nature Reviews Microbiology 8*(6), 423–435.

Kommineni, S., D. J. Bretl, V. Lam, R. Chakraborty, M. Hayward, P. Simpson, Y. Cao, P. Bousounis, C. J. Kristich, and N. H. Salzman (2015, October). Bacteriocin production augments niche competition by enterococci in the mammalian gastrointestinal tract. *Nature 526*(7575), 719–722.

Krishna Kumar, R., T. A. Meiller-Legrand, A. Alcinesio, D. Gonzalez, D. A. I. Mavridou, O. J. Meacock, W. P. J. Smith, L. Zhou, W. Kim, G. S. Pulcu, H. Bayley, and K. R. Foster (2021, December). Droplet printing reveals the importance of micron-scale structure for bacterial ecology. *Nature Communications 12*(1), 857.

Laubacher, M. E. and S. E. Ades (2008, March). The Rcs Phosphorelay Is a Cell Envelope Stress Response Activated by Peptidoglycan Stress and Contributes to Intrinsic Antibiotic Resistance. *Journal of Bacteriology 190*(6), 2065–2074.

LeRoux, M., R. L. Kirkpatrick, E. I. Montauti, B. Q. Tran, S. B. Peterson, B. N. Harding, J. C. Whitney, A. B. Russell, B. Traxler, Y. A. Goo, D. R. Goodlett, P. A. Wiggins, and J. D. Mougous (2015, February). Kin cell lysis is a danger signal that activates antibacterial pathways of *Pseudomonas aeruginosa*. *eLife 4*, e05701.

LeRoux, M., S. B. Peterson, and J. D. Mougous (2015, November). Bacterial danger sensing. *Journal of Molecular Biology 427*(23), 3744–3753.

Lories, B., S. Roberfroid, L. Dieltjens, D. De Coster, K. R. Foster, and H. P. Steenackers (2020, April). Biofilm Bacteria Use Stress Responses to Detect and Respond to Competitors. *Current Biology 30*(7), 1231–1244.

Ma, L.-S., A. Hachani, J.-S. Lin, A. Filloux, and E.-M. Lai (2014, July). *Agrobacterium Tumefaciens* Deploys a Superfamily of Type VI Secretion DNase Effectors as Weapons for Interbacterial Competition In Planta. *Cell Host & Microbe 16*(1), 94–104.

Majeed, H., O. Gillor, B. Kerr, and M. A. Riley (2011, January). Competitive interactions in *Escherichia coli* populations: The role of bacteriocins. *The ISME Journal 5*(1), 71–81.

Mariano, G., K. Trunk, D. J. Williams, L. Monlezun, H. Strahl, S. J. Pitt, and S. J. Coulthurst (2019, December). A family of Type VI secretion system effector proteins that form ion-selective pores. *Nature Communications 10*(1), 5484.

Mavridou, D. A., D. Gonzalez, W. Kim, S. A. West, and K. R. Foster (2018, February).

Bacteria Use Collective Behavior to Generate Diverse Combat Strategies. *Current Biology 28*(3), 345–355.

McCurdy, H. D. J. and T. H. MacRae (1974, February). Xanthacin. A bacteriocin of *Myxococcus xanthus* fb. *Canadian Journal of Microbiology 20*(2), 131–135.

Michel-Briand, Y. and C. Baysse (2002). The pyocins of *Pseudomonas aeruginosa*. *Biochimie 84*(5), 499–510.

Miller, C., L. E. Thomsen, C. Gaggero, R. Mosseri, H. Ingmer, and S. N. Cohen (2004, September). SOS Response Induction by β-Lactams and Bacterial Defense Against Antibiotic Lethality. *Science 305*(5690), 1629–1631.

Mitchell, A. M. and T. J. Silhavy (2019, July). Envelope stress responses: Balancing damage repair and toxicity. *Nature Reviews Microbiology 17*(7), 417–428.

Möller, J., P. Emge, I. A. Vizcarra, P. Kollmannsberger, and V. Vogel (2013, December). Bacterial filamentation accelerates colonization of adhesive spots embedded in biopassive surfaces. *New Journal of Physics 15*(12), 125016.

Munita, J. M. and C. A. Arias (2016, April). Mechanisms of Antibiotic Resistance. *Microbiology Spectrum 4*(2), VMBF–0016–2015.

Nadell, C. D., K. Drescher, and K. R. Foster (2016, July). Spatial structure, cooperation and competition in biofilms. *Nature Reviews Microbiology 14*, 589–600.

Nedialkova, L. P., R. Denzler, M. B. Koeppel, M. Diehl, D. Ring, T. Wille, R. G. Gerlach, and B. Stecher (2014, January). Inflammation Fuels Colicin Ib-Dependent Competition of *Salmonella* Serovar Typhimurium and *E. coli* in Enterobacterial Blooms. *PLoS Pathogens 10*(1), e1003844.

Oliveira, N. M., E. Martinez-Garcia, J. Xavier, W. M. Durham, R. Kolter, W. Kim, and K. R. Foster (2015, July). Biofilm Formation As a Response to Ecological Competition. *PLOS Biology 13*(7), e1002191.

Pabst, B., B. Pitts, E. Lauchnor, and P. S. Stewart (2016, October). Gel-Entrapped *Staphylococcus aureus* Bacteria as Models of Biofilm Infection Exhibit Growth in Dense Aggregates, Oxygen Limitation, Antibiotic Tolerance, and Heterogeneous Gene Expression. *Antimicrobial Agents and Chemotherapy 60*(10), 6294–6301.

Parijs, I. and H. P. Steenackers (2018, June). Competitive inter-species interactions underlie the increased antimicrobial tolerance in multispecies brewery biofilms. *The ISME Journal 12*, 2061–2075.

Paz-Yepes, J., B. Brahamsha, and B. Palenik (2013, July). Role of a Microcin-C-like biosynthetic gene cluster in allelopathic interactions in marine *Synechococcus*. *Proceedings of the National Academy of Sciences 110*(29), 12030–12035.

Phan, T. V., R. J. Morris, H. T. Lam, P. Hulamm, M. E. Black, J. Bos, and R. H. Austin (2018, December). Emergence of *Escherichia coli* critically buckled motile helices under stress. *Proceedings of the National Academy of Sciences 115*(51), 12979–12984.

Pissaridou, P., L. P. Allsopp, S. Wettstadt, S. A. Howard, D. A. I. Mavridou, and A. Filloux (2018, December). The *Pseudomonas aeruginosa* T6SS-VgrG1b spike is topped by a PAAR protein eliciting DNA damage to bacterial competitors. *Proceedings of the National Academy of Sciences 115*(49), 12519–12524.

Poole, K. (2012, September). Bacterial stress responses as determinants of antimicrobial resistance. *Journal of Antimicrobial Chemotherapy 67*(9), 2069–2089.

Prinsloo, H. E. (1966). Bacteriocins and phages produced by *Serratia marcescens*. *Journal of General Microbiology 45*(2), 205–212.

Pukatzki, S., A. T. Ma, A. T. Revel, D. Sturtevant, and J. J. Mekalanos (2007, September). Type VI secretion system translocates a phage tail spike-like protein into target cells where it cross-links actin. *Proceedings of the National Academy of Sciences 104*(39), 15508–15513.

Pukatzki, S., A. T. Ma, D. Sturtevant, B. Krastins, D. Sarracino, W. C. Nelson, J. F. Heidelberg, and J. J. Mekalanos (2006). Identification of a conserved bacterial pro-

tein secretion system in *Vibrio cholerae* using the Dictyostelium host model system. *Proceedings of the National Academy of Sciences 103*(5), 1528–1533.

Riley, M. A. and D. M. Gordon (1999). The ecological role of bacteriocins in bacterial competition. *Trends in Microbiology 7*(3), 129–133.

Roelofs, K. G., M. J. Coyne, R. R. Gentyala, M. Chatzidaki-Livanis, and L. E. Comstock (2016, September). *Bacteroidales* Secreted Antimicrobial Proteins Target Surface Molecules Necessary for Gut Colonization and Mediate Competition *In Vivo*. *mBio 7*(4), e01055–16.

Ross, B. D., A. J. Verster, M. C. Radey, D. T. Schmidtke, C. E. Pope, L. R. Hoffman, A. M. Hajjar, S. B. Peterson, E. Borenstein, and J. D. Mougous (2019, November). Human gut bacteria contain acquired interbacterial defence systems. *Nature 575*(7781), 224–228.

Ruhe, Z. C., D. A. Low, and C. S. Hayes (2020, September). Polymorphic Toxins and Their Immunity Proteins: Diversity, Evolution, and Mechanisms of Delivery. *Annual Review of Microbiology 74*(1), 497–520.

Ruhe, Z. C., P. Subramanian, K. Song, J. Y. Nguyen, T. A. Stevens, D. A. Low, G. J. Jensen, and C. S. Hayes (2018, November). Programmed Secretion Arrest and Receptor-Triggered Toxin Export during Antibacterial Contact-Dependent Growth Inhibition. *Cell 175*(4), 921–933.

Russell, A. B., R. D. Hood, N. K. Bui, M. LeRoux, W. Vollmer, and J. D. Mougous (2011, July). Type VI secretion delivers bacteriolytic effectors to target cells. *Nature 475*(7356), 343–347.

Russell, A. B., M. LeRoux, K. Hathazi, D. M. Agnello, T. Ishikawa, P. A. Wiggins, S. N. Wai, and J. D. Mougous (2013, April). Diverse type VI secretion phospholipases are functionally plastic antibacterial effectors. *Nature 496*(7446), 508–512.

Samuels, A. N., M. Roggiani, K. A. Smith, J. Zhu, M. Goulian, and R. M. Kohli (2020,

May). Deciphering the Role of Colicins during Colonization of the Mammalian Gut by Commensal *E. coli*. *Microorganisms 8*(5), 664.

Sassone-Corsi, M., S.-P. Nuccio, H. Liu, D. Hernandez, C. T. Vu, A. A. Takahashi, R. A. Edwards, and M. Raffatellu (2016, October). Microcins mediate competition among Enterobacteriaceae in the inflamed gut. *Nature 540*(7632), 280–283.

Sharp, C., C. Boinett, A. Cain, N. G. Housden, S. Kumar, K. Turner, J. Parkhill, and C. Kleanthous (2019, February). O-Antigen-Dependent Colicin Insensitivity of Uropathogenic *Escherichia coli*. *Journal of Bacteriology 201*(4), e00545–18.

Simmons, L. A., J. J. Foti, S. E. Cohen, and G. C. Walker (2008, February). The SOS Regulatory Network. *EcoSal Plus 3*(1), ecosalplus.5.4.3.

Slattery, M., I. Rajbhandari, and K. Wesson (2001). Competition-Mediated Antibiotic Induction in the Marine Bacterium *Streptomyces tenjimariensis*. *Microbial Ecology 41*, 90–96.

Smith, W. P. J., M. Brodmann, D. Unterweger, Y. Davit, L. E. Comstock, M. Basler, and K. R. Foster (2020, December). The evolution of tit-for-tat in bacteria via the type VI secretion system. *Nature Communications 11*(1), 5395.

Smith, W. P. J., A. Vettiger, J. Winter, T. Ryser, L. E. Comstock, M. Basler, and K. R. Foster (2020, May). The evolution of the type VI secretion system as a disintegration weapon. *PLOS Biology 18*(5), e3000720.

Soltani, S., R. Hammami, P. D. Cotter, S. Rebuffat, L. B. Said, H. Gaudreau, F. Bédard, E. Biron, D. Drider, and I. Fliss (2021, January). Bacteriocins as a new generation of antimicrobials: Toxicity aspects and regulations. *FEMS Microbiology Reviews 45*(1), fuaa039.

Souza, D. P., G. U. Oka, C. E. Alvarez-Martinez, A. W. Bisson-Filho, G. Dunger, L. Hobeika, N. S. Cavalcante, M. C. Alegria, L. R. Barbosa, R. K. Salinas, C. R. Guzzo, and C. S. Farah (2015, December). Bacterial killing via a type IV secretion system. *Nature Communications 6*(1), 6453.

Speare, L., A. G. Cecere, K. R. Guckes, S. Smith, M. S. Wollenberg, M. J. Mandel, T. Miyashiro, and A. N. Septer (2018, September). Bacterial symbionts use a type VI secretion system to eliminate competitors in their natural host. *Proceedings of the National Academy of Sciences 115*(36), E8528–E8537.

Steele, M. I., W. K. Kwong, M. Whiteley, and N. A. Moran (2017, December). Diversification of Type VI Secretion System Toxins Reveals Ancient Antagonism among Bee Gut Microbes. *mBio 8*(6), e01630–17.

Stempler, O., A. K. Baidya, S. Bhattacharya, G. B. Malli Mohan, E. Tzipilevich, L. Sinai, G. Mamou, and S. Ben-Yehuda (2017, December). Interspecies nutrient extraction and toxin delivery between bacteria. *Nature Communications 8*(1), 315.

Stewart, P. S. and M. J. Franklin (2008, March). Physiological heterogeneity in biofilms. *Nature Reviews Microbiology 6*(3), 199–210.

Stolle, A.-S., B. T. Meader, J. Toska, and J. J. Mekalanos (2021, January). Endogenous membrane stress induces T6SS activity in *Pseudomonas aeruginosa*. *Proceedings of the National Academy of Sciences 118*(1), e2018365118.

Storey, D., A. McNally, M. Åstrand, J. sa-Pessoa Graca Santos, I. Rodriguez-Escudero, B. Elmore, L. Palacios, H. Marshall, L. Hobley, M. Molina, V. J. Cid, T. A. Salminen, and J. A. Bengoechea (2020, March). *Klebsiella Pneumoniae* type VI secretion system-mediated microbial competition is PhoPQ controlled and reactive oxygen species dependent. *PLOS Pathogens 16*(3), e1007969.

Suzuki, H., J. Pangborn, and W. W. Kilgore (1967, February). Filamentous Cells of *Escherichia coli* Formed in the Presence of Mitomycin. *Journal of Bacteriology 93*(2), 683–688.

Tang, J. Y., N. P. Bullen, S. Ahmad, and J. C. Whitney (2018, February). Diverse NADase effector families mediate interbacterial antagonism via the type VI secretion system. *Journal of Biological Chemistry 293*(5), 1504–1514.

Tassinari, M., T. Doan, M. Bellinzoni, M. Chabalier, M. Ben-Assaya, M. Martinez, Q. Gaday, P. M. Alzari, E. Cascales, R. Fronzes, and F. Gubellini (2020, May). Central role and structure of the membrane pseudokinase YukC in the antibacterial *Bacillus subtilis* Type VIIb Secretion System. *bioRxiv*.

Tooke, C. L., P. Hinchliffe, E. C. Bragginton, C. K. Colenso, V. H. Hirvonen, Y. Takebayashi, and J. Spencer (2019, August). β-Lactamases and β-Lactamase Inhibitors in the 21st Century. *Journal of Molecular Biology 431*(18), 3472–3500.

Toska, J., B. T. Ho, and J. J. Mekalanos (2018, July). Exopolysaccharide protects *Vibrio cholerae* from exogenous attacks by the type 6 secretion system. *Proceedings of the National Academy of Sciences 115*(31), 7997–8002.

Unnikrishnan, M., C. Constantinidou, T. Palmer, and M. J. Pallen (2017, March). The Enigmatic Esx Proteins: Looking Beyond Mycobacteria. *Trends in Microbiology 25*(3), 192–204.

van der Ley, P., P. de Graaff, and J. Tommassen (1986, October). Shielding of *Escherichia coli* outer membrane proteins as receptors for bacteriophages and colicins by O-antigenic chains of lipopolysaccharide. *Journal of Bacteriology 168*(1), 449–451.

Vassallo, C. N., P. Cao, A. Conklin, H. Finkelstein, C. S. Hayes, and D. Wall (2017, August). Infectious polymorphic toxins delivered by outer membrane exchange discriminate kin in myxobacteria. *eLife 6*, e29397.

Virtanen, P., M. Wäneskog, and S. Koskiniemi (2019, March). Class II contact-dependent growth inhibition (CDI) systems allow for broad-range cross-species toxin delivery within the *Enterobacteriaceae* family. *Molecular Microbiology 111*(4), 1109–1125.

Walker, D., M. Rolfe, A. Thompson, G. R. Moore, R. James, J. C. D. Hinton, and C. Kleanthous (2004, February). Transcriptional Profiling of Colicin-Induced Cell Death of *Escherichia coli* MG1655 Identifies Potential Mechanisms by Which Bacteriocins Promote Bacterial Diversity. *Journal of Bacteriology 186*(3), 866–869.

Westhoff, S., G. P. van Wezel, and D. E. Rozen (2017, April). Distance-dependent danger responses in bacteria. *Current Opinion in Microbiology 36*, 95–101.

Whitney, J. C., S. Chou, A. B. Russell, J. Biboy, T. E. Gardiner, M. A. Ferrin, M. Brittnacher, W. Vollmer, and J. D. Mougous (2013, September). Identification, Structure, and Function of a Novel Type VI Secretion Peptidoglycan Glycoside Hydrolase Effector-Immunity Pair. *Journal of Biological Chemistry 288*(37), 26616–26624.

Whitney, J. C., S. B. Peterson, J. Kim, M. Pazos, A. J. Verster, M. C. Radey, H. D. Kulasekara, M. Q. Ching, N. P. Bullen, D. Bryant, Y. A. Goo, M. G. Surette, E. Borenstein, W. Vollmer, and J. D. Mougous (2017, July). A broadly distributed toxin family mediates contact-dependent antagonism between gram-positive bacteria. *eLife 6*, e26938.

Whitney, J. C., D. Quentin, S. Sawai, M. LeRoux, B. N. Harding, H. E. Ledvina, B. Q. Tran, H. Robinson, Y. A. Goo, D. R. Goodlett, S. Raunser, and J. D. Mougous (2015, October). An Interbacterial NAD(P)+ Glycohydrolase Toxin Requires Elongation Factor Tu for Delivery to Target Cells. *Cell 163*(3), 607–619.

Wholey, W.-Y., T. J. Kochan, D. N. Storck, and S. Dawid (2016, February). Coordinated Bacteriocin Expression and Competence in *Streptococcus pneumoniae* Contributes to Genetic Adaptation through Neighbor Predation. *PLOS Pathogens 12*(2), e1005413.

Wiener, P. (1996, July). Experimental studies on the ecological role of antibiotic production in bacteria. *Evolutionary Ecology 10*(4), 405–421.

Willett, J. L., Z. C. Ruhe, C. W. Goulding, D. A. Low, and C. S. Hayes (2015, November). Contact-Dependent Growth Inhibition (CDI) and CdiB/CdiA Two-Partner Secretion Proteins. *Journal of Molecular Biology 427*(23), 3754–3765.

Willey, J. M. and W. A. van der Donk (2007, October). Lantibiotics: Peptides of Diverse Structure and Function. *Annual Review of Microbiology 61*(1), 477–501.

Zhang, D., R. F. de Souza, V. Anantharaman, L. M. Iyer, and L. Aravind (2012). Polymorphic toxin systems: Comprehensive characterization of trafficking modes, process-

ing, mechanisms of action, immunity and ecology using comparative genomics. *Biology Direct* 7(1), 18.

Chapter 2

Filamentation as an escape strategy in *Escherichia coli*

2.1 Abstract

Filamentation is often observed in bacteria undergoing stress, including as a response to antibiotics. While often explained as a cellular repair mechanism, it has been suggested that filamentation could have a second function, as an escape mechanism. However, more evidence is needed. Here, we show that filamentation can indeed be beneficial in colonising new environments in the presence of toxins. We found that both the narrow-spectrum bacteriocin colicin E2 and the broad-spectrum drug mitomycin C trigger filamentation. We could not establish whether filamentation was beneficial in response to colicins, due to extensive filamentation in mutants deleted for known inhibitors of division. But we found that filamentation in response to the drug mitomycin C showed a net benefit to cells, helping them to colonise the edge of growing colonies. These results demonstrate that filamentation may work not only as a damage-repair mechanism but also as a way for cells to escape the causes of their stress. Whether this phenotype evolved, at least in part, to enable escape or whether this effect is just a by-product is a key question for future research.

2.2 Introduction

Bacteria have evolved strategies to cope with a wide range of stressors (Storz and Hengge, 2010). Examples of these strategies include responses to clinical antibiotics, but also the wide range of toxins that bacteria experience during competition with other strains and species of microbes (see Chapter 1). It is arguable that the majority of bacterial responses to clinical antibiotics first originated during competition with other bacteria. The wide distribution of these weapons across the bacterial phylogeny suggests that interbacterial conflicts are common (Ghoul and Mitri, 2016). More and more experimental evidence is also now building up to support the view that interference competition is common and a key interaction in microbial communities (Chassaing and Cascales, 2018; García-Bayona and Comstock, 2018; Parijs and Steenackers, 2018). One expected consequence of the omnipresence of conflict is that there is strong natural selection on bacteria to evolve ways to cope with high levels of aggression from other cells.

One key general response of bacteria to incoming stresses, including antibiotics, is biofilm formation. This response is often thought of as a strategy by which bacteria form a defensive group that can work together to survive potentially hostile conditions (a topic we will explore in chapter 3) (Hoffman et al., 2005; Oliveira et al., 2015). However, an obvious alternative is to attempt to move away from hostile environments and there is evidence that bacteria will sometimes do this too. This is particularly clear for swimming cells, which can perform negative chemotaxis whereby cells alter their behaviour and move down gradients of certain chemicals (Tso and Adler, 1974). A potential mechanism that is less well known is for a cell to change its shape in order to attempt to escape danger (Justice et al., 2008). Filamentation is the ability of a cell to grow without dividing and become abnormally long. The hypothesis is that, by becoming very long, cells have the potential to physically push themselves up and out of danger. This strategy is thought to help uropathogenic *Escherichia coli* (UPEC) cells escape and evade our immune cells during infection (Justice et al., 2006). More generally, *E. coli* exposed to minimum inhibitory concentrations of antibiotics will form

highly motile filaments, which, it has been argued, may allow cells to escape dangerous conditions (Phan et al., 2018). Filamentation has also been implicated as a way to endure stressful environments in other microorganisms (Jørgensen et al., 1995; Mattick et al., 2000; Heinrich et al., 2019). In *Pseudomonas aeruginosa*, Frost et al. (2018) noted cell elongation in response to carbenicillin (a β-lactam antibiotic), which they again speculated may help promote preferential access to the edge of growing colonies.

While there has been considerable discussion of the idea that filamentation may help cells to escape and compete better relative to cells that are not able to filament, direct experimental tests have been lacking. The best evidence to date comes from experiments with uropathogenic *E. coli* where it was shown that a mutant that was less able to filament was less virulent (Justice et al., 2006). However, this was in a complex and specific assay, which begs the question whether there is a general advantage to filamentation in bacterial groups. Phan et al. (2018) showed that chemically-inducing filamentation helped to increase the swimming speed of *E. coli* cells. While interesting, here filamentation is serving to enhance swimming motility rather than being a mechanism to physically push cells up and out of danger. Moreover, there is currently no experimental evidence that this swimming behaviour can lead to a competitive benefit to bacteria.

Our goal therefore was to explore the idea that filamentation, in response to incoming toxins, can provide a competitive benefit to bacteria. To date, the discussion of filamentation as an escape strategy has focussed on either the *in-vivo* context or the potential effects of clinical antibiotics. However, as discussed above, arguably a more important and ancient source of stress is competition with other bacteria. We wanted to ask, therefore, whether filamentation could be an escape strategy to bacterially derived bacteriocins, as well as broad-spectrum drugs.

Colicins are narrow-spectrum proteinaceous toxins produced by *E. coli* to compete with susceptible strains of the same or very closely related species (Riley and Gordon, 1999; Majeed et al., 2011). The genes encoding colicins are carried on plasmids that also encode a cognate immunity protein, which provides protection from the toxin to the producer and, in the case of group A colicins, a lysis protein that allows release of the

toxin (Cascales et al., 2007). Once released, these toxins need to bind and penetrate their targets in order for them to deploy their deadly activities, which they do by parasitising the victim's own import systems (Kleanthous, 2010; Housden and Kleanthous, 2012). Inside their victims, not all colicins act the same. While some form pores or inhibit peptidoglycan synthesis, others degrade the cells' RNA and DNA (Kleanthous, 2010; Cascales et al., 2007). Importantly for our question, the DNA damage that follows from DNase colicins' (E2, E7, E8 and E9) activity has the consequence to trigger the SOS response (Walker et al., 2004), which is expected to lead to cell division arrest (Huisman and D'Ari, 4 31) and filamentation (Figure 2.1).

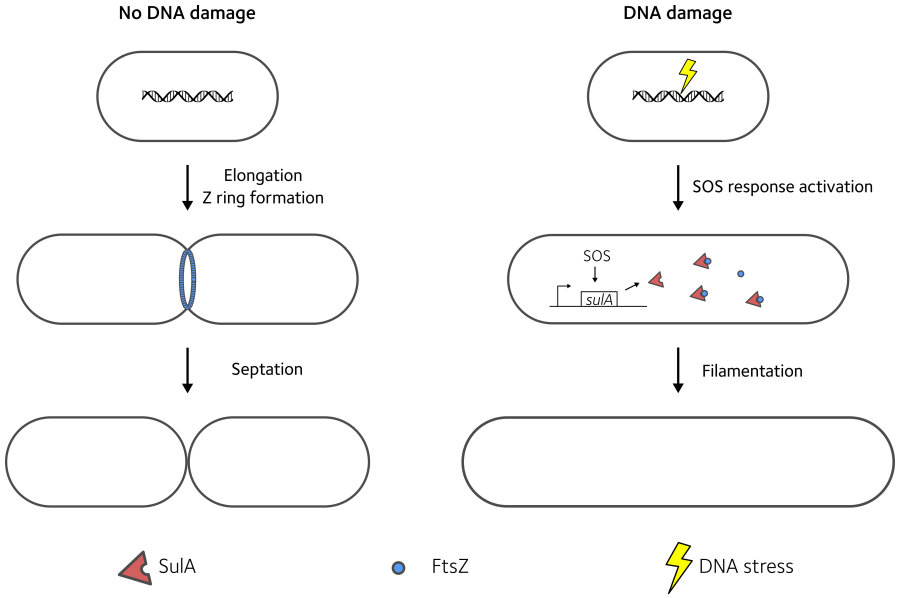

Figure 2.1: SulA prevents division by sequestering FtsZ. **Left**: In the absence of DNA damage, FtsZ monomers (blue circles) assemble to form the division ring (middle). The Z ring allows septation, leading to two daughter cells. **Right**: In the presence of DNA damage (top), the SOS response is activated. Transcription of *sulA* leads to the production of the SulA protein (red triangle). SulA binds to FtsZ and prevents Z ring formation (middle). As a consequence, cells filament (bottom).

Here we seek to understand whether filamentation — induced by colicins or the broad spectrum DNA-damaging drug, mitomycin C — leads to an escape benefit. We find that both toxins lead to filamentation in *E. coli*, as predicted by their ability to damage DNA and induce the SOS response. However, the two forms of filamentation also have differences. The response reaches extremes under colicin treatment, where

some individual filaments reach more than 100 microns, while cell elongation is less dramatic with mitomycin C. Despite exploring a range of potential mutants predicted to inhibit filamentation — including *sulA* (formerly known as *sfiA*) (Huisman et al., 1984), a key actor in blocking division during SOS response (Figure 2.1) — we were unable to find one that ablated the filamentation response to colicins. These results, unfortunately, mean that we are unable to test the potential adaptive significance of the colicin response. However, as compared to colicin treatment, *sulA* has more of an impact on filamentation under the presence of mitomycin C. Moreover, in support of the escape hypothesis, we provide evidence that filamentation in the presence of mitomycin C allows cells to better reach the edge of bacterial colonies and thereby outcompete cells that are less able to filament. These data support the notion that filamentation can provide cells with a competitive advantage by physically promoting their ability to disperse from groups.

2.3 Methods

2.3.1 Bacterial strains

The background strain used in all experiments was *E. coli* BZB1011, a gyrA spontaneous mutant of *E. coli* W3110 resistant to nalidixic acid with either a *sfgfp* or a *mscarlet-I* gene inserted at the *glmS* gene locus. The list of bacterial strains used in this study is shown in table 2.1.

2.3.2 Bacterial growth conditions

All liquid bacterial cultures, unless otherwise specified, were carried out in 3 mL of LB broth Miller (10g/L tryptone, 5g/L yeast extract, 10g/L NaCl) at 37°C with shaking (225 rotations per minute).

The solid medium used to grow bacteria, unless specified otherwise, was LB agar 1.5% w/v, Miller. Incubation of LB agar plates was done at 37°C in a static incubator.

The concentrations of antibiotics used are summarised in table 2.2. Alternative

Table 2.1: Bacterial strains used in this study

Name	Genotype
BZB1011[1]	λ^-, *gyrA*586 (NalR), IN(*rrnD-rrnE*)1, *rpsL*$^-$ (StrR), *rph-1*
BZB1011 GFP[2]	λ^-, *gyrA*586 (NalR), IN(*rrnD-rrnE*)1, *rpsL*$^-$ (StrR), *rph-1*, Pmax-*sfgfp*::Tn7
BZB1011 mScarlet[3]	λ^-, *gyrA*586 (NalR), IN(*rrnD-rrnE*)1, *rpsL*$^-$ (StrR), *rph-1*, Pmax-*mscarlet-I*::Tn7
BZB1011 GFP SulA$^-$ [3]	λ^-, *gyrA*586 (NalR), IN(*rrnD-rrnE*)1, *rpsL*$^-$ (StrR), *rph-1*, Δ*sulA*, Pmax-*sfgfp*::Tn7
BZB1011 mScarlet SulA$^-$ [3]	λ^-, *gyrA*586 (NalR), IN(*rrnD-rrnE*)1, *rpsL*$^-$ (StrR), *rph-1*, Δ*sulA*, Pmax-*mscarlet-I*::Tn7
BZB1011 GFP BtuB$^-$ [4]	λ^-, *gyrA*586 (NalR), IN(*rrnD-rrnE*)1, *rpsL*$^-$ (StrR), *rph-1*, Δ*btuB*, Pmax-*sfgfp*::Tn7
BZB1011 E2[1]	λ^-, *gyrA*586 (NalR), IN(*rrnD-rrnE*)1, *rpsL*$^-$ (StrR), *rph-1*, pColE2
BZB1011 E2 RFP[2]	λ^-, *gyrA*586 (NalR), IN(*rrnD-rrnE*)1, *rpsL*$^-$ (StrR), *rph-1*, Pmax-*mrfp1*::Tn7, pColE2

concentrations are indicated in the text where relevant.

Table 2.2: Antibiotics used in this study

Antibiotic	Standard working concentration	Standard stock concentration
Ampicillin	100 μg/mL	100 mg/mL
Kanamycin	50 μg/mL	50 mg/mL

2.3.3 Strain labelling

The BZB1011 GFP-labelled strain was previously generated by Mavridou et al. (2018). To label strains with mScarlet-I, the mini-Tn7 transposon method described by McKenzie and Craig (2006) was used. In brief, BZB1011 and BZB1011 SulA$^-$ were transformed with pGRG25-Pmax-*mscarlet-I* (by heat-shock for BZB1011, by electroporation

[1]Pugsley and Schwartz (1983)
[2]Mavridou et al. (2018)
[3]This study
[4]Krishna Kumar et al. (2021)

for BZB1011 SulA$^-$) using selection on ampicillin 100 μg/mL, recovery at 30°C for one hour and growth overnight at 30°C. The next day, colonies were checked for fluorescence using a Zeiss Axio Zoom.V16 stereoscope using the mRFP channel (Filter: 63 HE - Excitation: 572/25 nm - Emission: 629/62 nm - Beam Splitter: 590 nm). Three fluorescent colonies were picked and inoculated in LB supplemented with 0.5% w/v arabinose. The cultures were incubated overnight at 30°C. The next day 5 μL of each culture was streaked on LB agar + 0.5% w/v arabinose and incubated over the day 10 hours at 42°C. At the end of the day, fluorescence was checked and 5 fluorescent colonies were picked from each plate and streaked on LB agar. Plates were incubated at 42°C overnight. Colonies were then checked for fluorescence and 5 clones were picked, streaked on LB agar ampicillin and, using the same tip, inoculated in LB. Liquid cultures were incubated overnight at 37°C and the LB agar ampicillin plate was incubated at 30° overnight. Glycerol stocks (20% v/v final concentration) of the clones for which corresponding streak on LB ampicillin did not grow were made.

2.3.4 Chromosomal gene deletions

To delete genes in the chromosome of *E. coli*, the method described by Cianfanelli et al. (2020) was used. Briefly, the regions (700 base pairs) upstream and downstream of the genes to delete (*sulA*) were amplified by PCR and joined together in the pFOK plasmid using the NEB HiFi DNA Assembly Master Mix. In all, 5 μL of the reaction was then transformed into chemically competent *E. coli* Jke201 (recovery in 1mL of LB-Miller medium + 100 μM diamino pumilic acid (DAP) and selected on LB Miller agar plates supplemented with 100 μM DAP and 50 μg/mL kanamycin). Transformants were screened by colony PCR (GoTaq G2 polymerase) and sequenced (Source Bioscience) using the primers oOPC-614 and oOPC-615. Three clones carrying the correct plasmid (pTML1 for deletion of *sulA*) were then conjugated with BZB1011 non-tagged and BZB1011 *sfgfp*::Tn7. Transconjugants for which a second recombination event had occurred were then counter-selected. Clones were finally verified by colony PCR and sequencing (by using the primers TML-P15 and TML-P16) for deletion of the

sulA gene.

2.3.5 Heat-shock competent cells preparation and transformation

Preparation

The strain to transform was inoculated in LB overnight. The next day, the optical density of the overnight culture was measured using a spectrophotometer (Thermo Scientific, Genesys 10 S UV-VIS) by adding 100 μL of the overnight culture to 900 μL of fresh LB in a spectrophotometer cuvette (Fisherbrand^{TM} Polystyrene Semi Micro Cuvettes). 50 mL of LB were inoculated with the overnight culture to a concentration of optical density (OD) 0.05 and incubated at 37°C with shaking until the OD reached around 0.4 (checking the OD every hour until OD reaches 0.2, then every 30 minutes until it reaches OD 0.4). Once the OD was at the desired value, the cultures were placed on ice. They were immediately transferred in 2 conical 50 mL tubes dividing the volume equally between the two tubes and centrifuged for 10 minutes at 1734 g at 4°C. The supernatant was then discarded and each pellet resuspended gently in 12.5 mL of ice cold 100mM $CaCl_2$ + 15% v/v glycerol. The cultures were incubated on ice for 45 minutes and centrifuged again at 1734 g for 10 minutes at 4°. One pellet was resuspended in 5 mL of ice cold 100mM $CaCl_2$ + 15% v/v glycerol solution, and using this resuspension, the second pellet was resuspended. Following this, 200 μL of competent bacteria were aliquoted into 1.5-mL centrifuge tubes and directly frozen at -80°C.

Transformation

To transform heat-shock competent cells, 100 μL of competent cells were thawed on ice. DNA ($\sim$ 100 ng for plasmid or 5 μL of Gibson Assembly reaction mix) was added to the thawed cells. The cells were then kept on ice for 30 minutes. A heat shock was then applied by transferring the tube containing the cells into a 42°C water-bath for 45 seconds and transferring the tube back on ice for 2 minutes. The cells were then recovered by adding 900 μL of LB and by immediately incubating for an hour at 37°C (unless specified otherwise) with shaking. After one hour of recovery, 100 μL were plated

on selective LB agar. The remaining 900 μL were then centrifuged for 1 minute at 8000 g, followed by discarding 800 μL of the supernatant and the pellet resuspended in the residual 100 μL. The final 100 μL were then plated on selective LB agar. Both plates were then incubated overnight in a static incubator.

2.3.6 Electrocompetent cells preparation and transformation

Preparation

Electrocompetent cells were prepared at room temperature following the protocol described by Granato (2020). Cells were streaked on LB agar directly from the cryostock and grown overnight. Using a sterile 1 μL loop, one colony was scraped off the plate, resuspended in 700 μL sterile milliQ water in an Eppendorf tube and vortexed thoroughly. Cells were then spun down for 3 minutes at 5200 g. The supernatant was removed and the pellet resuspended in 700 μL sterile milliQ water and vortexed thoroughly. The cells were once again centrifuged for 3 minutes at 5200 g, the supernatant removed and the pellet resuspended in 40 μL sterile milliQ water.

Transformation

To transform the cells, about 50 ng of plamid was added to the cells. The mixture was then pipetted into a 1 mm electroporation cuvette (Bio-rad Gene Pulser, 0.1 cm gap) and electroporated at 2.5kV. The cells were recovered by adding 1 mL of LB to the cuvette, transferred to a 1.5 mL Eppendorf tube and incubated 1 hour at the desired temperature with shaking. After one hour of recovery, 100 μL were plated on selective LB agar. The remaining 900 μL were then centrifuged for 1 minute at 8000 g, 800 μL of the supernatant was discarded and the pellet resuspended in the residual 100 μL and plated on selective LB agar. Both plates were then incubated overnight in a static incubator.

2.3.7 Plasmid construction

All plasmids were designed in SnapGene and built using the NEB HiFI DNA builder.

2.3.8 Agarose droplets

The ability of cells to disperse via filamentation was studied under standard colony growth at the growing edge on agar (below), but also using an agarose droplet assay. Growth within agarose droplets is the basis of the 3D printing method the lab co-developed (Krishna Kumar et al., 2021) and form an alternate way to study bacterial growth in dense communities. For my experiments, I used single droplets, which are larger than the ones used in the printing, as I was not exploring the effects of spatial structure, but the principles are the same as in the 3D printing method. I detail the approach next.

Preparation

Cells were cultured in 3 mL of LB Broth Miller and incubated at 37°C with shaking (225 rpm/minute) overnight (16 hours). Custom holders for droplet formation and assays, hereafter called well arrays, were sterilised by submerging them in 70% v/v ethanol for at least an hour and drying them in a laminar flow hood. These well arrays, made of polymethylmethacrylate (PMMA), were generated using computer-aided design and a CNC (Computer Numerical Control) machine. The following day, cultures were diluted 100-fold in 2 mL of LB and incubated for 2 to 3 hours (sometimes more for colicin-producing strains) at 37°C with shaking until they reached mid-exponential phase (OD 0.2 to 0.7). Meanwhile, the well arrays were then filled with 200 μL oil (comprising of undecane and silicone oil AR20 at a volume ratio of 35:65 respectively) with a 3:1 or 2:1 molar ratio of DPhPC (1,2-diphytanoyl-sn-glycero-3-phosphocholine):POPC (1-palmitoyl-2-oleoyl-glycero-3-phosphocholine), a composition developed to optimise printing (Krishna Kumar et al., 2021).

Once cultures reached mid-exponential phase, the OD of the cultures was normalised to OD 3.5. The cultures were then diluted 100-fold to OD 0.035 (unless indicated otherwise) by doing two 10-fold serial dilutions in a mix of 75 μL of 2% w/v LB ultra low gelling temperature (ULGT) agarose and 15 μL of LB. Droplets were then formed in the well arrays by pipetting up 50 to 200 nL of the 1.5% w/v LB ULGT agarose

mixture containing the cells using a previously sterilised 0.2 μL Hamilton syringe (or a Gilson P2 pipette set on 0.2 μL) and expelling the mix in the oil forming an aqueous droplet. The droplets were then incubated 20 minutes at 4°C to allow gelling. The lipid layer surrounding the agarose droplet was then broken by adding 200 μL silicone oil in the well arrays and removing and discarding 200 μL of this mixture. This operation was performed 5 times in total. Droplets were then encased in LB using a sterile 10 μL Hamilton syringe by releasing some LB near the agarose droplets until the agarose droplet went into the LB pocket. This was done to ensure the agarose droplet would not dry when removing the remaining silicone oil. The remaining silicone oil was then thoroughly removed. 400 μL of LB were then added to the array leading to the cells-containing agarose droplets to bathe in LB (Figure 2.2).

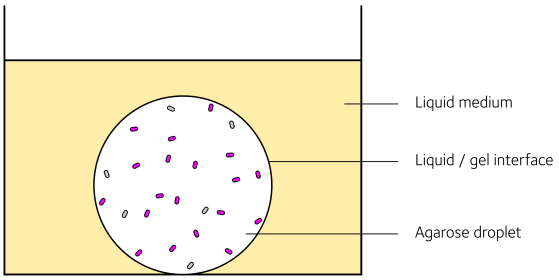

Figure 2.2: Schematic of cells (purple, susceptible cells; grey, colicin producer cells) embedded in an agarose droplet. The agarose droplet containing the cells sits in liquid LB medium. At the edge of the droplet, there is a liquid/gel interface.

The agarose droplet containing droplets were then incubated at 37°C either in a static incubator or under a heated microscope.

Imaging

Arrays containing the droplets were placed on a M-686K062 130x100 (PI) stage. All images were collected with a Zeiss LSM-700 laser scanning confocal microscope on a Zeiss Observer Z1 inverted microscope equipped with a Plan Apochromat 20X/0.8 DICII and an EC-Plan-Neofluar 40X/0.7 M27 objective. sfGFP fluorescence was excited with a 488 nm (10 mW) laser and collected using a SP 555 filter at 518 nm. The channel used for sfGFP was also used for the generation of transmitted light picture using the T-PMT function (PhotoMultiplier Tube for transmitted light). mRFP1 and propidium iodide fluorescence were excited with a 555 nm (10 mW) laser and collected at 585 nm. Images were acquired with a Zeiss Axiocam MRm controlled

with Zen Black 2011.

Escape assessment

Assessment of escape was carried out visually using microscopy and by sampling the medium surrounding the droplets in which both the colicin producer, the WT and the mutant are grown. This sample was then plated and colony forming units (CFU) for each strain counted (see Methods 2.3.11).

2.3.9 Colony Expansion Assay

This colony expansion assay was adapted from Frost et al. (2018). The fates of cells that filament (WT) and mutants that have reduced filamentation ($SulA^-$ or $BtuB^-$ strains) were studied in this assay.

Preparation

Strains were inoculated in 3 mL of LB and incubated at 37°C with shaking overnight (15 hours). The OD of the cultures were measured using a spectrophotometer by adding 100 μL of the overnight culture to 900 μL of fresh LB in a spectrophotometer cuvette (Fisherbrand^{TM} Polystyrene Semi Micro Cuvettes). Two tubes containing 3 mL of LB were then inoculated with the overnight cultures to normalise the OD to 0.05.

Diluted cultures were incubated for 2 hours at 37°C with shaking to allow the cells to reach exponential phase. The OD were then measured by pipetting 750 μL of the cultures into cuvettes and read using the spectrophotometer. The cells were then washed three times (centrifugation at 8000 g for 1 minute, discarding the supernatant, resuspending the pellet with 1 mL of PBS) and resuspended in 1 mL of PBS. Cultures were normalised to OD 0.3 using 1 mL as the desired final volume. Tubes were vortexed thoroughly and 200 μL of each strain culture (WT and mutant) were then mixed in a new Eppendorf tube. The mixture was then vortexed thoroughly.

- Either 5 one-μL droplets (technical replicates) were then deposited on LB agar containing either the supernatant of a colicin-producing strain or mitomycin C

(Figure 2.3.a).

- Or 4 one-μL droplets were placed at various distances (5, 15, 25 and 35 mm) from a colicin-producing strain spotted at the centre of a Petri dish containing LB agar ($100\,mm \times 15\,mm$) (Figure 2.3.b).

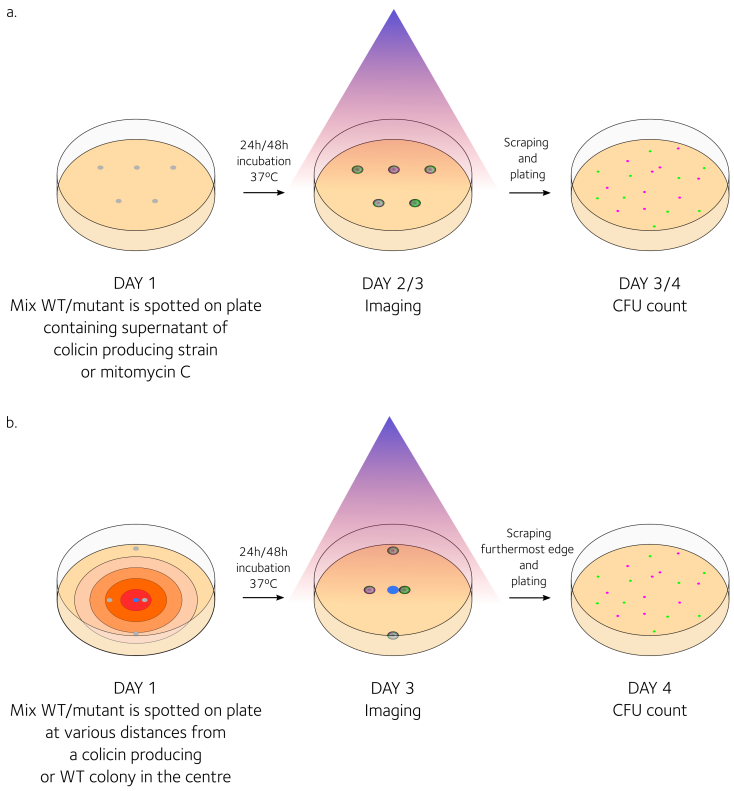

Figure 2.3: Colony expansion assay. **a.** A 1:1 mix of WT and mutant are spotted on LB agar containing the supernatant of either a colicin producer (E2 shown here) or a non-producer (WT) for experiments using colicins or either mitomycin C (for mitomycin C = 0 μg/mL, DMSO was added to the LB agar instead of mitomycin C). The spots are left to grow one or two days at 37°C. The colonies are then imaged, scraped, resuspended and plated (Day 2/3) to allow counting of CFU and estimation of the proportion of WT and SulA$^-$ cells in the colonies (Day 3/4). **b.** Same as in **a.** but the cells are spotted at various distances (5, 15, 25 and 35 mm) from a central colony (either colicin producing or non-colicin producing) on LB agar. The toxin comes from the central colony.

Droplets on the plates were set to dry under the flame for a few minutes until the spot appeared dry. Plates were then incubated statically at 37°C for 24 (for mitomycin C experiments) or 48 hours (for colicin experiments). After incubation, the colonies were imaged and scraped from the plate using a 10 μL plastic loop and resuspended in 200 μL filled well of a 96-well plate.

Imaging

Single cells. To assess whether any differences in the proportion of the strains competing in our colony assay came from filamentation, we looked at the edge of colonies under a microscope. Cells were grown on agar as described in section 2.3.9. Agar squares containing the colonies to image were cut using a scalpel and placed in 50 mm glass bottom (#1.5) dishes (MatTek Corporation). These dishes were then placed upside down (colony closer to the objective) on a SCAN IM 130x100-2mm (Märzhäuser) stage. All images were collected with a Zeiss LSM-880 laser scanning confocal microscope on a Zeiss Observer 7 inverted microscope equipped with an EC Epiplan-Neofluar 50X/0.8 objective DIC M27. sfGFP was excited with a 488 nm (35 mW) laser and collected using a MBS 488/561 filter at 506.25 nm. Images were acquired with a Zeiss Axiocam 506 mono controlled with ZEN 2.3 SP1 FP3 (black edition).

Whole colonies. To quickly assess whether colonies were enriched in one of the strains competing in our colony assays, whole colonies were imaged. Colonies were imaged directly on agar plates. All images were collected using a Zeiss Axio Zoom.V16 stereoscope equipped with a PlanApo Z 0.5X/0.125 FWD 114 mm objective. sfGFP was excited with a HXP 200 C illuminator and filtered using a 38 HE filter (Excitation: 470/40 nm - Emission: 525/50 nm - Beam Splitter: 495 nm). mRFP1 and mScarlet-I were excited using the same HXP 200 C light source but filtered using a 63 HE filter (Excitation: 572/25 nm - Emission: 629/62 nm - Beam Splitter: 590 nm). Images were acquired with a Zeiss Axiocam MRm controlled with ZEN Blue 2012. For each biological replicate, the zoom was adjusted to fit the biggest colony in the field of view (usually zoom 8X). Exposure time was set for each biological replicate using the 'Set Exposure' function on the first technical replicate on the control plate (no toxin) and kept constant within the remaining sample for that experiment.

Escape assessment

When colonies are grown on plates containing the supernatant of a colicin producer or mitomycin C, whole colonies are scraped, diluted and quantified by plating and counting CFUs (Figure 2.3.a). When colonies are grown next to a toxin-producing colony, the furthermost edge of the colony is scraped, diluted and quantified by plating and counting CFUs (2.3.b).

The proportion of each strain in the sample provides the relative ability of each strain to reach the edge of the colony (since the centre of the colony has a 1:1 ratio of WT and mutant). If the proportion of a strain is over 50%, this strains is in greater amount at the edge.

2.3.10 Filamentation quantification assay

To assess whether mutant strains were less able to filament, filamentation had to be quantified.

Preparation

Cells were inoculated overnight and diluted the next morning to OD 0.05 in the same way as above. The inocula were then incubated for 2 hours at 37°C with shaking (225 rpm) to allow the cells to reach exponential phase. After 2 hours, treatment was applied either by adding mitomycin C or a dilution of an overnight of E2 colicin-producing cells previously filter-sterilised using a 0.2 μm filter. The cultures were then put back at 37°C. After 4 hours of incubation, the cultures were sampled for imaging. This protocol was adapted from Suzuki et al. (1967).

Imaging

Cells were mounted between a glass slide and a cover slip (#1.5) and placed on a SCAN IM 130x100-2 mm (Märzhäuser) stage. All images were collected on a Zeiss Observer 7 inverted microscope equipped with a Plan Apochromat 20X/0.8 DICII and Plan Apochromat 63X/1.4 Oil M27. sfGFP fluorescence was excited with the Colibri LED module

- 475 nm light source at 480 nm at 20% of its maximum power and collected at 505 nm. Images were acquired with a Zeiss Axiocam 506 mono controlled with Zen Blue 2.6.

2.3.11 Colony Forming Units

Colony forming units in the colonies were determined by plating 50 μL of various dilutions of the colony resuspensions on LB agar. Incubations were done over approximately 24 hours at 30°C or overnight at 37°C or at room temperature until colonies were visible. Fluorescent colonies were then visualised and counted using the light source from the stereoscope Zeiss Axio Zoom.V16 set on GFP (Filter: 38 HE - Excitation: 470/40 nm - Emission: 525/50 nm - Beam Splitter: 495 nm).

2.3.12 Image analysis

Microscopy images were analysed with ImageJ2 version 2.3.0/1.53f and ZEN 2.3 (blue edition) and ZEN 2.3 SP1 FP2 (black edition).

FAST version 2.0.1 was used for measuring cell lengths from microscopy pictures (Meacock et al., 2021). The segmentations were carried out on the fluorescent channel of images taken at 20X. All parameters were kept the same between experiments and are summarised in table 2.3. Segmentation of the Keio mutant cells were carried out on the phase contrast channel. Some of the parameters used were modified from the ones used for the fluorescence images (Neighbourhood size: 7, Ridge scale: 15, Ridge threshold: 0.05, Minimum Ridge Area: 150 and Object area threshold (Low): 50).

2.3.13 Statistical analysis

Statistical analysis was performed using Matlab 2018a and Python 3.7.4 with the packages pyMannKendall for the Mann-Kendall tests (Hussain and Mahmud, 2019), SciPy (Virtanen et al., 2020) for the Wilcoxon rank-sum tests in figures 2.9 and 2.12 and the Kruskal-Wallis test in figure 2.15 and scikit-posthoc for the Steel-Dwass-Critchlow-Fligner test in figure 2.15 (Terpilowski, 2019). For all statistical tests, the significance threshold α was set at 0.05. All statistical tests outputs can be found in appendix A.2.

Table 2.3: FAST parameters used for the segmentation of cells

Parameter	Value
Neighbourhood size	5
Texture threshold	2.5
Ridge scale	20
Ridge threshold	0.08
Minimum ridge area	100
Watershed threshold	2.5
Object area threshold (High)	10000
Object area threshold (Low)	100

2.4 Results and Discussion

The goal of this chapter is to explore the potential for filamentation-mediated dispersal in response to bacterial toxins — colicins — and broad-spectrum drugs — mitomycin C (produced by the bacterium *Streptomyces caespitosus*), which is a strong inducer of the SOS response often used to trigger it. My work initially focussed on colicin toxins and this revealed a striking filamentation response. The majority of the subsequent results reported below comprise the search for strains, and an assay, where a clear test of my dispersal hypothesis could be performed. Ultimately, this search was not successful and the assays were either hampered by mutant cells retaining the ability to filament, or having pleiotropic effects. However, the assays with mitomycin C proceeded smoothly and did show a clear dispersal advantage to filamentation.

2.4.1 DNase colicins trigger filamentation in susceptible cells

We first studied filamentation during warfare between colicin-producing strains and susceptible cells in agarose droplets. Agarose droplets are 400 μm spheres of LB agarose, produced by ejecting molten LB agarose (1.5% w/v) in an oil/phospholipid solution (see Methods 2.3.8). Cells can be embedded in these droplets by incorporating the cells to the LB agarose before formation of the droplets (Krishna Kumar et al., 2021). The

droplets can then be cultured in liquid LB and observed over time using a microscope. This new method of culturing bacteria allows for competition to be carried out in 3 dimensions, at high density and in small volumes. Moreover, it allows the investigation of the liquid/gel interface (Figure 2.2), a feature of biofilms, which colonies do not easily permit.

While culturing susceptible cells in a droplet next to another droplet containing E2 colicin producing cells, we observed striking filamentation of the susceptible cells (Figure 2.4). This behaviour could also be observed when both susceptible and toxin producers were mixed in the same droplet (Supplementary Figure A.1). In both cases, filamentous cells would reach several tens of micrometers and appear to flux out of the droplets. Propidium iodide staining showed that many of these filamentous cells were dead (Supplementary Figure A.2). However, some filaments were seen resuming division once the colicin producer was removed from the environment indicating this phenotype to be reversible (Figure 2.4.c).

Little to no filamentation was observed in droplets containing susceptible cells grown next to droplets containing cells producing pore-forming colicins (Supplementary Figure A.3). This is consistent with the fact that these toxins do not target the DNA but rather form pores in their targets' membrane. They, therefore, do not trigger the SOS response.

Filamentation in colonies was also investigated. Filamentation could also be observed at the edge of colonies growing on agar containing the supernatant of a colicin producer (Figure 2.5.a), and in colonies growing near a colicin-producing colony (Figure 2.5.b).

2.4.2 Deleting *sulA* does not abolish filamentation in response to colicins

If filamentation is beneficial to escaping toxin-producing cells, cells able to filament should escape and disperse better than cells unable to filament when competing against one another in the the presence of toxins, or toxin producers. In order to test whether filamentation allows cells to escape toxin producers, we needed a strain unable to filament in response to DNase colicins.

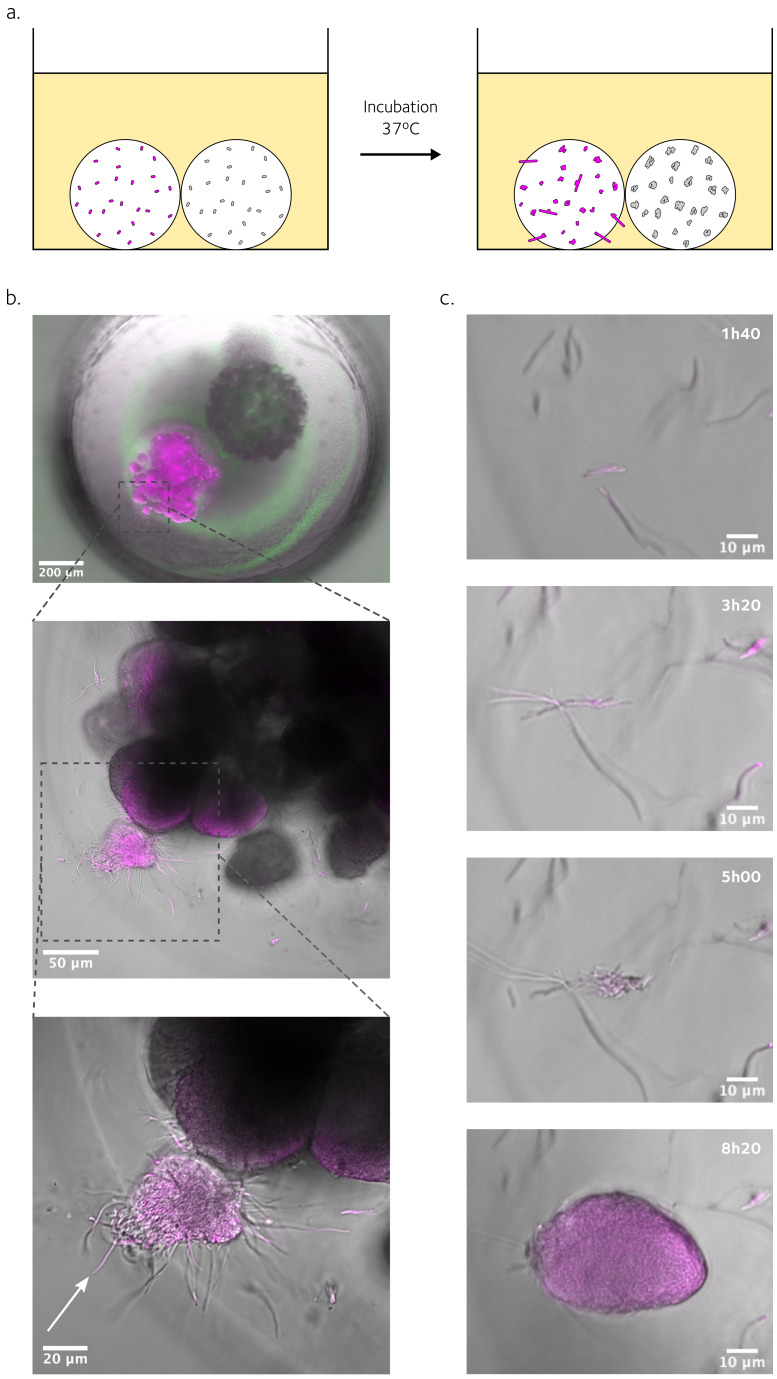

Figure 2.4: Filamentation of susceptible cells in response to DNase colicin E2 in agarose droplets. **a.** Susceptible and E2 producing cells are embedded in agarose droplet using the method described in section 2.3.8. The droplets are grown next to one another in LB and imaged. **b.** Susceptible cells embedded in an agarose droplet (top image, bottom left in purple) form microcolonies and a subpopulation filament in response to the colicins produced by the cells embedded in the neighbouring droplet (top image, top right in grey). The white arrow points to filaments. **c.** Time lapse of a filamentous cell in a droplet resuming division and forming a microcolony after the toxin-producing strain was removed from the environment. The time stamps indicate the time elapsed after the droplet containing the sensitive strain was separated from the droplet containing the colicin-producing cells and put into fresh LB medium.

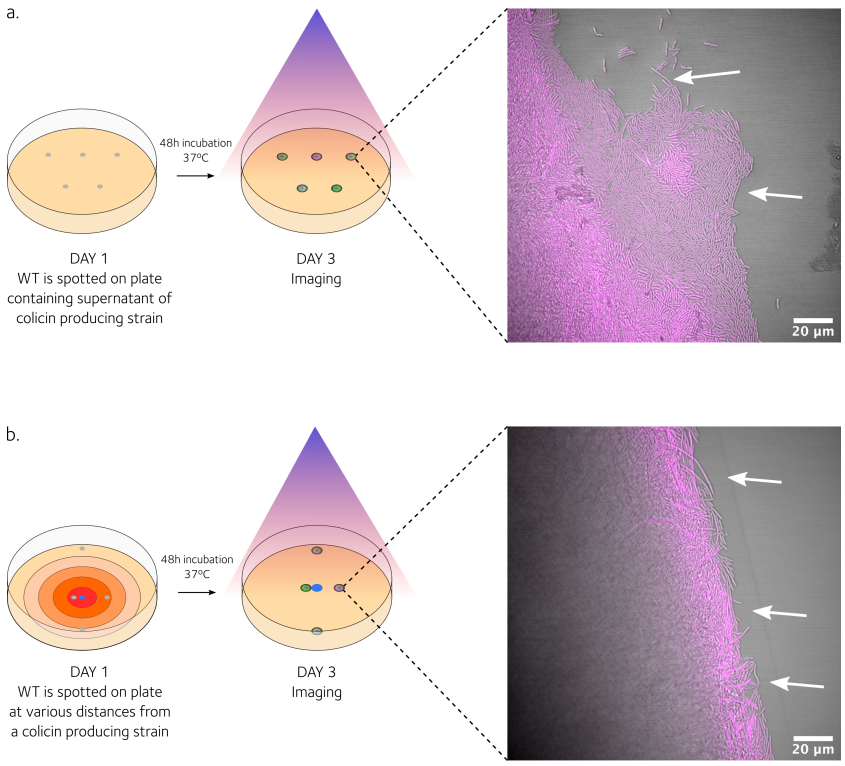

Figure 2.5: Filamentation of susceptible cells in response to DNase colicin E2 on agar plates. **a.** Susceptible cells are spotted on agar containing the supernatant of a colicin producer and incubated at 37°C for two days. After incubation, the edges of the colonies are imaged (photo, right). **b.** Susceptible cells are spotted next to a colony of colicin producers and incubated at 37°C for two days. After incubation, the edges of the colonies are imaged (photo, right). White arrows in microscopy images point to filamentous cells.

DNase colicins activate the SOS response (Walker et al., 2004). One of the genes activated during the SOS response is *sulA*, a gene encoding an inhibitor of division (Huisman and D'Ari, 4 31; Huisman et al., 1984; Simmons et al., 2008). D'Ari and Huisman (1983) identified another inhibitor of division at a locus they named sfiC, which is also activated during SOS response. However, Justice et al. (2006) reported that deleting *sulA* is sufficient to abolish filamentation *in vivo*. We therefore created a mutant lacking *sulA* (SulA$^-$) and assessed its ability to filament in response to colicin E2, initially in simple liquid culture (Figure 2.6)

In the absence of colicin treatment, SulA$^-$ cells were slightly elongated relative to WT cells. That is, SulA$^-$ and WT treated with the supernatant of a WT strain yielded mean cell lengths of 2.8 μm $\pm$ 0.9 μm and 2.2 μm $\pm$ 0.5 μm respectively. Moreover,

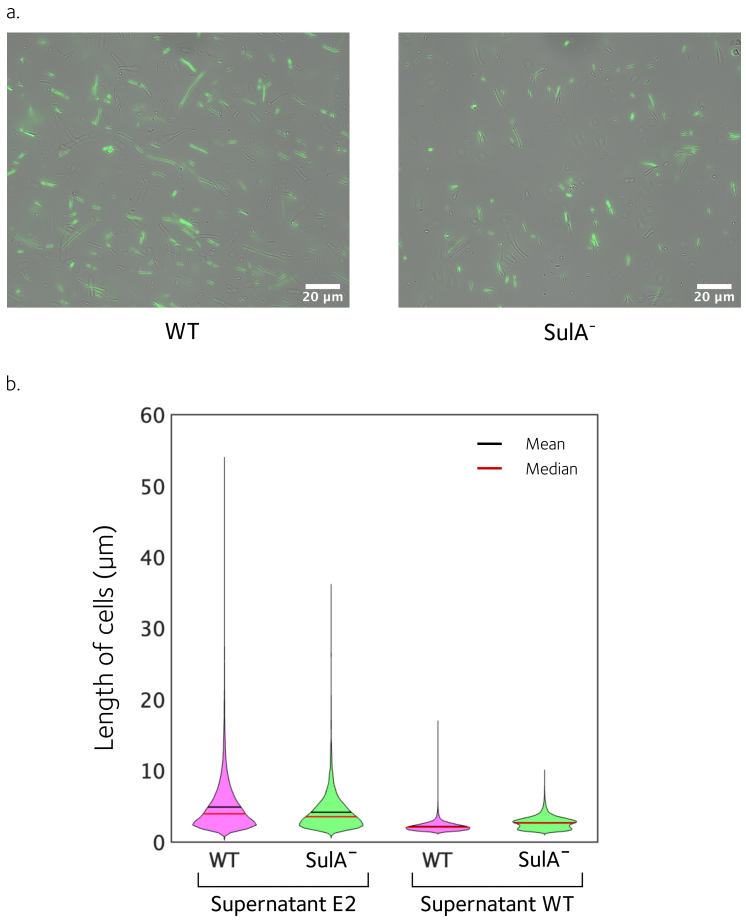

Figure 2.6: Deleting *sulA* does not abolish filamentation in response to colicins. **a.** Picture of cells (WT, left and SulA⁻, right) treated with the supernatant of a colicin E2 producer for 4 hours in liquid culture. **b.** Quantification of the amount of filamentation in these cultures. Number of cells measured from left to right: WT treated with E2 supernatant, 14294; SulA⁻ treated with E2 supernatant, 11842; WT treated with WT supernatant, 52881; SulA⁻ treated with WT supernatant, 45156. n=1 biological replicate.

when treated with colicins, the cells of both strains formed filaments. The cells deleted for *sulA* were slightly shorter than WT cells (Figure 2.6) with a mean length of 4.2 μm $\pm$ 2.5 μm vs. 5.0 μm $\pm$ 3.3 μm for the WT. However, there was still extensive filamentation in both strains, showing that the SulA⁻ strain was still able to elongate in response to colicin E2.

In order to focus on the cells that had undergone filamentation, we set a definition of filamentation as any cell longer than the mean length plus two standard deviations ($\mu + 2\sigma$) of WT cells treated with WT supernatant. The basis for this threshold is that

these cells under normal conditions would be considered significantly longer i.e. less than 5% of the total cells. With this measure, any cell longer than $2.2 + 2 * 0.5 = 3.2$ μm is taken as filamentous. Taking only filamentous cells, mean length of WT filaments was 6.4 μm $\pm$ 3.4 μm while that of the SulA$^-$ filaments was 5.5 μm $\pm$ 2.6 μm (Supplementary Figure A.4). The filamentous population in the E2 treatment represented 63.8% and 59.4% of the total population sampled for WT and SulA$^-$ respectively. In the controls (i.e. cells treated with WT supernatant), these proportions fell to 4.9% and 26.4% for the WT and SulA$^-$ respectively, which reflects the longer cells in the untreated condition for the mutant strain. Exposing cells to colicin E2 does, therefore, generate more of a response in the WT strain where the proportion of filamentous cells in the population increases 13-fold, as opposed to 2.25-fold for the SulA$^-$ strain.

We also quantified filamentation in the liquid surrounding droplets containing either the WT or the mutant SulA$^-$ strain in the presence of the E2 colicin producing strain (Figure 2.7.a). This revealed significant amounts of filamentation in both the WT and SulA$^-$ strains (Figure 2.7.b) with mean lengths of 37.2 μm $\pm$ 24.6 μm and 29.0 μm $\pm$ 18.8 μm respectively. These values remained unchanged when we excluded cells shorter than 3.2 μm. Filamentation is more extensive in the droplet assay than in liquid culture, which may be explained by a number of factors. In the droplets, the cells were exposed for longer to colicins (18 hours in the droplets vs. 4 hours in the liquid cultures) and exposure was gradual (very little colicins at the beginning and a lot at the end as the colicin-producing strain grew). By contrast, exposure was sudden and constant in the liquid cultures, excepting some colicin degradation. This means that cells in the droplet assay may have had time to ramp up progressively the stress responses which might have allowed them to survive long enough to filament more. Another important difference is that filaments were only measured after they left the droplet. As a result, if filaments are better at escaping the droplet, they should be present in a majority in the medium at the end of the experiment, skewing the length distribution towards longer cells.

In summary, we see that filamentation in response to colicin E2 in a strain deleted for *sulA* is only moderately reduced and not abolished. Consistent with this, a paper

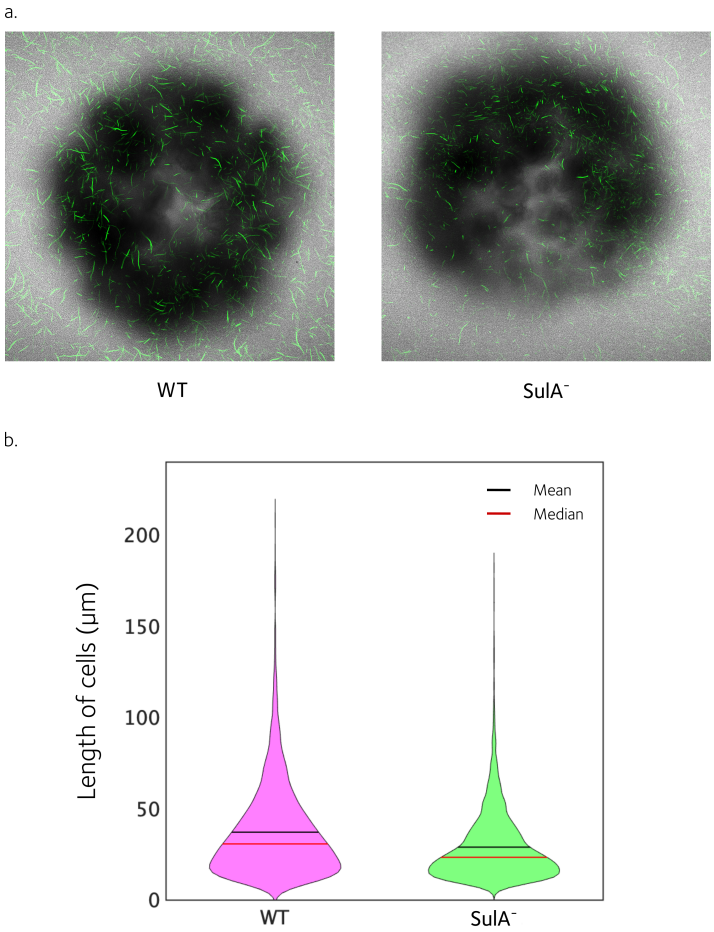

Figure 2.7: Deleting *sulA* reduces but does not abolish filamentation in response to colicins in the droplet assay. **a.** Picture of susceptible cells (WT, left and SulA$^-$, right) taken after 18 hours of growth in the presence of a colicin producer in an agarose droplet. Magnification: 400X. **b.** Quantification of the amount of filamentation in this assay. Number of cells measured from left to right: WT, 4211, SulA$^-$, 4622. n=1 biological replicate.

published after we did this work found that deleting *sulA* does not completely abolish filamentation in *E. coli* strain in which the SOS response is induced (Ansari et al., 2021). However, given there was a modest difference between the WT and the mutant strain, we decided to examine whether this was sufficient to lead to competitive difference in dispersal.

2.4.3 The difference in filamentation between WT and SulA$^-$ does not provide an advantage to WT in the presence of DNase colicins

We first examined the ability of the two strains to disperse from an agarose droplet when there was also a third E2 colicin-producer strain present. To assess dispersal, the liquid medium surrounding the droplet was sampled every hour for six hours (Figure 2.8). However, rather than demonstrating an advantage to the WT, the frequency of SulA$^-$ increased in the surrounding media across the experiment. This could be explained by the mutant SulA$^-$ being more resistant to colicins than the WT, a behaviour we later observed in response to mitomycin C (Figure 2.15). Certainly, there was no clear advantage to the WT.

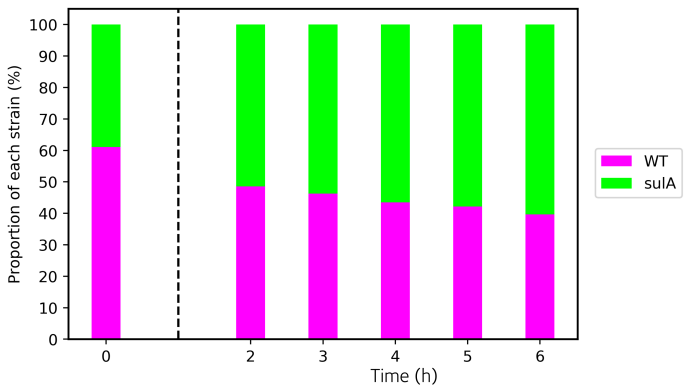

Figure 2.8: Competition between WT and SulA$^-$ and a colicin producer E2 strain in a droplet as described in 2.3.8. Proportion of WT and SulA$^-$ escaping from a droplet containing WT, SulA$^-$ and a colicin producer E2. E2's initial frequency is 1 in 500. The proportion of WT cells outside the droplet decreases over time. n=1 biological replicate.

We therefore next examined the competition at the expanding edge of bacterial colonies on agar as an alternative scenario. Here, we spotted a 1:1 mixture of WT and SulA$^-$ on agar containing colicin E2 and quantified the proportion of each strain in the colony after two days (see Methods 2.3.9 and Figure 2.3.a). To study the effects of colicins, a range of dilutions of cell-free supernatant of the colicin E2 strains were added to agar. Only two of these dilutions allowed growth of cells, 20000-fold and 2000-fold. Any concentration higher than that resulted in either no growth or growth of mutants insensitive to colicin E2 (exposing cells to E colicins frequently selects for BtuB mutants

that do not allow the import of these toxins anymore making them resistant).

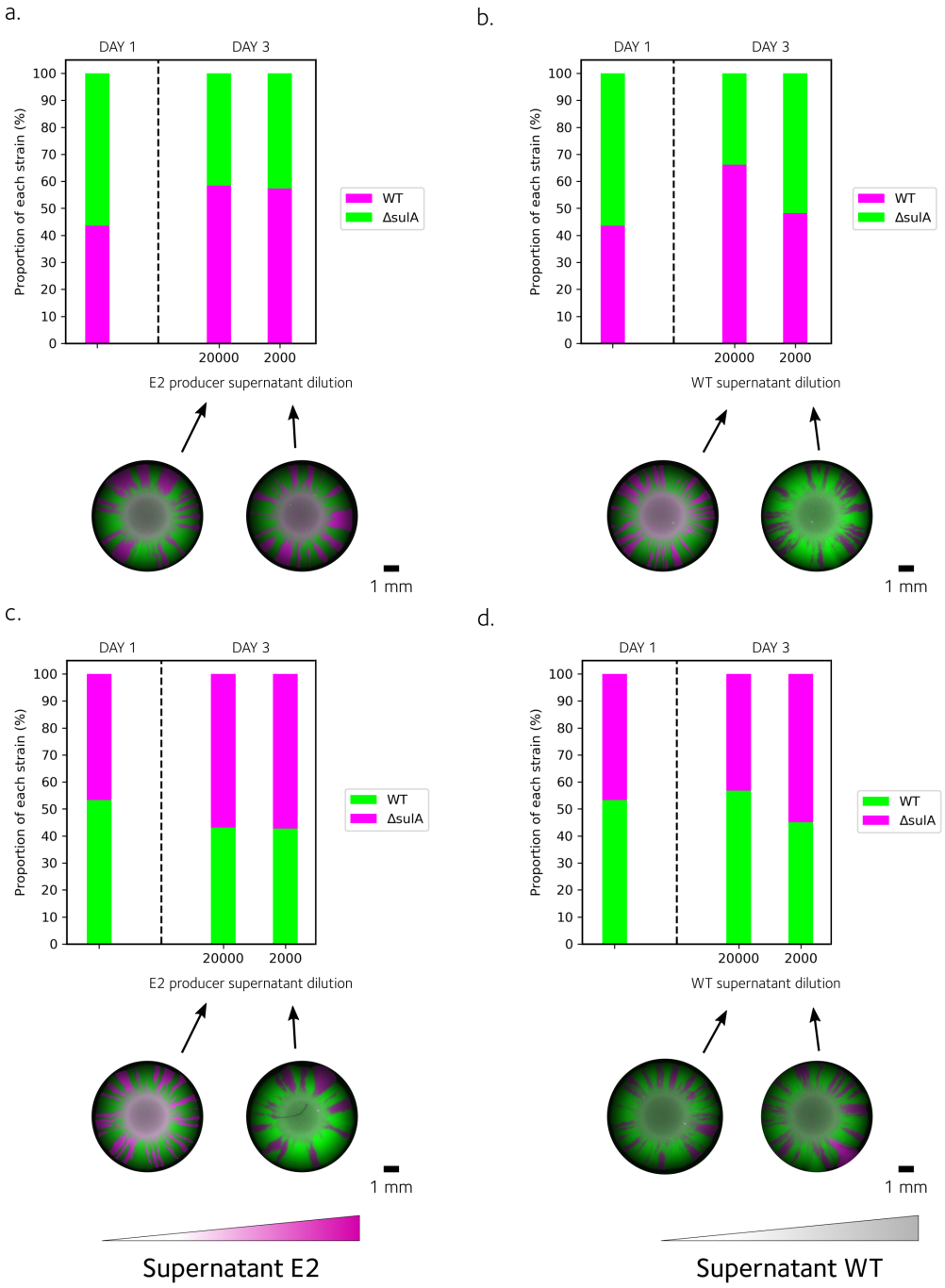

Figure 2.9: Competition between WT and SulA$^-$ on agar containing the supernatant of either a colicin producer (E2) or a non-producer (WT) as described in 2.3.9. Proportion of WT mScarlet-I and SulA$^-$ GFP (**a.** and **b.**) and WT GFP and SulA$^-$ mScarlet-I (**c.** and **d.**) in colonies after 2 days of growth (Day 3) and images of the colonies grown on colicins (E2, **a.** and **c.**) or non-producer supernatant (WT, **b.** and **d.**). Points in the bar charts indicate technical replicates and correspond to the proportion of WT in the colonies. n=1 biological replicate for each condition.

In both conditions, colonies were moderately enriched in the WT strain (Figure 2.9.a). However, the same trend could be observed for colonies grown on some of the plates containing the supernatant of non-producer WT strain, suggesting this result not to be attributable to the presence of colicins (Figure 2.9.b). Moreover, the effect in the presence of the colicin was not consistently robust to swapping the fluorescent markers used in each strain (Figure 2.9.c and d). Overall, the data suggests that the strain carrying the *mScarlet-I* marker were marginally slower growing and that this may explain the moderate differences seen in some conditions. Overall, the results did not support a clear advantage to the WT under conditions where filamentation was occurring.

All in all, none of the results above pointed to WT faring better than its SulA$^-$ counterpart. The likely interpretation of this is that there is simply not enough difference in the filamentation response between the WT and the SulA$^-$ strain to drive a consistent difference in their dispersal behaviour.

2.4.4 Response of inhibitor of division mutants to colicin E2

Since cells treated with colicin E2 and deleted for *sulA* were still able to filament, we searched through the literature for other candidate genes that might serve better to inhibit filamentation in the presence of colicin E2.

Walker et al. (2004) observed significant up-regulation of a number of cryptic prophages genes in response to colicin E3, an enzyme that cuts the 50 bases at the 5' end of the 16S rRNA of *E. coli*, thereby inhibiting translation and as a consequence protein synthesis. This raised the possibility that colicin E2 might similarly also activate ancient mobile elements. Some of these fossil prophages harbour inhibitors of cell division such as *dicB* from Qin (Cam et al., 1988), *kilR* from Rac (Conter et al., 1996), *ymfL* and *ymfM* (also known as sfiC) (Maguin et al., 1986; Ansari et al., 2021) from e14 (Mehta et al., 2004). Moreover, many of the genes carried by cryptic prophages are still functional when present within an ancient prophage (Wang et al., 2010). All of this suggests that such loci could play a role in filamentation in response to other SOS response-triggering

agents, like colicins. Other genes that have been reported to be involved in inhibiting division were also included in our screen. We chose to work with the Keio collection strains (Baba et al., 2006) to quickly assess whether deletion of any of these genes abolished or decreased filamentation (see Table 2.4).

Table 2.4: Loci screened for absence of filamentation

Gene	Mean length (μm)	Standard deviation (μm)	**Source**
WT	5.1	4.6	Burke et al. (2013); Ansari et al. (2021)
ymfL	5.0	4.3	Burke et al. (2013); Ansari et al. (2021)
ymfM	4.3	3.8	Burke et al. (2013); Ansari et al. (2021)
ycjY	4.7	3.7	Burke et al. (2013)
ykfI	4.3	3.6	Burke et al. (2013); Heller et al. (2017)
damX	3.9	3.5	Burke et al. (2013); Khandige et al. (2016)
sulA	3.6	2.6	Huisman et al. (1984); Justice et al. (2006)
dicB	3.7	3.2	Burke et al. (2013); Cam et al. (1988); Wang et al. (2010)
ytfB	4.7	4.0	Burke et al. (2013); Jorgenson and Young (2018)
kil	5.0	3.9	Burke et al. (2013); Conter et al. (1996)
yeeV	5.2	4.6	Tan et al. (2011); Heller et al. (2017)

All strains were studied when growing in the supernatant of the colicin E2 strain, and imaged (see Methods 2.3.10 and 2.3.12). Unfortunately, this revealed that all mutants were still able to filament. Indeed, SulA^{-}, our first target was the mutant exhibiting the

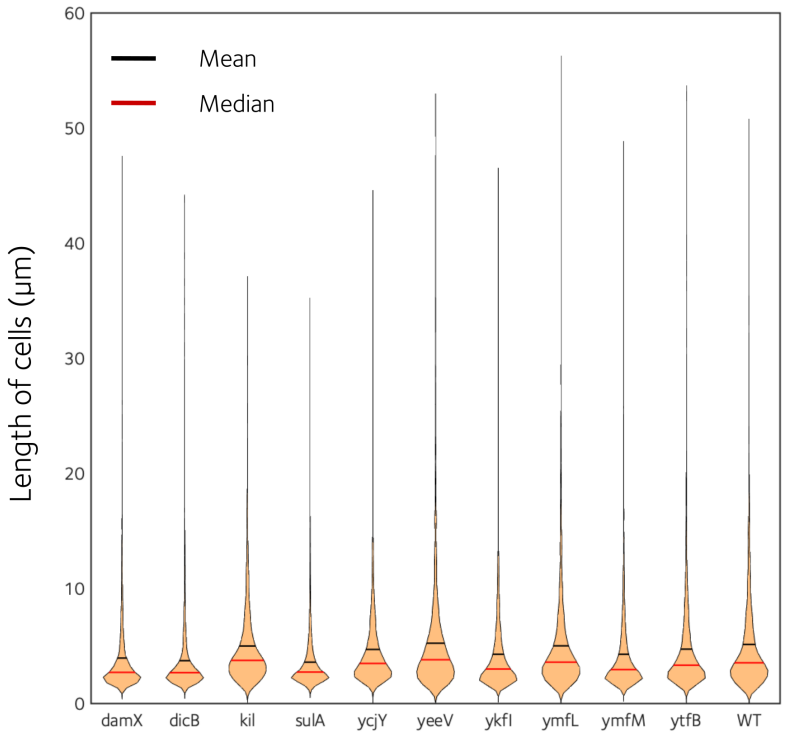

Figure 2.10: Mutants of genes involved in inhibiting division can still filament in response to colicin E2. From left to right, Keio mutants tested: damX, dicB, kil, sulA, ycjY, yeeV, ykfI, ymfL, ymfM, ytfB, BW25113 (WT). Number of cells measured from left to right: damX: 11298, dicB: 9390, kil: 3131, sulA: 13040, ycjY: 7972, yeeV: 3145, ykfI: 7525, ymfL: 3309, ymfM: 5796, ytfB: 6927, WT, 5449. n=1 biological replicate.

most reduced filamentation (mean length: 3.6 μm $\pm$ 2.6 μm as compared to 5.1 μm $\pm$ 4.6 μm for the WT, Figure 2.10 and Table 2.4). DicB$^-$ and DamX$^-$ strains also showed reduced amounts of filamentation (3.7 μm $\pm$ 3.2 μm and 3.9 μm $\pm$ 3.5 μm respectively). Interestingly, Khandige et al. (2016) proposed *damX* as an alternative gene involved in filamentation in the same strain used by Justice et al. (2006). In their *in vitro* assay (flow chamber infection model) and *in vivo*, strains deleted for *damX* were not able to filament. The authors suggest this indicates the existence of multiple strategy to filament during urinary tract infection (UTI). This supports our observation that *sulA* is not the only gene involved in filamentation.

2.4.5 Deleting *btuB* abolishes filamentation in response to colicins and renders this strain resistant

We were unable to find a mutant for a gene involved in inhibition of division that did not filament in the presence of colicins. We therefore changed our approach and turned to a strain resistant to the action of colicins, because such strains are not expected to filament. Specifically, we studied a strain with *btuB* deleted (BtuB$^-$), which encode the receptor used by *E. coli* to import vitamin B12. This receptor is hijacked by E class colicins to bind to cells before import, and its absence prevents E colicins from binding to cells. This effect renders cells lacking BtuB resistant to E colicins (Supplementary Figure A.5) (Housden et al., 2005; Krishna Kumar et al., 2021).

As expected, we found that the BtuB$^-$ cells were shorter than WT cells in the presence of colicin E2 with a mean length of 2.1 μm $\pm$ 0.6 μm against 5.0 μm $\pm$ 3.3 μm for the WT (Figure 2.11). Consistent with no increase in cell length and based on our 5% statistical cutoff for filamentation, we find that filamentous cells represented only 5.1% of the BtuB$^-$ cell population sampled while this population represented 63.80% in the WT.

2.4.6 WT is never at an advantage against BtuB$^-$ even at low concentrations of toxin

We competed this BtuB$^-$ strain, which does not filament in the presence of colicins, against a WT strain that does. An important difference, as compared to the previous experiments, is that the non-filamenting strain is now immune to the effects of the colicin. This means that the experimental design is very conservative in that any advantage to the WT must overcome the intrinsic disadvantage of being susceptive to the colicins. Consistent with this, competing the two strains on agar containing E2 colicin supernatant showed that the BtuB$^-$ strain was at an advantage compared to the WT in most conditions. At best, the WT strain did as well as the BtuB$^-$ strain (Supplementary Figure A.6).

To create a more modest colicin treatment, we adapted the assay and spotted either a

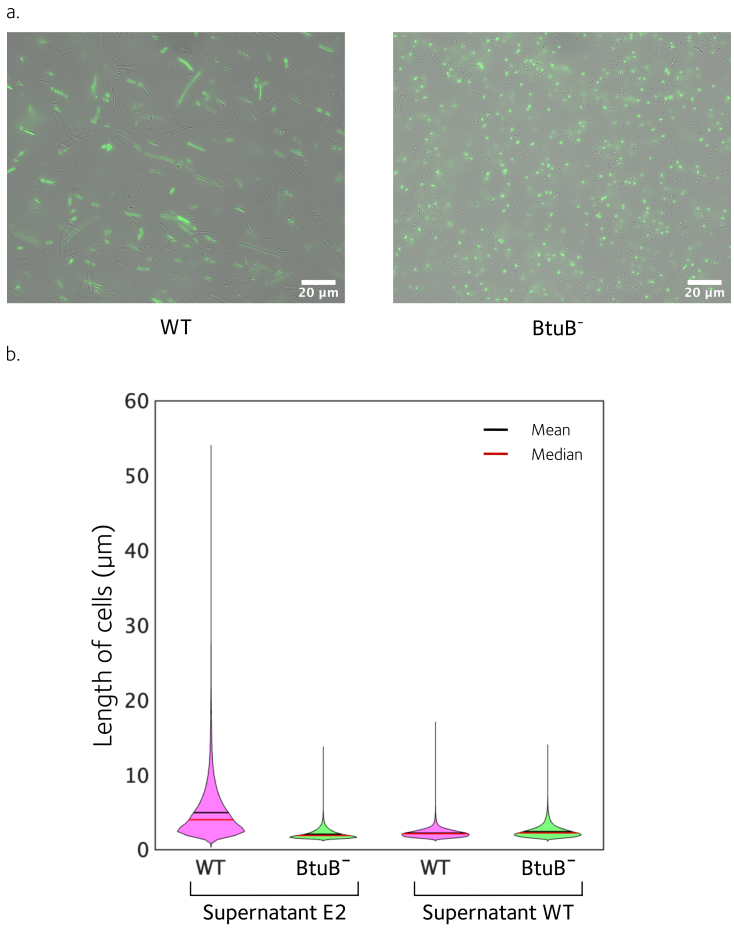

Figure 2.11: Deleting *btuB* abolishes filamentation in response to colicins. **a.** Picture of cells (WT, left and BtuB$^-$, right) treated with the supernatant of a colicin E2 producer for 4 hours in liquid culture. **b.** Quantification of the amount of filamentation in these cultures. Number of cells measured from left to right: WT treated with E2 supernatant, 14294; BtuB$^-$ treated with E2 supernatant, 19364; WT treated with WT supernatant, 52881; BtuB$^-$ treated with WT supernatant, 76029. n=1 biological replicate.

colicin E2 producer or a WT strain (control) in the centre of a Petri dish and a 1:1 mix of WT and BtuB$^-$ at a range of distances from the central colony (Figure 2.3.b). The agar concentration was also decreased to 1% to potentially facilitate filaments progressing on the surface of the plates. The edge of the mixed WT/BtuB$^-$ colonies furthest to the E2 colony looked enriched in WT as the distance decreased between the two colonies until it was so close that only the BtuB$^-$ strain survived. However, a similar trend was observed in colonies growing next to a WT colony (Figure 2.12). Moreover, the same assay carried out with E2 colonies or WT colonies spotted at both OD 10 and OD 0.01 yielded variable results with no clear advantage to the WT.

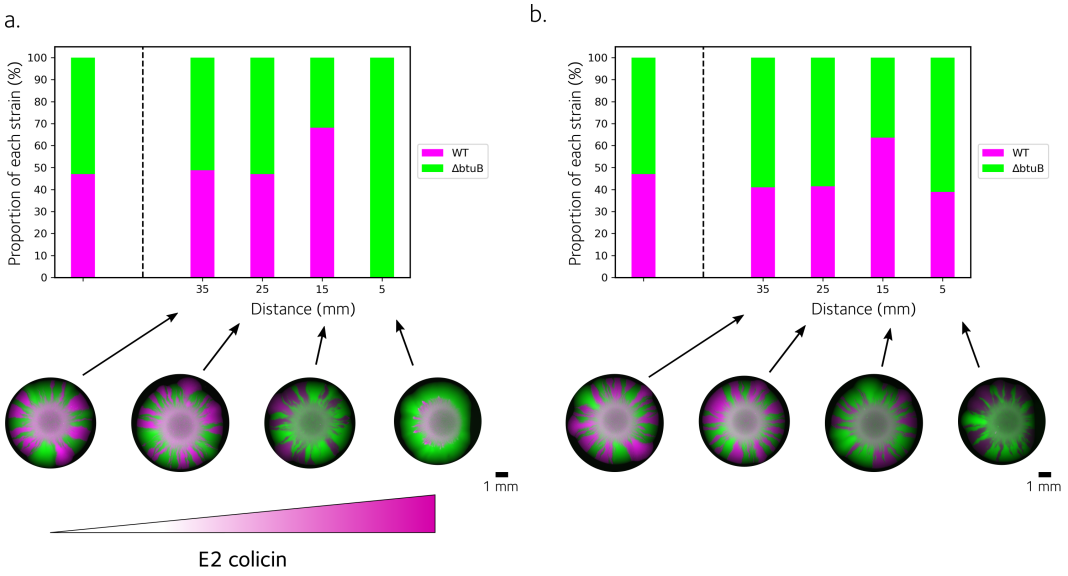

Figure 2.12: Competition between WT and BtuB$^-$ in a colony growing next to a colicin E2 producer or a non-producer WT strain. **a.** and **b.** Proportion of WT and BtuB$^-$ and images of the colonies grown next to a colicin producing colony spotted at OD 1 (left, **a.**) or non-producer WT colony also spotted at OD 1 (right, **b.**). n=1 biological replicate.

As a final test, as done for the SulA$^-$ mutant (see 2.4.3), we studied escape of the WT and BtuB$^-$ strains when competing in an agarose droplet in the presence of an E2 producing strain (Figure 2.13). Similar to the colony assay, at the best, the WT was able to match the mutant but we did not observe any conditions where it consistently did better in the droplets. Overall, we concluded there was no clear evidence of a robust advantage to the WT over BtuB$^-$ under any condition studied. Indeed, across these experiments, we find that the pleiotropic effect of BtuB$^-$ on colicin resistance dominated over any effects of reducing filamentation, which means we were unable to make conclusions based on the latter effect.

2.4.7 *sulA*-mediated filamentation allows cells to better access the colony edge when stressed with mitomycin C

In addition to narrow-spectrum toxins like colicins, *E. coli* may be faced with more broad spectrum toxins. We therefore also tested whether a broad-spectrum toxin could trigger escape by filamentation. We decided to use the drug mitomycin C as this is the

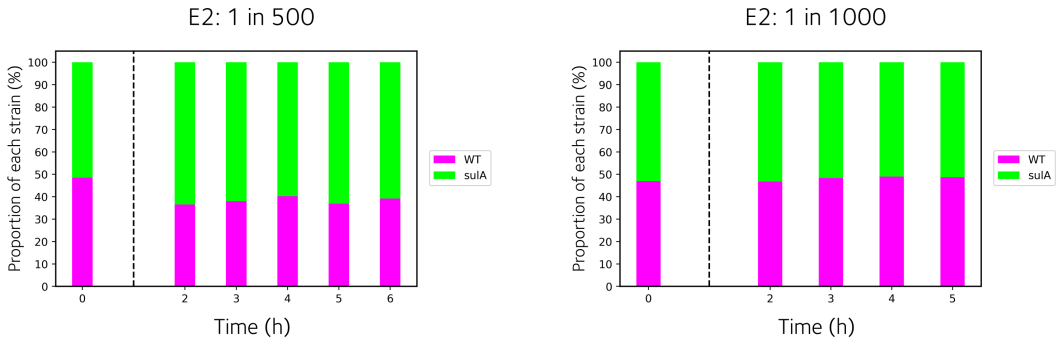

Figure 2.13: Competition between WT and BtuB$^-$ and a colicin producer E2 strain in a droplet as described in 2.3.8. Proportion of WT and BtuB$^-$ escaping from a droplet containing WT, BtuB$^-$ and a colicin producer E2. E2's initial frequency is 1 in 500 on the left and 1 in 1000 on the right. WT and BtuB$^-$ are equally represented at the start. n=1 biological replicate per condition.

standard way to induce the SOS response and it is known to trigger filamentation in an SOS-dependent manner in *E. coli* (Suzuki et al., 1967; Khil and Camerini-Otero, 2002). We found that, in response to mitomycin C too, both WT and SulA$^-$ filamented with a mean lengths of 5.2 μm $\pm$ 2.8 μm and 3.9 μm $\pm$ 1.8 μm respectively. While both filamented, the SulA$^-$ cells were as for colicins, a degree shorter on average than the WT cells. Indeed, the difference between the mean size of two cells types was greater for mitomycin C treatment than for colicins. With colicins, SulA$^-$ cells were on average 84% of WT cell length; with mitomycin C SulA$^-$ cells were on average 75% of WT cell length. Moreover, the variability in cell length was reduced under mitomycin C treatment, indicating that the differences in filamentation between the two genotypes would have more statistical impact in direct competition (Figure 2.14).

As with colicin E2, we decided to compete the WT and SulA$^-$ strains in mixed colonies growing on solid medium containing mitomycin C (see 2.4.2). Microscopy confirmed that filamentation occurred during these experiments at the growing edge (Figure 2.15.a). Consistent with the greater impact of SulA$^-$ on the filamentation phenotype, we found that the WT was better able to reach the edge than the SulA$^-$ strain when mitomycin C was present in the medium. These results were robust to swapping the fluorescent markers between the two genotypes (Figure 2.15.b). This advantage was not due to the WT being more resistant to mitomycin C, because growing both strains on their own on

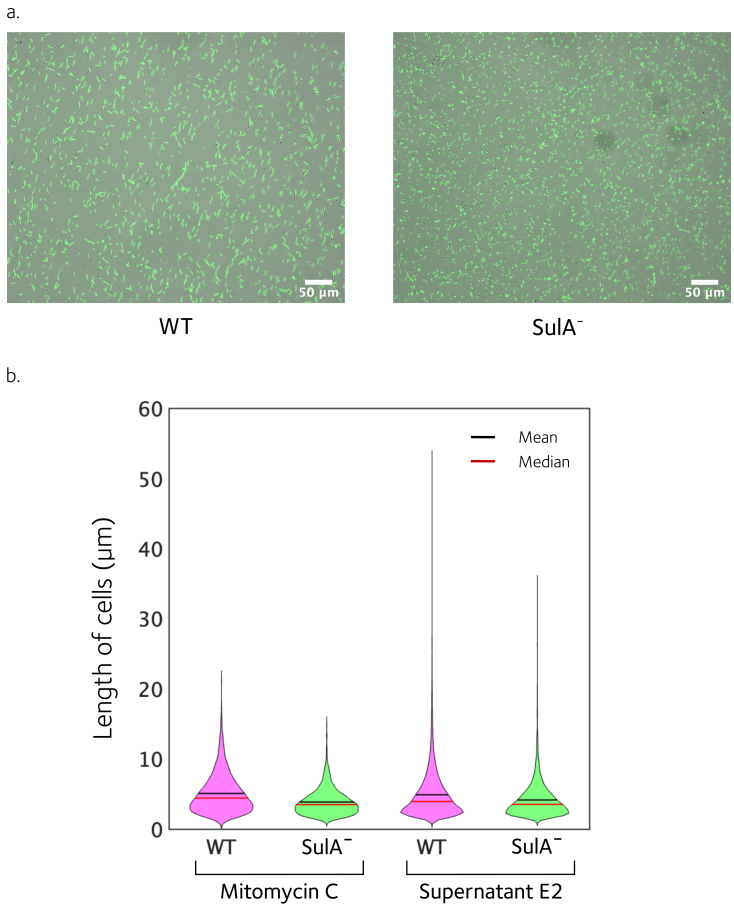

Figure 2.14: Deleting *sulA* reduces filamentation in response to mitomycin C **a.** Picture of cells (WT, left and SulA$^-$, right) treated with mitomycin C for 4 hours in liquid culture. **b.** Quantification of the amount of filamentation in cultures, comparing the effect of mitomycin C with that of colicin E2. Number of cells measured: WT treated with mitomycin C, 2046, SulA$^-$ treated with mitomycin C, 2709, WT treated with E2 supernatant, 14294, SulA$^-$ treated with E2 supernatant (E2 data as shown in figure 2.6). n=1 biological replicate.

mitomycin C did not show a difference in recovered CFU (Supplementary Figure A.7). In fact, at high mitomycin C concentrations, we see evidence that the SulA$^-$ strain is more resistant as it is the only one to survive (Figure 2.15.b, bottom rightmost colony). This latter observation, suggests that this experiment is a conservative test of the impacts of filamentation.

We find evidence, therefore, that filamentation driven by mitomycin C, a broad spectrum antibiotic, allows cells to gain better access to the edge of the growing colonies. The precise mechanism driving this phenomenon remains to be determined. Elongated

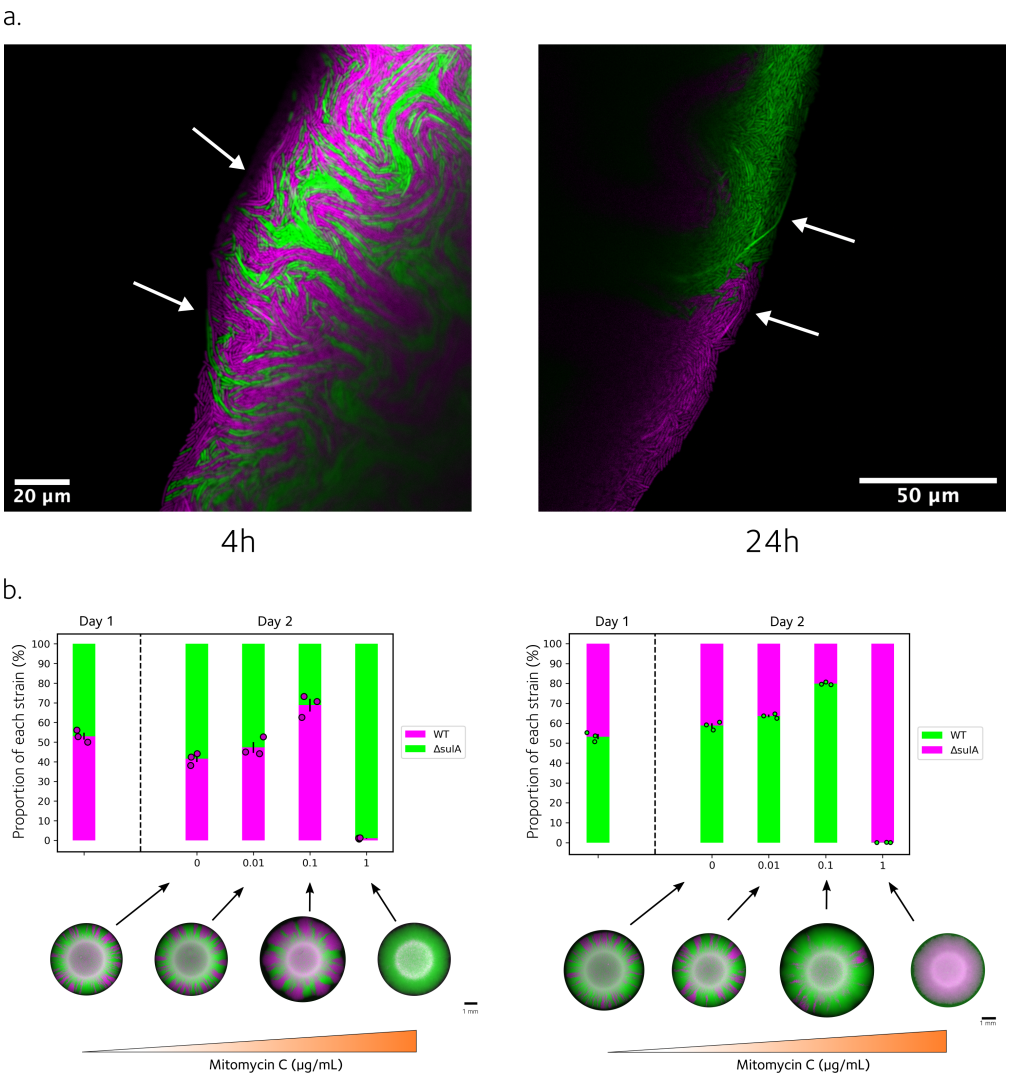

Figure 2.15: Susceptible cells stressed with mitomycin C allow cells to gain preferential access to the edge of the colony. **a.** Edge of a mixed WT/SulA$^-$ colony growing on medium containing mitomycin C (0.01 μg/mL) after 4 hours (left) and 24 hours (right) of growth. WT: purple, SulA$^-$: green. **b.** Proportion of WT and SulA$^-$ strains in colonies grown on agar containing increasing concentrations of mitomycin C. Left: WT mScarlet-I vs SulA$^-$ GFP. Right: WT GFP vs SulA$^-$ mScarlet-I .Points represent biological replicates and the error bars are the standard error of the mean. Bottom: Illustrative images of colonies grown on mitomycin C. Scale bar: 1 mm. A Kruskal-Wallis test was performed on the aggregated data of both sets of fluorescent markers to determine whether the frequency of WT in the colonies grown on different mitomycin C concentrations was different in at least one condition, yielding a p-value < 0.001 (n=6). A Steel-Dwass-Critchlow-Fligner test was then performed on the same data to determine which conditions significantly differed from one another. The p-values for each pairwise comparison between the treatments were as follows: $p_{0\,vs\,0.01} > 0.05$, $p_{0\,vs\,0.1} < 0.05$, $p_{0\,vs\,1} < 0.05$, $p_{0.01\,vs\,0.1} = 0.05$, $p_{0.01\,vs\,1} < 0.05$, $p_{0.1\,vs\,1} < 0.05$, indicating significant differences in the proportion of WT between the control (0 μg/mL mitomycin C) and colonies growing on both 0.1 and 1 μg/mL mitomycin C. n=6 for each comparison. See tests outputs in Appendix A.2.1. n=3 biological replicates for each fluorophore pairs.

cells might be better at accessing the edge due to their shape as simulations have shown (Frost et al., 2018) but it is also possible that they are producing more biomass per unit time than their non-filamentous counter-parts. The clear outcome of these experiments relative to the colicin experiments we believe is due to the better statistical properties of the SulA$^-$ mutation on the filamentation phenotype in the presence of mitomycin C (Figure 2.14). However, there are other differences, including the relative potency of individual toxin molecules. A single colicin molecule is thought to have the potential to kill a cell (Shannon and Hedges, 1967; Francis et al., 2021). This potency may explain the difficulty to find conditions where WT cells were filamenting in a more effective manner than SulA$^-$ cells, but not killed. On the other hand, cells seem to respond more gradually in a dose-dependent manner to mitomycin C with increased filamentation as mitomycin C concentration increased, which is consistent with previous work (Suzuki et al., 1967). This difference may allow cells to better filament and survive the process under mitomycin C, promoting the importance of filamentation as an escape response. Whatever the case, based on this work, we predict that a mutation that is better able to inhibit filamentation will reveal a dispersal benefit to cell elongation under both toxin treatments.

2.5 Conclusion

In this chapter, we investigated whether filamentation could be used as an escape mechanism by cells facing danger in the form of DNA-damaging toxins. We found that deleting *sulA*, a key actor in inhibiting division during the SOS response (which DNase colicins activate (Huisman et al., 1984; Walker et al., 2004; Mavridou et al., 2018)), does not abolish filamentation but rather quantitatively reduces it in response to both narrow-spectrum colicin E2 and broad-spectrum mitomycin C (Figures 2.6 and 2.14). This difference in filamentation provided no advantage to the WT strain in escaping colicins (Figures 2.8 and 2.9). However, this difference in filamentation was sufficient to provide a clear advantage to the WT under mitomycin C treatment (Figure 2.15).

These results add to the growing body of work suggesting filamentation can provide

a fitness benefit by allowing escape from danger. Frost et al. (2018) observed that filamentous cells are enriched at the growing edge of colonies. Confounding factors meant that the authors were not able to experimentally attribute this effect to filamentation. However, modelling work predicted that filamentation can indeed lead to cells accessing the edge of the colony better. Moreover, (Phan et al., 2018) showed that *E. coli* cells treated with minimum concentrations of cell-wall disrupting antibiotic cephalexin could make cells filamentous and highly motile in liquid suggesting filaments can be better at fleeing inhospitable regions. Finally, *in vivo* work also suggests filamentation is a key phenotype for the virulence of urinary tract infections and escape from the immune system (Justice et al., 2006). The present work shows direct evidence of the benefit of filamentation in a competition setting in colonies.

Whether this response has evolved at least in part for the purpose of evasion is hard to tell. On the one hand, filamentation is a striking phenotype and its potential benefits have been shown or speculated on in a multitude of contexts (Justice et al., 2006; Möller et al., 2013; Phan et al., 2018; Frost et al., 2018). On the other hand, this response is also a key step in allowing cells to replicate properly when they are experiencing DNA damage and enhanced evasion may just be a side effect of the DNA repair process. Whatever the case, filamentation has the potential to lead to strong fitness benefits under certain circumstances and this raises the clear possibility that the extent of the response seen is indeed an evolutionary adaptation.

The most dramatic filamentation response we observed was in the agarose droplet assay, where cells could reach one or even two hundred microns long (Figure 2.16). These cells can be seen physically pushing themselves out of the agarose droplets, consistent with them serving as an effective dispersal phenotype. It was this strong phenotype that motivated the large body of work presented herein to directly test for a competitive advantage from filamentation. While this was ultimately hampered by the limited impact of the *sulA* deletion and the other mutations studied, the filamentation phenotype is so clear that it remains suggestive that it can indeed serve to enable escape. This conclusion is further supported by our observation that some of the cells that have filamented have

the ability to remain viable and produce normal cells again, once the stress has been removed (Figure 2.4.c). Why were the filaments so long in the droplet assay, as compared to the liquid assay (Figures 2.7 and 2.6)? We speculate that a key difference was that the droplet assay were run for a longer period (4 h vs 18 h). More generally, the dynamic interplay of toxin production by a competing strain and cell growth in an escaping strain are likely to be critical to both the scale of filamentation and any advantage that it provides.

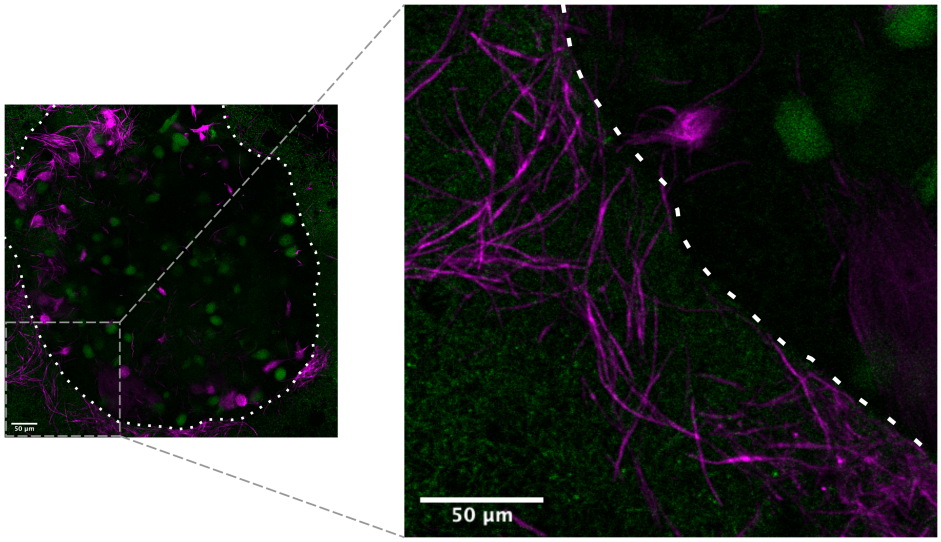

Figure 2.16: Filamentous cells fluxing out of an agarose droplet anchored to a glass surface. Susceptible WT cells (purple) grown in an agarose droplet alongside colicin E2 producer (green). WT cells filament extensively in response to toxin E2. The white dotted line represents the edge of the droplet.

While Justice et al. (2006) concluded that deleting *sulA* was able to completely abolish filamentation *in vivo*, we found this not to be the case in our *in vitro* assays. We found that deleting *sulA* only reduces filamentation. This result suggests that other genes must be involved in inhibiting division in response to colicins. Yet, SulA is the most studied inhibitor of division in *E. coli* and very few studies have investigated inhibition of division by alternative mechanisms. D'Ari and Huisman (1983) had discovered another SOS-induced inhibitor of division called *sfiC* (now *ymfM*), carried by a cryptic prophage. Very recently, Ansari et al. (2021) reported that deleting both *ymfM* and *sulA* leads to decreased filamentation during the SOS response compared to a strain only

deleted for *sulA*. They also noted that while deleting both *sulA* and *ymfM* decreased filamentation, it still did not abolish it completely suggesting yet other mechanisms are involved in filamentation during stress. Other cryptic prophages carry functional inhibitors of division, for example *dicB* from the prophage Qin and *kil* from the prophage Rac, and these might be involved too in inhibiting division during the SOS response. While the effect was again modest, our data (Figure 2.10) showed that a strain deleted for *dicB* filamented significantly less than the WT in response to colicins. This locus may be another one involved in the filamentation response to toxins and more work is clearly needed in this area to understand this response in *E. coli* and other bacteria.

In sum, we have identified a striking filamentation response in *E. coli* in response to the DNase colicin toxins made by some *E. coli* strains. Observation of this phenotype, particularly during growth in agarose droplets, suggest that it can help cells to physically escape from dense bacterial groups under toxin stress. However, our inability to find a mutant that ablated filamentation without pleiotropic effects means we were unable to directly test whether filamentation does indeed result in a competitive advantage. Nevertheless, the more modest phenotype seen under treatment with a drug, was amenable to these tests and here we find evidence that filamentation can enable dispersal and improve the ability to compete for the growing edge. Overall, this work suggests that filamentation can indeed serve to enable dispersal from bacterial communities.

2.6 Bibliography

Ansari, S., J. C. Walsh, A. L. Bottomley, I. G. Duggin, C. Burke, and E. J. Harry (2021, May). A Newly Identified Prophage Gene, *ymfM* , Causes SOS-Inducible Filamentation in *Escherichia coli*. *Journal of Bacteriology 203*(11), e00646–20.

Baba, T., T. Ara, M. Hasegawa, Y. Takai, Y. Okumura, M. Baba, K. A. Datsenko, M. Tomita, B. L. Wanner, and H. Mori (2006, January). Construction of *Escherichia coli* K-12 in-frame, single-gene knockout mutants: The Keio collection. *Molecular Systems Biology 2*(1).

Burke, C., M. Liu, W. Britton, J. A. Triccas, T. Thomas, A. L. Smith, S. Allen, R. Salomon, and E. Harry (2013, April). Harnessing Single Cell Sorting to Identify Cell Division Genes and Regulators in Bacteria. *PLoS ONE 8*(4), e60964.

Cam, K., S. Béjar, D. Gil, and J.-P. Bouché (1988). Identification and sequence of gene *dicB:* translation of the division inhibitor from an in-phase internal start. *Nucleic Acids Research 16*(14), 6327–6338.

Cascales, E., S. K. Buchanan, D. Duche, C. Kleanthous, R. Lloubes, K. Postle, M. Riley, S. Slatin, and D. Cavard (2007, March). Colicin Biology. *Microbiology and Molecular Biology Reviews 71*(1), 158–229.

Chassaing, B. and E. Cascales (2018, April). Antibacterial Weapons: Targeted Destruction in the Microbiota. *Trends in Microbiology 26*(4), 329–338.

Cianfanelli, F. R., O. Cunrath, and D. Bumann (2020, December). Efficient dual-negative selection for bacterial genome editing. *BMC Microbiology 20*(1), 129.

Conter, A., J. P. Bouché, and M. Dassain (1996, September). Identification of a new inhibitor of essential division gene *ftsZ* as the *kil* gene of defective prophage Rac. *Journal of Bacteriology 178*(17), 5100–5104.

D'Ari, R. and O. Huisman (1983, October). Novel mechanism of cell division inhibition

associated with the SOS response in *Escherichia coli*. *Journal of Bacteriology 156*(1), 243–250.

Francis, M.-L. R., M. N. Webby, N. G. Housden, R. Kaminska, E. Elliston, B. Chinthammit, N. Lukoyanova, and C. Kleanthous (2021, November). Porin threading drives receptor disengagement and establishes active colicin transport through *Escherichia coli* OmpF. *The EMBO Journal 40*(21), e108610.

Frost, I., W. P. J. Smith, S. Mitri, A. S. Millan, Y. Davit, J. M. Osborne, J. M. Pitt-Francis, R. C. MacLean, and K. R. Foster (2018, June). Cooperation, competition and antibiotic resistance in bacterial colonies. *The ISME Journal 12*(6), 1582–1593.

García-Bayona, L. and L. E. Comstock (2018, September). Bacterial antagonism in host-associated microbial communities. *Science 361*(6408), eaat2456.

Ghoul, M. and S. Mitri (2016, October). The Ecology and Evolution of Microbial Competition. *Trends in Microbiology 24*(10), 833–845.

Granato, E. T. (2020, August). Quick-n-dirty electrocompetent *E. coli* cells. *protocols.io*.

Heinrich, K., D. J. Leslie, M. Morlock, S. Bertilsson, and K. Jonas (2019, August). Molecular Basis and Ecological Relevance of *Caulobacter* Cell Filamentation in Freshwater Habitats. *mBio 10*(4), e01557–19.

Heller, D. M., M. Tavag, and A. Hochschild (2017, September). CbtA toxin of *Escherichia coli* inhibits cell division and cell elongation via direct and independent interactions with FtsZ and MreB. *PLOS Genetics 13*(9), e1007007.

Hoffman, L. R., D. A. D'Argenio, M. J. MacCoss, Z. Zhang, R. A. Jones, and S. I. Miller (2005, August). Aminoglycoside antibiotics induce bacterial biofilm formation. *Nature 436*(7054), 1171–1175.

Housden, N. G. and C. Kleanthous (2012, December). Colicin translocation across the *Escherichia coli* outer membrane. *Biochemical Society Transactions 40*(6), 1475–1479.

Housden, N. G., S. R. Loftus, G. R. Moore, R. James, and C. Kleanthous (2005, September). Cell entry mechanism of enzymatic bacterial colicins: Porin recruitment and the thermodynamics of receptor binding. *Proceedings of the National Academy of Sciences 102*(39), 13849–13854.

Huisman, O. and R. D'Ari (1981-04-31). An inducible DNA replication-cell division coupling mechanism in *E. coli*. *Nature 290*, 797–799.

Huisman, O., R. D'Ari, and S. Gottesman (1984, July). Cell-division control in *Escherichia coli*: Specific induction of the SOS function SfiA protein is sufficient to block septation. *Proceedings of the National Academy of Sciences 81*(14), 4490–4494.

Hussain, M. and I. Mahmud (2019, July). pyMannKendall: A python package for non parametric Mann Kendall family of trend tests. *Journal of Open Source Software 4*(39), 1556.

Jørgensen, F., P. Stephens, and S. Knøchel (1995, September). The effect of osmotic shock and subsequent adaptation on the thermotolerance and cell morphology of *Listeria monocytogenes*. *Journal of Applied Bacteriology 79*(3), 274–281.

Jorgenson, M. A. and K. D. Young (2018, July). YtfB, an OapA Domain-Containing Protein, Is a New Cell Division Protein in *Escherichia coli*. *Journal of Bacteriology 200*(13), e00046–18.

Justice, S. S., D. A. Hunstad, L. Cegelski, and S. J. Hultgren (2008, February). Morphological plasticity as a bacterial survival strategy. *Nature Reviews Microbiology 6*(2), 162–168.

Justice, S. S., D. A. Hunstad, P. C. Seed, and S. J. Hultgren (2006, December). Filamentation by *Escherichia coli* subverts innate defenses during urinary tract infection. *Proceedings of the National Academy of Sciences 103*(52), 19884–19889.

Khandige, S., C. A. Asferg, K. J. Rasmussen, M. J. Larsen, M. Overgaard, T. E. Andersen, and J. Møller-Jensen (2016, September). DamX Controls Reversible Cell Morphology Switching in Uropathogenic *Escherichia coli*. *mBio 7*(4), e00642–16.

Khil, P. P. and R. D. Camerini-Otero (2002, April). Over 1000 genes are involved in the DNA damage response of *Escherichia coli*. *Molecular Microbiology 44*(1), 89–105.

Kleanthous, C. (2010, December). Swimming against the tide: Progress and challenges in our understanding of colicin translocation. *Nature Reviews Microbiology 8*(12), 843–848.

Krishna Kumar, R., T. A. Meiller-Legrand, A. Alcinesio, D. Gonzalez, D. A. I. Mavridou, O. J. Meacock, W. P. J. Smith, L. Zhou, W. Kim, G. S. Pulcu, H. Bayley, and K. R. Foster (2021, December). Droplet printing reveals the importance of micron-scale structure for bacterial ecology. *Nature Communications 12*(1), 857.

Maguin, E., H. Brody, C. W. Hill, and R. D'Ari (1986, October). SOS-associated division inhibition gene *sfiC* is part of excisable element e14 in *Escherichia coli*. *Journal of Bacteriology 168*(1), 464–466.

Majeed, H., O. Gillor, B. Kerr, and M. A. Riley (2011, January). Competitive interactions in *Escherichia coli* populations: The role of bacteriocins. *The ISME Journal 5*(1), 71–81.

Mattick, K. L., F. Jørgensen, J. D. Legan, M. B. Cole, J. Porter, H. M. Lappin-Scott, and T. J. Humphrey (2000, April). Survival and Filamentation of *Salmonella enterica* Serovar Enteritidis PT4 and *Salmonella enterica* Serovar Typhimurium DT104 at Low Water Activity. *Applied and Environmental Microbiology 66*(4), 1274–1279.

Mavridou, D. A., D. Gonzalez, W. Kim, S. A. West, and K. R. Foster (2018, February). Bacteria Use Collective Behavior to Generate Diverse Combat Strategies. *Current Biology 28*(3), 345–355.

McKenzie, G. J. and N. L. Craig (2006). Fast, easy and efficient: Site-specific insertion of transgenes into Enterobacterial chromosomes using Tn7 without need for selection of the insertion event. *BMC Microbiology 6*(39).

Meacock, O. J., A. Doostmohammadi, K. R. Foster, J. M. Yeomans, and W. M. Durham

(2021, February). Bacteria solve the problem of crowding by moving slowly. *Nature Physics 17*(2), 205–210.

Mehta, P., S. Casjens, and S. Krishnaswamy (2004). Analysis of the lambdoid prophage element e14 in the *E. coli* K-12 genome. *BMC Microbiology 4*(4).

Möller, J., P. Emge, I. A. Vizcarra, P. Kollmannsberger, and V. Vogel (2013, December). Bacterial filamentation accelerates colonization of adhesive spots embedded in biopassive surfaces. *New Journal of Physics 15*(12), 125016.

Oliveira, N. M., E. Martinez-Garcia, J. Xavier, W. M. Durham, R. Kolter, W. Kim, and K. R. Foster (2015, July). Biofilm Formation As a Response to Ecological Competition. *PLOS Biology 13*(7), e1002191.

Parijs, I. and H. P. Steenackers (2018, June). Competitive inter-species interactions underlie the increased antimicrobial tolerance in multispecies brewery biofilms. *The ISME Journal 12*, 2061–2075.

Phan, T. V., R. J. Morris, H. T. Lam, P. Hulamm, M. E. Black, J. Bos, and R. H. Austin (2018, December). Emergence of *Escherichia coli* critically buckled motile helices under stress. *Proceedings of the National Academy of Sciences 115*(51), 12979–12984.

Pugsley, A. P. and M. Schwartz (1983, June). A genetic approach to the study of mitomycin-induced lysis of *Escherichia coli* K-12 strains which produce colicin E2. *Molecular and General Genetics 190*(3), 366–372.

Riley, M. A. and D. M. Gordon (1999). The ecological role of bacteriocins in bacterial competition. *Trends in Microbiology 7*(3), 129–133.

Shannon, R. and A. J. Hedges (1967). Kinetics of Lethal Adsorption of Colicin E2 by *Escherichia coli*. *Journal of Bacteriology 93*(4), 1353–1359.

Simmons, L. A., J. J. Foti, S. E. Cohen, and G. C. Walker (2008, February). The SOS Regulatory Network. *EcoSal Plus 3*(1), ecosalplus.5.4.3.

Storz, G. and R. Hengge (Eds.) (2010). *Bacterial Stress Responses*. John Wiley & Sons, Ltd.

Suzuki, H., J. Pangborn, and W. W. Kilgore (1967, February). Filamentous Cells of *Escherichia coli* Formed in the Presence of Mitomycin. *Journal of Bacteriology 93*(2), 683–688.

Tan, Q., N. Awano, and M. Inouye (2011, January). YeeV is an *Escherichia coli* toxin that inhibits cell division by targeting the cytoskeleton proteins, FtsZ and MreB. *Molecular Microbiology 79*(1), 109–118.

Terpilowski, M. (2019, April). Scikit-posthocs: Pairwise multiple comparison tests in Python. *Journal of Open Source Software 4*(36), 1169.

Tso, W.-W. and J. Adler (1974, May). Negative Chemotaxis in *Escherichia coli*. *Journal of Bacteriology 118*(2), 560–576.

Virtanen, P., R. Gommers, T. E. Oliphant, M. Haberland, T. Reddy, D. Cournapeau, E. Burovski, P. Peterson, W. Weckesser, J. Bright, S. J. van der Walt, M. Brett, J. Wilson, K. J. Millman, N. Mayorov, A. R. J. Nelson, E. Jones, R. Kern, E. Larson, C. J. Carey, İ. Polat, Y. Feng, E. W. Moore, J. VanderPlas, D. Laxalde, J. Perktold, R. Cimrman, I. Henriksen, E. A. Quintero, C. R. Harris, A. M. Archibald, A. H. Ribeiro, F. Pedregosa, P. van Mulbregt, SciPy 1.0 Contributors, A. Vijaykumar, A. P. Bardelli, A. Rothberg, A. Hilboll, A. Kloeckner, A. Scopatz, A. Lee, A. Rokem, C. N. Woods, C. Fulton, C. Masson, C. Häggström, C. Fitzgerald, D. A. Nicholson, D. R. Hagen, D. V. Pasechnik, E. Olivetti, E. Martin, E. Wieser, F. Silva, F. Lenders, F. Wilhelm, G. Young, G. A. Price, G.-L. Ingold, G. E. Allen, G. R. Lee, H. Audren, I. Probst, J. P. Dietrich, J. Silterra, J. T. Webber, J. Slavič, J. Nothman, J. Buchner, J. Kulick, J. L. Schönberger, J. V. de Miranda Cardoso, J. Reimer, J. Harrington, J. L. C. Rodríguez, J. Nunez-Iglesias, J. Kuczynski, K. Tritz, M. Thoma, M. Newville, M. Kümmerer, M. Bolingbroke, M. Tartre, M. Pak, N. J. Smith, N. Nowaczyk, N. Shebanov, O. Pavlyk, P. A. Brodtkorb, P. Lee, R. T. McGibbon, R. Feldbauer, S. Lewis, S. Tygier, S. Sievert, S. Vigna, S. Peterson, S. More, T. Pudlik, T. Oshima, T. J.

Pingel, T. P. Robitaille, T. Spura, T. R. Jones, T. Cera, T. Leslie, T. Zito, T. Krauss, U. Upadhyay, Y. O. Halchenko, and Y. Vázquez-Baeza (2020, March). SciPy 1.0: Fundamental algorithms for scientific computing in Python. *Nature Methods 17*(3), 261–272.

Walker, D., M. Rolfe, A. Thompson, G. R. Moore, R. James, J. C. D. Hinton, and C. Kleanthous (2004, February). Transcriptional Profiling of Colicin-Induced Cell Death of *Escherichia coli* MG1655 Identifies Potential Mechanisms by Which Bacteriocins Promote Bacterial Diversity. *Journal of Bacteriology 186*(3), 866–869.

Wang, X., Y. Kim, Q. Ma, S. H. Hong, K. Pokusaeva, J. M. Sturino, and T. K. Wood (2010, December). Cryptic prophages help bacteria cope with adverse environments. *Nature Communications 1*(1), 147.

Chapter 3

Biofilm formation as a response to bacterial warfare

3.1 Abstract

Most bacteria live in densely populated structures called biofilms. A key inducer of biofilm formation across diverse bacterial species is antibiotics, but the evolutionary basis for this response remains poorly understood. Here we explore the hypothesis that the origin of the biofilm response to antibiotics lies in bacterial competition. Specifically, we explore the idea that bacteria have evolved to increase biofilm formation in response to the incoming toxins of competing strains, because this improves their competitive ability. Using agent-based modelling, we first show that there is advantage to making thicker biofilms during competition because it allows better access to nutrients. We then introduce toxin-mediated warfare into the model, which reveals that thicker biofilms can improve both defence and attack in a focal strain. Our results show how both exploitative and interference competition should select for increased biofilm production when there is competition between bacterial strains. We conclude that biofilm formation evolved, at least in part, to enable bacterial warfare.

3.2 Introduction

One of the key ways that bacteria cope with stressors is to form a dense community known as a biofilm, a group of bacteria often embedded in a gel-like matrix of polymers (Costerton et al., 1995). There is extensive evidence from a wide diversity of bacterial species, both gram-negative and gram-positive, that sublethal concentrations of antibiotics trigger biofilm formation, including pathogens (Hoffman et al., 2005; Chang et al., 2010; Hsu et al., 2011) and non-pathogenic species (Schlomann et al., 2019). Often, these biofilm-associated bacteria display increased tolerance and resistance to antibiotics compared to their free-living counterparts, which can make biofilms a major challenge when trying to eliminate bacteria (Harms et al., 2016; Bernier et al., 2013; Fux et al., 2005).

We are interested in the evolutionary origin of this biofilm response. While the behaviour makes sense in terms of bacteria responding to and surviving antibiotic treatment, it is notable that it is seen very widely across the bacterial phylogeny, and in both pathogenic and non-pathogenic species (Flemming and Wuertz, 2019; Van Acker et al., 2014). This suggests that the response is likely to be the result of a general and ancient evolutionary pressure that predates the relatively short period that we have been treating bacteria with antibiotics (D'Costa et al., 2011). That is, it seems unlikely that the biofilm response to antibiotics evolved for the first time in the context of the clinical use of antibiotics. A clear alternative is that the response evolved in order for bacteria to deal with the toxins and stresses caused by competing strains and species.

The way that different strains of bacteria interact has been the focus of a large body of work in recent years, that studies traits including toxin and siderophore production as social behaviours (West et al., 2007). Over the past 15 years that social evolution ideas (Hamilton, 1964) have been applied to microbes, much of the focus has been on how microorganisms cooperate with one another. For example, many studies have focused on how public goods (e.g. biofilm production, siderophores) can evolve in spite of cheating (West et al., 2007; Nadell et al., 2010; Kümmerli et al., 2015; Irie et al., 2017). Sociomicrobiology resolves this apparent paradox by considering how related

individuals (i.e. individuals that share at minimum an identical genotype at the locus or loci governing the cooperative phenotype) preferentially benefit from the production of public goods. More generally, the field of sociomicrobiology has shown that it is important to study the evolution of microbes both when they are living alone and when they are together with competing genotypes. We follow this here, by asking whether the biofilm response can be explained by the need of a focal bacterial strain to cope with other strains within biofilms.

As we have seen in Chapter 1, a common source of toxins in the microbial world comes from the bacteria themselves (Granato et al., 2019). In fact, a large proportion of our antimicrobial arsenal finds its origins in bacteria (Johnson et al., 1945; Bunch and McGuire, 1953; Umezawa et al., 1957; Sensi, 1983; Nelson and Levy, 2011; Hutchings et al., 2019). How toxin production can evolve in spite of sometimes a tremendous cost to the producers (Granato and Foster, 2020) has also been studied through the lens of social evolution (Gardner et al., 2004; Inglis et al., 2009; Bucci et al., 2011). Here the prediction is that toxin production should be favoured most when producers are in contact with as many non-related cells as possible while still being able to kill (i.e. when the concentration of toxin is high enough to kill in the local neighbourhood). There is increasing evidence that interference competition in bacteria triggers biofilm formation, just like sublethal concentrations of antibiotics do (Oliveira et al., 2015; Lories et al., 2020). A key hypothesis that has emerged from these observations is that, when bacteria detect toxins from competing strains, they have evolved to up-regulate biofilm formation in order to cope with this competition. Indeed, more generally, it has been suggested that bacteria have evolved a wide range of such responses to competition. These responses are proposed to function via the many stress responses that bacteria have to detect incoming harm, serving to up-regulate traits that enable them to both defend themselves and attack their competitors. Such "competition sensing" is known to up-regulate toxin production (Cornforth and Foster, 2013; Mavridou et al., 2018), and a recent study showed that stress responses detect competition and up-regulate biofilm formation in *Salmonella enterica* (Lories et al., 2020).

In spite of the considerable evidence that biofilm formation is key to responding to harmful chemicals, and the growing evidence that this response functions during interbacterial warfare, the evolutionary incentives behind such responses are not well understood. When forming biofilms, bacterial cell density increases relative to planktonic states. A common view is that this serves to enhance bacterial defence via a variety of mechanisms, such as collective detoxification, toxin sequestration and diffusion limitation (Stewart and Franklin, 2008; Flemming et al., 2016). However, another possibility that has yet to be explored is that greater cell densities could also increase offensive capacity since bacteria often use toxins whose effectiveness relies on high producer densities (Chao and Levin, 1981). Did the biofilm response evolve as a defensive mechanism as is often assumed? Or could it be an offensive one that helps warring bacteria counter attack? Does it play another role altogether? These are the questions we set out to answer here.

To do this, we turned to a realistic agent-based model of biofilm formation. These models have proved to be a powerful way to explore the evolution of biofilm formation. They allow a large range of conditions and bacterial phenotypes to be explored in a manner that would be much more challenging with experimental work (Nadell et al., 2013). Agent-based models are particularly suited to our question since they allow one to capture effects emerging at the population level, for example spatiogenic structure (the patterning of different bacterial genotypes within a biofilm) which is known to be central for both biofilms and bacterial warfare (Nadell et al., 2010, 2016; Krishna Kumar et al., 2021). Moreover, they also account for population bottleneck effects (such as genetic drift and segregation) that continuum models overlook. Finally, this class of models have been used extensively to study both biofilms (Xavier et al., 2005; Xavier and Foster, 2007; Schluter et al., 2015) and interference competition (Smith et al., 2020; Bucci et al., 2011; Smith et al., 2020), where they have helped to understand a wide range of features of biofilm evolution (Nadell et al., 2016).

We developed an agent-based model (Smith et al., 2020, 2017, 2020) to study the fitness consequences of the biofilm response. Our model simulates biofilm formation by modulating the amount of cells dispersing so that thicker biofilms detach less and

retain more cells. We modelled bacteria growing alone and in competition with other strains to identify, in each case, the investment in biofilm formation that maximises fitness. We began by studying competition without any toxins in order to get a baseline for any biofilm response, i.e. the change in biofilm production, before toxin-mediated competition is considered. We found that, even here, there can be a major fitness advantage from a biofilm response, both in terms of dispersal and biomass share. This occurs because increasing investment into biofilm can be an effective way to obtain limited nutrients, and thereby outcompete other strains that threaten access to these nutrients. Introducing toxins into the competitions between strains further suggested that making a thick biofilm can help cells to both defend themselves against toxins, and overcome rivals' defences. Our work helps to provide an evolutionary rationale for the biofilm response to toxin-mediated stress caused by competitors: a thicker biofilm can help a strain in both exploitative and interference competition.

3.3 Methods

3.3.1 Agent-based model

Simulations were run using CellModeller 4 (`https://haselofflab.github.io/CellModeller/`), a Python modelling tool that uses OpenCL to efficiently model multicellular bacterial communities (Rudge et al., 2012, 2013), coupled with FEniCS, a tool that numerically solves partial differential equations (PDE) using the finite element method. This hybrid modelling framework was developed by Smith et al. (2017), mirroring previous hybrid approaches, such as BacSim, IDynomics and others (Kreft et al., 1998; Xavier et al., 2005; Lardon et al., 2011).

We here briefly describe the model. A full model description using the O.D.D. protocol (Overview, Design concepts, Details), a general framework to describe agent-based models in a standardised fashion to allow ease of comprehension, use and reproducibility, can be found in Appendix B.1 (Grimm et al., 2010, 2013, 2020).

We modelled a two-dimensional section of a biofilm attached to a solid substratum.

Cells are initially seeded onto the substratum and allowed to grow, divide and detach at the top of the biofilm section. Cells are initially seeded in equal numbers following Gardner et al. (2004) and Inglis et al. (2009) who predicted that equal competitor frequencies favoured toxin production. As described elsewhere, cells within the biofilm are rod-shaped and grow exponentially (Figure 3.1.a) (Rudge et al., 2012; Smith et al., 2020). Division occurs when the initial volume V_0 of the cell reaches $2V_0 + \eta_{volume}$, where η_{volume} is a uniform random noise. The orientation of daughter cells after division is subject to random jitter $\eta_{orientation}$ to simulate noise during the division process. Cell movement is driven by growth and results from cells pushing on one another.

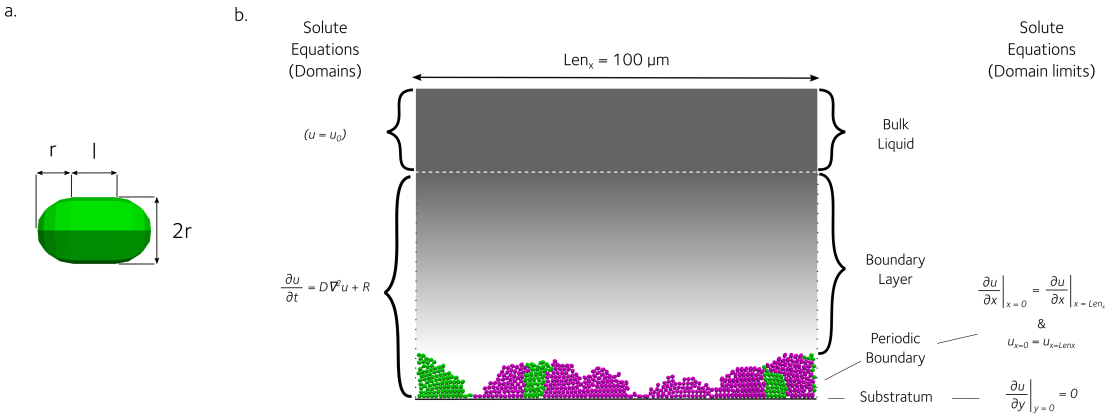

Figure 3.1: Geometry of the virtual cells and environment. **a.** Geometry of a cell composed of a cylindrical midsection of length l and radius r capped by two hemispheres of radius r. **b.** Environment in which the cells have been seeded (random configuration shown here). It is characterised by a base of length Len_x and two lateral periodic boundaries. The nutrient field (grey gradient) is governed by a reaction-diffusion equation within the boundary layer while the concentration in the bulk is constant and equal to u_0. Periodic boundaries imply that the nutrient concentration on the left of the domain equals that on the right.

The cells are assumed to be growing in a static liquid culture. The model can be coupled to a nutrient field to simulate nutrient-limited conditions, as often occur within biofilms (Flemming et al., 2016; Stewart and Franklin, 2008). Nutrients come from the bulk liquid at the top of the box and diffuse through the boundary layer (in which diffusion, rather than advection, governs the transport of solutes). Nutrient availability and rate of consumption then dictate the rate at which bacteria grow following Monod kinetics (Figure 3.1.b) (Monod, 1949; Picioreanu et al., 1998; Nadell et al., 2010).

All cells are implicitly subject to lateral shear forces sweeping over the colony. This causes cells to detach above a certain height from the substratum (Figure 3.2.a). Groups of cells need to be in contact with the substratum to resist shear forces; any group of cells not attached to the substratum is removed (Figure 3.2.b). Cells can invest in extracellular matrix production, paying a growth cost to produce a stronger, thicker biofilm. The cost paid by cells to invest in matrix production increases linearly with biofilm height. This is in contrast to Bucci et al. (2011) and others (Xavier et al., 2005) where cell detachment depends quadratically on height above the substratum. Cells investing less than their neighbours in biofilm formation can benefit from the neighbouring cells' investment.

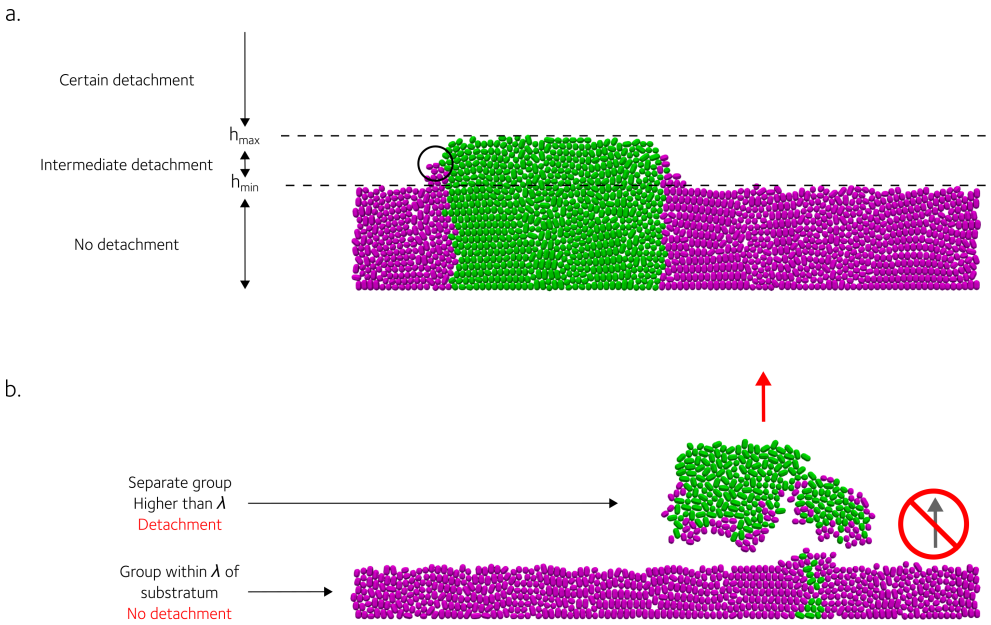

Figure 3.2: Detachment Rules. **a.** Cells below h_{min} do not detach, while cells above h_{max} automatically detach. The detachment height of the purple cells between h_{min} and h_{max} is the average detachment height of the cells within $r_{neighbourhood}$ (black circle) **b.** Group detachment occurs when the lowest cell of a group is higher than λ from the substratum. λ is a small value (here 2.4 μm) representing the minimum distance between groups of cells or groups of cells and the substratum. Below λ, the groups and/or substratum are considered attached.

3.3.2 Simulation protocols

Computation and post-processing

Agent-based simulations were run on a 2019 MacBook Pro laptop computer, with simulations distributed between an Intel® 2.3 GHz 8-Core i9 CPU and an AMD Radeon Pro 5500M compute engine. Simulations data were analysed using custom Matlab® scripts (version R2020a) and visualised using the Paraview software (version 5.9.0) (Ahrens et al., 2005).

3.3.3 Simulation metrics

Simulations are run long enough to reach a population equilibrium. In the case of a single strain biofilm, this means until the box is filled (i.e. cells have reached the detachment height on the whole length of the box). In a two-strain biofilm, this either means until one of the strains has been eliminated from the simulation and the remaining strain has filled the box or, in the case of simulations where the two strains remain, for 10000 steps, which is usually long enough for the volume of each strain to stop changing significantly over time.

Fitness metrics used in past models include the total number of divisions (Frost et al., 2018) and the division rate (Smith et al., 2017). We here chose detachment rate (number of cells of a given strain detaching from the biofilm per unit time, at equilibrium) as our fitness metric. Detachment rate gives a practical way to determine which strain dominates dispersal in a focal patch. Moreover, detachment rate is proportional to the amount of cells (weighted by growth rate) in the simulation so that detachment rate and biomass weighted by growth rate (a more local fitness metric) should align. Overall then, detachment rate reflects a bacterium's reproductive fitness both in the focal environment, and in other environments colonised through dispersal.

3.3.4 Theoretical model for detachment rate

In order to validate the underlying logic behind the optimal biofilm thickness for a single strain, we developed an analytical model for how detachment rate should, in theory, behave given a given cost and height. At equilibrium the number of cells in the biofilm is approximately constant and the number of cells detaching per unit time is approximately equal to the number of cells being born:

$$det_{rate} = \mu N, \tag{3.1}$$

where det_{rate} is the number of cells detaching per unit time, μ is the growth rate and N the number of cells at equilibrium. Both the growth rate and the number of cells at equilibrium depends on the amount invested in biofilm production and therefore on the height of the biofilm. Equation 3.1 is then

$$det_{rate} = \mu(h^*)N(h^*), \tag{3.2}$$

where h^* is the height of the biofilm at equilibrium. This becomes

$$det_{rate} = (1 - ch^*)N(h^*) \tag{3.3}$$

$N(h^*)$, the number of cells in the biofilm at equilibrium can be calculated by multiplying the total area occupied by the biofilm by the proportion of that area actually occupied by cells or the density of the cells (since cells are capsules that do not pack perfectly, the biofilm area is greater than the area of the cells composing it). We then have

$$N(h^*) = h^* w_{box} \rho, \tag{3.4}$$

where w_{box} is the width of the box and ρ is the density of the cells in the box. We know h^* and w_{box} (100 μm) and we can estimate ρ from the simulations.

If we replace $N(h^*)$ in equation 3.3 by 3.4, we then have

$$det_{rate} = (1 - ch^*) * (h^* w_{box} \rho) \tag{3.5}$$

3.4 Results and Discussion

3.4.1 Single-strain biofilms

Our goal is to understand why many bacterial species increase the thickness of their biofilms under toxin-mediated stress. Our key working assumption is that the detection of incoming toxins (or potentially nutrient deprivation) can be used to infer the presence of competing genotypes in the same biofilm. With this response, a strain has the opportunity to optimise biofilm thickness for two different growth conditions 1) growing alone (no competition detected); 2) growing in a mixed biofilm with another genotype (competition detected). For each condition, we ask what biofilm thickness maximises the number of cells produced by a given strain (a proxy of fitness). Our approach, therefore, does not require us to explicitly model the response to toxins itself. Instead, we can simply ask whether optimal biofilm thickness is predicted to change when one moves from condition one (no competition) to condition two (competition).

We began by investigating the optimum biofilm thickness for a strain that is growing alone. We assume that making a thicker biofilm comes at an increasing cost, which is consistent with the need for the release of polysaccharides, proteins and DNA to effectively attach cells within a biofilm (Flemming and Wingender, 2010; Dragoš et al., 2018; Dieltjens et al., 2020). Specifically, we assumed that biofilm production is a costly mechanism, where the cost increases linearly with height. We then ran single strain simulations under conditions of unlimited nutrients until each genotype (i.e. each level of investment in biofilm production) had reached its set biofilm thickness (Figure 3.3). These simulations revealed that, under the assumption that a thicker biofilm carries more cost, an intermediate biofilm thickness is the way for a strain to produce the most cells from a biofilm. A thicker biofilm contains more cells, which means more cells can potentially divide per unit time. This cell number effect favours making thicker biofilms

but, eventually, the cost of making thicker biofilms outweighs this benefit, leading to the optimum at intermediate thickness.

We devised a simple analytical model to evaluate this interpretation (Methods 3.3.4). This model predicted, as expected, that there is an intermediate investment at which dispersal per unit time from a biofilm is maximised (Figure 3.3.c red curve), which proved to be a good quantitative fit to the simulation results (Figure 3.3.c black curve). We also looked at another fitness metric, volume (i.e. biomass) weighted by growth rate, to validate our results. Indeed, the net production of offspring may depend on both a strain's ability to colonise other patches through dispersal but also on the strain's ability to dominate a local patch. The results for the volume weighted by growth rate yielded mostly similar results (Supplementary Figure B.4). This is because the number of cells a biofilm can disperse is dependent on the number of cells it can produce and is therefore proportional to biomass weighted by growth rate.

These first simulations, therefore, provide an estimate of optimal biofilm thickness for a single strain growing alone. However, their applicability to real biofilms is limited by the assumption of unlimited nutrient access. Rather, most microbes are expected to commonly experience nutrient limitation (Aldén et al., 2001; Cunrath and Bumann, 2019). Moreover, nutrient gradients often form in biofilms due to reduced diffusivity and consumption of the nutrients by the cells closest to the nutrient source (Stewart and Franklin, 2008; Flemming et al., 2016). In some cases, this severely limits nutrient access for all but those cells closest to the nutrient source (Figure 3.1) (Mitri et al., 2016).

Incorporating this well-documented effect into the simulations via explicit simulation of nutrient diffusion and their consumption by cells, revealed again that we can identify an evolutionary optimum biofilm thickness. However, importantly, this optimum is much thinner than for the case without nutrient limitation. Why is the optimum biofilm so much thinner? The reason is that, with nutrient limitation, only a relatively narrow band of cells at the surface of the biofilm are able to grow and divide. This growing-edge effect is well known from previous simulations and experiments with bacteria (Kim et al., 2014; Mitri et al., 2016; Nadell et al., 2010). This effect means that making a

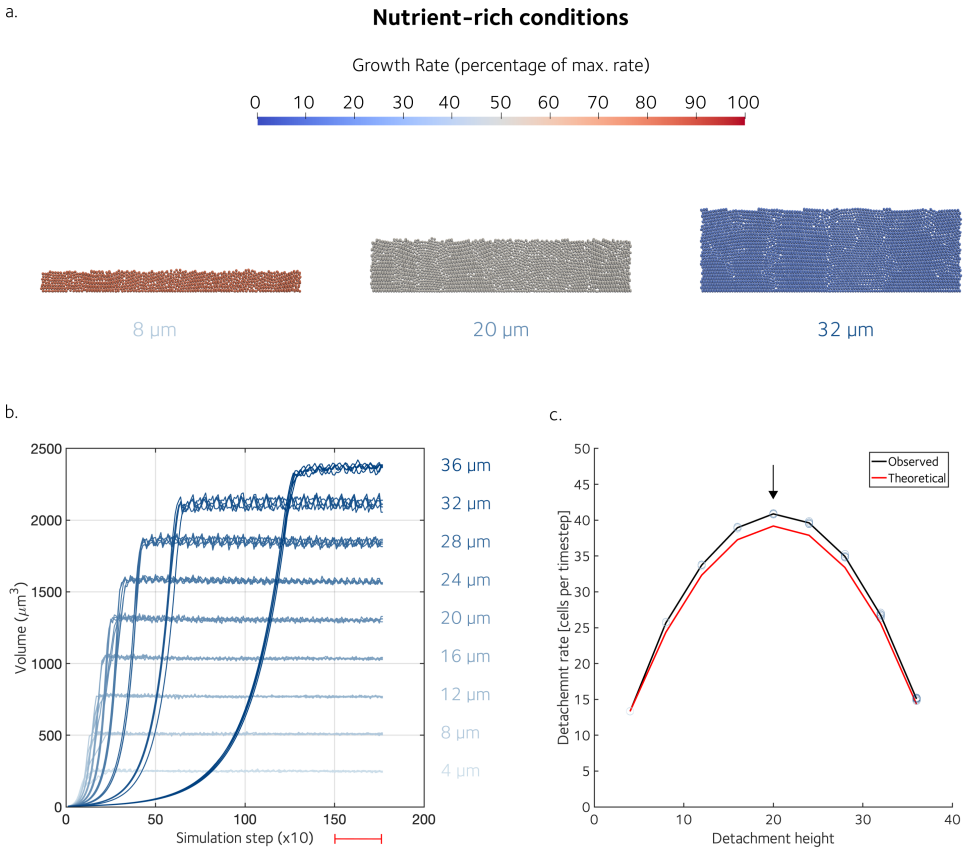

Figure 3.3: Single strain fitness optimum — nutrient-rich conditions. **a.** Illustrative snapshot of biofilms of different thickness coloured by growth rate. **b.** Total volume of biofilm of different thickness over time. The red bar indicates the window on which the average detachment rates were calculated **c.** Detachment rate of biofilm as a function of thickness. The black arrow points to the optimal detachment height. n=5 simulations for each condition.

thicker biofilm no longer increases the number of growing cells in the same way. Once the biofilm is thicker than the growing edge, no new dividing cells are added by making the biofilm thicker. For this reason, the optimum biofilm thickness is much lower than with unlimited nutrients throughout a biofilm (Figure 3.4 vs 3.3).

To evaluate this effect further, we modified the analytical model used for the unlimited nutrient case to assume that only the top most layer of cells can grow, where the thickness of this layer was estimated from the simulations (8 μm, Figure 3.4.a). As for the simulations, this model predicts that the optimal biofilm thickness is equal to the thickness of the growing edge (i.e. 8 μm). This result is in agreement with the idea that, beyond this thickness, there is no benefit to making a thicker biofilm because it will not

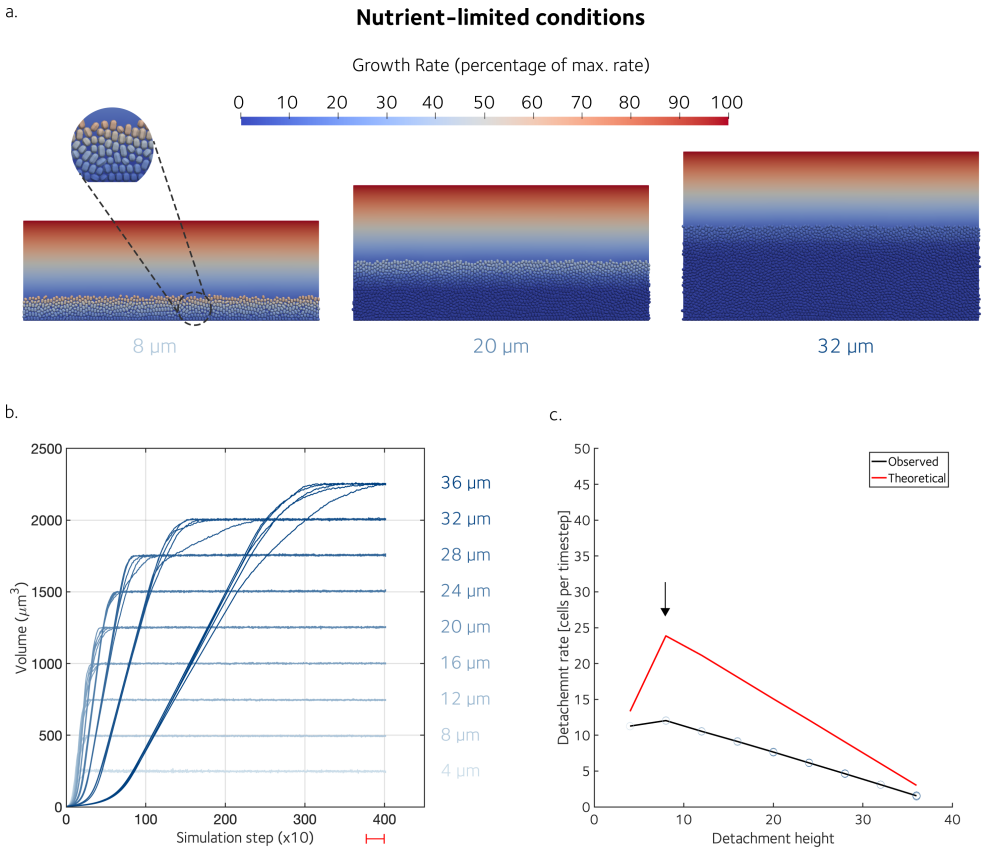

Figure 3.4: Single strain fitness optimum — nutrient-limited conditions. **a.** Illustrative snapshot of biofilms of different thickness coloured by growth rate. The nutrient field in each simulation is represented by a gradient from red (nutrient-rich) to blue (nutrient-poor) **b.** Total volume of biofilm of different thickness over time. The red bar indicates the window on which the average detachment rates were calculated **c.** Detachment rate of biofilm as a function of thickness. The black arrow points to the optimal detachment height. n=5 simulations for each condition.

increase the number of growing cells. While the same optimal thickness is predicted by both the analytical and the simulation models, the detachment rates differ between the analytical model and the simulations' outputs (Figure 3.4.c). This difference comes from the fact that the analytical model considers all cells in the top-most layer to be growing at the same maximum rate. In the simulations, nutrient access within the growing layer is inhomogeneous, with cells lower down growing slower than those closer to the biofilm surface (Figure 3.4). This effect results in the analytical model overestimating overall growth rates, but it nevertheless captures the qualitative properties of the simulations well.

3.4.2 Exploitative competition

We next investigated the optimal biofilm height of strains when they are in competition with another genotype. We began by studying pure exploitative competition for space and nutrients, such that competition is not influenced by the effects of toxins. This allows one to identify any effects of biofilm thickness on exploitative competition before the effects of toxins are introduced. We first looked at the nutrient-rich scenario in which cells only compete for space (Figure 3.5.a). We have seen in the previous section that the optimum biofilm height for a single strain is intermediate at 20 μm high for our standard parameters (Figure 3.3). How does this compare to a case where two strains are in competition? We can answer this by studying the outcome of a large number of pairwise competitions, where we systematically vary the maximal thickness of the biofilm made by the two strains. If, for example, we compete thicknesses of 16 μm against 20 μm, and 20 μm against 24 μm, one can see that a biofilm thickness of greater than 20 μm will win the contest, while a strain investing less loses (Figure 3.5.b). Thus, it seems that thicker biofilms would indeed be favoured during competition than when alone. This effect can be attributed to thicker biofilms being better able to gain space laterally than their competitors (Supplementary Figure B.5.a). However, this effect is only marginal. Competing a strain investing to grow at 24 μm against one growing at 28 μm reveals that the 24 μm strain wins (Figure 3.5.b, bottom row), which is predicted to be the evolutionary stable strategy under our modelling assumptions.

We asked whether this prediction was affected by the particulars of the competition scenario that we modelled. For example, initial cell density can be an important determinant of evolution in bacterial biofilms for some traits, but a sweep of cell density revealed that optimal biofilm thickness is not strongly affected by the initial cell density (Appendix B.6). Another factor known to often be important is spatiogenetic structure. In the simulations so far, the two genotypes were placed in single genotype groups side by side as an initial condition (high spatiogenetic structure). We can abolish this spatial structure by initially seeding cells at random in space with respect to their genotype. This change also has a small effect on the optimum biofilm thickness, such that now

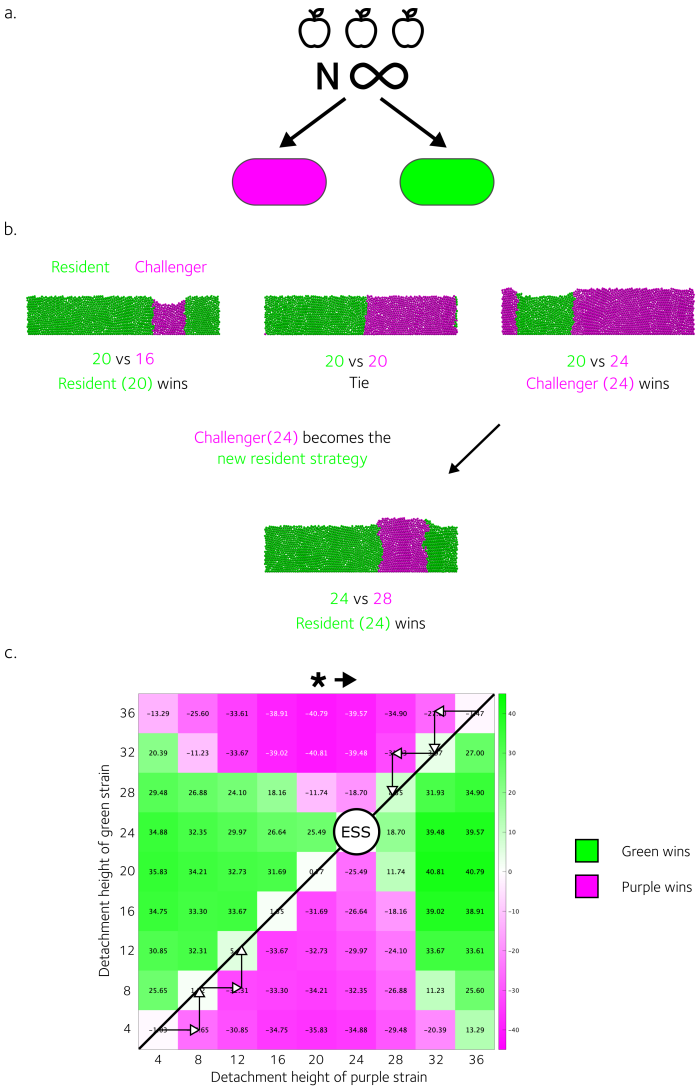

Figure 3.5: Optimal detachment height in a 2-strain exploitative competition in nutrient-rich conditions. **a.** Schematic of the competition. Purple and green cells have infinite nutrient (N∞) and only compete for space. **b.** Snapshots of simulation competing 2 strains with different detachment heights against one another. Top row from left to right: 16 μm vs. 20 μm, 20 μm vs. 20 μm, 20 μm vs. 24 μm. Bottom row: 24 μm vs. 28 μm. **c.** Heatmap of the net detachment rate of the green strain for intermediate initial density (6 vs. 6 cells). Arrows illustrate the progression of biofilm detachment heights converging on an evolutionary stable strategy height (ESS, white circle). The asterisk indicates the single-strain optimum and the arrow the shift in optimal strategy between single- and two-strains biofilms. n=3 simulations per case. Only the simulations on and above the black diagonal were run. The values were then mirrored for the bottom half as the cases are symmetrical. Apple image: Flaticon.com

the ESS lies within the 20 to 24 μm window (Supplementary Figure B.7). The slight decrease in the ESS can be explained by the fact that the slower growing strain (i.e.

the one investing more in biofilm formation) is now more at risk of being pushed out of the biofilm by surrounding faster growing cells of the other genotype. This effect can be observed when competing two strains that have the same detachment height but different growth rates (Supplementary Figure B.5.b). The increased likelihood of being excluded from the biofilm when growing slower therefore translates in a slightly lower optimum on average. But neither spatiogenetic structure nor initial cell density proved to be important factors for the ESS.

However, so far we have not considered nutrient limitation, which as discussed above is expected to be typical in many biofilms. Recall that for strains growing alone, the optimum biofilm thickness is much thinner under nutrient limitation, at around 8 μm for our parameters. What then happens to this optimum when there is competition with another strain? When we compete our strain optimised for detachment in the single strain case (optimum at 8 μm) against strains that invest less (4 μm) or more (12 μm) in biofilm formation (Figure 3.6.b, top row left and right respectively), we see that once again a thicker biofilm producer performs better. However, in contrast to the unlimited nutrient case where the impact of this effect was marginal, here we find that the benefit continues as we consider thicker and thicker biofilms (Figure 3.6.b, bottom row). As before, we can use the individual competitions to determine which height is predicted to be the evolutionary stable strategy (ESS) (Figure 3.6.c).

This approach reveals that the ESS for the co-culture case is much greater than for a single strain growing alone: the optimum detachment height trebles. What is driving this effect under nutrient limitation? The benefit of growing taller and accessing nutrients here strongly outweighs the cost of producing a thicker biofilm such that cells investing more than the single cell optimum grow better. This is the case up to a point (24 μm), beyond which accessing nutrients does not allow a faster growth owing to the cost of biofilm production. This means that a significant proportion of the cells' growth rate is invested in building a taller biofilm structure just to access nutrients to the detriment of cells at the bottom. Thus, in a scenario where biofilm production is costly and nutrients are limited, competing with another strain selects for thicker biofilms, which

is in agreement with previous models where biofilm thickness was modulated via the secretion of extracellular polymeric substances (Xavier and Foster, 2007).

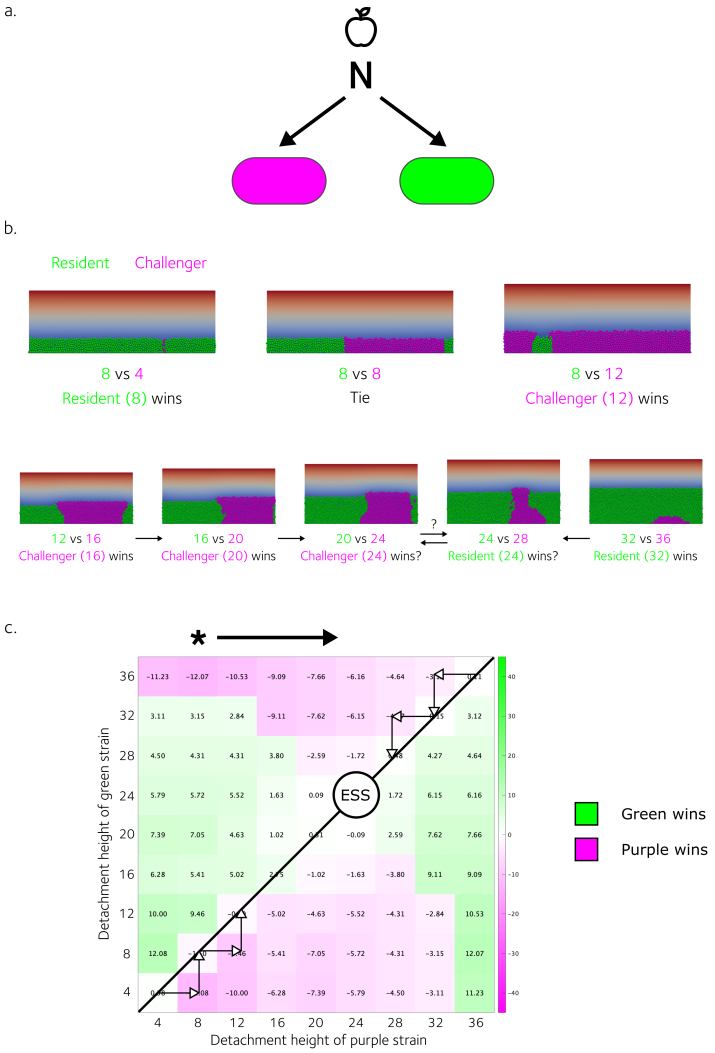

Figure 3.6: Optimal detachment height in a 2-strain exploitative competition in nutrient-limited conditions. **a.** Schematic of the competition. Purple and green cells have limited nutrient (N) and compete for space and nutrient. **b.** Snapshots of simulations competing 2 strains with different detachment heights against one another. Top row from left to right: 4 μm vs. 8 μm, 8 μm vs. 8 μm, 8 μm vs. 12 μm. Bottom row from left to right: 12 μm vs. 16, 16 μm vs. 20 μm, 20 μm vs. 24μm, 24 μm vs. 28μm, 28 μm vs. 32μm, 32 μm vs. 36μm. **c.** Heatmap of the net detachment rate of the green strain for intermediate initial density (6 vs. 6 cells). Arrows illustrate the progression of biofilm detachment heights converging on an evolutionary stable strategy height (ESS, white circle). n=3 simulations per case. The asterisk indicates the single-strain optimum and the arrow the shift in optimal strategy between single- and two-strains biofilms. Only the simulations on and above the black diagonal were run. The values were then mirrored for the bottom half as the cases are symmetrical to the ones above the diagonal. Apple image: Flaticon.com

3.4.3 Patch lifetime influences optimal biofilm height

We have so far explored a situation in which strain fitness, measured as dispersal per unit time, is evaluated only once biofilms have been allowed to reach their full thickness. At this equilibrium state, either one strain has eliminated the other or, if the two strains persist, in most cases the fraction of each strain in the biofilm does not change significantly. This situation reflects relatively long-lived environments. However, in some situations, local patches might experience disruptions and therefore not be allowed to reach equilibrium. One can imagine then that short-lived patches might favour thinner biofilms, since these have the faster population growth rates and can start dispersing cells at early time points. Can we then see a shift in the ESS towards thinner biofilms when we consider shorter-lived patches?

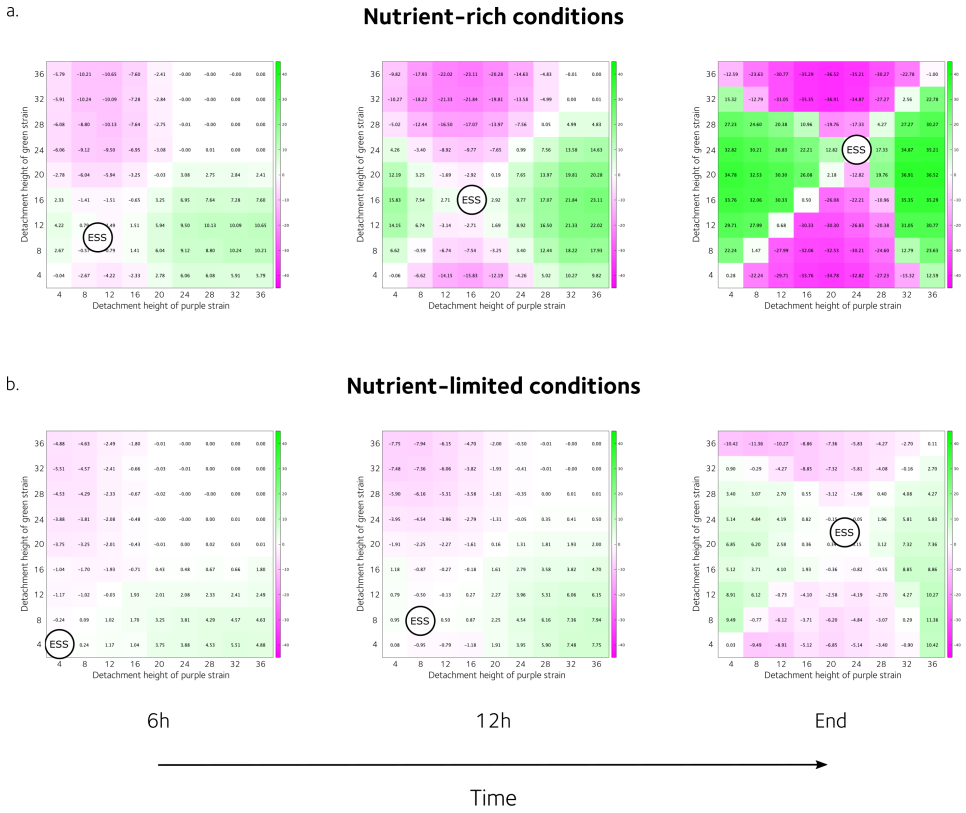

Figure 3.7: Optimal detachment height in a 2-strain exploitative competition as a function of patch life-span. **a.** Nutrient-rich conditions. **b.** Nutrient-limited conditions. Evolutionary stable strategy height (ESS, white circle). n=3 simulations per case. Only the simulations on and above the black diagonal were run. The values were then mirrored for the bottom half as the cases are symmetrical to the ones above the diagonal.

Consistent with this expectation, Figure 3.7 shows that for very short-lived patches (6 hours, first from the left), the optimal height is decreased for both nutrient-rich conditions and nutrient-limited conditions. As the lifespan of the patch increases so does the optimal biofilm height until equilibrium is reached and the optimum matches the one defined in section 3.4.2. Moreover, as seen previously, the segregated configuration favours slightly thicker biofilms throughout at all time points compared with a random configuration (Supplementary Figure B.8). Going forward, we will focus on longer lived patches where dispersal rate, at equilibrium, is key to fitness. However, we note that changing the duration that patches last can impact predictions.

3.4.4 Is biofilm formation a way to enhance toxin use?

While biofilms are often considered as a defensive mechanism that hampers the effects of toxins, the effects of biofilm formation on toxin production have received little attention. However, there is a growing body of work that shows that antimicrobials are indeed produced and used within biofilms (Kobayashi and Ikemoto, 2019; Rendueles et al., 2014). Being surrounded by clonemates in a biofilm offers the possibility of mounting a more effective attack using toxins: with more toxin producers contributing, greater and more effective toxin concentrations can be produced. Here, we explore the idea that building a thick biofilm could be a way for bacterial cells to build up a critical density of cells and produce enough toxin to wipe out competitors. We focus on the case where nutrients are limited within biofilms, given this is expected to be the most typical condition in nature.

Exploratory simulations revealed, as expected, that the effects of toxins in the simulations depend strongly upon toxin potency (the toxin concentration required to kill competitors, governed by the lethal toxin concentration parameter $u_{T_{crit}}$) and toxin production rate (the amount of toxin produced per unit time, governed by the parameter $D_{T,P}$). When toxins are not very potent ($u_{T_{crit}} = 6.5$), they have no impact in the simulations and the outcomes converge on the results without toxins (above). When toxins are very potent ($u_{T_{crit}} = 0.5$) and toxin production is high ($D_{T,P} = 0.1$), the

toxin producer rapidly wins across all biofilm thicknesses, and the simulations converge on the single strain optima (Supplementary Figure B.9).

At high toxin potencies ($u_{T_{crit}} = 0.5$) and low toxin production rates ($D_{T,P} = 0.01$) - when toxins are effective but not devastating - we see an interplay between biofilm thickness and the use of toxins (Figure 3.8). However, even here, the predicted optimal biofilm thickness in competition remains relatively thin and only slightly thicker than the single strain case. Note that here we are considering an asymmetrical competition in the sense that one strain has a toxin and the other strain does not. Unlike the previous analyses, the optimal biofilm thicknesses of the two strains may no longer be equal. For our toxin producer, therefore, we need to ask: what is the biofilm thickness that maximises reproductive output given the best response by the non-producer? The prediction is a relatively thin biofilm (12 μm for our parameters).

Why is the predicted optimum biofilm thickness relatively thin in this case? The reason is that the toxin producer need only make a biofilm that is thick enough to make effective use of its toxins. Meanwhile, thicker biofilms merely achieve competitor elimination at higher cost, on account of their greater investment in biofilm production. This characteristic thickness is closely linked to the thickness of the growing edge under nutrient limitation. The reason for this is that we assume that toxin production is tied to nutrient availability so that cells that have limited access to nutrients have correspondingly limited toxin production capabilities (Bucci et al., 2011). The result is that the optimum biofilm thickness to use toxins is predicted to be a relatively thin biofilm that can outcompete any biofilm thickness of a sensitive competitor. Thicker biofilms merely achieve competitor elimination at higher cost, on account of their greater investment in biofilm production.

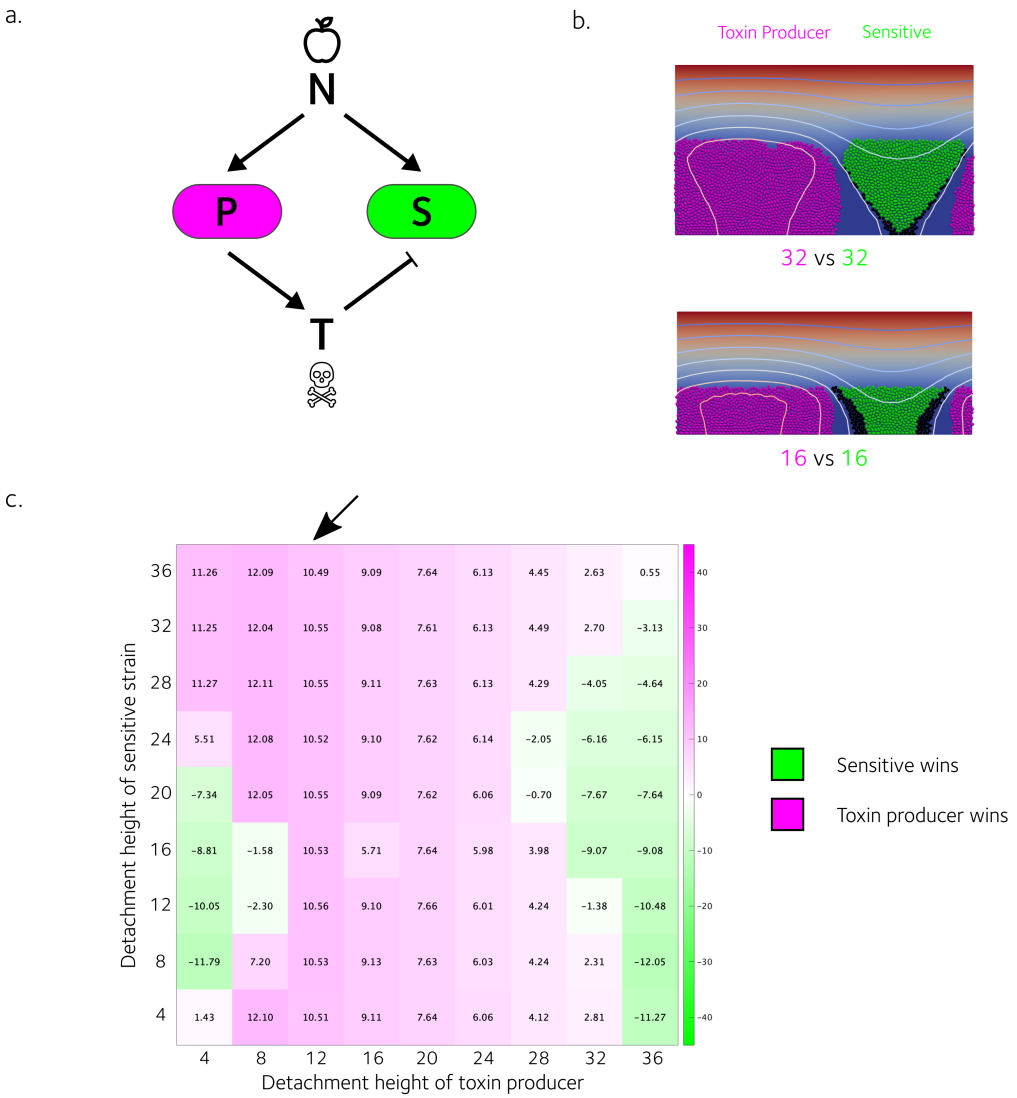

Figure 3.8: Optimal strategy for a toxin producer in competition with a sensitive strain — nutrient-limited conditions. **a.** Schematic of the competition. Toxin-producing cells (purple) and sensitive (green) cells have limited nutrient (N) and compete for space and nutrient. The toxin produced by the purple strain kills the green sensitive cells above a certain threshold. **b.** Snapshots of simulations competing a toxin-producing strain (purple) and a sensitive strain (green) for different heights. The isocontour lines represent gradients of toxin in the biofilm **c.** Heat map of a two-way competition in which one strain produces a toxin and another is sensitive to it and in which biofilm detachment height is varied. The optimal strategy for a toxin producer is indicated with an arrow. n=3 simulations per case. Toxin parameters used: $u_{T_{crit}} = 0.5$ (high potency) and $D_{T,P} = 0.01$ (low toxin production). Apple and crossbones skull images: Flaticon.com

3.4.5 Is biofilm formation a way to defend against toxins?

The previous section suggests that making a thick biofilm is not a means to help toxin producers outcompete sensitive strains. However, this analysis did not consider the possibility that making a biofilm can also help a sensitive strain better resist the attacks of a toxin producing strain. Experimental evidence shows that toxins can be absorbed by binding to receptors at the surface of cells or degraded by enzymes (e.g. β-lactamases) produced by non-producing cells (Frost et al., 2018; Inglis et al., 2013; Krishna Kumar et al., 2021). We, therefore, wanted to include this effect in our modelling and studied the effect of allowing the sensitive cells to act as toxin sinks, which remove toxins produced by their competitors, a feature absent from earlier models such as the one presented in Bucci et al. (2011). The idea is that, when more sensitive cells are in the biofilm, more toxin will be removed, potentially giving thicker biofilms a better ability to resist attacks.

We explored the effect of changing the rate at which toxins are removed by cells in the biofilms (Figure 3.9). With no removal, the analysis is the same as the previous section where the optimal biofilm height for a toxin producer is 12 μm. At this height, the sensitive strain is effectively eliminated from the biofilm, no matter the thickness it makes. As a result, there is predicted to be no natural selection on the sensitive strain to adopt any particular biofilm thickness. Moreover, even if we assume that the toxin producer is sometimes slightly off its optimum, the only evolutionary response predicted in the sensitive strain is to also make a relatively thin biofilm i.e. if the toxin producers make an 8 μm biofilm, the sensitive strain will make a 12 μm biofilm.

Introducing the possibility of defence via removal has a large effect on these predictions for both of the strains. When sensitive cells can remove toxin at a rate 10% that of the toxin production rate, making a thicker biofilm is favoured by natural selection. The optimal biofilm thickness for the sensitive strain increases to between 16 and 20 μm, which marks a large increase over the predicted thickness for a single strain biofilm (8 μm for these nutrient limited conditions). Allowing cells to defend themselves against toxins, therefore, leads to natural selection for making a thick biofilm. What is interest-

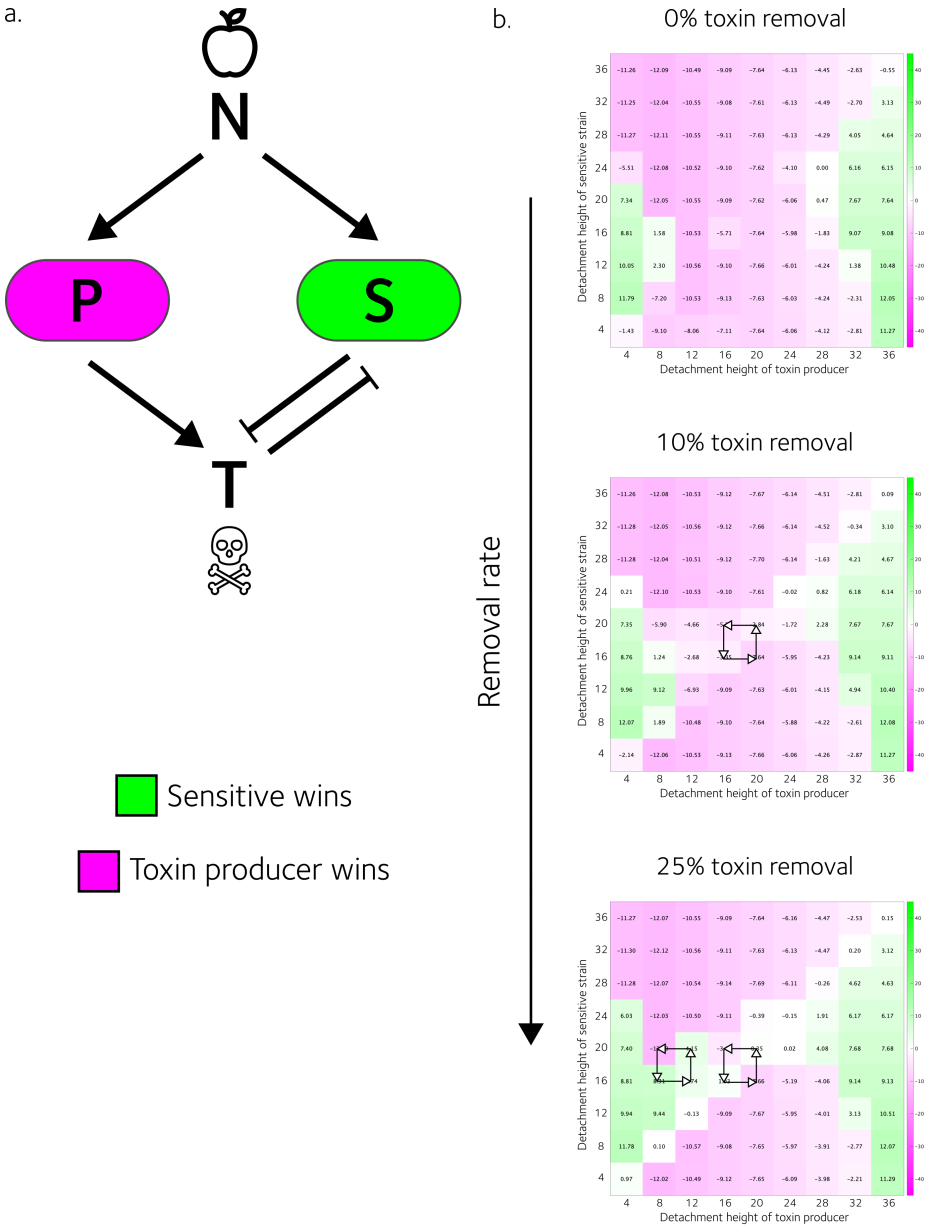

Figure 3.9: Optimal biofilm height for a sensitive strain in competition with a toxin producer — nutrient-limited conditions & low toxin production. **a.** Schematic of the competition. Toxin-producing cells (purple) and sensitive (green) cells have limited nutrient (N) and compete for space and nutrient. The toxin produced by the purple strain kills the green sensitive cells above a certain threshold. The green sensitive cells are able to remove some of the toxin produced by the toxin producer. **b.** Heat maps of the outcome of the competitions in this scenario. Toxin removal rate (relative to the toxin production rate) from top to bottom: 0% (as in Figure 3.8), 10%, 25%. Arrows indicate cycles of investment and disinvestment in biofilm production between the toxin producer and the toxin sensitive strain. n=3 simulations per case (except for 25% toxin removal, n=2). Toxin parameters used: $u_{T_{crit}} = 0.5$ (high potency) and $D_{T,P} = 0.01$ (low toxin production). Apple and crossbones skull images: Flaticon.com

ing is that this effect also impacts the optimum biofilm thickness for the toxin producer. A thin biofilm no longer suffices to create lethal levels of toxin, and so the toxin producer is now also selected to make a relatively thick biofilm.

The role played by biofilm thickness in attack and defence can be seen by considering the outcome of individual competitions for increasing biofilm thicknesses (Figure 3.9). Starting with relatively thin biofilms, the general pattern is that making a thicker biofilm improves the ability to attack for a toxin producer, and a reciprocal increase then improves the ability to defend. This pattern continues until both strains have the same 20 μm thickness and now, the best strategy for the toxin producer is to reduce its thickness and increase its growth rate, such that toxin mediated killing becomes more effective again. Here, the best counter move for the susceptible strain is to follow suit and invest more in growth rate than biofilm formation. The result is that the two strains are locked into a limit cycle where natural selection favours equal biofilm thickness in the sensitive strain and divergent in the toxin producer. Importantly, this cycling occurs at biofilm thicknesses that are much greater than the optimum thickness for a single strain.

Qualitatively similar results are seen at a higher rate of toxin removal (Figure 3.9, 25% toxin removal). If we increase removal any further, toxin production becomes ineffective and no longer influences the outcome of competition in the simulations. However, we also explored a case where both toxin production and toxin removal occurred at higher rates, so that toxins were still having an effect, in spite of high removal rates (Figure 3.10). We again see qualitatively similar dynamics, with the evolved biofilm thickness increasing above that of single strain biofilm. In sum, therefore, we find that making a thicker biofilm can play a role in improving both the use of toxins and defence against toxins.

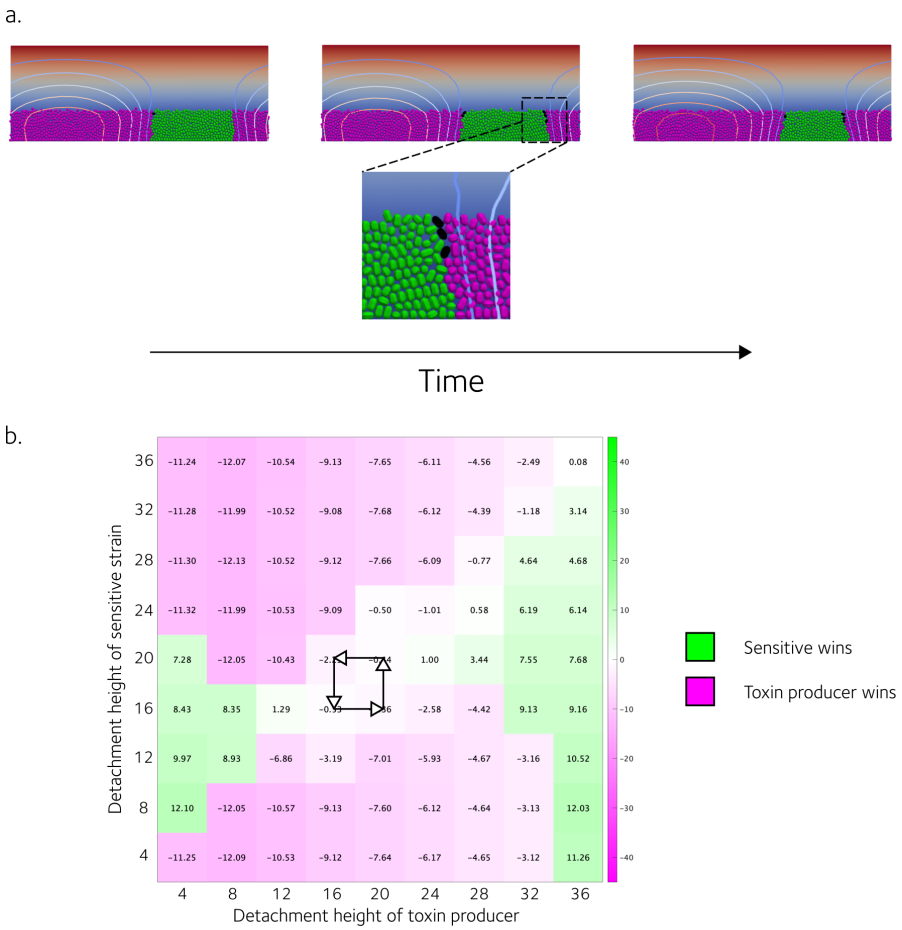

Figure 3.10: Optimal biofilm height for a sensitive strain in competition with a toxin producer — nutrient-limited conditions & high toxin production. **a.** Snapshots of a simulation at different points in time. Purple cells produce toxins at a high rate and green cell remove this toxin at a high rate. This results in cells dying at the interface (black cells) while still allowing sensitive cells to not be completely killed off. **b.** The optimal biofilm height for both the toxin producer and the toxin sensitive strain alternate between 16 and 20 μm (arrows). n=1 simulation per case. Toxin parameters used: $u_{T_{crit}} = 0.5$ (high potency) and $D_{T,P} = 0.1$ (low toxin production).

3.4.6 Competition between two toxin-producing strains

Finally, we considered the case that both strains use toxins to compete for the same patch. We extended our model to allow two strains to produce a toxin to which the other strain is sensitive. Here, we also assume again that each strain can remove its competitors toxin so that attack and defence can occur in both strains. As for the previous section, we investigated which biofilm investment strategy is optimal for both the low production/low removal case and the high production/high removal case. In both cases, the models predict that making a thicker biofilm upon detecting another strain would be beneficial.

When toxin production for both strains is low and removal is also low, there is an optimal biofilm height, and deviation from this height leads to a strain being eliminated by the competitors toxins. Below the optimum, biofilms are too thin to build up enough toxin to remain competitive against the other strain. Above the optimal height, biofilm investment is too high and cells grow too slowly, with the same outcome: cells are killed before they can produce enough toxin (ESS 16 μm, Figure 3.11). When toxin production for both strains is high and removal is also high, the ESS again lies at 16 μm (Figure 3.12.b). Deviations from this height again lead to a loss of competitive ability for the strains, although in this case the effects are less dramatic with the losing strain able to persist in the biofilm, owing to the high removal rate (Figure 3.12.a).

We find again, therefore, that an increase in biofilm thickness is favoured by competition between different genotypes. As for the case with a toxin producer and a sensitive strains, a thicker biofilm enable strains to both deploy toxins more effectively but also defend against these attacks. Overall, as with the exploitation competition scenarios, modelling predicts that interference competition can markedly increase cells' optimum investment in biofilm formation.

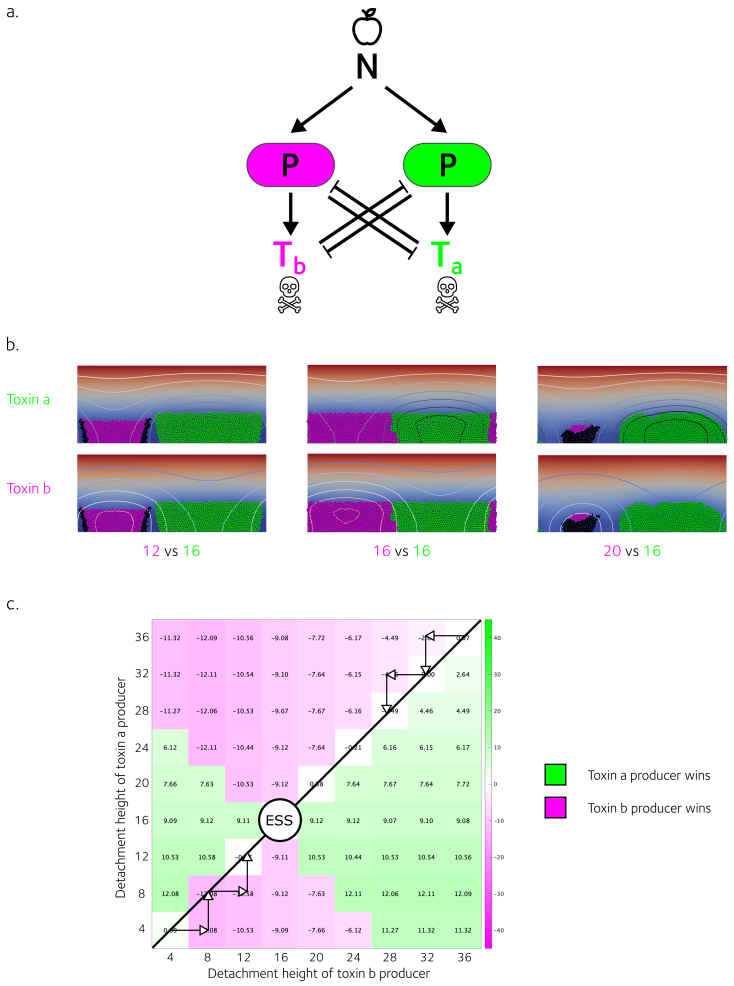

Figure 3.11: Optimal biofilm height for two toxin-producing strains competition — nutrient-limited conditions & low toxin production. **a.** Schematic of the two-toxin competition. Purple and green strains both produce a toxin (T_b and T_a respectively) to which the other is susceptible. Both strains are able to defend themselves by removing some of the other strain's toxin. Both strains compete for the same nutrient N. **b.** Snapshots of simulations competing 2 strains with different detachment heights against one another. 12 μm vs. 16 μm (snapshot taken before removal of purple cells), 16 μm vs. 16 μm (snapshot taken at the end of the simulation), 20 μm vs. 16 μm (snapshot taken before removal of purple cells). The first row displays contour lines for the toxin concentration of the toxin produced by the green strain (toxin a). The second row displays contour lines for the toxin concentration of the toxin produced by the purple strain (toxin b). Black cells are dead cells. **c.** Heatmap of the net detachment rate of the green strain. Arrows illustrate the progression of biofilm detachment heights converging on an evolutionary stable strategy height (ESS, white circle). n=1 simulations per case. Only the simulations on and above the black diagonal were run. The values were then mirrored for the bottom half as the cases are symmetrical. Toxin parameters used: $u_{T_{crit}} = 0.5$ (high potency) and $D_{T,P} = 0.01$ (low toxin production). Apple and crossbones skull images: Flaticon.com

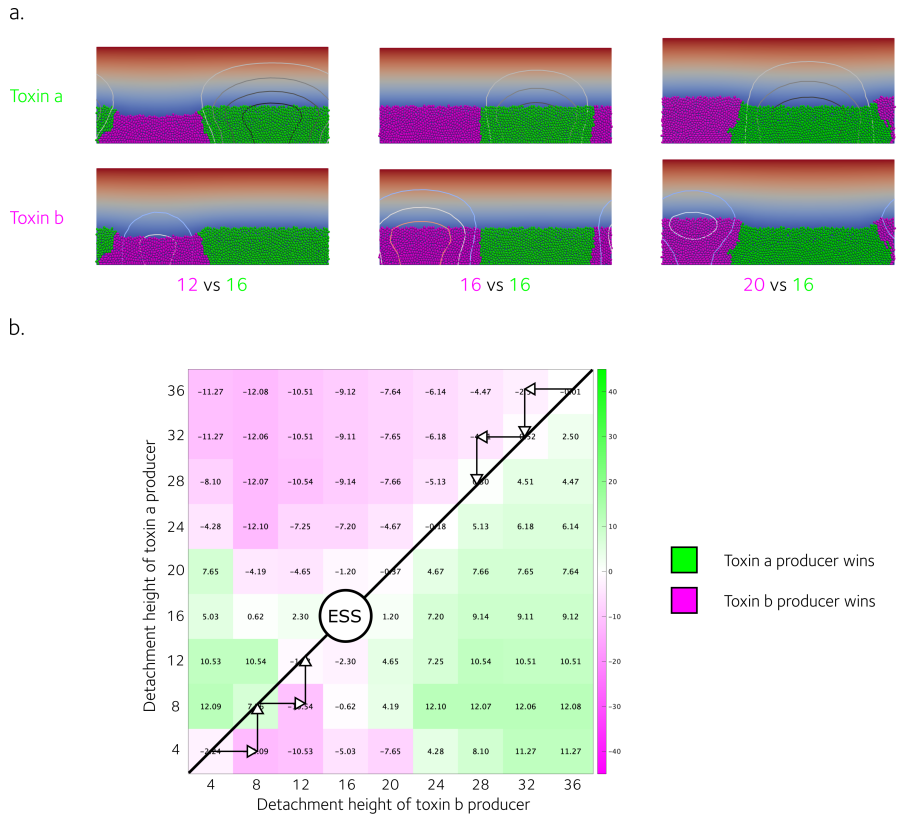

Figure 3.12: Optimal biofilm height for two toxin-producing strains competition — nutrient-limited conditions & high toxin production. **a.** Snapshots of simulations competing 2 strains with different detachment heights against one another. 12 μm vs. 16 μm, 16 μm vs. 16 μm, 20 μm vs. 16 μm. All snapshot taken at the end of the simulation. The first row displays contour lines for the toxin concentration of the toxin produced by the green strain (toxin a). The second row displays contour lines for the toxin concentration of the toxin produced by the purple strain (toxin b). Black cells are dead cells. **b.** Heatmap of the net detachment rate of the green strain. Arrows illustrate the progression of biofilm detachment heights converging on an evolutionary stable strategy height (ESS, white circle). n=5 simulations per case. Only the simulations on and above the black diagonal were run. The values were then mirrored for the bottom half as the cases are symmetrical. Toxin parameters used: $u_{T_{crit}} = 0.5$ (high potency) and $D_{T,P} = 0.1$ (high toxin production).

3.5 Conclusion

There is widespread evidence that biofilm production is up-regulated in response to toxins (Hoffman et al., 2005; Oliveira et al., 2015). Biofilms harbour a high density of bacteria, and therefore have the potential of increased offensive and defensive capabilities through increased toxin production and removal. Here, we have explored the idea that

biofilm formation is a means for bacteria to defend themselves against toxins, while also potentially allowing them to mount better attacks.

We began our analyses with the case of biofilms that do not contain toxin producers or, equally, toxins are present but ineffective at killing. Even here, we find a clear advantage to making a thick biofilm in response to inter-strain competition. In particular, we find that the optimal biofilm height for single strains growing alone depends crucially on how deep nutrients penetrate the biofilm. By contrast, when two different strains meet, natural selection can favour making much thicker biofilms in order to gain preferential access to the incoming nutrients. The importance of competition for the growing edge in bacterial biofilms is well known from previous studies (Kim et al., 2014; Nadell et al., 2010, 2016). However, to our knowledge, it has not been previously implicated in increasing biofilm cell number in response to interbacterial competition.

Introducing toxins into the simulations revealed that, in addition to benefits in exploitative competition, thick biofilms can help strains to attack and defend themselves during interference competition. An important caveat is that the impact of toxin production on our predictions depends crucially on the effectiveness of toxins (how much toxin is produced and how much is needed to kill). When toxins are too weak to kill, they have little impact on optimal biofilm height. Conversely, when toxins are highly potent and toxin removal is not sufficient to suppress the action of toxins, thick biofilms are no longer useful for attack or defence. Here, a thin biofilm will be sufficient for a toxin producer to eliminate its competitors and whichever thickness sensitive cells adopt, a toxin producer will prevail. However, whenever toxin removal is sufficient for strains to put some limits on the action of toxins, thicker biofilm are favoured by natural selection for defence. This, in turn, leads to natural selection for thicker biofilm formation in attackers, in order to attempt to overcome these defences.

The modelling presented in this chapter suggests an important interplay between the evolution of biofilm formation and bacterial warfare. However, as with all modelling frameworks, our work is subject to a number of features that may impact our conclusions. For example, we assume that the death of cells in response to intoxication only occurs

once a concentration threshold has been reached. This assumptions means that even if exposed to toxins, cell growth is unaffected below this threshold. In reality, toxins may slow down growth at concentrations well below this lethal threshold, which is a feature of some previous models (Bucci et al., 2011). This could then change the outcome of the competition if toxins are having an effect from the moment they encounter the sensitive cells. Therefore, a hybrid model where both inhibition and killing occur could be an interesting avenue to explore.

We also assumed that the cost of biofilm formation increases linearly with biofilm height. However, some studies use a quadratic detachment rates with no explicit penalty to model detachment (Bucci et al., 2011; Xavier et al., 2005). Investigating how alternative cost functions impact our model would be an interesting extension to this work to see the influence on predictions (see Stewart (1993) for interesting considerations about modelling detachment).

While we assume that biofilm formation comes at a cost, our modelling of toxin production is more simplistic and does not come at a cost to cells. Introducing a cost to toxins would allow one to study both optimum investment into biofilms and optimum investment into toxins, with the potential for interesting dependencies between the two. For example, this could potentially favour specialisation — strains which use either biofilm formation or toxins to overcome other strains, rather than the combined strategy we see here. Another assumption we make is that toxin production simply follows growth rate, after Bucci et al. (2011). This assumption makes sense because toxins are costly to produce and in the absence of nutrients, metabolic capabilities can be limited. However, some toxins are up-regulated under nutrient limitation (Gonzalez and Mavridou, 2019) and exploring the effects of such regulation on competition within biofilms is again an interesting prospect.

Finally, in the present chapter, only a limited range of values for nutrient availability and toxin production were explored. It will be important in future work to explore a wider range of these parameters.

To close, our modelling provides a clear rationale to the observation that bacteria

increase biofilm formation under toxin-generated stress. Making a thick biofilm can help a strain to compete for nutrients, defend against toxins, and deploy toxins itself. This supports the notion that biofilm formation is an important strategy that bacteria use to deal with competition from other strains and species.

3.6 Bibliography

Ahrens, J., B. Geveci, and C. Law (2005). ParaView: An End-User Tool for Large-Data Visualization. In *Visualization Handbook*, pp. 717–731. Elsevier.

Aldén, L., F. Demoling, and E. Bååth (2001, April). Rapid Method of Determining Factors Limiting Bacterial Growth in Soil. *Applied and Environmental Microbiology 67*(4), 1830–1838.

Bernier, S. P., D. Lebeaux, A. S. DeFrancesco, A. Valomon, G. Soubigou, J.-Y. Coppée, J.-M. Ghigo, and C. Beloin (2013, January). Starvation, Together with the SOS Response, Mediates High Biofilm-Specific Tolerance to the Fluoroquinolone Ofloxacin. *PLoS Genetics 9*(1), e1003144.

Bucci, V., C. D. Nadell, and J. B. Xavier (2011, December). The Evolution of Bacteriocin Production in Bacterial Biofilms. *The American Naturalist 178*(6), E162–E173.

Bunch, R. L. and J. M. McGuire (1953, September). Erythromycin, its salts, and methods of preparation.

Chang, Y.-M., W.-Y. Jeng, T.-P. Ko, Y.-J. Yeh, C. K.-M. Chen, and A. H.-J. Wang (2010, May). Structural study of TcaR and its complexes with multiple antibiotics from *Staphylococcus epidermidis*. *Proceedings of the National Academy of Sciences 107*(19), 8617–8622.

Chao, L. and B. R. Levin (1981). Structured habitats and the evolution of anticompetitor toxins in bacteria. *Proceedings of the National Academy of Sciences 78*(10), 6324–6328.

Cornforth, D. M. and K. R. Foster (2013, April). Competition sensing: The social side of bacterial stress responses. *Nature Reviews Microbiology 11*(4), 285–293.

Costerton, J. W., Z. Lewandowski, D. E. Caldwell, D. R. Korber, and H. M. Lappin-Scott (1995). Microbial Biofilms. *Annual Review of Microbiology 49*, 711–745.

Cunrath, O. and D. Bumann (2019, November). Host resistance factor SLC11A1 restricts *Salmonella* growth through magnesium deprivation. *Science 366*(6468), 995–999.

D'Costa, V. M., C. E. King, L. Kalan, M. Morar, W. W. L. Sung, C. Schwarz, D. Froese, G. Zazula, F. Calmels, R. Debruyne, G. B. Golding, H. N. Poinar, and G. D. Wright (2011, September). Antibiotic resistance is ancient. *Nature 477*(7365), 457–461.

Dieltjens, L., K. Appermans, M. Lissens, B. Lories, W. Kim, E. V. Van der Eycken, K. R. Foster, and H. P. Steenackers (2020, December). Inhibiting bacterial cooperation is an evolutionarily robust anti-biofilm strategy. *Nature Communications 11*(1), 107.

Dragoš, A., H. Kiesewalter, M. Martin, C.-Y. Hsu, R. Hartmann, T. Wechsler, C. Eriksen, S. Brix, K. Drescher, N. Stanley-Wall, R. Kümmerli, and Á. T. Kovács (2018, June). Division of Labor during Biofilm Matrix Production. *Current Biology 28*(12), 1903–1913.e5.

Flemming, H.-C. and J. Wingender (2010, September). The biofilm matrix. *Nature Reviews Microbiology 8*(9), 623–633.

Flemming, H.-C., J. Wingender, U. Szewzyk, P. Steinberg, S. A. Rice, and S. Kjelleberg (2016, September). Biofilms: An emergent form of bacterial life. *Nature Reviews Microbiology 14*(9), 563–575.

Flemming, H.-C. and S. Wuertz (2019, April). Bacteria and archaea on Earth and their abundance in biofilms. *Nature Reviews Microbiology 17*(4), 247–260.

Frost, I., W. P. J. Smith, S. Mitri, A. S. Millan, Y. Davit, J. M. Osborne, J. M. Pitt-Francis, R. C. MacLean, and K. R. Foster (2018, June). Cooperation, competition and antibiotic resistance in bacterial colonies. *The ISME Journal 12*(6), 1582–1593.

Fux, C., J. Costerton, P. Stewart, and P. Stoodley (2005, January). Survival strategies of infectious biofilms. *Trends in Microbiology 13*(1), 34–40.

Gardner, A., S. A. West, and A. Buckling (2004, July). Bacteriocins, spite and virulence. *Proceedings of the Royal Society of London. Series B: Biological Sciences 271*(1547), 1529–1535.

Gonzalez, D. and D. A. Mavridou (2019, November). Making the Best of Aggression: The Many Dimensions of Bacterial Toxin Regulation. *Trends in Microbiology 27*(11), 897–905.

Granato, E. T. and K. R. Foster (2020, July). The Evolution of Mass Cell Suicide in Bacterial Warfare. *Current Biology 30*(14), 2836–2843.

Granato, E. T., T. A. Meiller-Legrand, and K. R. Foster (2019, June). The Evolution and Ecology of Bacterial Warfare. *Current Biology 29*(11), R521–R537.

Grimm, V., U. Berger, D. L. DeAngelis, J. G. Polhill, J. Giske, and S. F. Railsback (2010, November). The ODD protocol: A review and first update. *Ecological Modelling 221*(23), 2760–2768.

Grimm, V., G. Polhill, and J. Touza (2013). Documenting Social Simulation Models: The ODD Protocol as a Standard. In B. Edmonds and R. Meyer (Eds.), *Simulating Social Complexity*, pp. 117–133. Berlin, Heidelberg: Springer Berlin Heidelberg.

Grimm, V., S. F. Railsback, C. E. Vincenot, U. Berger, C. Gallagher, D. L. DeAngelis, B. Edmonds, J. Ge, J. Giske, J. Groeneveld, A. S. Johnston, A. Milles, J. Nabe-Nielsen, J. G. Polhill, V. Radchuk, M.-S. Rohwäder, R. A. Stillman, J. C. Thiele, and D. Ayllón (2020). The ODD Protocol for Describing Agent-Based and Other Simulation Models: A Second Update to Improve Clarity, Replication, and Structural Realism. *Journal of Artificial Societies and Social Simulation 23*(2), 7.

Hamilton, W. (1964, July). The genetical evolution of social behaviour. I. *Journal of Theoretical Biology 7*(1), 1–16.

Harms, A., E. Maisonneuve, and K. Gerdes (2016, December). Mechanisms of bacterial persistence during stress and antibiotic exposure. *Science 354*(6318), aaf4268.

Hoffman, L. R., D. A. D'Argenio, M. J. MacCoss, Z. Zhang, R. A. Jones, and S. I. Miller (2005, August). Aminoglycoside antibiotics induce bacterial biofilm formation. *Nature 436*(7054), 1171–1175.

Hsu, C.-Y., M.-H. Lin, C.-C. Chen, S.-C. Chien, Y.-H. Cheng, I.-N. Su, and J.-C. Shu (2011, November). Vancomycin promotes the bacterial autolysis, release of extracellular DNA, and biofilm formation in vancomycin-non-susceptible *Staphylococcus aureus*. *FEMS Immunology & Medical Microbiology 63*(2), 236–247.

Hutchings, M. I., A. W. Truman, and B. Wilkinson (2019, October). Antibiotics: Past, present and future. *Current Opinion in Microbiology 51*, 72–80.

Inglis, R. F., A. Gardner, P. Cornelis, and A. Buckling (2009, April). Spite and virulence in the bacterium *Pseudomonas aeruginosa*. *Proceedings of the National Academy of Sciences 106*(14), 5703–5707.

Inglis, R. F., A. R. Hall, and A. Buckling (2013, February). The role of 'soaking' in spiteful toxin production in *Pseudomonas aeruginosa*. *Biology Letters 9*, 20120569.

Irie, Y., A. E. L. Roberts, K. N. Kragh, V. D. Gordon, J. Hutchison, R. J. Allen, G. Melaugh, T. Bjarnsholt, S. A. West, and S. P. Diggle (2017, July). The *Pseudomonas aeruginosa* PSL Polysaccharide Is a Social but Noncheatable Trait in Biofilms. *mBio 8*(3), e00374–17.

Johnson, B. A., H. Anker, and F. L. Meleney (1945, October). Bacitracin: A new antibiotic produced by a member of the *B. subtilis* group. *Science 102*(2650), 376–377.

Kim, W., F. Racimo, J. Schluter, S. B. Levy, and K. R. Foster (2014, April). Importance of positioning for microbial evolution. *Proceedings of the National Academy of Sciences 111*(16), E1639–E1647.

Kobayashi, K. and Y. Ikemoto (2019, October). Biofilm-associated toxin and extracellular protease cooperatively suppress competitors in *Bacillus subtilis* biofilms. *PLOS Genetics 15*(10), e1008232.

Kreft, J.-U., G. Booth, and J. W. T. Wimpenny (1998, December). BacSim, a simulator for individual-based modelling of bacterial colony growth. *Microbiology 144*(12), 3275–3287.

Krishna Kumar, R., T. A. Meiller-Legrand, A. Alcinesio, D. Gonzalez, D. A. I. Mavridou, O. J. Meacock, W. P. J. Smith, L. Zhou, W. Kim, G. S. Pulcu, H. Bayley, and K. R. Foster (2021, December). Droplet printing reveals the importance of micron-scale structure for bacterial ecology. *Nature Communications 12*(1), 857.

Kümmerli, R., L. A. Santorelli, E. T. Granato, Z. Dumas, A. Dobay, A. S. Griffin, and S. A. West (2015, December). Co-evolutionary dynamics between public good producers and cheats in the bacterium *Pseudomonas aeruginosa*. *Journal of Evolutionary Biology 28*(12), 2264–2274.

Lardon, L. A., B. V. Merkey, S. Martins, A. Dötsch, C. Picioreanu, J.-U. Kreft, and B. F. Smets (2011, September). iDynoMiCS: Next-generation individual-based modelling of biofilms: iDynoMiCS for Biofilm Modelling. *Environmental Microbiology 13*(9), 2416–2434.

Lories, B., S. Roberfroid, L. Dieltjens, D. De Coster, K. R. Foster, and H. P. Steenackers (2020, April). Biofilm Bacteria Use Stress Responses to Detect and Respond to Competitors. *Current Biology 30*(7), 1231–1244.

Mavridou, D. A., D. Gonzalez, W. Kim, S. A. West, and K. R. Foster (2018, February). Bacteria Use Collective Behavior to Generate Diverse Combat Strategies. *Current Biology 28*(3), 345–355.

Mitri, S., E. Clarke, and K. R. Foster (2016). Resource limitation drives spatial organization in microbial groups. *The ISME journal 10*(6), 1471–1482.

Monod, J. (1949). The growth of bacterial cultures. *Annual Review of Microbiology 3*, 371–394.

Nadell, C. D., V. Bucci, K. Drescher, S. A. Levin, B. L. Bassler, and J. B. Xavier (2013, January). Cutting through the complexity of cell collectives. *Proceedings of the Royal Society B: Biological Sciences 280*(1755), 20122770–20122770.

Nadell, C. D., K. Drescher, and K. R. Foster (2016, July). Spatial structure, cooperation and competition in biofilms. *Nature Reviews Microbiology 14*, 589–600.

Nadell, C. D., K. R. Foster, and J. B. Xavier (2010, March). Emergence of Spatial Structure in Cell Groups and the Evolution of Cooperation. *PLoS Computational Biology 6*(3), e1000716.

Nelson, M. L. and S. B. Levy (2011, December). The history of the tetracyclines: The history of the tetracyclines. *Annals of the New York Academy of Sciences 1241*(1), 17–32.

Oliveira, N. M., E. Martinez-Garcia, J. Xavier, W. M. Durham, R. Kolter, W. Kim, and K. R. Foster (2015, July). Biofilm Formation As a Response to Ecological Competition. *PLOS Biology 13*(7), e1002191.

Picioreanu, C., M. C. M. van Loosdrecht, and J. J. Heijnen (1998, April). Mathematical modeling of biofilm structure with a hybrid differential-discrete cellular automaton approach. *Biotechnology and Bioengineering 58*(1), 101–116.

Rendueles, O., C. Beloin, P. Latour-Lambert, and J.-M. Ghigo (2014, June). A new biofilm-associated colicin with increased efficiency against biofilm bacteria. *The ISME Journal 8*(6), 1275–1288.

Rudge, T. J., F. Federici, P. J. Steiner, A. Kan, and J. Haseloff (2013, December). Cell Polarity-Driven Instability Generates Self-Organized, Fractal Patterning of Cell Layers. *ACS Synthetic Biology 2*(12), 705–714.

Rudge, T. J., P. J. Steiner, A. Phillips, and J. Haseloff (2012, August). Computational Modeling of Synthetic Microbial Biofilms. *ACS Synthetic Biology 1*(8), 345–352.

Schlomann, B. H., T. J. Wiles, E. S. Wall, K. Guillemin, and R. Parthasarathy (2019, October). Sublethal antibiotics collapse gut bacterial populations by enhancing aggregation and expulsion. *Proceedings of the National Academy of Sciences 116*(43), 21392–21400.

Schluter, J., C. D. Nadell, B. L. Bassler, and K. R. Foster (2015, January). Adhesion as a weapon in microbial competition. *The ISME Journal 9*(1), 139–149.

Sensi, P. (1983, July). History of the Development of Rifampin. *Clinical Infectious Diseases 5*(Supplement_3), S402–S406.

Smith, W. P. J., M. Brodmann, D. Unterweger, Y. Davit, L. E. Comstock, M. Basler, and K. R. Foster (2020, December). The evolution of tit-for-tat in bacteria via the type VI secretion system. *Nature Communications 11*(1), 5395.

Smith, W. P. J., Y. Davit, J. M. Osborne, W. Kim, K. R. Foster, and J. M. Pitt-Francis (2017, January). Cell morphology drives spatial patterning in microbial communities. *Proceedings of the National Academy of Sciences 114*(3), E280–E286.

Smith, W. P. J., A. Vettiger, J. Winter, T. Ryser, L. E. Comstock, M. Basler, and K. R. Foster (2020, May). The evolution of the type VI secretion system as a disintegration weapon. *PLOS Biology 18*(5), e3000720.

Stewart, P. S. (1993, January). A model of biofilm detachment. *Biotechnology and Bioengineering 41*(1), 111–117.

Stewart, P. S. and M. J. Franklin (2008, March). Physiological heterogeneity in biofilms. *Nature Reviews Microbiology 6*(3), 199–210.

Umezawa, H., M. Ueda, K. Maeda, K. Yagishita, S. Kondo, Y. Okami, R. Utahara, Y. Osato, K. Nitta, and T. Takeuchi (1957, September). Production and isolation of a new antibiotic, Kanamycin. *The Journal of Antibiotics, Series A 10*(5), 181–188.

Van Acker, H., P. Van Dijck, and T. Coenye (2014, June). Molecular mechanisms of antimicrobial tolerance and resistance in bacterial and fungal biofilms. *Trends in Microbiology 22*(6), 326–333.

West, S. A., S. P. Diggle, A. Buckling, A. Gardner, and A. S. Griffin (2007, December). The Social Lives of Microbes. *Annual Review of Ecology, Evolution, and Systematics 38*(1), 53–77.

West, S. A., A. S. Griffin, and A. Gardner (2007, August). Evolutionary Explanations for Cooperation. *Current Biology 17*(16), R661–R672.

Xavier, J. B. and K. R. Foster (2007, January). Cooperation and conflict in microbial biofilms. *Proceedings of the National Academy of Sciences 104*(3), 876–881.

Xavier, J. B., C. Picioreanu, S. A. Rani, M. C. M. van Loosdrecht, and P. S. Stewart (2005, December). Biofilm-control strategies based on enzymic disruption of the extracellular polymeric substance matrix – a modelling study. *Microbiology 151*(12), 3817–3832.

Xavier, J. B., C. Picioreanu, and M. C. M. van Loosdrecht (2005, August). A framework for multidimensional modelling of activity and structure of multispecies biofilms. *Environmental Microbiology 7*(8), 1085–1103.

Chapter 4

The Evolution and Ecology of Bacterial Warfare

Current Biology
Review

CellPress

The Evolution and Ecology of Bacterial Warfare

Elisa T. Granato[1,2,3], Thomas A. Meiller-Legrand[1,2,3], and Kevin R. Foster[1,2,*]
[1]Department of Zoology, University of Oxford, Oxford, UK
[2]Department of Biochemistry, University of Oxford, Oxford, UK
[3]Equal contribution
*Correspondence: kevin.foster@zoo.ox.ac.uk
https://doi.org/10.1016/j.cub.2019.04.024

Bacteria have evolved a wide range of mechanisms to harm and kill their competitors, including chemical, mechanical and biological weapons. Here we review the incredible diversity of bacterial weapon systems, which comprise antibiotics, toxic proteins, mechanical weapons that stab and pierce, viruses, and more. The evolution of bacterial weapons is shaped by many factors, including cell density and nutrient abundance, and how strains are arranged in space. Bacteria also employ a diverse range of combat behaviours, including pre-emptive attacks, suicidal attacks, and reciprocation (tit-for-tat). However, why bacteria carry so many weapons, and why they are so often used, remains poorly understood. By comparison with animals, we argue that the way that bacteria live — often in dense and genetically diverse communities — is likely to be key to their aggression as it encourages them to dig in and fight alongside their clonemates. The intensity of bacterial aggression is such that it can strongly affect communities, via complex coevolutionary and eco-evolutionary dynamics, which influence species over space and time. Bacterial warfare is a fascinating topic for ecology and evolution, as well as one of increasing relevance. Understanding how bacteria win wars is important for the goal of manipulating the human microbiome and other important microbial systems.

Introduction

Bacteria commonly live in dense, multispecies communities where there is competition over scarce resources. A key requirement for evolutionary success in these complex environments is the ability to survive and divide in the presence of other strains and species [1–4]. As a result, metabolism and the ability to acquire nutrients are key determinants of success in a given community [5]. For example, mammalian gut bacteria employ a wide range of enzymes and transporters to break down and import carbohydrates [6]. Such mechanisms of **exploitative competition**, however, are only part of the story. It is becoming increasingly clear that bacteria also rely heavily on mechanisms of **interference competition** for their ecological and evolutionary success [7–14]. (See the Glossary in Box 1 for key terms denoted in bold text.)

Advances in genomics, biochemistry and imaging have revealed that bacteria employ an amazing diversity of mechanisms to harm, inhibit and kill off their competitors (Figures 1–3). These bacterial **weapons** include mechanisms for chemical warfare via **toxins**, complex mechanical weapons that punch holes, and the use of viruses in biological warfare [15]. Deployment of these weapons can be extremely costly; at the extreme, a cell may go so far as to lyse and die to attack others. And yet, many species carry multiple types of weapons and sometimes multiple variants of each type (Figures 2 and 3). It is not yet clear what drove the evolution of all of these bacterial weapons. This is perhaps surprising insofar as the 1928 discovery of the antibiotic penicillin marked the starting point of close to a century of intense investigation of antimicrobial compounds, many of which first evolved as mechanisms for microbial **competition**. However, the focus on the drugs' mechanisms of action and clinical application has meant that a literature replete with examples of antibacterial mechanisms rarely considers their evolution or original function [16].

Outside of microbiology, the evolution of **combat** has been long discussed, following the classic paper of Maynard Smith and Price [17] that introduced **game theory** into evolutionary biology. However, the focus was animal combat and more specifically why animals that have weapons rarely use them in pairwise **contests** [17–19]. This focus contrasts with what we know about bacterial contests, where encounters can involve many millions of individuals on each side and, moreover, contests are often intense and lethal [5,16]. The evolution of **warfare** in bacteria, therefore, demands dedicated study. In the years following the development of evolutionary game theory, some authors employed theory and experiment to ask when bacterial weapons are favoured [20–26] and how weapons can affect genetic diversity [27–33]. Most recently, some studies have begun to consider the evolution of the behavioural strategies used when bacteria fight, including responses to nutrient levels [16], reciprocation [34] and provocation [35]. Nevertheless, there is much to learn. In particular, we do not understand why bacteria appear to be so very aggressive, both in terms of how often they attack other strains and the amount of weaponry they carry.

Here we showcase the diverse mechanisms that bacteria have evolved to harm and kill their competitors. We discuss both the evolution of the weapons themselves and the evolution of the strategies employed during contests, where we draw comparisons to the much-studied contests of animals. Finally, we turn to the consequences of such prevalent **aggression** for the ecological and evolutionary dynamics of bacterial communities. Bacterial warfare encompasses many major themes in evolution and ecology, including collective behaviour, behavioural ecology, social evolution and the study of ecological networks. Understanding how bacteria win their contests also has growing importance for microbiology and medicine, where many disease



Box 1. Glossary

Aggression	How often and how severely an individual attacks.
Coevolution	Reciprocal evolutionary adaptations in different individuals or species that evolved in response to one another.
Collective behaviour	Behaviour that emerges from the interactions of individuals in a group.
Combat	Fighting involving weapons between two or more individuals.
Competition (as an evolved adaptation [158])	Negative effect of one cell on other cells' survival and reproduction, which evolved at least in part because of this effect.
Competition sensing	A physiological response that detects harm caused by other cells and that evolved, at least in part, for that purpose.
Contest	A fight or battle between two or more individuals.
Cue	A feature that provides another organism with information but that has not evolved for that purpose.
Division of labour	The division of a collective phenotype into separate tasks performed by different individuals.
Exploitative competition	Competition driven by increased uptake and use of nutrients by a focal cell.
Game theory	Theory seeking best performing strategies, where the best strategy will often depend on the strategy of others.
Interference competition	Competition that interferes with the access of other cells to resources, but not driven by increased nutrient uptake in a focal cell.
Quorum sensing	Density-dependent response that occurs via the secretion and detection of dedicated molecules (autoinducers).
Signal	An evolved means of conveying information to receivers (often restricted to cooperative information only [139]).
Strategy	Rule(s) defining the decisions of an actor in response to prevailing conditions (for example, fight back if attacked).
Tactics	Behaviours displayed in a given contest (the realised output of a strategy).
Toxin	Substance that disrupts cell physiology.
Warfare	Conflict involving weapons between two or more groups.
Weapon	Competitive phenotype that damages and/or disrupts the physiology of recipients, and that evolved, at least in part, for that purpose (for example, bacteriocin production).

outcomes rest upon whether a strain can invade or persist in the diverse human microbiota.

The Diversity of Bacterial Weapons

Weapons are extremely common in culturable bacteria (Figure 2). In the best-studied species, it is typical to find multiple mechanisms for damaging competitors, and, moreover, multiple variants of each of these mechanisms (Figure 3). A striking example is the opportunistic pathogen *Pseudomonas aeruginosa*, which is a major concern owing to its ability to cause diverse infections and withstand many antibiotics. A single cell of *P. aeruginosa* has the option of generating a vast arsenal including: many different types of diffusing protein toxins (including S pyocins) [36,37]; multiple types of poisoned molecular speargun (type VI secretion systems) [38]; poisoned proteinaceous sticks (contact-dependent growth inhibition system) [39]; two different mechanical weapons that punch holes in other cells (R and F pyocins) [36]; and viruses (phages) that kill non-clonemates [40,41]. And, though it is less clear they evolved for this purpose, *P. aeruginosa* also makes molecules like hydrogen cyanide [42] and pyocyanin [43], and membrane vesicles [44] that can harm other bacteria. *P. aeruginosa* may be a relatively extreme case, but the widespread occurrence of weapons in the best-studied species (Figure 3) as well as in other cultured bacteria (Figure 2) suggest that, when we look, we will commonly find weaponry in bacteria.

The full extent of bacterial weapons, however, remains unknown. To demonstrate that a protein or pathway functions in interbacterial competition requires culturing and experimental work, which has only been performed for a tiny fraction of bacterial species. Moreover, this fraction is biased as the best-studied species are often pathogens that only cover a minority of the bacterial phylogeny (Figure S1). Pathogens appear to be particularly prone to weapon evolution [45], and it is possible that some unstudied groups may differ so fundamentally in their ecology that the evolution of weaponry is much more limited. For example, the Candidate Phyla Radiation is a fascinating and enigmatic group of ultra-small bacteria that may comprise around a quarter of all bacterial diversity [46]. They have reduced genomes and are thought to live as symbiotic parasites on the outside of larger bacteria [47], and whether they need or use weaponry is not yet clear. Caveats aside, it is clear that many bacteria do employ weapons and, moreover, that these weapons are important for their ability to invade and compete in natural communities [12,13,48–51], particularly in the mammalian microbiome where much attention has been focussed [9,10,12,48,50–57].

Bacterial weapons can be divided up broadly by the way they damage cells (Figure 1). There are some mechanical weapons, which physically damage cells. However, more common are biological (virus) and particularly chemical (toxin) warfare, which

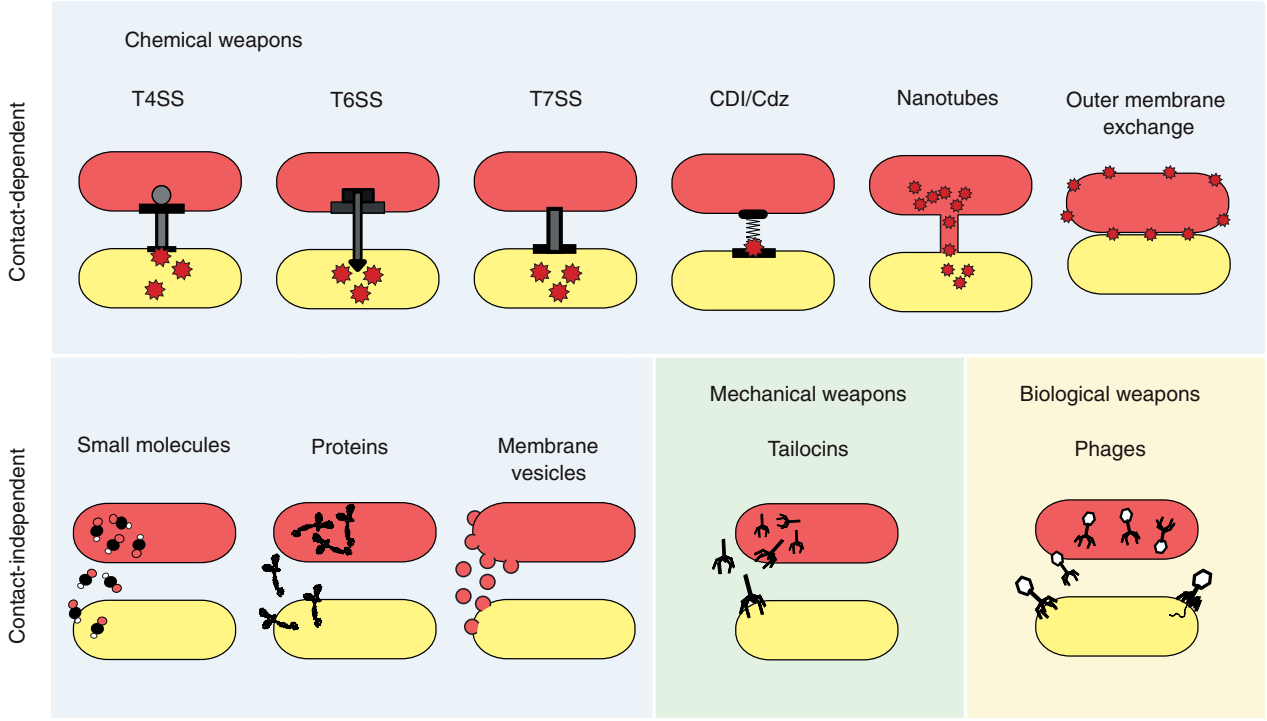

Figure 1. Types of bacterial weapons.
Type IV secretion systems (*T4SS*) translocate DNA and proteins in Gram-negative bacteria and have recently been implicated in targeting toxins towards competitors. *Type VI secretion systems* (*T6SS*) are widespread in Gram-negative bacteria and allow direct delivery of toxin effectors to competitor cells using a repurposed contractile phage tail. *Type VII secretion systems* (*T7SS*) are involved in contact-dependent toxin delivery in Gram-positive bacteria, although little is yet known about their structure and mechanism of delivery. *Contact-dependent growth inhibition* (*CDI*) *systems* (and the functionally similar Cdz systems) involve a filamentous protein containing a toxic domain and a second protein responsible for export and anchoring to the cell surface of the attacker. Upon contact of the filament to a target cell, the toxic domain is translocated into the victim. Cdz toxicity also involves formation of filaments on the cell surface of the attacker. *Nanotubes* are structures bridging the cytoplasm of neighbouring bacteria, allowing the direct transfer of toxins and other molecules between cells. *Outer membrane exchange* (*OME*) mechanisms involve the delivery of toxic proteins embedded in the outer membrane. A cell can poison non-immune neighbours by transferring toxin-containing membrane fragments upon cell–cell contact. *Small molecule toxins* include peptides and antibiotics, less than 10 kDa in size, that are released and diffuse to target cells. *Protein toxins* are those bigger than 10 kDa that are released, often by cell lysis, allowing them to diffuse to target cells. *Membrane vesicles* are produced by diverse bacteria [69] and can kill other cells by, for example, delivery of enzymes that digest the cell wall [44]. The vesicles deliver many molecules, however, and the importance of vesicle production for bacterial competition needs further verification (they do not yet meet the inclusion criteria for Figure 2). *Tailocins* are derived from phages and lack the nucleic acid containing capsular head. These multi-protein assemblies are released into the environment and physically puncture the membrane of their target. *Phages* include many viruses integrated into bacterial genomes that when released will kill competitors but not clonemates that also carry the virus. See main text for more details and Table S1 for references.

dominates the current list of examples. This dominance may partially reflect the historical focus of research on antibiotics, but it is nevertheless clear that toxin-based interference competition is common to many bacteria.

Chemical Warfare

Bacteria use diverse toxins to disrupt the physiology of target cells, ranging from small molecules to large proteins and other molecules. Small toxins often bind to other molecules and interfere with their function [58], whereas protein toxins can have more complex actions, and include large enzymes that digest cell components [59]. Like clinical antibiotics, bacterial toxins typically act on a cell's envelope or its core metabolism. Many toxins made by bacteria damage membranes, including last-line polymyxin antibiotics like colistin [60]. More sophisticated are protein toxins that insert themselves into the target cell membrane and form a pore [61]. These pores weaken or ablate the chemical gradients needed to keep a cell functioning, often leading to cell death. Another major target in the envelope is the cell wall, and its associated protein cytoskeleton, which is again affected by a range of toxins, including beta-lactams and other classes of antibiotics [58]. The last-line antibiotic vancomycin, for example, is made by the soil bacterium *Amycolatopsis orientalis* and destabilizes the cell wall of susceptible cells, leading to death by osmotic lysis [58,62]. Inside the cell, major targets include the transcription and translation machineries, as well as a competitor's DNA and RNA, which are targeted by nuclease toxins [49,61,63].

Regardless of the target, the impact of many toxins rests upon interfering with the cell's ability to grow and divide. The potency of antimicrobial toxins for growing cells makes it imperative that the producer cell has a way to avoid self-intoxication, which is achieved via mechanisms including the use of immunity proteins that block a toxin's activity [61,64], expressing a resistant form of

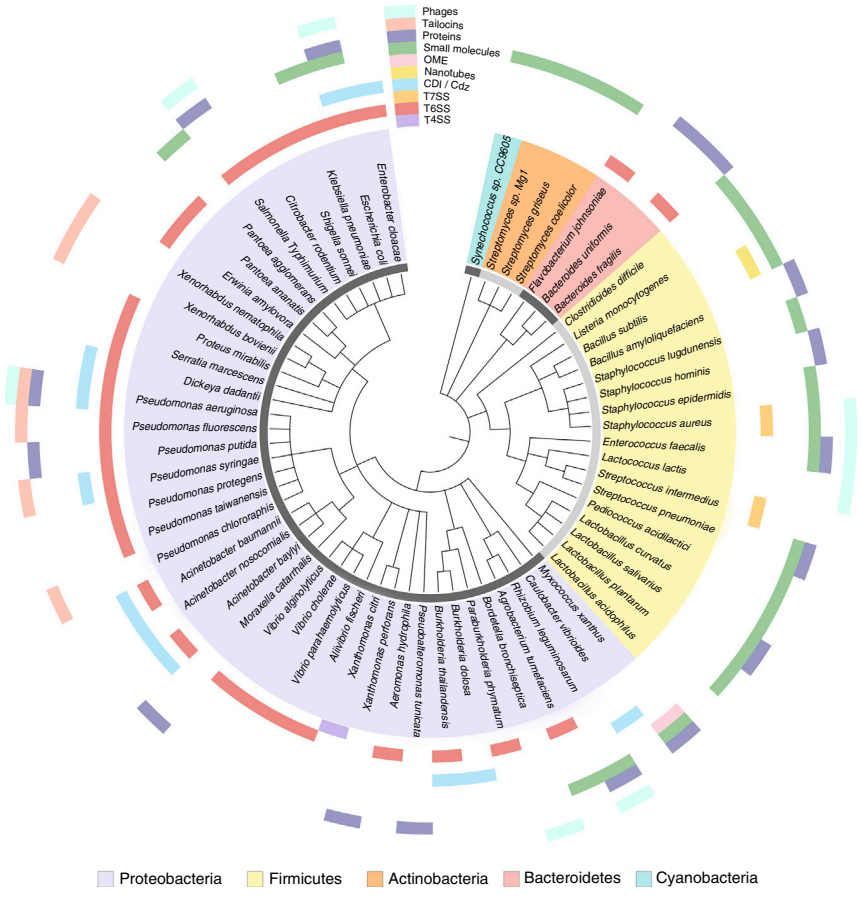

Figure 2. Distribution of documented weapon systems in bacteria.
We performed a literature search to identify studies that provide empirical evidence of a weapon in a given species. Our search used multiple sources and strategies to identify candidates and we then applied fairly stringent criteria for inclusion in the figure (see Table S1 for studies included). Specifically, we required that two strains of the same genetic background were compared with and without the putative weapon system (or toxin of the system) using a competition experiment, which either pitted the two strains against each other or against a third-party strain. We included studies when the presence of the putative weapon resulted in removal and/or inhibition of the competitor in the mixed culture experiment. In a few cases included, the regulation of the weapon needed to be artificially induced to elicit a phenotype. Although many species shown here have multiple weapons, our stringent inclusion criteria mean that many will actually have further weapons that have yet to be validated (for example, prophages). Moreover, the great majority of bacterial diversity is missing as most bacterial species have not yet been cultured, let alone studied in this context (Figure S1). The bacterial phylogeny was built using the NCBI common tree tool [214]. Visualisation and annotation of the tree was performed using iTOL [215].

the toxin's target, synthesizing an inactive precursor, or exporting the toxin to prevent its build-up [65,66]. A catch is that a weapon may be rendered ineffective if a target strain picks up these mechanisms by horizontal gene transfer (see "Ecological and Evolutionary Dynamics" below). Why have bacteria evolved to primarily attack core cellular functions of their victims, like cell wall and DNA synthesis? Most obviously, core functions are often essential for cell viability. Targeting a core function also brings with it the potential to harm a diverse set of competing species. However, to be effective a toxin must be able to reach its target. For this purpose, bacteria have evolved ingenious, and sometimes spectacular, methods of toxin delivery, which we discuss next.

Toxin Delivery: Secretion, Suicide and Stabbing

To employ a chemical attack, a cell must first export its toxins. Small toxins may diffuse out of the producing cell, often via protein pores, or are released by active transport across the cell envelope [67,68]. Other toxins are released in membrane vesicles that bleb from the surface of the producing cell and can deliver many molecules to a target cell in one go [44,69]. At the extreme, several well-known bacteria — including *Escherichia coli*, *P. aeruginosa* and *Salmonella enterica* — have been shown to lyse themselves using dedicated enzymes to release large protein toxins [36,61], thus benefitting their non-lysing clonemates; a particularly clear example of **division of labour** in microbes (below) [34].

Most toxins must cross the membranes of the target cell to have an effect. Again, small molecules may simply diffuse across, and this property has made them particularly attractive for use as clinical antibiotics as they can enter and affect a variety of species [67]. Larger molecules require more sophisticated mechanisms to enter a cell. One elaborate and well-studied mechanism is employed by the colicin toxins of *E. coli*. These large proteins employ a Trojan horse strategy by binding specifically to outer-membrane receptors normally used to import small essential molecules such as vitamin B12, iron-carrying siderophores, or nucleosides. The colicin toxins are massive compared to the intended molecules but, astonishingly, colicins are able to both bind the same receptors and translocate into the cell, either directly or by recruiting host porins [70,71]. The complexity of this entry mechanism, however, makes these toxins highly specific; they fail to bind and enter bacterial species lacking the specific target proteins needed for entry [61].

Whereas many toxins must diffuse from producer to target cell, others are delivered directly to the target. Physical delivery includes direct transfer of membrane components containing toxins when cells touch [72] and the enigmatic formation of 'nanotubes' that appear able to exchange cytoplasmic content, including toxins [73]. Better understood is the appropriately named contact-dependent growth inhibition (CDI) system [74–76]. Something akin to a shape-shifting poison-tipped stick, CDI involves the expression of a filamentous protein, tens of nanometers long, from the cell [77]. Upon contact with the target cell, the toxic domain is delivered to the tip, cleaved [78], and translocated into the target cell [79]. As for protein bacteriocins,

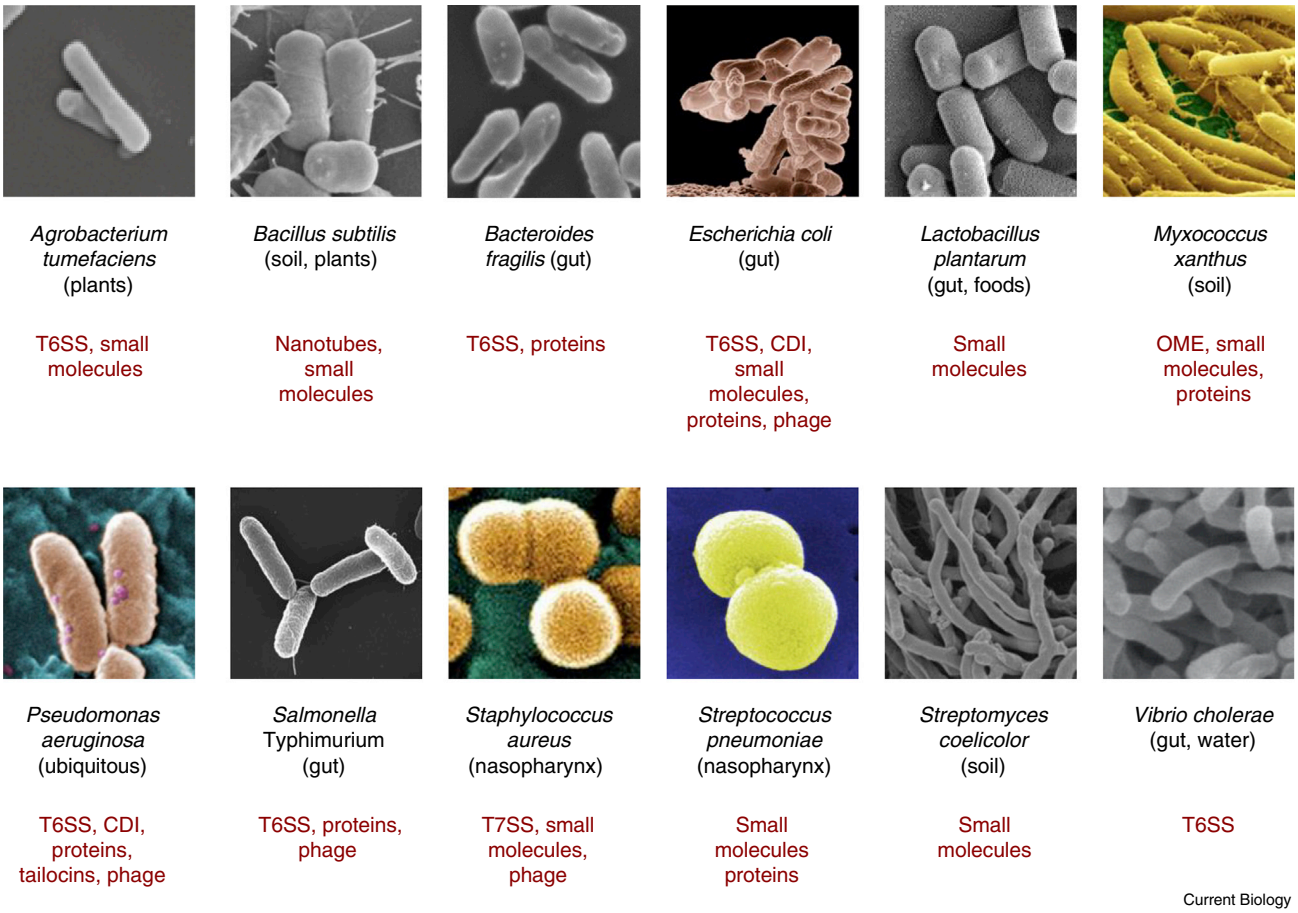

Figure 3. Weapons of well-studied bacteria.
A typical environment for each bacterium is shown in parentheses. Gut and nasopharynx colonization refers primarily to humans, although all of the species can be found in additional environments to those listed. Weapons listed are only those that have been experimentally shown to mediate bacterial competition as described in Figure 2. See Figure 1 legend for details on weapons and abbreviations. Image sources: *A. tumefaciens* (credit: taken from [216] © 2013 John Wiley & Sons Ltd); *B. fragilis* (credit: taken from [217] (CC BY 4.0)); *B. subtilis* (credit: taken from [218] © Zweers *et al.* licensee BioMed Central Ltd. 2008 (CC BY 2.0)); *E. coli* (credit: Eric Erbe, digital colorization by Christopher Pooley, both of USDA, ARS, EMU); *L. plantarum* (credit: taken from [219] and reproduced with permission from American Society for Microbiology); *M. xanthus* (credit: Jürgen Berger, Supriya Kadam, Gregory Velicer, Max Planck Institute for Developmental Biology, Tübingen, Germany); *P. aeruginosa* (credit: Janice Haney Carr, PD-USGov-HHS-CDC); *S. coelicolor* (credit: taken from [220] CC BY 4.0); *S. aureus* (credit: Janice Haney Carr, Centers for Disease Control and Prevention); *S. pneumococcus* (credit: Richard Facklam, CDC-PHIL); *S. Typhimurium* (credit: Volker Brinkmann, Max Planck Institute for Infection Biology, Berlin, Germany); *V. cholerae* (credit: Ronald Taylor, Tom Kirn, Louisa Howard, Dartmouth Electron Microscope Facility).

the need to translocate into the cell makes CDI a narrow-spectrum weapon that targets members of the same species [80]. A growing number of such contact-dependent weapon systems are being discovered, and strikingly, all appear to have independent evolutionary origins. This suggests that these complex weapons have convergently evolved multiple times across the bacterial phylogeny, testament to the importance of warfare for bacterial evolution. More recently discovered systems include the functionally similar Cdz (Contact-Dependent inhibition by glycine Zipper proteins) system [81], the type VII secretion system [82,83], and the type IV secretion system, a long-studied secretion system that was only recently found to mediate interbacterial competition [84].

Our final example of toxin delivery is the type VI secretion system, whose dry name belies its status as one of the most fascinating structures made by bacteria. Initially implicated in infections [85], the type VI secretion system was later shown to be a powerful mediator of interbacterial competition [64,86,87], and is carried by many Gram-negative bacteria [88]. Best envisaged as a poisoned molecular speargun, the type VI secretion system solves the problem of toxin release and delivery in one step by firing a toxin-carrying needle into a target cell, via a spring-loaded contractile sheath [89–91]. Cells that use the system achieve immunity to the diverse toxic 'effector' proteins carried on the needle through the expression of cognate immunity proteins, which also ensures that hitting a clonemate does not cause harm. Gram-positive species are often resistant to this type of weapon, possibly due to their thick cell walls. Nevertheless, the type VI secretion system is a versatile weapon that can kill diverse species, and there is growing evidence of its importance for bacterial competition, particularly in the mammalian gut microbiota [12,54,56,92,93].

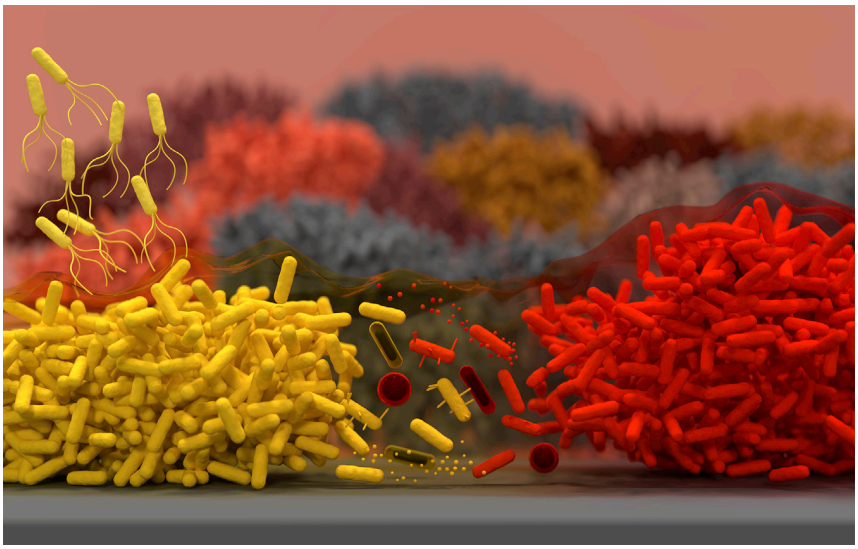

Figure 4. Illustration of warfare in a multispecies bacterial biofilm.
Bacteria commonly live in dense bacterial communities, called biofilms, where cells live encased in a self-produced, extracellular polymeric matrix, often comprised of carbohydrates, proteins and DNA. These communities can be extremely diverse, with many species and strains, but often develop distinct patches of tightly packed cells of a single genotype. Competitive interactions occur at the interface between genotypes (in the case of contact-dependent and -independent mechanisms), as well as throughout the biofilm whenever diffusible compounds are involved. Weapon use on both sides results in dead cells at the interface, shown here with a black interior and/or a rounded shape (caused by toxins that compromise the cell wall). Although dispersal from the edge of a biofilm is possible (yellow cells, top left), movement is generally restricted due to the cells being surrounded by the extracellular matrix. Artwork by Enrico Khatchapuridze.

Alternative Functions of Toxins and Delivery Systems: Metabolism, Virulence and Signalling

Not all bacterial toxins or delivery systems are antimicrobial weapons. For example, many bacteria express several toxin–antitoxin protein pairs in their cells, where the toxins degrade more slowly than the antitoxin. As a result, inactivation of expression leads to self-intoxication, which appears to be a crude but effective way to shut down metabolism and generate dormant, toxin-resistant cells (called persisters) [94]. Other toxins leave the cell but are used on eukaryotic targets during infections [95], or to overcome a single-celled predator [96]. Delivery systems, including some versions of the type VI systems, are also used to target eukaryotic cells [91,97–99], and some type VI systems also appear to be involved in metal ion uptake [100,101].

Caution must be applied, therefore, when assigning function to any bacterial toxin or delivery system. Even mechanisms that do appear to serve as weapons can have additional functions. For example, many weapons also deliver toxins to clonemates as well as competing strains. In some cases, this allows the toxin-receiving cells to detect their toxin-producing clonemates and is used to increase investment into attacks [34] or group formation (specifically biofilms; Figure 4) [102]. An extreme example of functional diversity is the redox-active molecule pyocyanin, made by *P. aeruginosa* (Figure 3). There is experimental evidence that pyocyanin can serve in bacterial warfare [43], cell–cell signalling among clonemates [103], pathogenesis [104], and metabolism (as an alternative electron acceptor for respiration) [105]. Despite each of these effects having its own literature, it remains unclear which of these are true evolutionary functions [106] in the sense that they are important for the fitness of *P. aeruginosa* in nature.

Mechanical Warfare

The weapons of humans and other animals often function via physical damage. In bacteria, the clearest examples of such weapons evolved from the viruses (phage) that infect bacteria. For example, R-type pyocins produced by *P. aeruginosa* resemble phage tails that lack the capsid shell on top that holds the viral DNA [36]. Known as tailocins, the result is a macromolecular machine that binds preferentially to sugar residues on the outer membrane of non-clonemates and physically punches a hole, which leads to massive membrane depolarization and death [107]. Like some protein toxins, the releasing cell must lyse to release R pyocins, making this again a particularly costly mode of attack. The use of mechanical weapons appears less common than chemical weapons and is only known from relatively few species [108]. However, they have a wide phylogenetic distribution and, compared to chemical weapons, they have not been looked for as intensively during the antibiotic era.

Biological Warfare

Many bacteria carry dormant viruses encoded in their genomes. Under stressful conditions, the dormant form (called the prophage) becomes activated to produce large numbers of virulent progeny, which typically leave a cell by lysis [109]. The viruses that can make a prophage are known as temperate phages and have commonly been viewed as pathogens owing to the catastrophic way they often leave a cell, and the potential for subsequent virulent replication [110]. Indeed, once activated and released from a cell, they have the potential to infect and kill vast numbers of bacteria before potentially integrating into new host genomes. However, the characterisation of temperate phages as pathogens of bacteria is questionable given a key feature of their biology. Bacteria that carry a prophage are often immune to infection by copies of the same virus through mechanisms including cell surface modifications that block viral attachment [111]. When a prophage excises itself from the genome and leaves a host cell, therefore, it will typically not harm the clonemates of that cell, as they will carry the same prophage. However, it does have the potential to infect and kill competing strains. In this way, temperate phages may function as powerful biological weapons for the strains that carry them [25,40,112,113].

The cost of carrying a prophage is that a bacterial strain will lose some cells during phage release, but the benefit is that surviving cells can experience greatly reduced competition. These

benefits may be short lived if the phages integrate into the genomes of competitors and immunise them [114]. However, if a cell carries multiple different prophages in its genome, this can reduce the probability of any given target being completely immune [115]. Are temperate phages biological weapons in the strict sense that they have evolved to enable bacteria to kill competitors, or are they simply agents of their own replication that happen to sometimes benefit bacteria [110]? This is a challenging question, and the answer rests on whether bacteria have evolved to allow, or coordinate, phage release. The potential for strong fitness benefits suggests that bacteria may indeed have evolved to enable the use of temperate phages against competitors. Broadly consistent with this, phage release is sometimes co-regulated with the production of the protein toxins used in warfare [116]. Whatever the case, prophage carriage can be a key determinant of bacterial competition, whose importance may prove to rival chemical warfare.

Other Ways to Interfere: Stickiness, Slime, Shape, Speed, and Signals

There are a wide range of other phenotypes in bacteria that allow them to interfere with each other's growth and survival without necessarily causing damage (reviewed in [2,5,117,118]). These mechanisms are more weapon-like than weapons in a strict sense. They include several physical mechanisms that allow bacteria to position and push themselves into nutrient-rich locations, including adhesion [119], the secretion of slimy polymers (extracellular polymeric substances) that allow cells to spread out and smother competitors [120,121], and even cell shape [122]. Movement is another way to gain the best position in a community [123], and there is even the potential for 'information warfare', whereby one species interrupts cell–cell signalling (**quorum sensing**) in another by consuming their signalling molecules [5,124].

The Evolution of Bacterial Warfare

Why Evolve a Weapon?

The incredible abundance and diversity of weapons in bacterial communities raises many questions for evolution and ecology. Most fundamentally, what drives the evolution of **weapons**? Close to forty years ago, two seminal papers showed that the evolutionary benefits to *E. coli* of making colicin toxins were greatest when a producer strain is locally abundant [21,125]. These presaged later studies suggesting that both local frequency and density favour toxin use, because each increases the likelihood that toxins build up enough to be effective [25,26,33,59,126–128]. Gardner *et al.* subsequently highlighted that costly toxin production was a particularly compelling example of 'spiteful' behaviour in the vernacular of sociobiology, as it is costly to the personal fitness of both the actor (toxin producer) and recipient (victim) [22]. They also made the point that, in a sense, toxin production is actually most beneficial at an *intermediate* frequency of producers — too low, and not enough toxin builds up, too high, and there is no one to kill — which was supported by subsequent experiments and agent-based modelling [20,23,24].

Toxin production may also be most favoured at an intermediate level of nutrients. Having some nutrients is important for the evolution of warfare so that a cell can afford to invest in toxin production [129,130]. However, an abundance of nutrients can also favour investing in rapid growth rather than interference, to use up the nutrients first [16]. It may be then that limited — but not too limited — nutrient conditions favour the greatest investment into toxins. Another important correlate of cell density is spatiogenetic structure, that is, the arrangement of different genotypes in space [2]. More work here is needed, but low structure — mixing of different genotypes — can make weapons more favourable as it allows attacking genotypes better access to victims, something that is particularly true for short range weapons like the type VI secretion systems [32]. That said, low structure can also correlate with a low density of any given strain [131], which — as just discussed — disfavours the use of diffusing toxins.

In summary, density, frequency, nutrients, and spatial structure are all predicted to influence the evolution of weapons. However, the effects can be complex and are likely to affect various weapon types differently. For example, whereas diffusing toxins function poorly at low cell density, releasing phages can help a rare strain to invade a community [25]. There is much then to still understand.

Tactics and Strategy: When Should Weapons Be Used?

Once a weapon has evolved, when should a cell actually use it? Decades of work on antibiotics and other toxins made by bacteria have shown that production is often tightly regulated [16,59,61,132]. However, little is known about how these regulatory networks map to the actual behaviours (or **tactics**) and **strategies** used during bacterial contests [16,34]. By contrast, there is a large body of literature on how animals behave during contests [133]. Though little discussed in microbiology [34,35], this literature is useful for thinking about how bacteria use their weapons and highlights both similarities and differences to animals.

Models of animal contests typically consider two individuals and a disputed resource to ask which decisions — such as starting a fight, staying in a fight, and retreating — are favoured by natural selection (for a detailed review see [19]). Rooted in evolutionary **game theory**, these models couch decisions in the context of a wide range of possible strategies, which might be as simple as 'always fight' or 'never fight' but also include more complex behaviours that depend on what the competitor is doing, such as 'retaliate if attacked' (known as a 'tit-for-tat' behaviour). The most discussed case is the 'hawk–dove' model, which asks whether an always-fight (hawk) or never-fight (dove) **strategy** will evolve. This makes the important prediction that fighting is not universally beneficial. Once hawks are common in the population, they will meet other hawks, leading to costly contests that can favour the persistence of doves in the population [19]. This, and later models, went on to identify several factors important in the decision to fight, including the cost of fighting, fighting ability ('resource holding potential'), and the value of a disputed resource [17,19,134,135]. Such factors seem likely to be important for bacteria as well. For example, recent work suggests that *E. coli* strains will only benefit from mounting a strong attack when they have superior fighting ability because, if not, they risk provoking a fierce counterattack that leads to a high cost of fighting [34,35].

The Importance of Information: Competition Sensing, Cues, and Signals

A major theme in the study of animal contests is the importance of information: what exactly can a focal individual glean about

the competitor and the resource, and when is this information available? For example, in animal **combat**, if an assessment can only be made by challenging a competitor, the likelihood of fighting will necessarily increase [19]. In bacteria, information is similarly critical, and the expectation is that a strain will evolve to regulate attacks based upon information that allows it to use weapons prudently but effectively. As in animals [19], we expect bacteria will tend to fight more over high-value resources than low-value ones. However, bacteria often consume resources during a contest, and therefore they may respond to resource levels in different ways to animals. For example, low nutrients can indicate high cell density and a good time to invest in weapons, and data show that nutrient stress promotes toxin production in diverse bacterial species [16]. Nutrient type can also be important. The production of some antibiotics is increased more by the limitation of a cell's preferred carbon source than by depletion of other carbon sources [136], perhaps because this indicates the most threatening form of nutrient competition for bacteria [16].

Another important source of information for a bacterium is cell damage, which may indicate an incoming attack, and there are many links between indicators of cell damage and toxin production in bacteria [16]. These observations led to the idea of **competition sensing**, which argues that bacteria commonly use their stress responses — those that detect nutrient stress and cell damage — as a means to detect and respond to competitors, both defensively and aggressively [16,132,137]. A key corollary of competition sensing is that bacteria, like animals, have evolved the ability to retaliate to incoming attacks. Further evidence of this ability comes from studies on the type VI secretion systems. Whereas many species appear to fire this weapon randomly, *P. aeruginosa* has a type VI system that is fired in response to incoming type VI system attacks, an example of an aggressive tit-for-tat behaviour in bacteria [138].

Both animals and bacteria, therefore, respond to cues from competitors when deciding whether to fight. In evolutionary biology, something is considered a **cue** when information is inadvertently provided by one individual to another, for example one strain consuming nutrients and the other detecting it [139]. This contrasts with a **signal** that evolved to allow one individual to actively communicate with another [139]. This distinction is important as true signals are a critical factor in many animal contests where contestants communicate fighting ability, social status, or intent [133,140,141]. Male red deer, for example, roar to signal their size and strength [142], and rubyspot damselflies display their bright red wing spots to communicate fighting ability [143]. There is a large literature on such signals, suggesting that they evolve to allow individuals to avoid costly fights when the outcome can be easily predicted [133]. It is unclear if bacteria have equivalents of the signals seen in animal contests [144]. Signalling one's quality requires information processing in the receiver that can both decipher the signal and also respond appropriately, and the evolution of such communication is clearly more constrained by bacterial regulatory networks than by animal brains. In addition, these signals are expected to replace weapon use, and lead to mostly peaceful outcomes, which contrasts with many studies suggesting that bacterial weapons are both extensively used and important for competitive outcomes [7,8,10–14,34,40,48–56,72–74,82,84,86,145–147].

Signalling between competitors, therefore, may prove uncommon during bacterial warfare. However, signalling between *cooperators* does occur in the form of **quorum sensing** [139,148–150], and there are many similar responses that can serve to detect or infer a quorum of clonemates [151], such as changes in pH [16]. Such communication among clonemates is commonly used to upregulate toxins, presumably because it indicates high-density conditions where toxin release is effective [5,16]. Bacteria also eavesdrop on competitors' signals: the soil bacterium *Chromobacterium violaceum* detects quorum-sensing molecules of *Burkholderia thailandensis* and upregulates production of antimicrobials [152].

Some weapons double as a means to communicate. Virulent strains of the gut bacterium *Enterococcus faecalis* release a two-subunit toxin (cytolysin) that dissociates upon binding to a range of target cells. One subunit remains and functions as a toxin, and the other is released to function as an autoinducer that activates further toxin production [153]. Cleverly, this signal ensures that toxin is only produced when sufficient numbers of both attackers and targets are present. Interbacterial communication also appears to occur via the contact-dependent growth inhibition system (Figure 1), which promotes group (biofilm) formation when it hits clonemates rather than a competitor [102]. These, and other examples [34], suggest that toxins can serve as signals and cues between clonemates, as well as weapons. What is much less clear is whether antibiotics function as signals between species to allow them to coordinate community functions, as has been suggested, motivated by the observation that bacteria show widespread regulatory responses to sub-inhibitory antibiotic concentrations [154–157]. The prevalence of competition in natural environments [1,158] suggests that these responses to antibiotics are better explained by cells preparing themselves for incoming attacks, and that the antibiotic is serving as an inadvertent cue rather than a signal between species [16,159,160].

In summary, bacteria have the capacity to integrate a wide range of information including nutrient level, nutrient type, cell damage and information on quorum in deciding when to attack. However, bacteria vary in which inputs are used — even within a species [34] — and an interesting challenge is to understand why different bacteria value different information sources differently [16].

Sociality and Sessility: When Contests Become Warfare

The way that bacteria and animals use information during contests, therefore, may differ greatly. In particular, animals are known to often resolve contests using signalling rather than fighting, something with no clear equivalent in bacteria. A second set of differences arises from the fact that many animal fights involve only two, or a few, individuals (Figure 5) [19]. By contrast, bacterial contests often occur in dense bacterial communities, known as biofilms, containing millions of individuals from many different species [161–163]. Moreover, because bacteria can undergo rapid asexual reproduction, a given cell may be surrounded by clonemates in addition to any competitors (Figure 4) [2].

Having clonemates around opens up the possibility of combat strategies that make use of **collective behaviours** involving

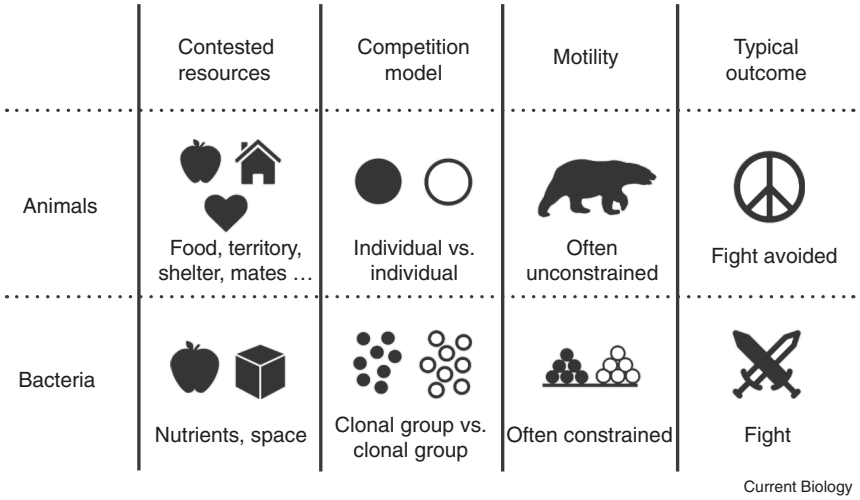

Figure 5. Key differences between the classical game theory of animal contests and bacterial warfare.
Contested resources: Animals typically compete over access to limiting resources such as food, territory, shelter and mates. Bacteria are thought to mostly compete over nutrients and space. *Competition model*: Models of animal contests have typically focused on cases with only two — or a few — individuals, whereas bacterial contests often occur in dense communities comprised of millions of individuals. Moreover, because bacteria can undergo rapid asexual reproduction, a given cell may be surrounded by clonemates in addition to any competitors. *Motility*: The ability to leave a fight is an important option in many animal contests, such as male polar bears fighting over a mate, but bacteria within large communities may become effectively sessile, as their dispersal is highly constrained. *Typical outcome*: Animals commonly evolve behaviours to avoid costly fights, including signals that allow contestants to predict the outcome of fights without actually engaging. This contrasts with what we know about bacterial contests, in which encounters are often intense and lethal.

multiple group members [164], including the use of quorum sensing to coordinate attacks, as just discussed. Cells may also warn others of incoming attacks. *E. coli* cells at the edge of a colony will sense certain incoming toxins and produce their own toxin in response. This production can be detected by their clonemates around and behind them who make their own toxin, triggering yet more toxin production to generate a coordinated and powerful counterattack (Figure 6) [34]. Although not captured by the dyadic models of animal contests that focus on just two individuals [19], such collective behaviour has a striking analogy in group-living animals, where incoming threats often drive alarm signalling. For example, all the major groups of eusocial insects — including bees, ants, wasps, and termites — have independently evolved the use of alarm pheromones that coordinate counterattacks [165].

There are further similarities between bacteria and social animals (Figure 6). A key feature of insect societies is the **division of labour**, in which different individuals perform distinct tasks. This includes the division between reproductive individuals, such as queens, and the workers who often launch vicious attacks on competitors at considerable personal cost [166]. Species like the army-ant *Eciton burchellii* show further specialisation with the production of soldier castes with larger mandibles and bigger bodies than regular workers [167]. Specialisation is also seen in bacterial warfare; antibiotic production in the soil bacterium *Streptomyces coelicolor* (Figure 3) is often performed by a subset of cells (Figure 6) [168]. Moreover, as discussed above, the insects' tendency for self-sacrifice is also seen in bacteria, with several species using cell lysis to release toxins [34,61,169]. The evolution of such traits — those that are costly to an actor's lifetime personal fitness — is the focus of a large literature on social evolution (or sociobiology [170,171]). This literature has shown that behaviours like suicidal attacks only make sense in a social group, where surviving clonemates or family members can benefit to pass on copies of the attacker's genes [22,170].

A final feature of social organisms that may contribute to increased aggression is a decreased ability to leave contests. Although dispersal from the edge of a biofilm is possible (Figure 4) [172], bacteria within large communities can become effectively sessile; so too can social insects that construct large, immovable nests. This constraint on dispersal, as well as the challenges of finding another high value site, may favour aggression to hold a territory and keep out intruders. Consistent with this, social insects are commonly extremely aggressive near their nest [165], and there is evidence for pre-emptive attacks in bacteria from the seemingly constitutive production of antimicrobials (Figure 6) [61,173,174] and contact-dependent toxins [175]. A link between sessile lifestyle and aggression is also known from sessile marine invertebrates, such as sponges, which constitutively produce toxins to kill neighbouring species (Figure 6) [176].

The aggression of bacteria, therefore, may have been promoted by their social and semi-sessile lifestyle, and perhaps also a limited ability to resolve conflicts via signalling (Figure 5). However, much is still unknown, and other factors need consideration. Central among these is the potential for complex evolutionary and ecological dynamics associated with weapons evolution.

Evolutionary and Ecological Dynamics

The diversity, abundance and common use of weapons in bacterial communities brings with it the potential for many knock-on effects. These effects are expected to be particularly important within a species as many bacterial weapons target conspecifics [59] or at least strains in the same physical or metabolic niche [177–179]. This targeting makes sense as these strains are likely to compete strongly for resources [180]. The evolution of a weapon, therefore, has the potential to set off coevolutionary dynamics between species, but the strongest effects may occur within species [181].

Arms Race Evolution

A target strain may evolve resistance to a weapon, in turn generating natural selection on the aggressor to evolve their weapons. Such **coevolution** can then lead to escalation, as in the classic arms race, where each party invests in a greater number of

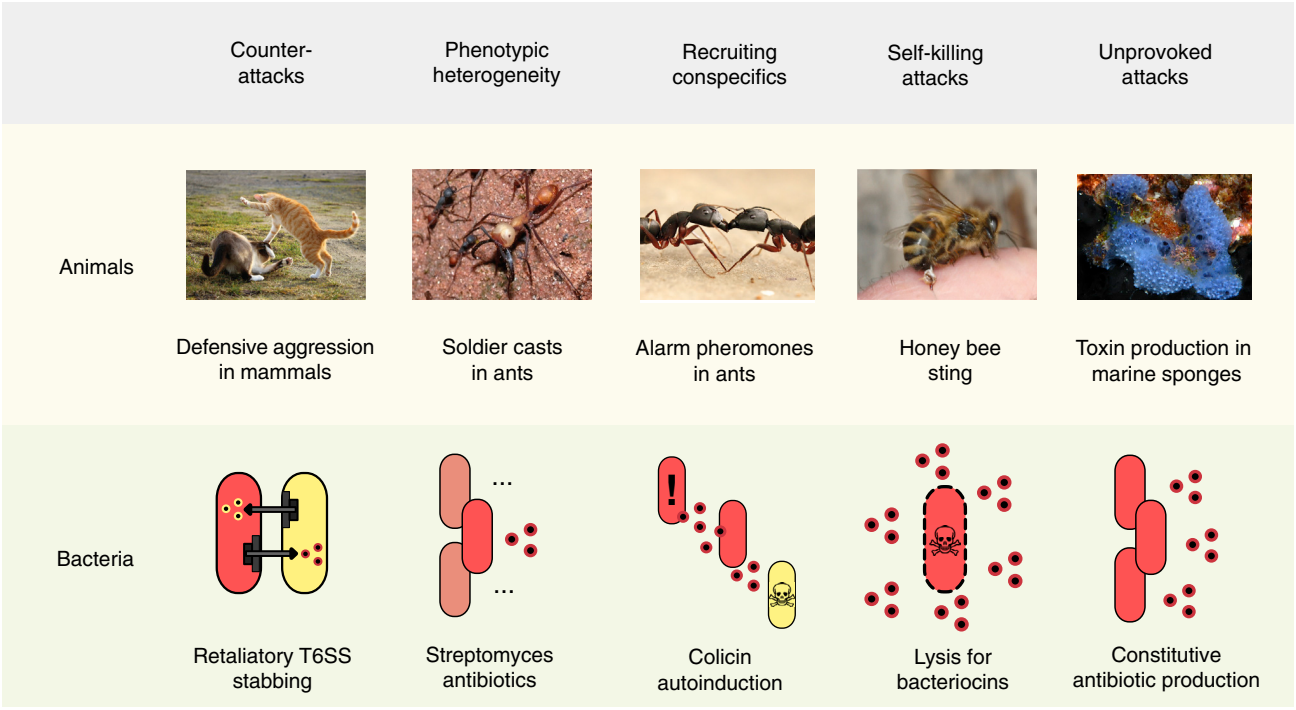

Figure 6. Combat behaviours seen in both bacteria and animals.
Counterattacks: The human pathogen *P. aeruginosa* fires its type VI secretion system into a neighbouring cell in response to an incoming attack, an example of a counterattack behaviour in bacteria [138]. Defensive aggression (retaliation in response to an attack) is also found in animals [221]. *Phenotypic heterogeneity*: The soil bacterium *S. coelicolor* uses a bistable gene switch to ensure that only a fraction of the population engages in the production of a certain antibiotic at low cell densities [168]. The army ant *Eciton burchellii* exhibits extreme physical polymorphism, where specialized soldier ants develop larger mandibles and bigger bodies than regular workers [167]. *Recruiting conspecifics*: *E. coli* cells sense incoming toxins and produce their own toxin in response. This production can be detected by their clonemates who then make their own toxin, triggering a coordinated counterattack [34]. Similarly, eusocial insects commonly use alarm pheromones to recruit conspecifics to the site of conflict [165]. *Self-killing attacks*: Many bacterial toxins — for example, colicins in *E. coli* — require the producing cell to lyse in order to be released [61]. Similarly, honeybee workers use their sting to protect the hive at a considerable cost, often leading to the worker's death [166]. *Unprovoked attacks*: Some bacteria constitutively produce antimicrobial compounds, even when growing alone and unchallenged by a competitor [174]. The marine sponge *Dysidea* sp. also appears to constitutively produce toxins to kill neighbouring species [176]. Image sources: domestic cats (credit: rihaij/Pixabay); soldier ant (© Alex Wild, used by permission); two ants communicating (credit: Rakeshkdogra/Wikimedia Commons (CC BY-SA 3.0)); honeybee (credit: Waugsberg/Wikimedia Commons (CC BY-SA 3.0)); *Dysidea* sponge (credit: Flower Garden Banks National Marine Sanctuary).

weapons and/or defences, resulting in reciprocal directional natural selection [182]. This process may have contributed to the general aggression exhibited by many bacteria, both in terms of how often, and how many, weapons are used. Identifying escalation and the evolutionary forces that drove it is challenging after the fact. However, when one strain of bacteria — specifically soil bacteria of the genus *Streptomyces* — inhibits another strain, it is more likely than average to be inhibited in return, possibly indicating the escalation of arms between competitors [183]. Particularly compelling is the case of *Streptomyces clavuligerus,* which makes multiple beta-lactam (penicillin-type) antibiotics, including cephamycin C. In many other species, resistance to these antibiotics is conferred by beta-lactamase enzymes that digest the antibiotics. However, *S. clavuligerus* has evolved to produce an additional compound, clavulanic acid, which inhibits the beta-lactamases of potential competitors [184]. So powerful is the cocktail of beta-lactam antibiotic and beta-lactamase inhibitor, it has long been used as a combination drug therapy in the clinic [185].

In addition to such specific mechanisms, the evolution of weapons appears to have driven the evolution of general defences in many bacterial species. Key candidates include the use of efflux pumps to remove toxins [67], the formation of protective biofilms (Figure 4) in response to cell damage [180], and the production of a small number of non-dividing persister cells that can survive extreme toxin concentrations [94,186].

Cyclical Coevolution, Frequency Dependence, and the Evolution of Diversity

Evolution does not always escalate [181]. The evolution of resistance by one strain can simply favour reduced use, or loss, of a weapon by an attacking strain [187]. The loss of the weapon, in turn, can favour the loss of resistance, which can itself be costly. This may lead to what is known as a 'rock-paper-scissors' dynamic that cycles through strategies of toxin production, resistance and susceptibility — a scenario that has been shown experimentally in *E. coli* [31,188]. Further diversity and complexity may be created if the resistance mechanism actively degrades the antibiotic so that one strain or species may protect others in the community [29].

Once resistance for one toxin is common, natural selection is also expected to favour strains that produce a different, rarer toxin for which resistance has not yet evolved [59]. This can

lead to cyclical evolutionary dynamics in which a large diversity of toxins is maintained in a population [27]. Consistent with rapid evolutionary turnover in weapons and defences, the strength of antagonism between bacterial strains is often poorly correlated with their phylogeny [177,178,189]. Moreover, while a given strain will often produce inhibitory factors, it may only kill a small subset of potential target strains [177,183], perhaps because it may be cheaper to carry genes for resistance than for weaponry [178]. This raises the intriguing possibility that coevolutionary dynamics may lead to a situation where, at any one time, bacteria are investing heavily in weapons that are largely ineffective.

Central to many models of weapon turnover is what is known as negative frequency-dependent selection, whereby rare strategies tend to have an advantage. Negative frequency dependence is a general process that generates genetic diversity [181], and is a major theme in the evolutionary game theory of animal combat, where a diversity of strategies is commonly predicted (mixed evolutionarily stable strategies) [17,19,34]. Whereas the benefits of having a rare toxin can generate negative frequency dependence, at smaller spatial scales there is also the potential for positive frequency-dependent selection. This is because, as discussed, a locally abundant strain can generate high toxin concentrations to kill competitors [21,125]. This effect can remove diversity locally but, when combined with stochasticity in which genotype colonises each position, the result can be a patchwork quilt where each genotype dominates locally but not further afield. Such spatial ecology appears to mirror coral reefs, where clonal groups of coral polyps exist in close proximity [190–192] and stochastic immigration, competition and chemical warfare are important [193,194].

Horizontal Gene Transfer and Multi-Level Selection In Bacterial Warfare

Unlike animals, bacteria are often able to pick up and express small pieces of DNA via horizontal gene transfer. This, and the modular organisation of bacterial genomes, means that bacteria have the potential to rapidly gain and lose a wide diversity of weapons. Weapon acquisition can even occur during contests, as some species co-regulate DNA uptake with the use of chemical weapons [195,196]. A similar link is seen in certain temperate phages that, upon infecting a new bacterial strain, generate some phage particles containing DNA of the bacterial victim instead of their own phage DNA. These particles are then picked up by the original bacterial host in large numbers allowing the killer to widely sample the DNA of the victim [197]. In these examples, weapons can then be used to steal the weapons and defences of competitors, as well as to kill [198].

Horizontal gene transfer has the potential to strongly shape bacterial communities by allowing diverse strains to acquire the same phenotypes [199]. Such horizontal acquisition of weapons and defences may explain the surprising result from marine bacteria that strains from a given community are less likely to kill each other than those from other communities [200]. Indeed, many bacterial weapons are associated with mobile genetic elements [59], which means that the ecology and evolution of weapons can be partially decoupled from the bacteria that carry them. For example, a plasmid for a given toxin may occur in a niche that is overlapping with, but distinct from, all of its bacterial hosts [199]. Evolutionarily, there can be conflicts of interests between the mobile elements carrying the weapons and their bacterial hosts, something that is most clear when a prophage of one bacterial strain integrates into a competing strain and immunizes it from further attack [114]. The potential for multi-level selection to shape the evolution of mobile genetic elements has long been recognized [201], but its impact on bacterial warfare remains little explored.

Conclusions and Applications

Microbes affect many aspects of our lives; they shape ecosystems, agriculture, industrial processes, health, and disease. There is particular interest in the plant- and animal-associated communities that are central to the health and welfare of their host [202–205]. The study of bacterial warfare can help with understanding and manipulating these vital communities [206].

Most simply, possession of a weapon can predict whether a particular pathogen will invade or a symbiont persist [7–14,48–56,207,208]. Weapon use also has the potential for complex effects that ripple through communities, as each species may affect multiple others via nutrient competition and release, in addition to warfare [2–6,118,158]. Host-associated communities also enable audacious forms of bacterial warfare that work by provoking the host to attack the whole community [209]. For example, the gut pathogen *Salmonella enterica* serovar Typhimurium uses a sub-population of cells to invade the host gut epithelium and provoke a massive immune response. This devastates the bacterial populations in the gut, but the remaining *S.* Typhimurium use a chemical byproduct of the immune response to respire and rapidly proliferate [210]. A challenge looking forward is to understand the causes and consequences of warfare within such complex ecological systems, both for individual species and for system-level properties like community stability [29,211].

We also need ways to manipulate microbial communities. Broad-spectrum antibiotics are commonly used to suppress pathogens, but they also harm many other species in the microbiota. Considering the full diversity of bacterial weapons reveals many narrow-spectrum alternatives, such as the protein bacteriocins [212]. Further specificity may be achieved by identifying probiotic species that release toxins right next to a pathogen being targeted [51,206]. Probiotics also have the potential to evolve, raising the possibility that resistance evolution will be less of an issue than for antibiotics. The evolution of resistance will nevertheless be a problem, both for drugs and for probiotic strategies. The study of bacterial behaviour during contests can help, as some species reveal new toxins, and mechanisms of drug resistance, when in competition with other species [16,132]. Finally, there is the intriguing potential to treat disease with small amounts of drugs that provoke bacteria to fight, and thereby eliminate one another [35].

For close to a century, microbiologists have studied mechanisms of bacterial warfare [213]. This has revealed an astonishing abundance and diversity of weapons, many of which are used despite considerable costs of deployment. Understanding the causes and consequences of bacterial aggression is an open challenge for evolutionary biology and ecology. And as we

seek to remove problem strains, or manipulate microbial communities, we would do well to remember that bacteria have spent the last three billion years doing just this.

SUPPLEMENTAL INFORMATION

Supplemental Information includes one figure, one table and supplemental references and can be found with this article online at https://doi.org/10.1016/j.cub.2019.04.024.

ACKNOWLEDGEMENTS

The authors are grateful to Sean Cameron Booth, Olivier Cunrath, Kayla King, Rolf Kümmerli, Carey Nadell, Connor Sharp and Sofia van Moorsel for providing comments on the manuscript. We would also like to thank Enrico Khatchapuridze for generating the illustration shown in Figure 4. E.T.G. is funded by a Postdoc Mobility Fellowship from the Swiss National Science Foundation (P2ZHP3_174751). T.A.M.-L. acknowledges funding from the University of Oxford, the EPSRC & BBSRC Centre for Doctoral Training in Synthetic Biology (grant EP/L016494/1). K.R.F. is funded by European Research Council Grant 787932 and Wellcome Trust Investigator award 209397/Z/17/Z.

REFERENCES

1. Foster, K.R., and Bell, T. (2012). Competition, not cooperation, dominates interactions among culturable microbial species. Curr. Biol. *22*, 1845–1850.
2. Nadell, C.D., Drescher, K., and Foster, K.R. (2016). Spatial structure, cooperation and competition in biofilms. Nat. Rev. Microbiol. *14*, 589–600.
3. Stubbendieck, R.M., and Straight, P.D. (2016). Multifaceted interfaces of bacterial competition. J. Bacteriol. *198*, 2145–2155.
4. West, S.A., Diggle, S.P., Buckling, A., Gardner, A., and Griffin, A.S. (2007). The social lives of microbes. Annu. Rev. Ecol. Evol. Syst. *38*, 53–77.
5. Hibbing, M.E., Fuqua, C., Parsek, M.R., and Peterson, S.B. (2010). Bacterial competition: surviving and thriving in the microbial jungle. Nat. Rev. Microbiol. *8*, 15–25.
6. Flint, H.J., Bayer, E.A., Rincon, M.T., Lamed, R., and White, B.A. (2008). Polysaccharide utilization by gut bacteria: potential for new insights from genomic analysis. Nat. Rev. Microbiol. *6*, 121–131.
7. Bosák, J., Micenková, L., Hrala, M., Pomorská, K., Kunova Bosakova, M., Krejci, P., Göpfert, E., Faldyna, M., and Šmajs, D. (2018). Colicin FY inhibits pathogenic *Yersinia enterocolitica* in mice. Sci. Rep. *8*, 12242.
8. Chassaing, B., and Cascales, E. (2018). Antibacterial weapons: targeted destruction in the microbiota. Trends Microbiol. *26*, 329–338.
9. Gillor, O., Giladi, I., and Riley, M.A. (2009). Persistence of colicinogenic *Escherichia coli* in the mouse gastrointestinal tract. BMC Microbiol. *9*, 165.
10. Kommineni, S., Bretl, D.J., Lam, V., Chakraborty, R., Hayward, M., Simpson, P., Cao, Y., Bousounis, P., Kristich, C.J., and Salzman, N.H. (2015). Bacteriocin production augments niche competition by enterococci in the mammalian gastrointestinal tract. Nature *526*, 719–722.
11. Russell, A.B., Wexler, A.G., Harding, B.N., Whitney, J.C., Bohn, A.J., Goo, Y.A., Tran, B.Q., Barry, N.A., Zheng, H., Peterson, S.B., *et al.* (2014). A type VI secretion-related pathway in bacteroidetes mediates interbacterial antagonism. Cell Host Microbe *16*, 227–236.
12. Sana, T.G., Flaugnatti, N., Lugo, K.A., Lam, L.H., Jacobson, A., Baylot, V., Durand, E., Journet, L., Cascales, E., and Monack, D.M. (2016). *Salmonella* Typhimurium utilizes a T6SS-mediated antibacterial weapon to establish in the host gut. Proc. Natl. Acad. Sci. USA *113*, E5044–E5051.
13. Speare, L., Cecere, A.G., Guckes, K.R., Smith, S., Wollenberg, M.S., Mandel, M.J., Miyashiro, T., and Septer, A.N. (2018). Bacterial symbionts use a type VI secretion system to eliminate competitors in their natural host. Proc. Natl. Acad. Sci. USA *115*, E8528–E8537.
14. Wexler, A.G., Bao, Y., Whitney, J.C., Bobay, L.-M., Xavier, J.B., Schofield, W.B., Barry, N.A., Russell, A.B., Tran, B.Q., Goo, Y.A., *et al.* (2016). Human symbionts inject and neutralize antibacterial toxins to persist in the gut. Proc. Natl. Acad. Sci. USA *113*, 3639–3644.
15. Brown, S.P., Fredrik Inglis, R., and Taddei, F. (2009). Evolutionary ecology of microbial wars: within-host competition and (incidental) virulence. Evol. Appl. *2*, 32–39.
16. Cornforth, D.M., and Foster, K.R. (2013). Competition sensing: the social side of bacterial stress responses. Nat. Rev. Microbiol. *11*, 285–293.
17. Maynard Smith, J., and Price, G.R. (1973). The logic of animal conflict. Nature *246*, 15–18.
18. Enquist, M., and Leimar, O. (1990). The evolution of fatal fighting. Anim. Behav. *39*, 1–9.
19. Kokko, H. (2013). Dyadic contests: modelling fights between two individuals. In Animal Contests, I.C.W. Hardy, and M. Briffa, eds. (Cambridge: Cambridge University Press), pp. 5–32.
20. Bucci, V., Nadell, C.D., and Xavier, J.B. (2011). The evolution of bacteriocin production in bacterial biofilms. Am. Nat. *178*, E162–E173.
21. Chao, L., and Levin, B.R. (1981). Structured habitats and the evolution of anticompetitor toxins in bacteria. Proc. Natl. Acad. Sci. USA *78*, 6324–6328.
22. Gardner, A., West, S.A., and Buckling, A. (2004). Bacteriocins, spite and virulence. Proc. Biol. Sci. *271*, 1529–1535.
23. Inglis, R.F., Gardner, A., Cornelis, P., and Buckling, A. (2009). Spite and virulence in the bacterium *Pseudomonas aeruginosa*. Proc. Natl. Acad. Sci. USA *106*, 5703–5707.
24. Inglis, R.F., Roberts, P.G., Gardner, A., and Buckling, A. (2011). Spite and the scale of competition in *Pseudomonas aeruginosa*. Am. Nat. *178*, 276–285.
25. Brown, S.P., Le Chat, L., De Paepe, M., and Taddei, F. (2006). Ecology of microbial invasions: amplification allows virus carriers to invade more rapidly when rare. Curr. Biol. *16*, 2048–2052.
26. Levin, B.R. (1988). Frequency-dependent selection in bacterial populations. Philos. Trans. R. Soc. B Biol. Sci. *319*, 459–472.
27. Biernaskie, J.M., Gardner, A., and West, S.A. (2013). Multicoloured greenbeards, bacteriocin diversity and the rock-paper-scissors game. J. Evol. Biol. *26*, 2081–2094.
28. Czárán, T.L., Hoekstra, R.F., Pagie, L., and Levin, S.A. (2002). Chemical warfare between microbes promotes biodiversity. Proc. Natl. Acad. Sci. USA *99*, 786–790.
29. Kelsic, E.D., Zhao, J., Vetsigian, K., and Kishony, R. (2015). Counteraction of antibiotic production and degradation stabilizes microbial communities. Nature *521*, 516–519.
30. Kerr, B., Riley, M.A., Feldman, M.W., and Bohannan, B.J.M. (2002). Local dispersal promotes biodiversity in a real-life game of rock-paper-scissors. Nature *418*, 171–174.
31. Kirkup, B.C., and Riley, M.A. (2004). Antibiotic-mediated antagonism leads to a bacterial game of rock–paper–scissors in vivo. Nature *428*, 412–414.
32. McNally, L., Bernardy, E., Thomas, J., Kalziqi, A., Pentz, J., Brown, S.P., Hammer, B.K., Yunker, P.J., and Ratcliff, W.C. (2017). Killing by Type VI secretion drives genetic phase separation and correlates with increased cooperation. Nat. Commun. *8*, 14371.
33. Rendueles, O., Amherd, M., and Velicer, G.J. (2015). Positively frequency-dependent interference competition maintains diversity and pervades a natural population of cooperative microbes. Curr. Biol. *25*, 1673–1681.
34. Mavridou, D.A.I., Gonzalez, D., Kim, W., West, S.A., and Foster, K.R. (2018). Bacteria use collective behavior to generate diverse combat strategies. Curr. Biol. *28*, 345–355.
35. Gonzalez, D., Sabnis, A., Foster, K.R., and Mavridou, D.A.I. (2018). Costs and benefits of provocation in bacterial warfare. Proc. Natl. Acad. Sci. USA *115*, 7593–7598.

36. Michel-Briand, Y., and Baysse, C. (2002). The pyocins of *Pseudomonas aeruginosa*. Biochimie *84*, 499–510.

37. Ghequire, M.G.K., and De Mot, R. (2014). Ribosomally encoded antibacterial proteins and peptides from *Pseudomonas*. FEMS Microbiol. Rev. *38*, 523–568.

38. Russell, A.B., Peterson, S.B., and Mougous, J.D. (2014). Type VI secretion system effectors: poisons with a purpose. Nat. Rev. Microbiol. *12*, 137–148.

39. Mercy, C., Ize, B., Salcedo, S.P., de Bentzmann, S., and Bigot, S. (2016). Functional characterization of *Pseudomonas* contact dependent growth inhibition (CDI) systems. PLoS One *11*, e0147435.

40. Davies, E.V., James, C.E., Kukavica-Ibrulj, I., Levesque, R.C., Brockhurst, M.A., and Winstanley, C. (2016). Temperate phages enhance pathogen fitness in chronic lung infection. ISME J. *10*, 2553–2555.

41. Rice, S.A., Tan, C.H., Mikkelsen, P.J., Kung, V., Woo, J., Tay, M., Hauser, A., McDougald, D., Webb, J.S., and Kjelleberg, S. (2009). The biofilm life cycle and virulence of *Pseudomonas aeruginosa* are dependent on a filamentous prophage. ISME J. *3*, 271–282.

42. Anderson, R.D., Roddam, L.F., Bettiol, S., Sanderson, K., and Reid, D.W. (2010). Biosignificance of bacterial cyanogenesis in the CF lung. J. Cyst. Fibros. *9*, 158–164.

43. Korgaonkar, A.K., and Whiteley, M. (2011). *Pseudomonas aeruginosa* enhances production of an antimicrobial in response to N-acetylglucosamine and peptidoglycan. J. Bacteriol. *193*, 909–917.

44. Kadurugamuwa, J.L., Mayer, A., Messner, P., Ra, M.S., Sleytr, U.B., and Beveridge, T.J. (1998). S-layered *Aneurinibacillus* and *Bacillus* spp. are susceptible to the lytic action of *Pseudomonas aeruginosa* membrane vesicles. J. Bacteriol. *180*, 2306–2311.

45. Sharp, C., Bray, J., Housden, N.G., Maiden, M.C.J., and Kleanthous, C. (2017). Diversity and distribution of nuclease bacteriocins in bacterial genomes revealed using Hidden Markov Models. PLoS Comput. Biol. *13*, e1005652.

46. Castelle, C.J., and Banfield, J.F. (2018). Major new microbial groups expand diversity and alter our understanding of the tree of life. Cell *172*, 1181–1197.

47. Bor, B., McLean, J.S., Foster, K.R., Cen, L., To, T.T., Serrato-Guillen, A., Dewhirst, F.E., Shi, W., and He, X. (2018). Rapid evolution of decreased host susceptibility drives a stable relationship between ultrasmall parasite TM7x and its bacterial host. Proc. Natl. Acad. Sci. USA *115*, 12277–12282.

48. Hsieh, P.-F., Lu, Y.-R., Lin, T.-L., Lai, L.-Y., and Wang, J.-T. (2019). *Klebsiella pneumoniae* Type VI secretion system contributes to bacterial competition, cell invasion, Type-1 fimbriae expression, and in vivo colonization. J. Infect. Dis. *219*, 637–647.

49. Ma, L.-S., Hachani, A., Lin, J.-S., Filloux, A., and Lai, E.-M. (2014). *Agrobacterium tumefaciens* deploys a superfamily of Type VI secretion DNase effectors as weapons for interbacterial competition in planta. Cell Host Microbe *16*, 94–104.

50. Roelofs, K.G., Coyne, M.J., Gentyala, R.R., Chatzidaki-Livanis, M., and Comstock, L.E. (2016). *Bacteroidales* secreted antimicrobial proteins target surface molecules necessary for gut colonization and mediate competition *in vivo*. mBio *7*, e01055–16.

51. Sassone-Corsi, M., Nuccio, S.-P., Liu, H., Hernandez, D., Vu, C.T., Takahashi, A.A., Edwards, R.A., and Raffatellu, M. (2016). Microcins mediate competition among Enterobacteriaceae in the inflamed gut. Nature *540*, 280–283.

52. Chatzidaki-Livanis, M., Geva-Zatorsky, N., and Comstock, L.E. (2016). *Bacteroides fragilis* type VI secretion systems use novel effector and immunity proteins to antagonize human gut Bacteroidales species. Proc. Natl. Acad. Sci. USA *113*, 3627–3632.

53. Nakatsuji, T., Chen, T.H., Narala, S., Chun, K.A., Two, A.M., Yun, T., Shafiq, F., Kotol, P.F., Bouslimani, A., Melnik, A.V., *et al*. (2017). Antimicrobials from human skin commensal bacteria protect against *Staphylococcus aureus* and are deficient in atopic dermatitis. Sci. Transl. Med. *9*, eaah4680.

54. Verster, A.J., Ross, B.D., Radey, M.C., Bao, Y., Goodman, A.L., Mougous, J.D., and Borenstein, E. (2017). The landscape of Type VI secretion across human gut microbiomes reveals its role in community composition. Cell Host Microbe *22*, 411–419.

55. Zipperer, A., Konnerth, M.C., Laux, C., Berscheid, A., Janek, D., Weidenmaier, C., Burian, M., Schilling, N.A., Slavetinsky, C., Marschal, M., *et al*. (2016). Human commensals producing a novel antibiotic impair pathogen colonization. Nature *535*, 511–516.

56. García-Bayona, L., and Comstock, L.E. (2018). Bacterial antagonism in host-associated microbial communities. Science *361*, eaat2456.

57. O'Sullivan, J.N., Rea, M.C., O'Connor, P.M., Hill, C., and Ross, R.P. (2019). Human skin microbiota is a rich source of bacteriocin-producing staphylococci that kill human pathogens. FEMS Microbiol. Ecol. *95*, fiy241.

58. Kohanski, M.A., Dwyer, D.J., and Collins, J.J. (2010). How antibiotics kill bacteria: from targets to networks. Nat. Rev. Microbiol. *8*, 423–435.

59. Riley, M.A., and Chavan, M.A. (2007). Bacteriocins, First edition (Berlin: Springer).

60. Shaheen, M., Li, J., Ross, A.C., Vederas, J.C., and Jensen, S.E. (2011). *Paenibacillus polymyxa* PKB1 produces variants of Polymyxin B-type antibiotics. Chem. Biol. *18*, 1640–1648.

61. Cascales, E., Buchanan, S.K., Duche, D., Kleanthous, C., Lloubes, R., Postle, K., Riley, M., Slatin, S., and Cavard, D. (2007). Colicin biology. Microbiol. Mol. Biol. Rev. *71*, 158–229.

62. Huang, K.C., Mukhopadhyay, R., Wen, B., Gitai, Z., and Wingreen, N.S. (2008). Cell shape and cell-wall organization in Gram-negative bacteria. Proc. Natl. Acad. Sci. USA *105*, 19282–19287.

63. Beck, C.M., Morse, R.P., Cunningham, D.A., Iniguez, A., Low, D.A., Goulding, C.W., and Hayes, C.S. (2014). CdiA from *Enterobacter cloacae* delivers a toxic ribosomal RNase into target bacteria. Structure *22*, 707–718.

64. Hood, R.D., Singh, P., Hsu, F., Güvener, T., Carl, M.A., Trinidad, R.R.S., Silverman, J.M., Ohlson, B.B., Hicks, K.G., Plemel, R.L., *et al*. (2010). A Type VI secretion system of *Pseudomonas aeruginosa* targets a toxin to bacteria. Cell Host Microbe *7*, 25–37.

65. Cundliffe, E. (1989). How antibiotic-producing organisms avoid suicide. Annu. Rev. Microbiol. *43*, 207–233.

66. Hopwood, D.A. (2007). How do antibiotic-producing bacteria ensure their self-resistance before antibiotic biosynthesis incapacitates them? Mol. Microbiol. *63*, 937–940.

67. Masi, M., Réfregiers, M., Pos, K.M., and Pagès, J.-M. (2017). Mechanisms of envelope permeability and antibiotic influx and efflux in Gram-negative bacteria. Nat. Microbiol. *2*, 17001.

68. Zheng, S., and Sonomoto, K. (2018). Diversified transporters and pathways for bacteriocin secretion in Gram-positive bacteria. Appl. Microbiol. Biotechnol. *102*, 4243–4253.

69. Toyofuku, M., Nomura, N., and Eberl, L. (2019). Types and origins of bacterial membrane vesicles. Nat. Rev. Microbiol. *17*, 13–24.

70. Housden, N.G., and Kleanthous, C. (2012). Colicin translocation across the *Escherichia coli* outer membrane. Biochem. Soc. Trans. *40*, 1475–1479.

71. Kleanthous, C. (2010). Swimming against the tide: progress and challenges in our understanding of colicin translocation. Nat. Rev. Microbiol. *8*, 843–848.

72. Vassallo, C.N., Cao, P., Conklin, A., Finkelstein, H., Hayes, C.S., and Wall, D. (2017). Infectious polymorphic toxins delivered by outer membrane exchange discriminate kin in myxobacteria. Elife *6*, e29397.

73. Stempler, O., Baidya, A.K., Bhattacharya, S., Malli Mohan, G.B., Tzipilevich, E., Sinai, L., Mamou, G., and Ben-Yehuda, S. (2017). Interspecies nutrient extraction and toxin delivery between bacteria. Nat. Commun. *8*, 315.

74. Aoki, S.K., Pamma, R., Hernday, A.D., Bickham, J.E., Braaten, B.A., and Low, D.A. (2005). Contact-dependent inhibition of growth in *Escherichia coli*. Science *309*, 1245–1248.

75. Aoki, S.K., Diner, E.J., t'Kint de Roodenbeke, C., Burgess, B.R., Poole, S.J., Braaten, B.A., Jones, A.M., Webb, J.S., Hayes, C.S., Cotter, P.A., *et al*. (2010). A widespread family of polymorphic contact-dependent toxin delivery systems in bacteria. Nature *468*, 439–442.

76. Perault, A.I., and Cotter, P.A. (2018). Three distinct contact-dependent growth inhibition systems mediate interbacterial competition by the cystic fibrosis pathogen *Burkholderia dolosa*. J. Bacteriol. *200*, e00428–18.

77. Ruhe, Z.C., Low, D.A., and Hayes, C.S. (2013). Bacterial contact-dependent growth inhibition. Trends Microbiol. *21*, 230–237.

78. Ruhe, Z.C., Subramanian, P., Song, K., Nguyen, J.Y., Stevens, T.A., Low, D.A., Jensen, G.J., and Hayes, C.S. (2018). Programmed secretion arrest and receptor-triggered toxin export during antibacterial contact-dependent growth inhibition. Cell *175*, 921–933.

79. Hayes, C.S., Koskiniemi, S., Ruhe, Z.C., Poole, S.J., and Low, D.A. (2014). Mechanisms and biological roles of contact-dependent growth inhibition systems. Cold Spring Harb. Perspect. Med. *4*, a010025.

80. Ruhe, Z.C., Wallace, A.B., Low, D.A., and Hayes, C.S. (2013). Receptor polymorphism restricts contact-dependent growth inhibition to members of the same species. mBio *4*, e00480–13.

81. García-Bayona, L., Guo, M.S., and Laub, M.T. (2017). Contact-dependent killing by *Caulobacter crescentus* via cell surface-associated, glycine zipper proteins. Elife *6*, e24869.

82. Cao, Z., Casabona, M.G., Kneuper, H., Chalmers, J.D., and Palmer, T. (2017). The type VII secretion system of *Staphylococcus aureus* secretes a nuclease toxin that targets competitor bacteria. Nat. Microbiol. *2*, 16183.

83. Whitney, J.C., Peterson, S.B., Kim, J., Pazos, M., Verster, A.J., Radey, M.C., Kulasekara, H.D., Ching, M.Q., Bullen, N.P., Bryant, D., *et al*. (2017). A broadly distributed toxin family mediates contact-dependent antagonism between Gram-positive bacteria. Elife *6*, e26938.

84. Souza, D.P., Oka, G.U., Alvarez-Martinez, C.E., Bisson-Filho, A.W., Dunger, G., Hobeika, L., Cavalcante, N.S., Alegria, M.C., Barbosa, L.R.S., Salinas, R.K., *et al*. (2015). Bacterial killing via a type IV secretion system. Nat. Commun. *6*, 6453.

85. Pukatzki, S., Ma, A.T., Sturtevant, D., Krastins, B., Sarracino, D., Nelson, W.C., Heidelberg, J.F., and Mekalanos, J.J. (2006). Identification of a conserved bacterial protein secretion system in *Vibrio cholerae* using the *Dictyostelium* host model system. Proc. Natl. Acad. Sci. USA *103*, 1528–1533.

86. MacIntyre, D.L., Miyata, S.T., Kitaoka, M., and Pukatzki, S. (2010). The *Vibrio cholerae* type VI secretion system displays antimicrobial properties. Proc. Natl. Acad. Sci. USA *107*, 19520–19524.

87. Schwarz, S., West, T.E., Boyer, F., Chiang, W.-C., Carl, M.A., Hood, R.D., Rohmer, L., Tolker-Nielsen, T., Skerrett, S.J., and Mougous, J.D. (2010). *Burkholderia* type VI secretion systems have distinct roles in eukaryotic and bacterial cell interactions. PLoS Pathog. *6*, e1001068.

88. Boyer, F., Fichant, G., Berthod, J., Vandenbrouck, Y., and Attree, I. (2009). Dissecting the bacterial type VI secretion system by a genome wide in silico analysis: what can be learned from available microbial genomic resources? BMC Genomics *10*, 104.

89. Basler, M. (2015). Type VI secretion system: secretion by a contractile nanomachine. Philos. Trans. R. Soc. B Biol. Sci. *370*, 20150021.

90. Basler, M., Pilhofer, M., Henderson, G.P., Jensen, G.J., and Mekalanos, J.J. (2012). Type VI secretion requires a dynamic contractile phage tail-like structure. Nature *483*, 182–186.

91. Ho, B.T., Dong, T.G., and Mekalanos, J.J. (2014). A view to a kill: the bacterial type VI secretion system. Cell Host Microbe *15*, 9–21.

92. Anderson, M.C., Vonaesch, P., Saffarian, A., Marteyn, B.S., and Sansonetti, P.J. (2017). *Shigella sonnei* encodes a functional T6SS used for interbacterial competition and niche occupancy. Cell Host Microbe *21*, 769–776.

93. Zhao, W., Caro, F., Robins, W., and Mekalanos, J.J. (2018). Antagonism toward the intestinal microbiota and its effect on *Vibrio cholerae* virulence. Science *359*, 210–213.

94. Harms, A., Maisonneuve, E., and Gerdes, K. (2016). Mechanisms of bacterial persistence during stress and antibiotic exposure. Science *354*, aaf4268.

95. Ramachandran, G. (2014). Gram-positive and Gram-negative bacterial toxins in sepsis: A brief review. Virulence *5*, 213–218.

96. Matz, C., Deines, P., Boenigk, J., Arndt, H., Eberl, L., Kjelleberg, S., and Jurgens, K. (2004). Impact of violacein-producing bacteria on survival and feeding of bacterivorous nanoflagellates. Appl. Environ. Microbiol. *70*, 1593–1599.

97. Pukatzki, S., Ma, A.T., Revel, A.T., Sturtevant, D., and Mekalanos, J.J. (2007). Type VI secretion system translocates a phage tail spike-like protein into target cells where it cross-links actin. Proc. Natl. Acad. Sci. USA *104*, 15508–15513.

98. Suarez, G., Sierra, J.C., Erova, T.E., Sha, J., Horneman, A.J., and Chopra, A.K. (2010). A type VI secretion system effector protein, VgrG1, from *Aeromonas hydrophila* that induces host cell toxicity by ADP ribosylation of actin. J. Bacteriol. *192*, 155–168.

99. Wan, B., Zhang, Q., Ni, J., Li, S., Wen, D., Li, J., Xiao, H., He, P., Ou, H., Tao, J., *et al*. (2017). Type VI secretion system contributes to Enterohemorrhagic *Escherichia coli* virulence by secreting catalase against host reactive oxygen species (ROS). PLoS Pathog. *13*, e1006246.

100. Chen, W.-J., Kuo, T.-Y., Hsieh, F.-C., Chen, P.-Y., Wang, C.-S., Shih, Y.-L., Lai, Y.-M., Liu, J.-R., Yang, Y.-L., and Shih, M.-C. (2016). Involvement of type VI secretion system in secretion of iron chelator pyoverdine in *Pseudomonas taiwanensis*. Sci. Rep. *6*, 32950.

101. Wang, T., Si, M., Song, Y., Zhu, W., Gao, F., Wang, Y., Zhang, L., Zhang, W., Wei, G., Luo, Z.-Q., *et al*. (2015). Type VI secretion system transports Zn2+ to combat multiple stresses and host immunity. PLoS Pathog. *11*, e1005020.

102. Garcia, E.C., Perault, A.I., Marlatt, S.A., and Cotter, P.A. (2016). Interbacterial signaling via *Burkholderia* contact-dependent growth inhibition system proteins. Proc. Natl. Acad. Sci. USA *113*, 8296–8301.

103. Dietrich, L.E.P., Price-Whelan, A., Petersen, A., Whiteley, M., and Newman, D.K. (2006). The phenazine pyocyanin is a terminal signalling factor in the quorum sensing network of *Pseudomonas aeruginosa*. Mol. Microbiol. *61*, 1308–1321.

104. Hall, S., McDermott, C., Anoopkumar-Dukie, S., McFarland, A., Forbes, A., Perkins, A., Davey, A., Chess-Williams, R., Kiefel, M., Arora, D., *et al*. (2016). Cellular effects of pyocyanin, a secreted virulence factor of *Pseudomonas aeruginosa*. Toxins *8*, 236.

105. Price-Whelan, A., Dietrich, L.E.P., and Newman, D.K. (2006). Rethinking "secondary" metabolism: physiological roles for phenazine antibiotics. Nat. Chem. Biol. *2*, 71–78.

106. Williams, G.C. (1966). Adaptation and Natural Selection. (Princeton: Princeton University Press).

107. Scholl, D. (2017). Phage tail–like bacteriocins. Annu. Rev. Virol. *4*, 453–467.

108. Gebhart, D., Williams, S.R., Bishop-Lilly, K.A., Govoni, G.R., Willner, K.M., Butani, A., Sozhamannan, S., Martin, D., Fortier, L.-C., and Scholl, D. (2012). Novel high-molecular-weight, R-type bacteriocins of *Clostridium difficile*. J. Bacteriol. *194*, 6240–6247.

109. Howard-Varona, C., Hargreaves, K.R., Abedon, S.T., and Sullivan, M.B. (2017). Lysogeny in nature: mechanisms, impact and ecology of temperate phages. ISME J. *11*, 1511–1520.

110. Koch, A.L. (2007). Evolution of temperate pathogens: the bacteriophage/bacteria paradigm. Virol. J. *4*, 121.

111. Bondy-Denomy, J., and Davidson, A.R. (2014). When a virus is not a parasite: the beneficial effects of prophages on bacterial fitness. J. Microbiol. *52*, 235–242.

112. Li, X.-Y., Lachnit, T., Fraune, S., Bosch, T.C.G., Traulsen, A., and Sieber, M. (2017). Temperate phages as self-replicating weapons in bacterial competition. J. R. Soc. Interface *14*, 20170563.

113. Stewart, F.M., and Levin, B.R. (1984). The population biology of bacterial viruses: Why be temperate. Theor. Popul. Biol. *26*, 93–117.

114. Gama, J.A., Reis, A.M., Domingues, I., Mendes-Soares, H., Matos, A.M., and Dionisio, F. (2013). Temperate bacterial viruses as double-edged swords in bacterial warfare. PLoS One *8*, e59043.

115. Burns, N., James, C.E., and Harrison, E. (2015). Polylysogeny magnifies competitiveness of a bacterial pathogen *in vivo*. Evol. Appl. *8*, 346–351.

116. Fornelos, N., Browning, D.F., and Butala, M. (2016). The use and abuse of LexA by mobile genetic elements. Trends Microbiol. *24*, 391–401.

117. Ghigo, J.-M., and Rendueles, O. (2015). Mechanisms of competition in biofilm communities. In Microbial Biofilms, Second Edition, P.K. Mukherjee, M. Ghannoum, M. Whiteley, and M. Parsek, eds. (Washington, D.C.: American Society of Microbiology), pp. 319–342.

118. Ghoul, M., and Mitri, S. (2016). The ecology and evolution of microbial competition. Trends Microbiol. *24*, 833–845.

119. Schluter, J., Nadell, C.D., Bassler, B.L., and Foster, K.R. (2015). Adhesion as a weapon in microbial competition. ISME J. *9*, 139–149.

120. Kim, W., Racimo, F., Schluter, J., Levy, S.B., and Foster, K.R. (2014). Importance of positioning for microbial evolution. Proc. Natl. Acad. Sci. USA *111*, E1639–E1647.

121. Xavier, J.B., and Foster, K.R. (2007). Cooperation and conflict in microbial biofilms. Proc. Natl. Acad. Sci. USA *104*, 876–881.

122. Smith, W.P.J., Davit, Y., Osborne, J.M., Kim, W., Foster, K.R., and Pitt-Francis, J.M. (2017). Cell morphology drives spatial patterning in microbial communities. Proc. Natl. Acad. Sci. USA *114*, E280–E286.

123. Klausen, M., Aaes-Jørgensen, A., Molin, S., and Tolker-Nielsen, T. (2003). Involvement of bacterial migration in the development of complex multicellular structures in *Pseudomonas aeruginosa* biofilms: Biofilm mushrooms with a twitch. Mol. Microbiol. *50*, 61–68.

124. Xavier, K.B., and Bassler, B.L. (2005). Interference with AI-2-mediated bacterial cell–cell communication. Nature *437*, 750–753.

125. Adams, J., Kinnew, T., Thompson, S., Rubin, L., and Helling, R.B. (1979). Frequency-dependent selection for plasmid-containing cells of *Escherichia coli*. Genetics *91*, 627–637.

126. Durrett, R., and Levin, S. (1997). Allelopathy in spatially distributed populations. J. Theor. Biol. *185*, 165–171.

127. Gordon, D.M., and Riley, M.A. (1999). A theoretical and empirical investigation of the invasion dynamics of colicinogeny. Microbiology *145*, 655–661.

128. Greig, D., and Travisano, M. (2008). Density-dependent effects on allelopathic interactions in yeast. Evolution *62*, 521–527.

129. Frank, S.A. (1994). Spatial polymorphism of bacteriocins and other allelopathic traits. Evol. Ecol. *8*, 369–386.

130. Wloch-Salamon, D.M., Gerla, D., Hoekstra, R.F., and de Visser, J.A.G. (2008). Effect of dispersal and nutrient availability on the competitive ability of toxin-producing yeast. Proc. Biol. Sci. *275*, 535–541.

131. Nadell, C.D., Foster, K.R., and Xavier, J.B. (2010). Emergence of spatial structure in cell groups and the evolution of cooperation. PLoS Comput. Biol. *6*, e1000716.

132. Traxler, M.F., and Kolter, R. (2015). Natural products in soil microbe interactions and evolution. Nat. Prod. Rep. *32*, 956–970.

133. I.C.W. Hardy, and M. Briffa, eds. (2013). Animal Contests (Cambridge: Cambridge University Press).

134. Parker, G.A. (1974). Assessment strategy and the evolution of fighting behaviour. J. Theor. Biol. *47*, 223–243.

135. Enquist, M., and Leimar, O. (1983). Evolution of fighting behaviour: Decision rules and assessment of relative strength. J. Theor. Biol. *102*, 387–410.

136. Sánchez, S., Chávez, A., Forero, A., García-Huante, Y., Romero, A., Sánchez, M., Rocha, D., Sánchez, B., Ávalos, M., Guzmán-Trampe, S., *et al*. (2010). Carbon source regulation of antibiotic production. J. Antibiot. (Tokyo) *63*, 442–459.

137. Abrudan, M.I., Smakman, F., Grimbergen, A.J., Westhoff, S., Miller, E.L., van Wezel, G.P., and Rozen, D.E. (2015). Socially mediated induction and suppression of antibiosis during bacterial coexistence. Proc. Natl. Acad. Sci. USA *112*, 11054–11059.

138. Basler, M., Ho, B.T., and Mekalanos, J.J. (2013). Tit-for-tat: type VI secretion system counterattack during bacterial cell-cell interactions. Cell *152*, 884–894.

139. Diggle, S.P., Gardner, A., West, S.A., and Griffin, A.S. (2007). Evolutionary theory of bacterial quorum sensing: when is a signal not a signal? Philos. Trans. R. Soc. B Biol. Sci. *362*, 1241–1249.

140. Morina, D.L., Demarais, S., Strickland, B.K., and Larson, J.E. (2018). While males fight, females choose: male phenotypic quality informs female mate choice in mammals. Anim. Behav. *138*, 69–74.

141. van Staaden, M.J., Searcy, W.A., and Hanlon, R.T. (2011). Chapter 3-Signaling Aggression. In Aggression Advances in Genetics., R. Huber, D.L. Bannasch, and P. Brennan, eds. (Amsterdam: Elsevier Academic Press), pp. 23–49.

142. Clutton-Brock, T.H., and Albon, S.D. (1979). The roaring of red deer and the evolution of honest advertisement. Behaviour *69*, 145–170.

143. González-Santoyo, I., González-Tokman, D.M., Munguía-Steyer, R.E., and Córdoba-Aguilar, A. (2014). A mismatch between the perceived fighting signal and fighting ability reveals survival and physiological costs for bearers. PLoS One *9*, e84571.

144. Cornforth, D.M., and Foster, K.R. (2015). Antibiotics and the art of bacterial war. Proc. Natl. Acad. Sci. USA *112*, 10827–10828.

145. Chatzidaki-Livanis, M., Coyne, M.J., and Comstock, L.E. (2014). An antimicrobial protein of the gut symbiont *Bacteroides fragilis* with a MACPF domain of host immune proteins. Mol. Microbiol. *94*, 1361–1374.

146. Dorosky, R.J., Yu, J.M., Pierson, L.S., and Pierson, E.A. (2017). *Pseudomonas chlororaphis* produces two distinct R-tailocins that contribute to bacterial competition in biofilms and on roots. Appl. Environ. Microbiol. *83*, e00706–e00717.

147. Paz-Yepes, J., Brahamsha, B., and Palenik, B. (2013). Role of a Microcin-C-like biosynthetic gene cluster in allelopathic interactions in marine *Synechococcus*. Proc. Natl. Acad. Sci. USA *110*, 12030–12035.

148. Abisado, R.G., Benomar, S., Klaus, J.R., Dandekar, A.A., and Chandler, J.R. (2018). Bacterial quorum sensing and microbial community interactions. mBio *9*, e02331–17.

149. Miller, M.B., and Bassler, B.L. (2001). Quorum sensing in bacteria. Annu. Rev. Microbiol. *55*, 165–199.

150. Papenfort, K., and Bassler, B.L. (2016). Quorum sensing signal–response systems in Gram-negative bacteria. Nat. Rev. Microbiol. *14*, 576–588.

151. Schluter, J., Schoech, A.P., Foster, K.R., and Mitri, S. (2016). The evolution of quorum sensing as a mechanism to infer kinship. PLoS Comput. Biol. *12*, e1004848.

152. Chandler, J.R., Heilmann, S., Mittler, J.E., and Greenberg, E.P. (2012). Acyl-homoserine lactone-dependent eavesdropping promotes competition in a laboratory co-culture model. ISME J. *6*, 2219–2228.

153. Coburn, P.S. (2004). *Enterococcus faecalis* senses target cells and in response expresses cytolysin. Science *306*, 2270–2272.

154. Davies, J., Spiegelman, G.B., and Yim, G. (2006). The world of subinhibitory antibiotic concentrations. Curr. Opin. Microbiol. *9*, 445–453.

155. Fajardo, A., and Martínez, J.L. (2008). Antibiotics as signals that trigger specific bacterial responses. Curr. Opin. Microbiol. *11*, 161–167.

156. Linares, J.F., Gustafsson, I., Baquero, F., and Martinez, J.L. (2006). Antibiotics as intermicrobial signaling agents instead of weapons. Proc. Natl. Acad. Sci. USA *103*, 19484–19489.

157. Yim, G., Wang, H.H., and Davies, J. (2007). Antibiotics as signalling molecules. Philos. Trans. R. Soc. B Biol. Sci. *362*, 1195–1200.

158. Mitri, S., and Foster, K.R. (2013). The genotypic view of social interactions in microbial communities. Annu. Rev. Genet. *47*, 247–273.

159. Bernier, S.P., and Surette, M.G. (2013). Concentration-dependent activity in natural environments. Front. Microbiol. *4*, 20.

160. Ratcliff, W.C., and Denison, R.F. (2011). Alternative actions for antibiotics. Science *332*, 547–548.

161. Berne, C., Ellison, C.K., Ducret, A., and Brun, Y.V. (2018). Bacterial adhesion at the single-cell level. Nat. Rev. Microbiol. *16*, 616–627.

162. Costerton, J.W., Lewandowski, Z., Caldwell, D.E., Korber, D.R., and Lappin-Scott, H.M. (1995). Microbial biofilms. Annu. Rev. Microbiol. *49*, 711–745.

163. Flemming, H.-C., Wingender, J., Szewzyk, U., Steinberg, P., Rice, S.A., and Kjelleberg, S. (2016). Biofilms: an emergent form of bacterial life. Nat. Rev. Microbiol. *14*, 563–575.

164. Sumpter, D.J. (2006). The principles of collective animal behaviour. Philos. Trans. R. Soc. B Biol. Sci. *361*, 5–22.

165. Blum, M.S. (1969). Alarm pheromones. Annu. Rev. Entomol. *14*, 57–80.

166. Nouvian, M., Reinhard, J., and Giurfa, M. (2016). The defensive response of the honeybee *Apis mellifera*. J. Exp. Biol. *219*, 3505–3517.

167. Jaffé, R., Kronauer, D.J., Bernhard Kraus, F., Boomsma, J.J., and Moritz, R.F. (2007). Worker caste determination in the army ant *Eciton burchellii*. Biol. Lett. *3*, 513–516.

168. Mehra, S., Charaniya, S., Takano, E., and Hu, W.-S. (2008). A bistable gene switch for antibiotic biosynthesis: the butyrolactone regulon in *Streptomyces coelicolor*. PLoS One *3*, e2724.

169. Bayramoglu, B., Toubiana, D., van Vliet, S., Inglis, R.F., Shnerb, N., and Gillor, O. (2017). Bet-hedging in bacteriocin producing *Escherichia coli* populations: the single cell perspective. Sci. Rep. *7*, 42068.

170. Hamilton, W.D. (1964). The genetical evolution of social behaviour. I. J. Theor. Biol. *7*, 1–16.

171. Nadell, C.D., Xavier, J.B., and Foster, K.R. (2009). The sociobiology of biofilms. FEMS Microbiol. Rev. *33*, 206–224.

172. Kaplan, J.B. (2010). Biofilm dispersal: mechanisms, clinical implications, and potential therapeutic uses. J. Dent. Res. *89*, 205–218.

173. Franz, C.M.A.P., Worobo, R.W., Quadri, L.E.N., Schillinger, U., Holzapfel, W.H., Vederas, J.C., and Stiles, M. (1999). Atypical genetic locus associated with constitutive production of Enterocin B by *Enterococcus faecium* BFE 900. Appl. Environ. Microbiol. *65*, 2170–2178.

174. McAuliffe, O., O'Keeffe, T., Hill, C., and Ross, R.P. (2001). Regulation of immunity to the two-component lantibiotic, lacticin 3147, by the transcriptional repressor LtnR. Mol. Microbiol. *39*, 982–993.

175. Weber, B.S., Miyata, S.T., Iwashkiw, J.A., Mortensen, B.L., Skaar, E.P., Pukatzki, S., and Feldman, M.F. (2013). Genomic and functional analysis of the Type VI Secretion System in *Acinetobacter*. PLoS One *8*, e55142.

176. Thacker, R.W., Becerro, M.A., Lumbang, W.A., and Paul, V.J. (1998). Allelopathic interactions between sponges on a tropical reef. Ecology *79*, 1740–1750.

177. Bruce, J.B., West, S.A., and Griffin, A.S. (2017). Bacteriocins and the assembly of natural *Pseudomonas fluorescens* populations. J. Evol. Biol. *30*, 352–360.

178. Kinkel, L.L., Schlatter, D.C., Xiao, K., and Baines, A.D. (2014). Sympatric inhibition and niche differentiation suggest alternative coevolutionary trajectories among Streptomycetes. ISME J. *8*, 249–256.

179. Russel, J., Røder, H.L., Madsen, J.S., Burmølle, M., and Sørensen, S.J. (2017). Antagonism correlates with metabolic similarity in diverse bacteria. Proc. Natl. Acad. Sci. USA *114*, 10684–10688.

180. Oliveira, N.M., Martinez-Garcia, E., Xavier, J., Durham, W.M., Kolter, R., Kim, W., and Foster, K.R. (2015). Biofilm formation as a response to ecological competition. PLoS Biol. *13*, e1002191.

181. Thompson, J.N. (2005). The Geographic Mosaic of Coevolution (Chicago: University of Chicago Press).

182. Dawkins, R., and Krebs, J.R. (1979). Arms races between and within species. Proc. Biol. Sci. *205*, 489–511.

183. Vetsigian, K., Jajoo, R., and Kishony, R. (2011). Structure and evolution of *Streptomyces* interaction networks in soil and in silico. PLoS Biol. *9*, e1001184.

184. Reading, C., and Cole, M. (1977). Clavulanic acid: a beta-lactamase-inhibiting beta-lactam from *Streptomyces clavuligerus*. Antimicrob. Agents Chemother. *11*, 852–857.

185. Bush, K. (2015). A resurgence of β-lactamase inhibitor combinations effective against multidrug-resistant Gram-negative pathogens. Int. J. Antimicrob. Agents *46*, 483–493.

186. Brauner, A., Fridman, O., Gefen, O., and Balaban, N.Q. (2016). Distinguishing between resistance, tolerance and persistence to antibiotic treatment. Nat. Rev. Microbiol. *14*, 320–330.

187. Gerardin, Y., Springer, M., and Kishony, R. (2016). A competitive trade-off limits the selective advantage of increased antibiotic production. Nat. Microbiol. *1*, 16175.

188. Kerr, B., Riley, M.A., Feldman, M.W., and Bohannan, B.J.M. (2002). Local dispersal promotes biodiversity in a real-life game of rock–paper–scissors. Nature *418*, 171–174.

189. Vos, M., and Velicer, G.J. (2009). Social conflict in centimeter-and global-scale populations of the bacterium *Myxococcus xanthus*. Curr. Biol. *19*, 1763–1767.

190. Brickner, I. (2006). Energy integration between the solitary polyps of the clonal coral *Lobophyllia corymbosa*. J. Exp. Biol. *209*, 1690–1695.

191. Ayre, D.J., and Grosberg, R.K. (1995). Aggression, habituation, and clonal coexistence in the sea anemone *Anthopleura elegantissima*. Am. Nat. *146*, 427–453.

192. Wulff, J.L. (1986). Variation in clone structure of fragmenting coral reef sponges. Biol. J. Linn. Soc. *27*, 311–330.

193. Connell, J.H. (1973). Population ecology of reef-building corals. In Biology and Geology of Coral Reefs (Amsterdam: Elsevier), pp. 205–245.

194. Connell, J.H., Hughes, T.P., Wallace, C.C., Tanner, J.E., Harms, K.E., and Kerr, A.M. (2004). A long-term study of competition and diversity of corals. Ecol. Monogr. *74*, 179–210.

195. Borgeaud, S., Metzger, L.C., Scrignari, T., and Blokesch, M. (2015). The type VI secretion system of *Vibrio cholerae* fosters horizontal gene transfer. Science *347*, 63–67.

196. Mignolet, J., Fontaine, L., Sass, A., Nannan, C., Mahillon, J., Coenye, T., and Hols, P. (2018). Circuitry rewiring directly couples competence to predation in the gut dweller *Streptococcus salivarius*. Cell Rep. *22*, 1627–1638.

197. Haaber, J., Leisner, J.J., Cohn, M.T., Catalan-Moreno, A., Nielsen, J.B., Westh, H., Penadés, J.R., and Ingmer, H. (2016). Bacterial viruses enable their host to acquire antibiotic resistance genes from neighbouring cells. Nat. Commun. *7*, 13333.

198. Thomas, J., Watve, S.S., Ratcliff, W.C., and Hammer, B.K. (2017). Horizontal gene transfer of functional type VI killing genes by natural transformation. mBio *8*, e00654–17.

199. Niehus, R., Mitri, S., Fletcher, A.G., and Foster, K.R. (2015). Migration and horizontal gene transfer divide microbial genomes into multiple niches. Nat. Commun. *6*, 8924.

200. Cordero, O.X., Wildschutte, H., Kirkup, B., Proehl, S., Ngo, L., Hussain, F., Le Roux, F., Mincer, T., and Polz, M.F. (2012). Ecological populations of bacteria act as socially cohesive units of antibiotic production and resistance. Science *337*, 1228–1231.

201. Eberhard, W.G. (1990). Evolution in bacterial plasmids and levels of selection. Q. Rev. Biol. *65*, 3–22.

202. Foster, K.R., Schluter, J., Coyte, K.Z., and Rakoff-Nahoum, S. (2017). The evolution of the host microbiome as an ecosystem on a leash. Nature *548*, 43–51.

203. Gilbert, J.A., Blaser, M.J., Caporaso, J.G., Jansson, J.K., Lynch, S.V., and Knight, R. (2018). Current understanding of the human microbiome. Nat. Med. *24*, 392–400.

204. Lamont, R.J., Koo, H., and Hajishengallis, G. (2018). The oral microbiota: dynamic communities and host interactions. Nat. Rev. Microbiol. *16*, 745–759.

205. Tropini, C., Earle, K.A., Huang, K.C., and Sonnenburg, J.L. (2017). The gut microbiome: connecting spatial organization to function. Cell Host Microbe *21*, 433–442.

206. Raffatellu, M. (2018). Learning from bacterial competition in the host to develop antimicrobials. Nat. Med. *24*, 1097–1103.

207. Bernal, P., Allsopp, L.P., Filloux, A., and Llamas, M.A. (2017). The *Pseudomonas putida* T6SS is a plant warden against phytopathogens. ISME J. *11*, 972–987.

208. Shen, P., Lees, J.A., Bee, G.C.W., Brown, S.P., and Weiser, J.N. (2019). Pneumococcal quorum sensing drives an asymmetric owner–intruder competitive strategy during carriage via the competence regulon. Nat. Microbiol. *4*, 198–208.

209. Brown, S.P., Le Chat, L., and Taddei, F. (2008). Evolution of virulence: triggering host inflammation allows invading pathogens to exclude competitors. Ecol. Lett. *11*, 44–51.

210. Rivera-Chávez, F., and Bäumler, A.J. (2015). The pyromaniac inside you: *Salmonella* metabolism in the host gut. Annu. Rev. Microbiol. *69*, 31–48.

211. Coyte, K.Z., Schluter, J., and Foster, K.R. (2015). The ecology of the microbiome: networks, competition, and stability. Science *350*, 663–666.

212. Behrens, H.M., Six, A., Walker, D., and Kleanthous, C. (2017). The therapeutic potential of bacteriocins as protein antibiotics. Emerg. Top. Life Sci. *1*, 65–74.

213. Gratia, A. (1925). Sur un remarquable exemple d'antagonisme entre deux souches de colibacille. C.R. Séances Soc. Biol. Ses. Fil. *93*, 1040–1041.

214. Sayers, E.W., Barrett, T., Benson, D.A., Bryant, S.H., Canese, K., Chetvernin, V., Church, D.M., DiCuccio, M., Edgar, R., Federhen, S., *et al.* (2009). Database resources of the National Center for Biotechnology Information. Nucleic Acids Res. *37*, D5–D15.

215. Letunic, I., and Bork, P. (2016). Interactive tree of life (iTOL) v3: an online tool for the display and annotation of phylogenetic and other trees. Nucleic Acids Res. *44*, W242–W245.

216. Xu, J., Kim, J., Koestler, B.J., Choi, J.-H., Waters, C.M., and Fuqua, C. (2013). Genetic analysis of *Agrobacterium tumefaciens* unipolar polysaccharide production reveals complex integrated control of the motile-to-sessile switch. Mol. Microbiol. *89*, 929–948.

217. Deng, H., Li, Z., Tan, Y., Guo, Z., Liu, Y., Wang, Y., Yuan, Y., Yang, R., Bi, Y., and Zhi, F. (2016). A novel strain of *Bacteroides fragilis* enhances phagocytosis and polarises M1 macrophages. Sci. Rep. *6*, 29401.

218. Zweers, J.C., Barák, I., Becher, D., Driessen, A.J., Hecker, M., Kontinen, V.P., Saller, M.J., Vavrová, L., and van Dijl, J.M. (2008). Towards the development of *Bacillus subtilis* as a cell factory for membrane proteins and protein complexes. Microb. Cell Fact. *7*, 10.

219. Bron, P.A., Marco, M., Hoffer, S.M., Van Mullekom, E., de Vos, W.M., and Kleerebezem, M. (2004). Genetic characterization of the bile salt response in *Lactobacillus plantarum* and analysis of responsive promoters in vitro and in situ in the gastrointestinal tract. J. Bacteriol. *186*, 7829–7835.

220. Bhatia, S.K., Lee, B.R., Sathiyanarayanan, G., Song, H.S., Kim, J., Jeon, J.M., Yoon, J.J., Ahn, J., Park, K., and Yang, Y.H. (2016). Biomass-derived molecules modulate the behavior of *Streptomyces coelicolor* for antibiotic production. 3 Biotech *6*, 223.

221. Koolhaas, J.M., Coppens, C.M., de Boer, S.F., Buwalda, B., Meerlo, P., and Timmermans, P.J.A. (2013). The resident-intruder paradigm: a standardized test for aggression, violence and social stress. J. Vis. Exp. *77*, e4367.

Chapter 5

Conclusion and Discussion

Each of the results chapters have their own conclusion and discussion. Here, I summarise the key findings of the thesis and discuss how these results broadly integrate in what is known about interbacterial defences as well as potential new avenues for research.

5.1 Summary

5.1.1 Chapter 2 — Filamentation as an escape strategy in *Escherichia coli*

- We found that like many DNA damaging toxins, DNase colicins trigger filamentation in *E. coli*. This response leads to the elongation of cells up to several dozen times the length of an unstressed cell and seems to lead to an escape-like behaviour.
- Deleting *sulA*, an inhibitor of division expressed in response to DNA damage, did not abolish filamentation but only reduced it. Cells deleted for *sulA* did not fare worse than WT cells when challenged with colicins. This suggests the difference in filamentation between WT and the SulA$^-$ strain is not enough to favour the WT over the mutant.
- Other genes were tested to ablate filamentation but none were able to completely abolish it or had pleiotropic effects dominating over the potential benefits of fila-

mentation.

- Mitomycin C, a broad-spectrum DNA damaging drug, also makes *E. coli* cells filament. Filamentation in this case is more modest than in response to colicins. However, cells fully able to filament do have an advantage in gaining access to the leading edge of a colony over cells with reduced filamentation capabilities.

- Overall, our results suggest filamentation can be used as an escape mechanism. However, this was only observed in response to mitomycin C but not with colicins since we did not have a strain unable to filament under colicin stress.

5.1.2 Chapter 3 — Biofilm formation as a response to warfare

- We developed an agent-based model to study the role of biofilm formation during bacterial warfare.

- We found that, in single strain biofilms, the optimal investment in biofilm formation is dependent on the cost of biofilm and the availability of nutrients. This means that biofilms should be as thick as the depth of penetration of nutrients. With nutrient limitation, therefore, biofilms are predicted to evolve to be relatively thin.

- In competition, with other strains, thick biofilms are beneficial even without toxins because it allows cells to reach nutrients first. When a competitor makes a toxin, we find that making a thick biofilm can serve to mop up toxins and protect a susceptible strain. Finally, making a thick biofilm can also help a toxin producer to overcome another strain's defences.

- In summary, we find there are good reasons why bacteria will make thicker biofilms when they meet competitors: thicker biofilms can help with both exploitative (nutrient) and interference competition.

5.2 Concluding remarks and outlook

5.2.1 Biofilm formation and filamentation: integral parts of bacterial lifecycles?

It is clear that biofilm formation and filamentation are two very different ways to respond to aggression and stress. However, the fact that both are up-regulated by stress responses raises the possibility that they may be used together by bacteria to cope with challenging environments. Consistent with this, there is growing evidence that both phenotypes can be observed in a single species during its lifecycle.

Uropathogenic *E. coli* (UPEC), for example, undergo both a biofilm phase and a filamentation phase at different stages of urinary tract infections, which is thought to help to maximise a strain's chances of survival and dissemination. UPEC cells initially invade epithelial cells to form intracellular bacterial colonies (IBCs), akin to a simple biofilm. Then, upon being attacked by the immune system, a subpopulation filaments and disperses to colonise new host cells (Justice et al., 2004). Justice et al. (2014) noted that these behaviours are not restricted to *E. coli* but were also observed in several other pathogens. For example, it has been observed that *Klebsiella pneumoniae* similarly form IBCs during UTIs and filaments could readily be observed in the urine of infected animals (Rosen et al., 2008). In *Haemophilus influenza* infections, immune system-induced transient nutrient-depletion triggers filamentation. These filaments can then form biofilms with an altered architecture that is lace-like in structure. Mutants deleted for the gene responsible for filamentation do not produce these biofilms and are less persistent during infections while also leading to less severe disease (Szelestey et al., 2013). These observations indicate that such filamentation phenotypes may be widespread and of general importance for the fitness of pathogenic bacteria.

Filamentation also appears to play a role in biofilm life outside of pathogenic settings. When outside the host, *Vibrio cholerae* cells can be found in marine environments. There, they colonise and feed on chitin particles. Wucher et al. (2019) showed that filamentous *V. cholerae* cells had a competitive advantage in the colonisation of these

particles over non-filamentous cells. The filamentous cells produce biofilms whose architecture relied on the entanglement of the filaments onto the particle. The authors proposed that these transient and loose biofilms allow cells to rapidly colonise marine particle and that this is particularly advantageous when the particles are frequently disturbed. If left undisturbed, filamentous cells have the initial colonisation advantage but non-filamentous EPS-secreting cells outcompete, in the long-run, filamentous cells in the biofilm. This suggests again that filamentation and biofilm formation may be part of the normal lifecycle of bacteria.

Finally, Heinrich et al. (2019) showed that *Caulobacter crescentus* filaments in response to environmental stress similar to the one they experience during algal blooms. They speculate that this might allow cells at the bottom of the biofilm, experiencing starvation, to bridge the top of the biofilm to better scavenge nutrients and better disperse cells (as well as increasing predation evasion when in the planktonic phase).

It appears then that biofilm formation and filamentation may work together to respond to various stresses. Our findings also support this idea. We observed that both biofilm formation and filamentation can play a role in the competitive ability of cells growing on surfaces (Chapters 2 and 3). However, beyond the potential for both being induced by stress, we still understand little of how the two phenotypes are regulated, or indeed co-regulated at the molecular level. A better understanding of this regulation would be a useful way to interrogate the functional logic of each response, and how they are used in nature, either alone or in concert. This would be particularly useful for filamentation whose regulation and control is the most enigmatic, as we found during our attempts to inhibit filamentation genetically in Chapter 2.

5.2.2 Bacterial defences' role in bacterial warfare

The study of bacterial warfare has focused strongly on the mechanisms that bacteria use to kill one another. No doubt the complexity and sophistication of many of these antibacterial mechanisms helps to explain this focus. However, the research focus on weapons has arguably led to an important bias. Experimenters studying a weapon will

tend to select target cells that are highly susceptible in order to demonstrate the action of a weapon and study the mechanism of killing. In reality, as we have touched upon in this thesis, many bacteria might not be so helpless when attacked, both in terms of constitutive defences and regulated ones. In particular, a key message of my thesis is that a focus on how bacteria kill can lead us to overlook how the targets of these attacks respond against such aggression, and that these responses are a central part of the dynamics at play during bacterial warfare.

The use of antibiotics has led to a wealth of studies focussing on how bacterial cells are able to resist bacterial toxins and related compounds. This literature does provide important insights on how bacteria defend themselves. However, the result is that the majority of our current understanding comes from a clinical context, either through the study of antibiotics, infection models, or both. There are, as a result, important caveats. First, there is a strong bias towards human pathogens and there is likely to be a lot we can learn from the study of non-pathogenic bacteria. For example, Molina-Santiago et al. (2019) studied the competitive interactions between two plant-beneficial bacteria, *Bacillus subtilis* and *Pseudomonas chlororaphis*. They observed that the sporulation rate in *B. subtilis* was higher in competition with *P. chlororaphis* possessing an intact T6SS than in competition with the same organism deleted for the T6SS. Sporulation, they suggest, acts as a defence mechanism in *B. subtilis* when faced with an aggressive competitor. While the notion that spores can protect against antibiotics was known from the clinical literature (Louie et al., 2012), therefore, this study revealed that sporulation also can be a *response* in bacteria, which appears to improve survival.

A second important caveat to using the antibiotic literature to understand bacterial defences is that antibiotics only represent one class of toxic molecules that bacteria use to kill one another. We have seen in Chapters 1 and 4 that bacteria have a very diverse arsenal they can use to target competitors (Granato et al., 2019). So far, the evidence suggests that many of the responses activated in response to antibiotics can also be activated by bacterial warfare, giving support to the competition sensing hypothesis (Cornforth and Foster, 2013). For example, the SOS response is activated in response

to antibiotics (Baharoglu and Mazel, 2014) but also multiple types of weapons, such as the T6SS (Jana et al., 2019) and bacteriocins (Walker et al., 2004; Mavridou et al., 2018). Similarly the envelope stress response can be activated by antibiotics (Laubacher and Ades, 2008) and the T6SS (Hersch et al., 2020). How these responses are used and provide defensive capabilities in the context of bacterial warfare is however so far poorly understood.

There is, therefore, a need for more dedicated work on the use of defences in bacterial warfare. For example, it has only recently been observed that *P. aeruginosa*, a widely studied organism, up-regulates biofilm formation in response to pyocins, bacteriocins used by *P. aeruginosa* to target closely related competitors (Oliveira et al., 2015). The exact role biofilm formation plays in facing the challenges posed by these toxins still remains unclear. In Chapter 3, we investigated this question with agent-based models. This work suggests that competition with other strains favours increased biofilm production. This effect is actually seen whether there is toxin competition or not. So it may be that the primary function of biofilm formation is to enable competition for the growing edge, rather than as a direct defence to incoming antibiotics. However, it is consistent with biofilm being used as part of the competitive strategy of bacteria during chemical warfare. Biofilm formation is just one phenotype that bacteria can use during competition. Moreover, it is clear that there are many other types of defences that bacteria can employ during warfare. For example, protection against the T6SS has long thought to be solely mediated by immunity proteins, which bind the toxic effectors and protect the producer cell and its kin. A recent review by Hersch et al. (2020), however, highlights that various mechanisms beyond canonical immunity are at play when bacteria are attacked by the T6SS. The same authors, for example, demonstrated that cells expressing immunity proteins could still be sensitive to the effect of the T6SS if they were not able to activate the envelope stress response (Hersch et al., 2020) and that this response was essential for full immunity. Other mechanisms influencing survival against the T6SS include the general stress response (Lories et al., 2020), the reactive oxygen species response or the presence of EPS or a capsule surrounding the target cell (Toska et al.,

2018; Flaugnatti et al., 2021). Some recent work from our lab has also illustrated how bacteria respond and survive attacks with examples of strong counter attacks (Mavridou et al., 2018) and shielding by clonemates (Krishna Kumar et al., 2021).

Decades of work on antibiotic resistance, persistence and tolerance in bacteria have shown that bacteria can skilfully escape death by using a wide range of responses and defence mechanisms. It emerges that many of these responses and defences are also key to microbes' survival during bacterial warfare. It is clear then that understanding bacterial warfare dynamics and evolution requires a better understanding of the role that defence mechanisms play.

5.2.3 Understanding bacterial defences to better fight them

The study of defences is also important for the goal of controlling and manipulating bacterial communities. Because bacteria have evolved in a warring landscape, they can be already well-equipped to respond to any new antimicrobial we use against them. The data presented in Chapter 2 suggests, for example, that filamentation in *E. coli*, a behaviour observed in response to colicins and antibiotics, can promote dispersal from endangered groups. Moreover, in Chapter 3, we have seen that competition can lead to up-regulation of biofilm formation, which promotes resilience in bacteria. Understanding bacterial defences and how they operate under natural conditions, therefore, is likely to be an important part of improving the effectiveness of treatment strategies.

There is growing evidence of the link between bacterial warfare and susceptibility to antibiotic treatment. Koch et al. (2014), showed, for example, that resistance to vancomycin could emerge from competition within biofilms in methicillin resistant *Staphylococcus aureus*. This resistant phenotype emerged in response to bacteriocins without exposure to the antibiotic they become resistant to. This clearly demonstrates that antibiotic-resistance can emerge from bacterial interference competition.

More recently, Meirelles et al. (2021) also showed that a naturally occurring toxin, pyocyanin, can increase resilience to some antibiotics in *P. aeruginosa*. Pyocyanin, which shares structural similarities with fluoroquinolones, can prime *P. aeruginosa* and

other bacteria against similar threats (i.e. antibiotic treatment). This is an important observation that suggests that bacterial warfare can activate defences in pathogens prior to antibiotic treatment in a manner that renders them more tolerant. However, the opposite effect can also occur. The authors and others (Schiessl et al., 2019; Zhu et al., 2019) noted that susceptibility to cationic peptides could conversely be increased by exposure to the same molecule (pyocyanin). These observations suggests that there might be trade-offs in which activation of some defences against one type of molecule can lead to increased susceptibility to other compounds. Thus, understanding how bacteria defend themselves when competing against one another can be critical to choosing the appropriate course of treatment.

Using the right drug against the right pathogen is increasingly important as antibiotic resistance spreads. Bacteriocins are often proposed as a viable alternative or as an additional tool to fight infections. These toxins are often more targeted and therefore friendlier to the microbiota but also potentially more efficient because evolved to specifically target certain bacteria (Behrens et al., 2017). As attractive as bacteriocins may seem, they do suffer from the same pitfalls as antibiotics, such as emergence of resistance and triggering potential defence mechanisms in competitors. Moreover targeted approaches might not be as targeted as once thought. As discussed in Chapter 1, some bacteria mount strong counterattacks when assaulted (Basler et al., 2013; Mavridou et al., 2018). These behaviours may have unexpected consequences on surrounding members of the community. Chatterjee et al. (2021) recently showed that bacteria being attacked by phages or antibiotics can trigger their T7SS in response and kill neighbouring bacteria. Therapeutics aiming at more targeted treatment of infections should therefore be wary that bacteria have evolved a variety of responses aimed at surviving assaults from neighbours and that antibiotic treatments might inadvertently activate them with unexpected consequences.

A strategy often discussed to circumvent the limitations of the use of antibiotics and toxins are probiotics or biotherapeutics, e.g. the use of bacteria to directly fight pathogens or prevent them from establishing. This approach is an attractive strategy

because bacteria have naturally evolved to fight and defend themselves against other bacteria. Using probiotics could therefore mean having a treatment able to keep up, in an evolutionary sense, with the evading mechanisms and defences pathogens often develop. Although, this is true only provided the probiotic's fitness is contingent on the pathogens' demise. Moreover, the success of such a strategy relies on the probiotic strains being able to establish in the community and persist there long enough for the treatment to be effective (Suez et al., 2019). Many intestinal microorganisms possess weapons that they use to compete with one another and prevent competitors from establishing (García-Bayona and Comstock, 2018; Chassaing and Cascales, 2018). Understanding how microbes can defend themselves against these weapons will therefore be key to successfully designing probiotics that can withstand these attacks and successfully invade and survive in these communities.

It also follows that, if the probiotics are to successfully fight pathogens to prevent infections using interference competition, one needs to understand which defences pathogenic bacteria possess. As discussed in the previous section, most of the defence systems we know bacteria to possess come from the study of pathogens and how they respond to antibiotic treatment. We, thus, know that pathogens can successfully defend themselves against many types of assaults (Hersch et al., 2020; Munita and Arias, 2016). Additionally, pathogens can become more virulent when under attack (Lories et al., 2020). So preventing increases in virulence is also a critical consideration in any probiotic strategies.

Whatever the strategy we employ to fight bacterial infections, a deeper understanding of how both pathogens and commensals respond to aggression will be warranted. As the story of antibiotic use and misuse so far tells us, we must be cautious that any new drugs or therapies have the potential to fall foul of bacterial defences, either ancient or newly evolved.

5.3 Bibliography

Baharoglu, Z. and D. Mazel (2014, November). SOS, the formidable strategy of bacteria against aggressions. *FEMS Microbiology Reviews 38*(6), 1126–1145.

Basler, M., B. T. Ho, and J. J. Mekalanos (2013, February). Tit-for-Tat: Type VI Secretion System Counterattack during Bacterial Cell-Cell Interactions. *Cell 152*(4), 884–894.

Behrens, H. M., A. Six, D. Walker, and C. Kleanthous (2017, April). The therapeutic potential of bacteriocins as protein antibiotics. *Emerging Topics in Life Sciences 1*(1), 65–74.

Chassaing, B. and E. Cascales (2018, April). Antibacterial Weapons: Targeted Destruction in the Microbiota. *Trends in Microbiology 26*(4), 329–338.

Chatterjee, A., J. L. E. Willett, G. M. Dunny, and B. A. Duerkop (2021, January). Phage infection and sub-lethal antibiotic exposure mediate *Enterococcus faecalis* type VII secretion system dependent inhibition of bystander bacteria. *PLOS Genetics 17*(1), e1009204.

Cornforth, D. M. and K. R. Foster (2013, April). Competition sensing: The social side of bacterial stress responses. *Nature Reviews Microbiology 11*(4), 285–293.

Flaugnatti, N., S. Isaac, L. F. Lemos Rocha, S. Stutzmann, O. Rendueles, C. Stoudmann, N. Vesel, M. Garcia-Garcera, A. Buffet, T. G. Sana, E. P. C. Rocha, and M. Blokesch (2021, December). Human commensal gut Proteobacteria withstand type VI secretion attacks through immunity protein-independent mechanisms. *Nature Communications 12*(1), 5751.

García-Bayona, L. and L. E. Comstock (2018, September). Bacterial antagonism in host-associated microbial communities. *Science 361*(6408), eaat2456.

Granato, E. T., T. A. Meiller-Legrand, and K. R. Foster (2019, June). The Evolution and Ecology of Bacterial Warfare. *Current Biology 29*(11), R521–R537.

Heinrich, K., D. J. Leslie, M. Morlock, S. Bertilsson, and K. Jonas (2019, August). Molecular Basis and Ecological Relevance of *Caulobacter* Cell Filamentation in Freshwater Habitats. *mBio 10*(4), e01557–19.

Hersch, S. J., K. Manera, and T. G. Dong (2020, October). Defending against the Type Six Secretion System: Beyond Immunity Genes. *Cell Reports 33*(2), 108259.

Hersch, S. J., N. Watanabe, M. S. Stietz, K. Manera, F. Kamal, B. Burkinshaw, L. Lam, A. Pun, M. Li, A. Savchenko, and T. G. Dong (2020, May). Envelope stress responses defend against type six secretion system attacks independently of immunity proteins. *Nature Microbiology 5*(5), 706–714.

Jana, B., C. M. Fridman, E. Bosis, and D. Salomon (2019, December). A modular effector with a DNase domain and a marker for T6SS substrates. *Nature Communications 10*(1), 3595.

Justice, S. S., A. Harrison, B. Becknell, and K. M. Mason (2014, November). Bacterial differentiation, development, and disease: Mechanisms for survival. *FEMS Microbiology Letters 360*(1), 1–8.

Justice, S. S., C. Hung, J. A. Theriot, D. A. Fletcher, G. G. Anderson, M. J. Footer, and S. J. Hultgren (2004, February). Differentiation and developmental pathways of uropathogenic *Escherichia coli* in urinary tract pathogenesis. *Proceedings of the National Academy of Sciences 101*(5), 1333–1338.

Koch, G., A. Yepes, K. U. Förstner, C. Wermser, S. T. Stengel, J. Modamio, K. Ohlsen, K. R. Foster, and D. Lopez (2014, August). Evolution of Resistance to a Last-Resort Antibiotic in *Staphylococcus aureus* via Bacterial Competition. *Cell 158*(5), 1060–1071.

Krishna Kumar, R., T. A. Meiller-Legrand, A. Alcinesio, D. Gonzalez, D. A. I. Mavridou, O. J. Meacock, W. P. J. Smith, L. Zhou, W. Kim, G. S. Pulcu, H. Bayley, and K. R. Foster (2021, December). Droplet printing reveals the importance of micron-scale structure for bacterial ecology. *Nature Communications 12*(1), 857.

Laubacher, M. E. and S. E. Ades (2008, March). The Rcs Phosphorelay Is a Cell Envelope Stress Response Activated by Peptidoglycan Stress and Contributes to Intrinsic Antibiotic Resistance. *Journal of Bacteriology 190*(6), 2065–2074.

Lories, B., S. Roberfroid, L. Dieltjens, D. De Coster, K. R. Foster, and H. P. Steenackers (2020, April). Biofilm Bacteria Use Stress Responses to Detect and Respond to Competitors. *Current Biology 30*(7), 1231–1244.

Louie, A., B. D. VanScoy, D. L. Brown, R. W. Kulawy, H. S. Heine, and G. L. Drusano (2012, March). Impact of Spores on the Comparative Efficacies of Five Antibiotics for Treatment of *Bacillus anthracis* in an *In Vitro* Hollow Fiber Pharmacodynamic Model. *Antimicrobial Agents and Chemotherapy 56*(3), 1229–1239.

Mavridou, D. A., D. Gonzalez, W. Kim, S. A. West, and K. R. Foster (2018, February). Bacteria Use Collective Behavior to Generate Diverse Combat Strategies. *Current Biology 28*(3), 345–355.

Meirelles, L. A., E. K. Perry, M. Bergkessel, and D. K. Newman (2021, March). Bacterial defenses against a natural antibiotic promote collateral resilience to clinical antibiotics. *PLOS Biology 19*(3), e3001093.

Molina-Santiago, C., J. R. Pearson, Y. Navarro, M. V. Berlanga-Clavero, A. M. Caraballo-Rodriguez, D. Petras, M. L. García-Martín, G. Lamon, B. Haberstein, F. M. Cazorla, A. de Vicente, A. Loquet, P. C. Dorrestein, and D. Romero (2019, December). The extracellular matrix protects *Bacillus subtilis* colonies from *Pseudomonas* invasion and modulates plant co-colonization. *Nature Communications 10*(1), 1919.

Munita, J. M. and C. A. Arias (2016, April). Mechanisms of Antibiotic Resistance. *Microbiology Spectrum 4*(2), VMBF–0016–2015.

Oliveira, N. M., E. Martinez-Garcia, J. Xavier, W. M. Durham, R. Kolter, W. Kim, and K. R. Foster (2015, July). Biofilm Formation As a Response to Ecological Competition. *PLOS Biology 13*(7), e1002191.

Rosen, D. A., J. S. Pinkner, J. M. Jones, J. N. Walker, S. Clegg, and S. J. Hultgren (2008, July). Utilization of an Intracellular Bacterial Community Pathway in *Klebsiella pneumoniae* Urinary Tract Infection and the Effects of FimK on Type 1 Pilus Expression. *Infection and Immunity 76*(7), 3337–3345.

Schiessl, K. T., F. Hu, J. Jo, S. Z. Nazia, B. Wang, A. Price-Whelan, W. Min, and L. E. P. Dietrich (2019, December). Phenazine production promotes antibiotic tolerance and metabolic heterogeneity in *Pseudomonas aeruginosa* biofilms. *Nature Communications 10*(1), 762.

Suez, J., N. Zmora, E. Segal, and E. Elinav (2019, May). The pros, cons, and many unknowns of probiotics. *Nature Medicine 25*(5), 716–729.

Szelestey, B. R., D. R. Heimlich, F. K. Raffel, S. S. Justice, and K. M. Mason (2013, October). Haemophilus Responses to Nutritional Immunity: Epigenetic and Morphological Contribution to Biofilm Architecture, Invasion, Persistence and Disease Severity. *PLoS Pathogens 9*(10), e1003709.

Toska, J., B. T. Ho, and J. J. Mekalanos (2018, July). Exopolysaccharide protects *Vibrio cholerae* from exogenous attacks by the type 6 secretion system. *Proceedings of the National Academy of Sciences 115*(31), 7997–8002.

Walker, D., M. Rolfe, A. Thompson, G. R. Moore, R. James, J. C. D. Hinton, and C. Kleanthous (2004, February). Transcriptional Profiling of Colicin-Induced Cell Death of *Escherichia coli* MG1655 Identifies Potential Mechanisms by Which Bacteriocins Promote Bacterial Diversity. *Journal of Bacteriology 186*(3), 866–869.

Wucher, B. R., T. M. Bartlett, M. Hoyos, K. Papenfort, A. Persat, and C. D. Nadell (2019, July). *Vibrio Cholerae* filamentation promotes chitin surface attachment at the expense of competition in biofilms. *Proceedings of the National Academy of Sciences 116*(28), 14216–14221.

Zhu, K., S. Chen, T. A. Sysoeva, and L. You (2019, December). Universal antibiotic

tolerance arising from antibiotic-triggered accumulation of pyocyanin in *Pseudomonas aeruginosa*. *PLOS Biology 17*(12), e3000573.

Appendix A

Supplementary information for Chapter 2: "Filamentation as an escape strategy in *Escherichia coli*"

A.1 Supplementary Figures

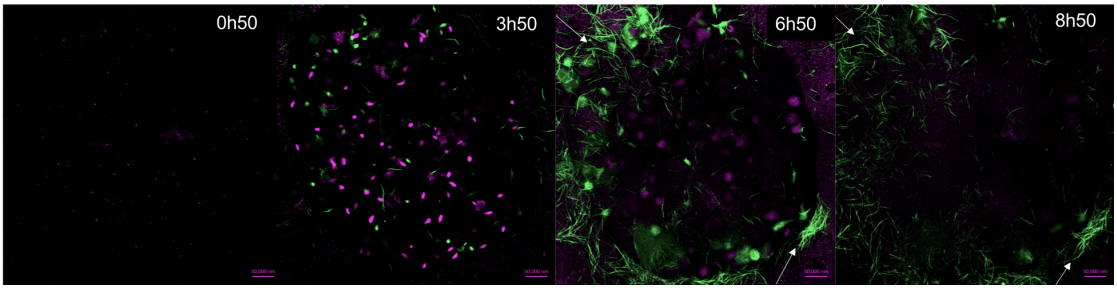

Figure A.1: Time lapse of sensitive cells filamenting out of a droplet containing a strain producing a colicin (E2). Green: BZB1011 GFP, purple: BZB1011 E2 RFP.

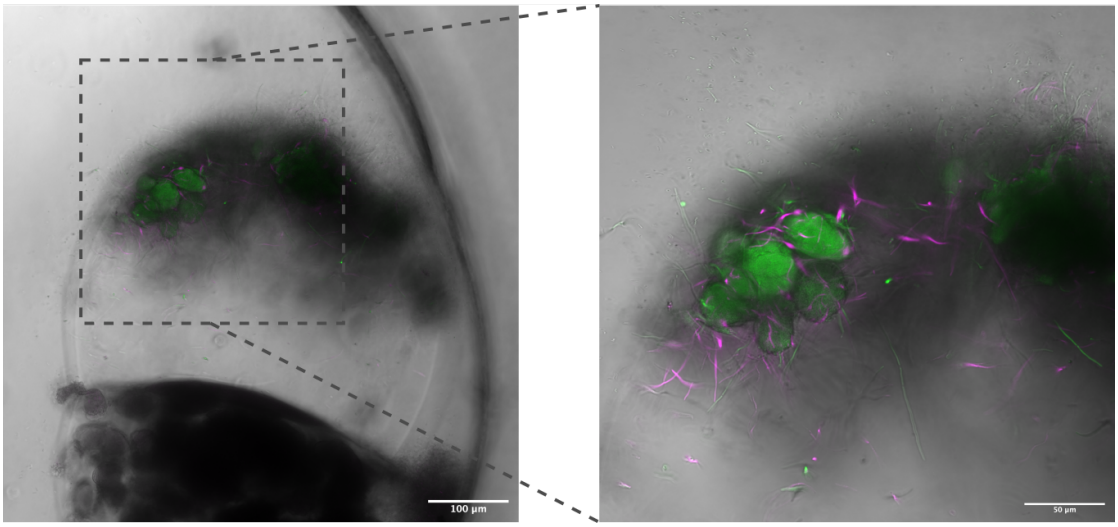

Figure A.2: Droplets treated with Propidium Iodide. Sensitive cells exposed to colicin E2 can be positive for propidium iodide (PI, purple) staining which indicates the loss of membrane integrity and therefore death. However, a fraction of the population (green) remains impermeable to PI which suggests some of them are still alive.

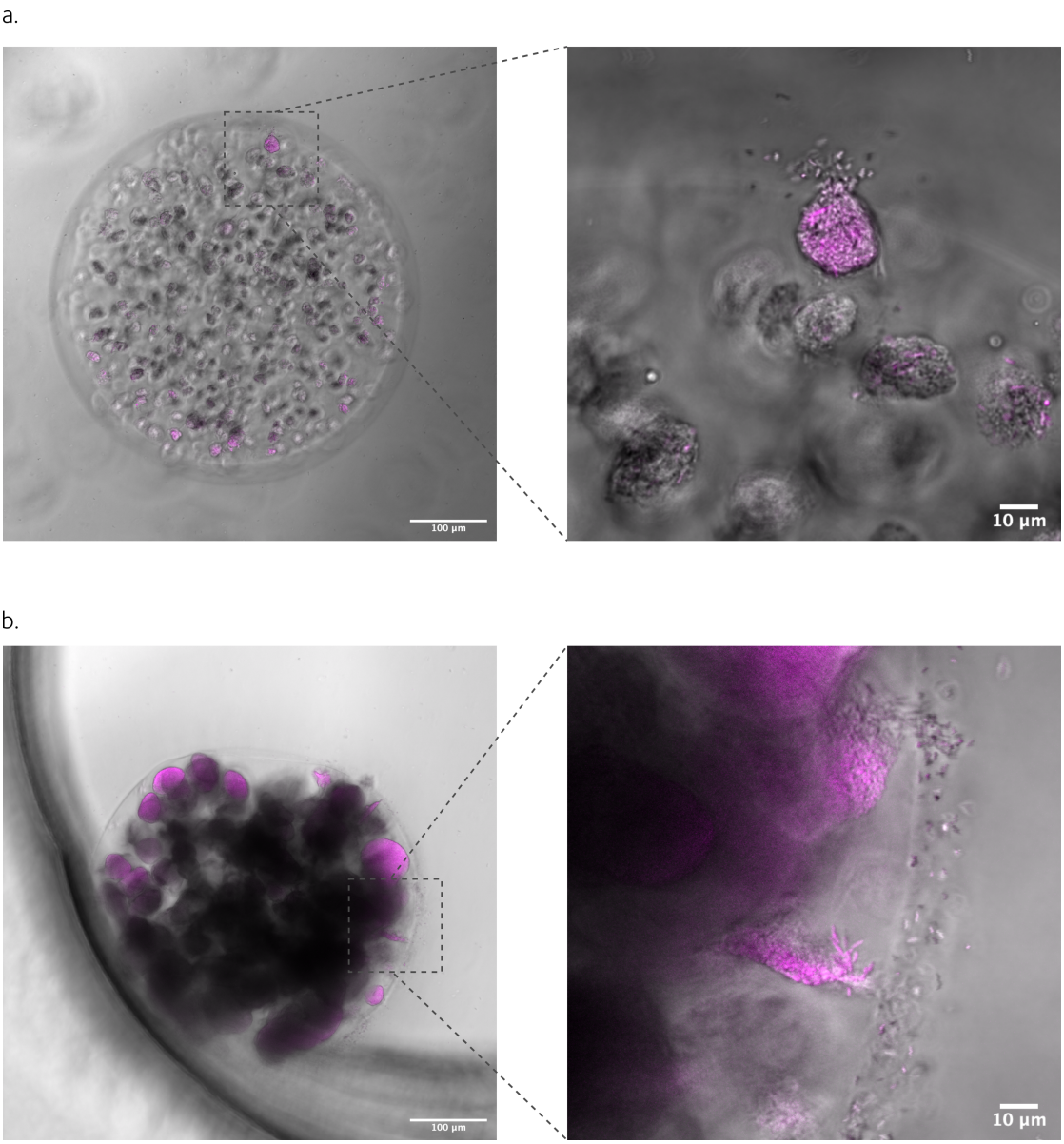

Figure A.3: Susceptible cells do not filament in response to pore-forming colicins. **a.** A droplet containing susceptible cells after being in contact with a droplet containing a strain producing colicin A. The susceptible cells managed to form microcolonies with little to no filamentation observed. **b.** Same as in a. but colicin K was produced by the toxin-producing strain. Microcolony morphology is different than the one observed in response to colicin A.

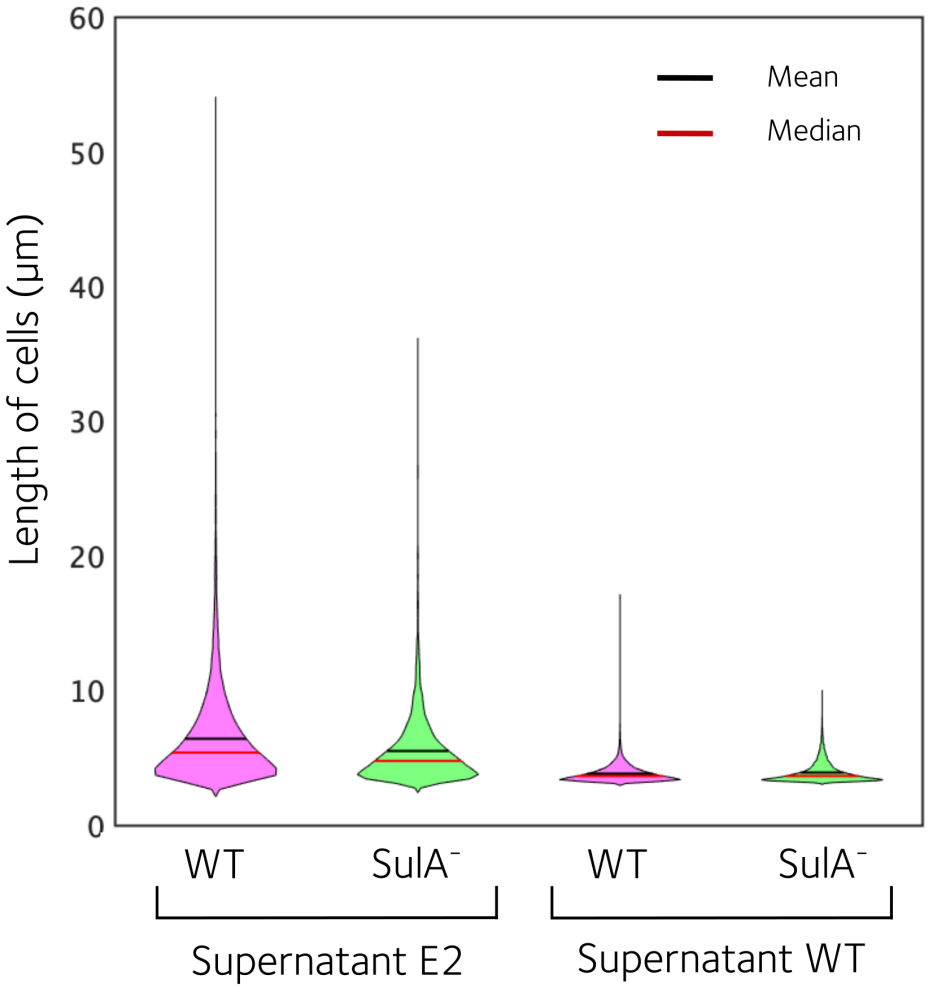

Figure A.4: Distribution of the length of filaments in a culture exposed to either E2 or WT supernatant. Number of cells measured from left to right: WT treated with E2 supernatant, 9120, SulA$^-$ treated with E2 supernatant, 7029, WT treated with WT supernatant, 2605, SulA$^-$ treated with WT supernatant, 11897.

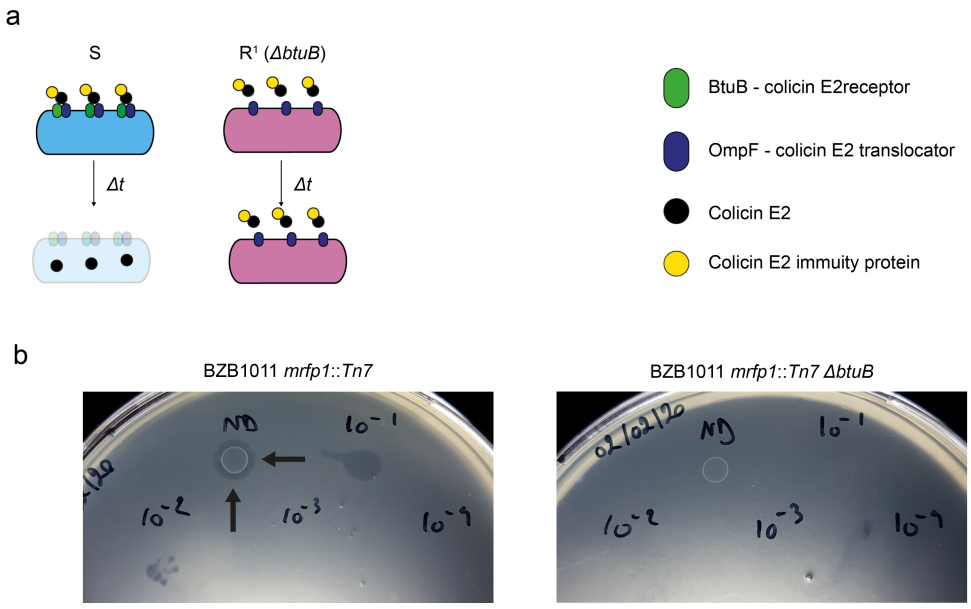

Figure A.5: Competition with colicin-resistant strains. **a.** Interaction of colicin E2 with susceptible cells (S), and resistant cells made by *btuB* deletion (R1). **b.** Images of LB-Miller agar plates for assessing resistance to colicin E2 for BZB1011 *mrfp1*::Tn7 (S), BZB1011 *mrfp1*::Tn7 BtuB$^-$ (R1). Inhibition is only seen for BZB1011 *mrfp1*::Tn7 as indicated by the two arrows. In b, BZB1011 pColE2 was spotted on top of the strains of interest without dilution (ND), and after dilution, by 10^1, 10^2, 10^3, and 10^4-fold. See Methods for growth inhibition assays in Appendix D. These experiments were performed to show that the genetic modification did indeed produce the phenotypic resistance to colicin E2. Figure adapted with permission from Krishna Kumar et al. (2021).

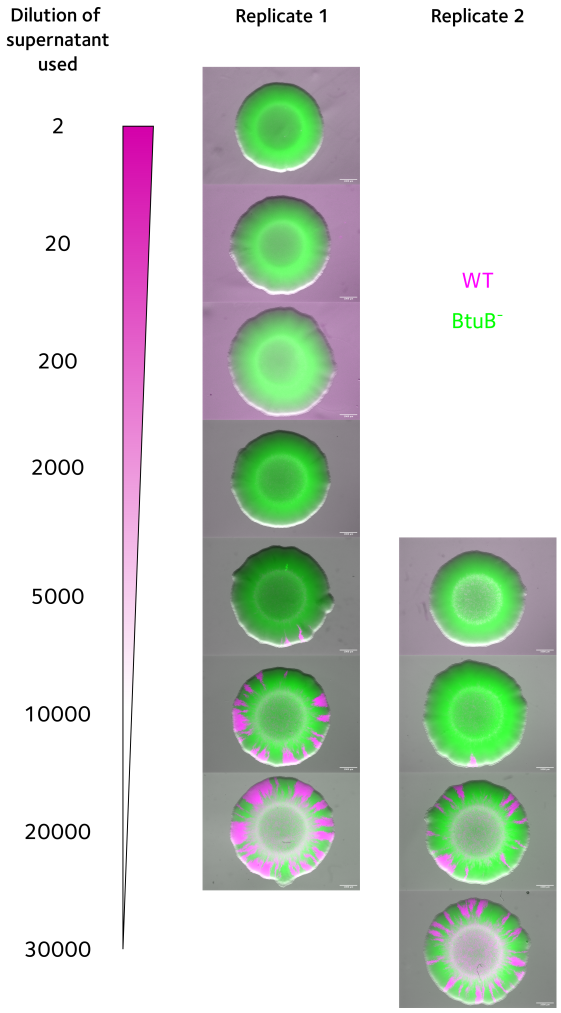

Figure A.6: Competition between WT and BtuB$^-$ on agar 1.5% containing the supernatant of an E2 colicin producer. From top to bottom are decreasing concentrations of colicin E2. **Left**: Replicate 1. **Right**: Replicate 2.

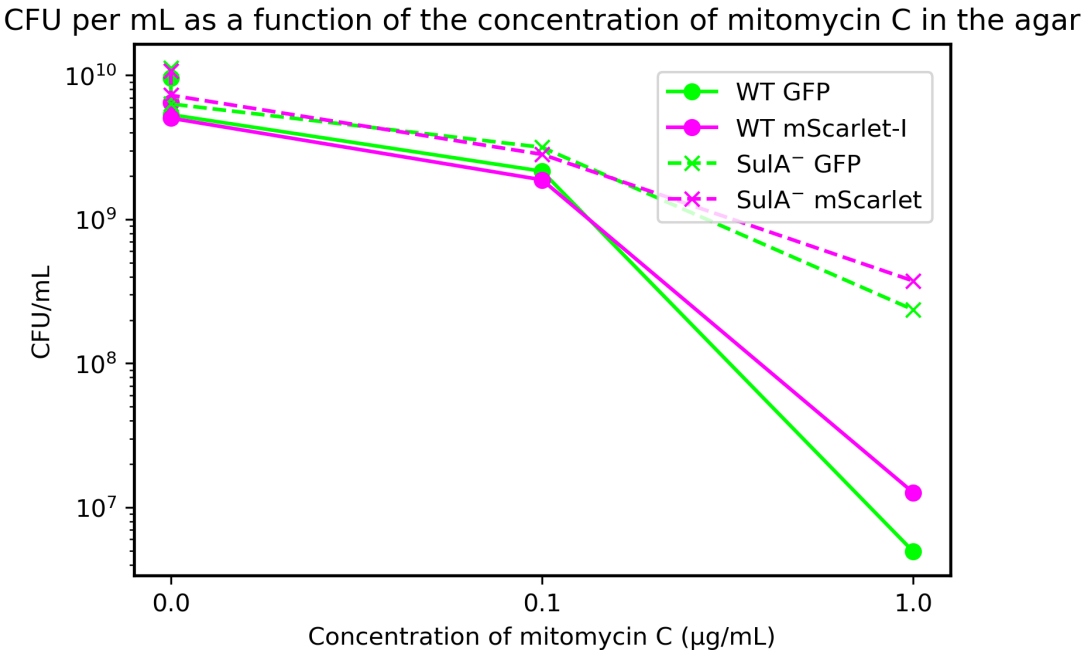

Figure A.7: CFU of WT and SulA⁻ colonies grown alone on LB agar supplemented with mitomycin C.

A.2 Statistical tests outputs

A.2.1 Outputs for figure 2.15

Table A.1: Output of the Kruskal-Wallis test comparing the proportion of WT between all treatments

Statistic	Value
p-value	0.00023926722295776137
statisitc	19.28

Table A.2: Output of the *post hoc* Steel-Dwass-Critchlow-Fligner test comparing the proportion of WT between all treatments

	0 μg/mL	0.01 μg/mL	0.1 μg/mL	1 μg/mL
0 μg/mL	1.0	0.566107	0.020607	0.020607
0.01 μg/mL	0.566107	1.0	0.050937	0.020607
0.1 μg/mL	0.020607	0.050937	1.0	0.020607
1 μg/mL	0.020607	0.020607	0.020607	1.0

A.3 Bibliography

Krishna Kumar, R., T. A. Meiller-Legrand, A. Alcinesio, D. Gonzalez, D. A. I. Mavridou, O. J. Meacock, W. P. J. Smith, L. Zhou, W. Kim, G. S. Pulcu, H. Bayley, and K. R. Foster (2021, December). Droplet printing reveals the importance of micron-scale structure for bacterial ecology. *Nature Communications 12*(857).

Appendix B

Supplementary information for Chapter 3: "Biofilm formation as a response to bacterial warfare"

B.1 Model description using the O.D.D. protocol

Below we use the O.D.D. protocol (Overview, Design concepts, Details) to describe the model used in this study. The O.D.D. protocol is a general framework to describe agent-based models in a standardised fashion to allow ease of comprehension, use and reproducibility (Grimm et al., 2010, 2013, 2020).

B.1.1 Purpose

The purpose of this model is to study the role played by biofilms, as high density aggregates of cells, in the context of interference competition. We sought to:

- disentangle the intrinsic value biofilms carry when two strains compete for resources
- investigate whether biofilms help in protecting cells from toxin-producer competitors

- understand whether biofilms help toxin-producer carry more effective attacks through building more biomass.

In this work, biofilm formation is conceptualised as a reduction in cell detachment such that local cell density increases where detachment decreases.

B.1.2 Entities, state variables and scales

The entities or agents in the simulations of this study are bacterial cells. Each cell carries a neutral, heritable genetic label (green or purple), and has a fixed phenotype (growth rate, detachment height, sensitive or resistant to toxin, toxin producer or not) linked to that label.

Entities and state variables

The biofilm is comprised of n individual cells. The cells are rod-shaped and represented by rigid capsules composed of a cylindrical midsection of variable length l and radius r capped with hemispheres of radius r (Figure B.1.a). Each cell has a unique identifier i. Each cell's position, orientation and length at time t are given by the generalised position of the cell:

$$x_i(t) = (c_x, c_y, c_z, \phi_x, \phi_y, \phi_z, L)^T$$

where c_x, c_y and c_z are the coordinates of the cell centre of mass, ϕ_x, ϕ_y, ϕ_z its orientation and L its length (Rudge et al., 2012).

The state variables for cells are summarised in table B.1.

The cells are assumed to be growing in a static liquid culture. The model can be coupled to a nutrient field to simulate nutrient-limited conditions, as often occur within biofilms (Flemming et al., 2016; Stewart and Franklin, 2008). Nutrients come from the bulk liquid at the top of the box and diffuse through the boundary layer (in which diffusion, rather than advection, governs the transport of solutes). Nutrient availability and rate of consumption then dictate the rate at which bacteria grow following Monod kinetics (Monod, 1949; Picioreanu et al., 1998; Nadell et al., 2010),

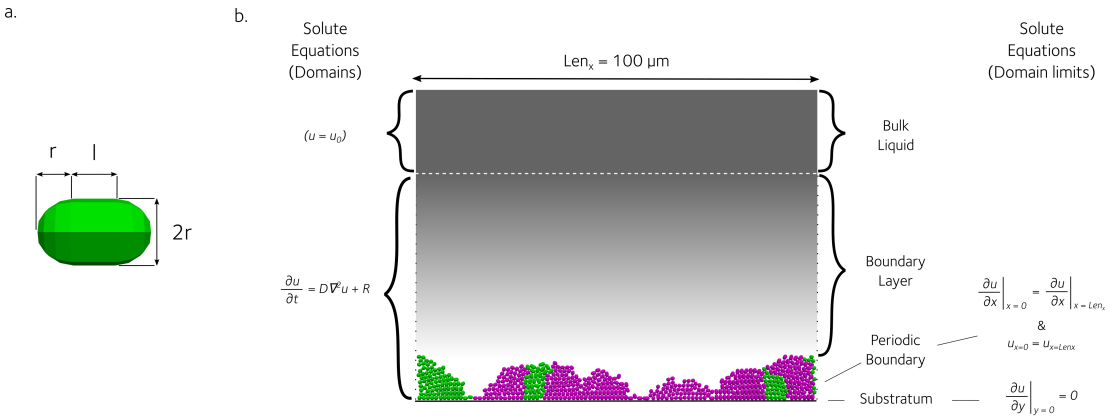

Figure B.1: Geometry of the virtual cells and environment. **a.** Geometry of a cell composed of a cylindrical midsection of length l and radius r capped by two hemispheres of radius r. **b.** Environment in which the cells have been seeded (random configuration shown here). It is characterised by a base of length Len_x and two lateral periodic boundaries. The nutrient field (grey gradient) is governed by a reaction-diffusion equation within the boundary layer while the concentration in the bulk is constant and equal to u_0. Periodic boundaries imply that the nutrient concentration on the left of the domain equals that on the right. As Figure 3.1 from the main text.

$$\mu_i = \mu_{max} \frac{u_n(p_i)}{K + u_n(p_i)},$$

where μ_max is the maximum growth rate of the strain, $u_n(p_i)$ is the concentration of nutrients evaluated at the ith cell's centre p and K is the carrying capacity or saturation constant. In nutrient rich conditions, $\text{u} = \infty$ and $\mu_\text{i} = \mu_\text{max}$.

Using a similar system, a toxin field can also be simulated when cells are programmed to produce a toxin. The amount of toxin produced by the cells is proportional to their growth rate adjusted for nutrient availability so that strains experiencing limited access to nutrients have limited toxin production capabilities,

$$\underbrace{\frac{\partial u_T}{\partial t}}_{\text{Accumulation}} = \underbrace{D_T \nabla^2 u_T}_{\text{Diffusion}} + \underbrace{\alpha_T \rho \mu_{max} \left(\frac{u_n}{u_N + K_N}\right) \phi_P}_{\text{Production}} - \underbrace{\beta_T \rho \nu_{max} \left(\frac{u_T}{u_T + K_T}\right) \phi_S}_{\text{Removal}},$$

where u_T is the concentration of toxin, D_T is the toxin diffusivity, α_T and β_T are the toxin yield and removal per unit biomass respectively, ρ is the biomass density, ϕ_P and

Table B.1: State variables

Name	Symbol
Genetic label	-
Radius	r
Length	L
Coordinates	x, y, z
Orientation	ϕ_x, ϕ_y, ϕ_z
Growth rate	μ
ID	i

ϕ_S are the volume fractions of the producer cells and sensitive cells respectively, ν_{max} is the maximal toxin removal rate and K_N and K_T are Monod half-saturation constants for nutrient consumption and toxin removal respectively. In practice, toxin production is modulated using the Damköhler number $D_{T,P}$, which is related to the toxin range parameter L_{bac} used by Bucci et al. (2011) (Smith, 2017). Producers are here always immune to the toxin they produce. Although toxin production can incur a cost to the producer, we here simplify by having no cost to toxin production (Cascales et al., 2007; Kerr et al., 2002). Sensitive cells are unaffected by the toxin under the critical concentration $\mathrm{u_{T_{crit}}}$, but die if exposed to concentrations exceeding this threshold. Cell death translates to a null growth rate and an inability to divide. Lysis and therefore removal of the dead cells occurs after a delay $\mathrm{t_{lysis}}$.

Spatial and temporal scales

Cells exist within a two-dimensional (2-D) cartesian space and are constrained to a rectangular box defined by a solid base and periodic lateral edges.

We simulate a 100 μm-wide 2-D section of biofilm, resulting in a computationally tractable population. To avoid artefacts due to having rigid walls on either side of the biofilm, the lateral edges obey periodic boundary conditions, rendering the domain cylindrical (i.e. cells on one side are in contact with the cells on the other side). The periodicity does not yet hold for group formation (i.e. cells moving on the other side of the simulation when going over the periodic boundary get assigned to a new group,

see Methods B.1.7). In practice, this means that any cell disappearing from one side to reappear on the other will be considered to be their own group if no other cell is present next to the boundary at the site where the cell crosses over and detach immediately making it harder for thicker biofilms to colonise the whole box from both sides. However, this is expected to only slow but not prevent thicker biofilms from invading the domain when they already are doing so thus not changing the expected outcome.

Simulations are run long enough to reach a population equilibrium. In the case of a single strain biofilm, this means until the box is filled (i.e. cells have reached the detachment height on the whole length of the box). In a two-strain biofilm, this either means until one of the strains has been eliminated from the simulation and the remaining strain has filled the box or, in the case of simulations where the two strains remain, for 250 steps after the volume of each strain stops changing significantly over time. This equilibrium is dynamic. In theory it is reached when the number of cells born is equal to the number of cells detaching (see Methods 3.3.4). In practice, we do observe slight variations up and down the theoretical equilibrium (Figures 3.3 and 3.4). Therefore, once equilibrium is reached, simulations are run for at least 250 additional steps to allow averaging of metrics over equilibrium states.

One time step is 0.025 h. No simulation was run for no more than 10000 steps (i.e. 250 hours or $\sim$ 10.5 days).

B.1.3 Process overview and scheduling

The model is generally organised in the following fashion:

1. The environment is first set up (see Methods B.1.5).

2. The cells are then initialised setting values for the growth rate, the volume at which cells should divide, the countdown before lysis and the local toxin concentration.

3. The simulation is updated at each time step. At every step, the following processes occur:

   (a) **Cell Detachment**. Strains can differ in the amount they invest in biofilm

formation. This results in different detachment heights with more investment resulting in a higher detachment height, and so a thicker biofilm. In this model, we only consider two strains. The one investing the least in biofilm production will have the lower detachment height (h_{min}) while the other one will have the higher (h_{max}) (Figure B.2.a).

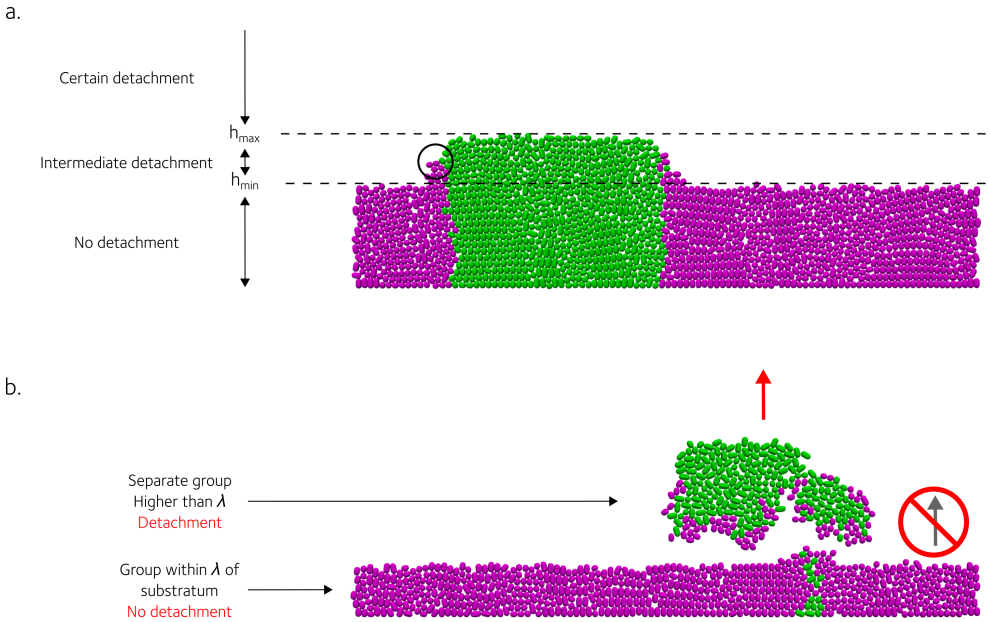

Figure B.2: Detachment Rules. **a.** Cells below h_{min} do not detach, while cells above h_{max} automatically detach. The detachment height of the purple cells between h_{min} and h_{max} is the average detachment height of the cells within $r_{neighbourhood}$ (black circle) **b.** Group detachment occurs when the lowest cell of a group is higher than λ from the substratum. λ is a small value (here 2.4 μm) representing the minimum distance between groups of cells or groups of cells and the substratum. Below λ, the groups and/or substratum are considered attached. As Figure 3.2 from the main text.

Each cell is checked against the detachment heights (Figure B.2.a):

i. First, it is checked against the minimum detachment height. Any cells below it do not detach and are not checked against the other detachment heights.

ii. Second, the remaining cells (the ones above the minimum detachment height) are checked against the maximum detachment height. Any cell above this height should detach and is removed from the simulation.

iii. Third, all the cells in between the minimum and maximum detachment

heights that are of the type that has the minimum detachment height are checked against an intermediate detachment height determined by the weighted average detachment height of the cells in its neighbourhood. This allows weak biofilm forming cells to potentially benefit from the investment of the neighbouring strong biofilm producer cells.

All detachment events are counted to monitor the amount of cells detaching. This is analysed in post-processing.

(b) **Group Detachment**. Cells are assigned to a group using a pruned Delaunay triangulation where edges longer than minimum length λ have been removed (see Methods B.1.7). Cells belong to the same group when they are close enough together that they are implicitly mechanically connected (e.g. via EPS). We use the variable λ as the critical value within which neighbouring cells are connected to one another. Cells belong to different groups if they are further away than λ from one another and none of the cells in the network of implicitly-connected neighbouring cells are either. If the lowest cell in a group is further away than λ from the base of the box, this group is set to detach and the cells within it are removed from the simulation (Figure B.2.b). We term this phenomenon group detachment.

(c) **Division**. The volume of each cell is checked against the target division volume. If it is above it, cells divide. Cells divide lengthwise and results in two identical daughter cells.

(d) **Growth**. The growth rate of each cell is evaluated based on detachment height and local nutrient concentration. More precisely, each time step a cell will grow by μV where V is the volume of the cell. In the presence of a nutrient gradient, cells growth rate follows a Monod equation (Monod, 1949; Picioreanu et al., 1998; Nadell et al., 2010).

(e) **Death**. The local toxin concentration around each cell is checked against the lethal toxin concentration. If it is higher, the cells change type (type 2, only used for dead cells), their growth rate is evaluated to 0 and the lysis

countdown starts. Once the countdown reaches 0, cells are removed from the simulation.

B.1.4 Design concepts

Basic principles

1. **Detachment**.
    - All cells are implicitly subject to lateral shear forces sweeping over the colony. This causes cells to detach above a certain height from the substratum.
    - Groups of cells need to be in contact with the substratum to resist shear forces. Any group of cells not attached to the substratum is removed.
    - Cells can invest in extracellular matrix production. This results in thicker colonies. Cells producing stronger, thicker biofilms pay a growth cost to do so.
    - The cost paid by cells to invest in matrix production increases linearly with biofilm height.
    - Cells investing less than their neighbours in biofilm formation can benefit from the neighbouring cells' investment.
2. **Movement**. Cell movement is driven by growth and results from cells pushing on one another.

Objectives

We chose detachment rate (number of cells of a given strain detaching from the biofilm per unit time, at equilibrium) as our fitness metric. Detachment rate is proportional to the amount of cells (weighted by growth rate) in the simulation so that detachment rate and biomass weighted by growth rate align.

Perceiving

Cells can perceive the local nutrient concentration. This will affect the cells' behaviour (e.g. growth rate).

Sensitive cells can also perceive the local toxin concentration. Their ability to continue to grow and divide depends on this local concentration. Cells' sensitivity to a toxin is described by $u_{T_{crit}}$, which is the concentration of toxin above which cells die.

Interaction

Cells interact in various ways:

1. They physically interact by pushing one another.
2. They compete for nutrients. All cells consume nutrients based on the local nutrients concentration. Consumption depletes the supply of nutrients entering the system from the bulk layer (upper boundary). This follows well-established hybrid models of nutrient competition (for example Nadell et al. (2010)).
3. Some cells can produce a toxin that will affect sensitive cells.
4. The implicit extracellular matrix produced by cells influences cells in the vicinity. A strong biofilm producer surrounded by strong biofilm producers is less likely to detach. Conversely, a weak biofilm producer surrounded by other weak biofilm formers will detach easily. But a weak biofilm producer surrounded by strong biofilm producers might benefit from the strong biofilm producer's investment in forming a biofilm and detach higher, potentially resulting in better access to nutrients and better opportunities for dispersal.

Stochasticity

The division volume of each cell contains some stochasticity. Cells divide when they reach twice their initial volume (target volume) plus some noise (drawn at random between 0 and 9% percent of the target volume) (Rudge et al., 2012; Smith et al., 2017).

The orientation of daughter cells after division is subject to random jitter $\eta_{\text{orientation}}$ to simulate noise during the division process.

Collectives

Cells can form groups, defined as a group of cells within λ from one another. Whole groups can detach when they are not attached to the substrate (i.e. further away than λ away from the box).

Although toxin-producer cells' toxin production is fixed and unregulated (i.e. it does not depend on the density of the producer strain), collectives of toxin-producers create locally higher toxin concentrations than producer cells alone. This potentially allows these collectives to produce enough toxin to kill competitors where this could not be achieved by individual cells.

Observation

A CSV file is created containing the number of cells of each type that have detached at each step. In post-processing, these are used to calculate the detachment rates at equilibrium as well as the total number of cells shed over the span of the simulation.

Every s steps (here $s = 10$), the simulation configuration (i.e. ids, cell types, volume, radius, length, position, orientation and growth rate of all the cells) is saved as a `.pickle` file. In post-processing, these are converted to `.vtp` files (ParaView VTK Poly Data). This is a file format readable by the Visualization Toolkit (VTK) developed by Kitware Inc., which ParaView uses to allow visualisation of the simulations (Ahrens et al., 2005) (see Methods 3.3.2). These are also used to calculate the cumulative volume of the cells at the end of the simulations.

B.1.5 Initialisation

Simulation initialisation is specified in a CellModeller model file.

- The environment is set up.
  - The size of the domain is set at 100 μm in the x axis.

  - The lateral boundaries are specified as periodic.

- The cells' state variables are initialised.

  - **Position**. Cells are always seeded in a 1:1 ratio. 6 cells of each of the two types are seeded along the base of the simulation domain, representing founder cells that first encounter the surface. The configuration of the initial seeding can be specified to be side by side (i.e. all the cells of each type are randomly seeded on different side of the box) or random (i.e. all the cells are randomly scattered on along the base regardless of their type).
  - **Orientation**. All the cells are initially lying flat on the surface (i.e. their long axis is parallel to the base of the simulation) as is often the case when bacteria commit to a surface-associated lifestyle and irreversibly attach to a substrate (Kimkes and Heinemann, 2020).
  - **Growth rate**. Their growth rate is initially set at 0.
  - **Initial volume**. The initial volume is set at 0.54.
  - **Radius**. the radius of the cells is set at 0.5.
  - **Division volume**. The volume at which cells should divide is set at two times the initial volume plus some noise (drawn at random between 0 and 9% percent of the target volume).
  - **Detachment height**. The detachment height for each type is fixed (varies between simulations).
  - **Nutrient concentration**. The initial amount of nutrient each cell is experiencing at its centre is evaluated (depends on the proximity of other cells that might be competing for nutrients).
  - **Toxin concentration**. The initial amount of toxin each cell is experiencing at its centre is evaluated (depends on the proximity of toxin producing cells).
  - **Lethal toxin concentration**. Value depends on the simulations. Set at 0.5 for a potent toxin and 6.5 for a weak toxin.

  - **Lysis delay time**. Set at 10 steps (i.e. 15 minutes).

  This cell initialisation stage is not constrained to the initialisation of the simulation as new cells born over the span of the run will be initialised in the same manner.

- The nutrient field parameters are specified.
- The toxin field parameters are specified.

B.1.6 Input data

The model does not use input data to represent time-varying processes.

B.1.7 Submodels

We here describe the subprocesses carried out during the update function and therefore occurring at every step.

Cell detachment

The number of cells detaching per step is initialised to 0. Each cell is checked against the detachment heights in the following order:

1. First, it is checked against the minimum detachment height. Any cells below it do not detach and are not checked against the other detachment heights. No further action is undertaken.

2. Second, the remaining cells (the ones above the minimum detachment height) are checked against the maximum detachment height. If their cell centres are above the maximum detachment height, they should detach and the cells growth rate is evaluated to 0, they are not allowed to divide anymore and they are flagged for removal. The counter for the number of cells detaching of each type is incremented by the number of cells of each type that has been removed.

3. All the remaining cells that are of the type that detaches above the minimum detachment height, i.e. the ones between the minimum and maximum detachment

heights and might be able to detach, are checked against an intermediate detachment height computed as the weighted average sloughing height of the cells within a $r_{neighbour}$ radius. If their cell centres are above this height, the cells should be removed from the simulation, their growth rate is evaluated to 0, they are not allowed to divide anymore and are flagged for removal. The count of the number of cells detaching during that step is incremented by 1 for each cell removed. If not, no other action is taken.

4. The count of the number of cells of each type that have detached during that step is appended to an array which is exported as a CSV file for further processing.

5. If there is only one type of cell left in the simulation, a countdown starts to allow the now single strain biofilm to reach equilibrium and at least an additional 250 steps.

For every step, the algorithm counts the number of each cell type that has detached in two variables. At the beginning of every new step, these variables are therefore reset to 0 to allow the count of detached cells to start anew for this step. Every time a cell detaches, the counter for the corresponding type is incremented by 1. At the end of the step, these two variables are concatenated and appended to an array. This array therefore contains all the values of the number of cells that have been removed from the simulation through detachment in the current step and all the previous ones. Finally, this array is exported as a CSV file.

Group detachment

In addition to cells detaching because they have reached their detachment height, the model implements a group detachment functionality. Indeed, in biofilms, detachment can also occur through cluster shedding (Petrova and Sauer, 2016) and can potentially significantly contribute to the detached biomass (Stoodley et al., 2001). The algorithm for group formation functions the following way:

1. An empty list of cells to be removed from the simulation is first created.

2. If cells have started to detach (i.e. the total number of cells detached of either type is above 0) and there are more than 3 cells in the simulation (necessary for triangulation) and cells are not all aligned (i.e. they are not just lined up on the base of the box), we perform a Delaunay triangulation (Fig. B.3, step 3).

3. This triangulation is used by a custom function that removes edges longer than λ. In brief this function locates the triangles that have edges longer than λ and removes them. The function outputs the set of remaining simplices (Figure B.3, step 4).

4. Two new lists are created that will accommodate the IDs and the position of centre of the cells.

5. If the list of simplices returned by the previous function is not empty (i.e. there is at least one group of cell with more than one cell), we need to determine which cells belong to which group. We arbitrarily start with a cell and search for which other nodes form the triangle in which the focal node is involved. Once we found these (called sister nodes), we repeat the process for these cells and so on until we cannot find more cells involved in neighbouring triangles. This forms one group. A list of cells that have not been assigned yet is generated and the whole process is repeated until all the cells have been tried (Fig. B.3, step 5).

6. If a cell has not been assigned to a group (which is possible if a couple of cells are linked by a simplice which occurs when both were within λ of one another but further than λ from all the other cells or in the case of a single cell), each individual cell not accounted for forms its own group.

7. In the unlikely event that all cells are further away than λ from one another, each cell is considered as a group.

8. We then look at whether the lowest cell in each group is further away than λ from the base of the box (i.e. y=0). If it is the case, then all the cells in this group are flagged as needing to be removed (growth rate evaluated to 0, unable to divide

and flagged for removal).

9. The counter for the number of cells detached during that step is incremented for the number of cells of each type that has detached similarly to the single cell detachment.

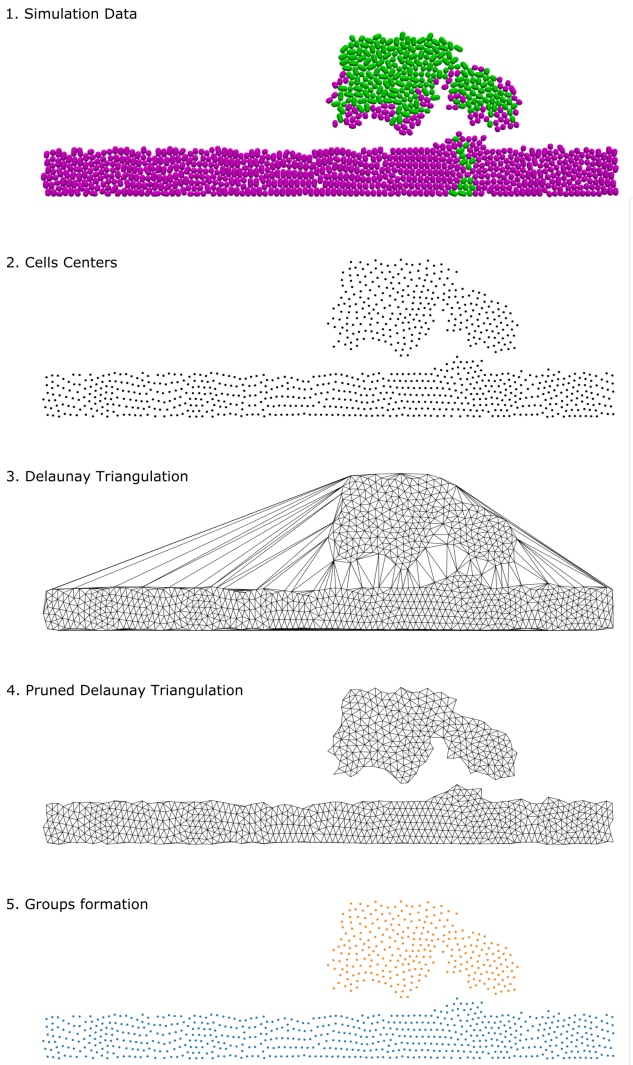

Figure B.3: Group formation illustrated. **1.** Visual representation of a time point in a simulation where a separate group is forming. **2.** Representation of the cells' centres used for the subsequent steps. **3.** Delaunay triangulation of the cells' centres. **4.** Triangulation after the edges longer than λ have been removed. **5.** Identification of the groups.

Growth

In the nutrient-limited case, the growth rate is evaluated as follows:

$$\mu_i = (\mu_{max} - ch)\frac{u_n(p_i)}{K + u_n(p_i)}$$

where μ_{max} is the the maximal growth rate of the cells, c is the cost per μm to invest in biofilm production, h is the maximum height at which the cell can grow (and therefore ch represents the metabolic cost of producing a biofilm), $u_n(p_i)$ is the concentration of nutrient at the cell's centre p_i and K is a saturation constant.

In nutrient-rich conditions, we have $u_n(p_i) = \infty$ and therefore, the growth rate is evaluated as:

$$\mu_i = (\mu_{max} - ch)$$

Division

The volume of each cell is checked against the division volume. If it is above it, then cells are instructed to divide. Cells divide symmetrically and therefore form two identical daughter cells.

Death

The toxin concentration at every cell's centre is evaluated. If this concentration is higher than $u_{T_{crit}}$ and the cell is of sensitive type, then:

1. The type of the cell is changed to 2 (assigned to dead cells).
2. The growth rate is set to 0.
3. The cells are forbidden to divide.
4. The lysis countdown starts. Any dead cell take 10 steps to lyse (i.e. to be removed from the simulation). Every step, the countdown of all the cells of type 2 is checked.

If it is below 1, the cell lyses and is removed from the simulation. If not, the cell remains in the simulation and the lysis countdown decreases by 1.

We chose to focus on a lytic mode of action for the toxin to begin with as it is easier to decouple the effects of toxin-based and nutrient-based competition. Moreover, most toxins need time to lyse cells (Smith et al., 2020) and can range from very rapid lysis (less than a minute) to slow lysis (several hours). We then picked an intermediate value for lysis of about 15 minutes. We do not expect lysis delay values to have much effect in nutrient-rich conditions (cells will likely be pushed out of the simulation by growing cells), but it could prove to have stronger effects in nutrient-limited conditions where dead cells might prevent other cells to take over the biofilm.

Parameters

Table B.2: Parameters used in this study

Parameter	Symbol	Value	Unit	Reference
Cells				
Cell radius	r	0.5	μm	(Smith et al., 2020)
Initial volume	V_i	0.54	μm^3	(Smith et al., 2017)
Growth rate	μ_{max}	1	h^{-1}	(Rudge et al., 2012)
Maximum cell division volume noise	η_{volume}	9	%	(Rudge et al., 2012)
Cell division orientation noise	$\eta_{orientation}$	0.2	%	(Rudge et al., 2012)
Detachment height	h	Variable	μm	This study
Biofilm formation cost	c	0.025	μm^{-1}	This study
Neighbourhood radius	$r_{neighbour}$	4	μm	This study
Critical distance between two groups	λ	2.4	μm	This study
Lethal toxin concentration	$u_{T_{crit}}$	0.5 & 6.5	-	This study
Lysis delay time	t_{lysis}	10	step	This study
Space and time				
Box width	Len_x	100	μm	This study
Time step	Δt	0.025	h	(Rudge et al., 2012)
Mesh element size	h_n	10	μm	This study
Biomass density	ρ	$2.9.10^{-13}$	$g/\mu m^3$	(Smith et al., 2017)
PDE solver				
Newton solver tolerance	ϵ_n	1.10^{-3}	-	(Smith et al., 2017)
Maximum Newton solver iterations	N_{iter}	500	-	(Smith et al., 2017)
Maximum contact iterations	M_{iter}	8	-	(Rudge et al., 2012)
Nutrient diffusivity	D_N	4.10^4	$\mu m^2/h$	(Bucci et al., 2011)
Toxin diffusivity	D_T	7.10^4	$\mu m^2/h$	(Bucci et al., 2011)
Toxin production yield per unit biomass	α_T	1.10^{-7}	g_T/g_X	(Bucci et al., 2011)
Toxin removal yield per unit biomass	β_T	1.10^{-7}	g_T/g_X	(Bucci et al., 2011)
Damköhler nutrient uptake	$D_{N,R}$	0.01	-	This study
Monod half-saturation concentration scaled by the bulk concentration	η_N	0.033	-	This study
Damköhler toxin production	$D_{T,P}$	0.01 & 0.1	-	This study
Damköhler toxin removal	$D_{T,R}$	0.0 & 1	-	This study

Monod half-saturation concentration for toxin removal scaled by the lethal concentration	η_T	1.0	-	This study

B.2 Bibliography

Ahrens, J., B. Geveci, and C. Law (2005). ParaView: An End-User Tool for Large-Data Visualization. In *Visualization Handbook*, pp. 717–731. Elsevier.

Bucci, V., C. D. Nadell, and J. B. Xavier (2011, December). The Evolution of Bacteriocin Production in Bacterial Biofilms. *The American Naturalist 178*(6), E162–E173.

Cascales, E., S. K. Buchanan, D. Duche, C. Kleanthous, R. Lloubes, K. Postle, M. Riley, S. Slatin, and D. Cavard (2007, March). Colicin Biology. *Microbiology and Molecular Biology Reviews 71*(1), 158–229.

Flemming, H.-C., J. Wingender, U. Szewzyk, P. Steinberg, S. A. Rice, and S. Kjelleberg (2016, September). Biofilms: An emergent form of bacterial life. *Nature Reviews Microbiology 14*(9), 563–575.

Grimm, V., U. Berger, D. L. DeAngelis, J. G. Polhill, J. Giske, and S. F. Railsback (2010, November). The ODD protocol: A review and first update. *Ecological Modelling 221*(23), 2760–2768.

Grimm, V., G. Polhill, and J. Touza (2013). Documenting Social Simulation Models: The ODD Protocol as a Standard. In B. Edmonds and R. Meyer (Eds.), *Simulating Social Complexity*, pp. 117–133. Berlin, Heidelberg: Springer Berlin Heidelberg.

Grimm, V., S. F. Railsback, C. E. Vincenot, U. Berger, C. Gallagher, D. L. DeAngelis, B. Edmonds, J. Ge, J. Giske, J. Groeneveld, A. S. Johnston, A. Milles, J. Nabe-Nielsen, J. G. Polhill, V. Radchuk, M.-S. Rohwäder, R. A. Stillman, J. C. Thiele, and D. Ayllón (2020). The ODD Protocol for Describing Agent-Based and Other Simulation Models: A Second Update to Improve Clarity, Replication, and Structural Realism. *Journal of Artificial Societies and Social Simulation 23*(2), 7.

Kerr, B., M. A. Riley, M. W. Feldman, and B. J. M. Bohannan (2002, July). Local dispersal promotes biodiversity in a real-life game of rock–paper–scissors. *Nature 418*(6894), 171–174.

Kimkes, T. E. P. and M. Heinemann (2020, January). How bacteria recognise and respond to surface contact. *FEMS Microbiology Reviews 44*(1), 106–122.

Monod, J. (1949). The growth of bacterial cultures. *Annual Review of Microbiology 3*, 371–394.

Nadell, C. D., K. R. Foster, and J. B. Xavier (2010, March). Emergence of Spatial Structure in Cell Groups and the Evolution of Cooperation. *PLoS Computational Biology 6*(3), e1000716.

Petrova, O. E. and K. Sauer (2016, April). Escaping the biofilm in more than one way: Desorption, detachment or dispersion. *Current Opinion in Microbiology 30*, 67–78.

Picioreanu, C., M. C. M. van Loosdrecht, and J. J. Heijnen (1998, April). Mathematical modeling of biofilm structure with a hybrid differential-discrete cellular automaton approach. *Biotechnology and Bioengineering 58*(1), 101–116.

Rudge, T. J., P. J. Steiner, A. Phillips, and J. Haseloff (2012, August). Computational Modeling of Synthetic Microbial Biofilms. *ACS Synthetic Biology 1*(8), 345–352.

Smith, W. P. J. (2017, June). *Influences of Cell Shape in Microbial Communities*. Ph. D. thesis, University of Oxford, Oxford.

Smith, W. P. J., Y. Davit, J. M. Osborne, W. Kim, K. R. Foster, and J. M. Pitt-Francis (2017, January). Cell morphology drives spatial patterning in microbial communities. *Proceedings of the National Academy of Sciences 114*(3), E280–E286.

Smith, W. P. J., A. Vettiger, J. Winter, T. Ryser, L. E. Comstock, M. Basler, and K. R. Foster (2020, May). The evolution of the type VI secretion system as a disintegration weapon. *PLOS Biology 18*(5), e3000720.

Stewart, P. S. and M. J. Franklin (2008, March). Physiological heterogeneity in biofilms. *Nature Reviews Microbiology 6*(3), 199–210.

Stoodley, P., S. Wilson, L. Hall-Stoodley, J. D. Boyle, H. M. Lappin-Scott, and J. W.

Costerton (2001, December). Growth and Detachment of Cell Clusters from Mature Mixed-Species Biofilms. *Applied and Environmental Microbiology 67*(12), 5608–5613.

B.3 Supplementary Figures

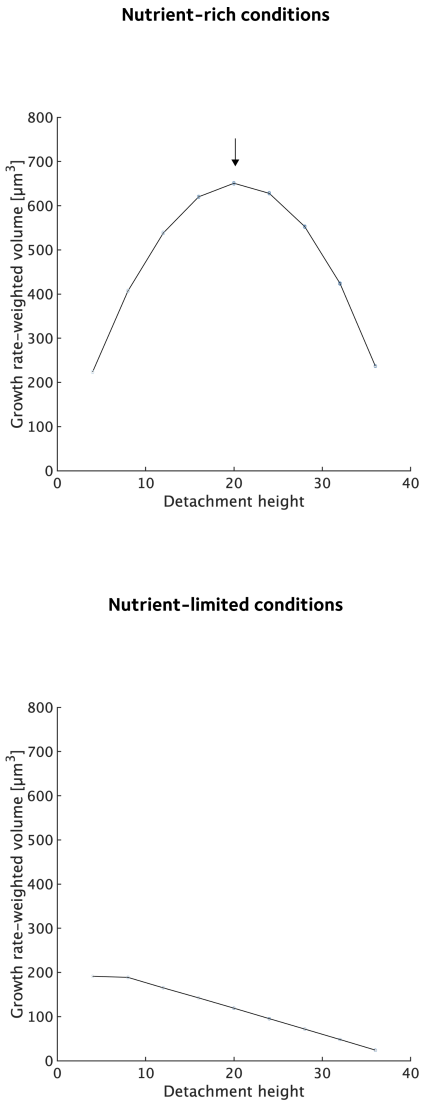

Figure B.4: Single strain fitness optimum — volume weighted by growth rate. **Top**: Volume of biofilm weighted by growth rate as a function of thickness in nutrient-rich conditions. **Bottom**: Volume of biofilm weighted by growth rate as a function of thickness in nutrient-limited conditions. The black arrows point to the optimal detachment height.

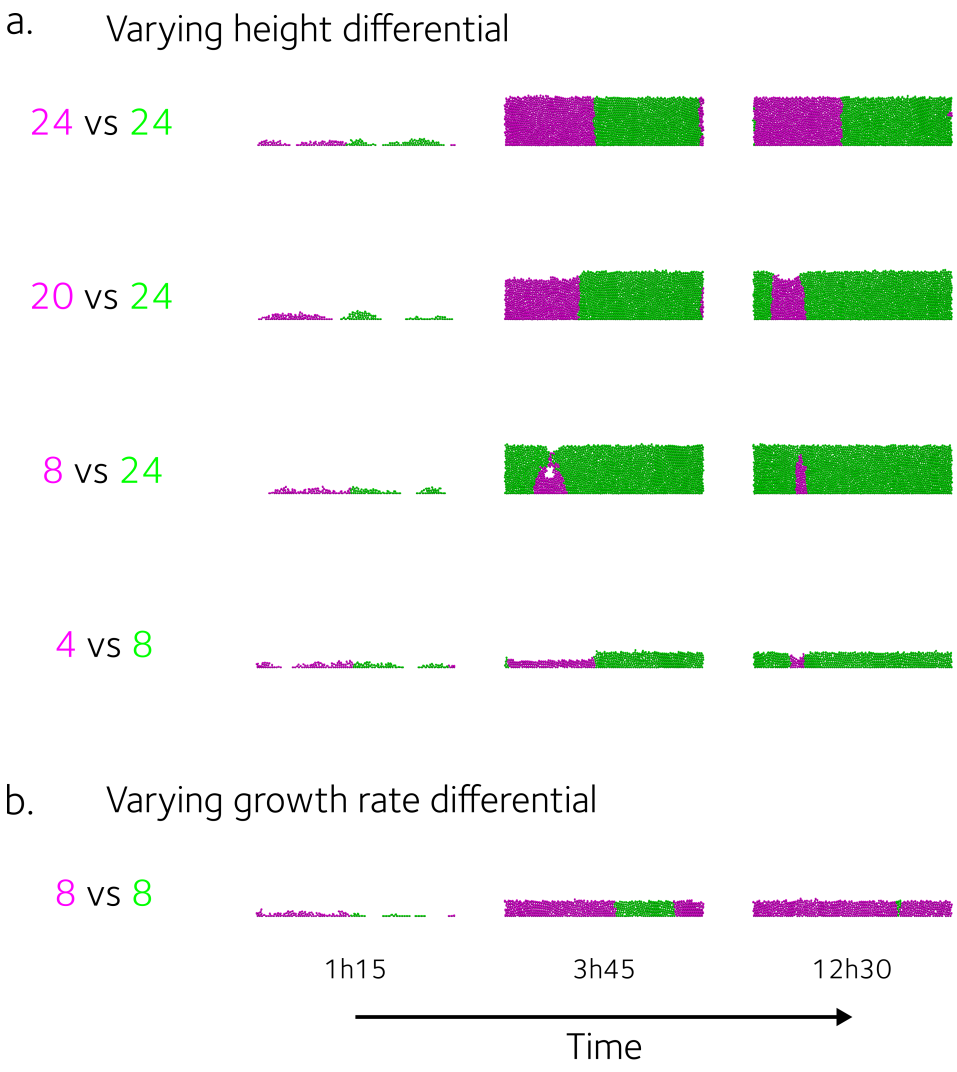

Figure B.5: Snapshots of competition where strains reach different heights but have the same growth rate. **a.** Strains invest the same amount irrespective of their detachment height. When strains grow at the same height, the two strains coexist (top: 24 μm against 24 μm). When a strain grows thinner, it is being pushed by the thicker biofilm. Thicker biofilms are better able to push thin biofilm than relatively thinner ones. **b.** Strains invest different amounts in biofilm formation irrespective of their detachment height. The green strain pays more for building its biofilm and is being pushed by the purple strain, which is faster growing.

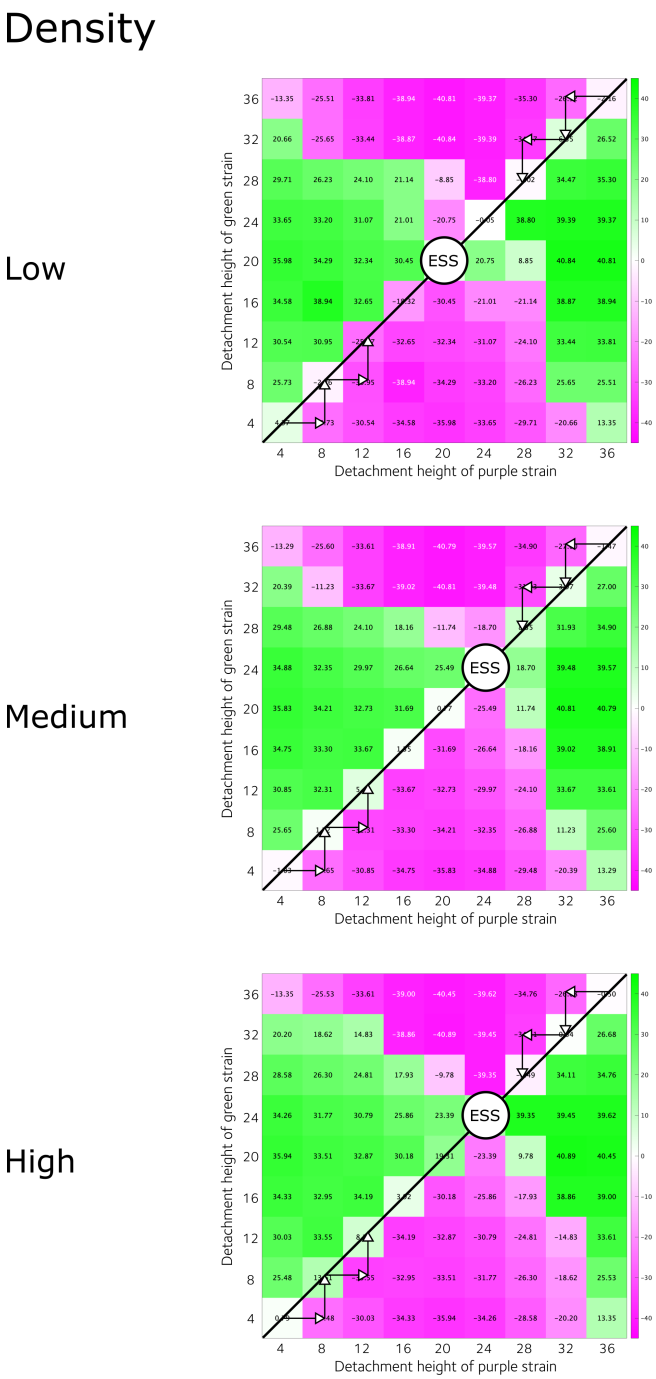

Figure B.6: ESS in nutrient-rich conditions depending on initial density — side by side configuration. **Top**: Low initial density (2 cells of each strain seeded). n=1 simulation per case. **Middle**: Medium initial density (6 cells of each strain seeded). n = 3 simulation per case. As seen in figure 3.5. **Bottom**: High initial density (18 cells of each strain seeded). n=1 simulation per case. As in 3.5, simulations above the diagonal have been mirrored below as simulations are symmetrical.

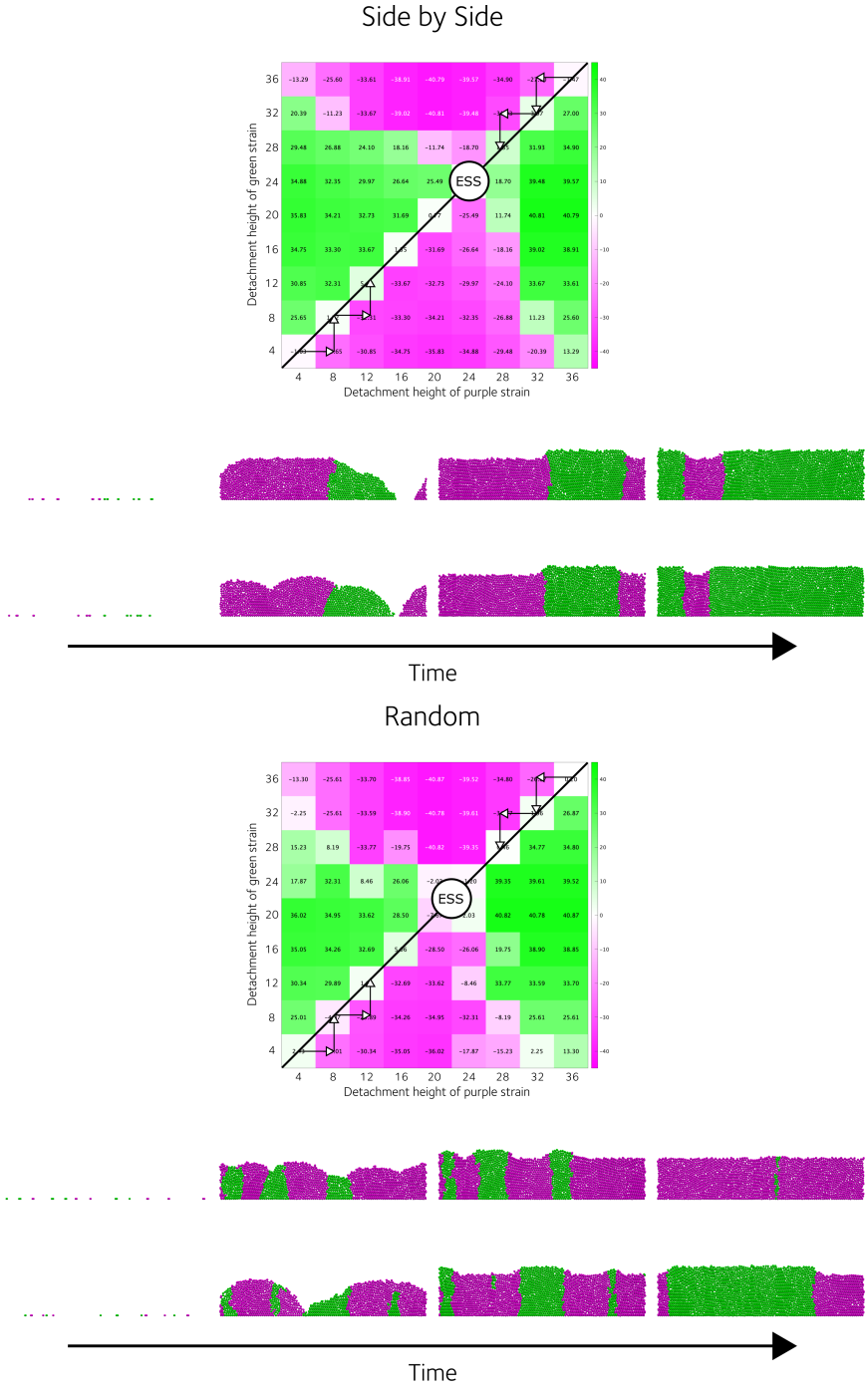

Figure B.7: ESS in nutrient-rich conditions depending on initial configuration of cells. **Top**: Side by side initial configuration as seen in figure 3.5. Arrows illustrate the progression of biofilm detachment heights converging on an evolutionary stable strategy height (ESS, white circle). n=3 simulation per case. **Bottom**: Random initial configuration. n = 3 simulation per case. Each row of snapshots represent two different replicates of the same pair of heights for each initial condition. Only the simulations on and above the black diagonal were run. The values were then mirrored for the bottom half as the cases are symmetrical.

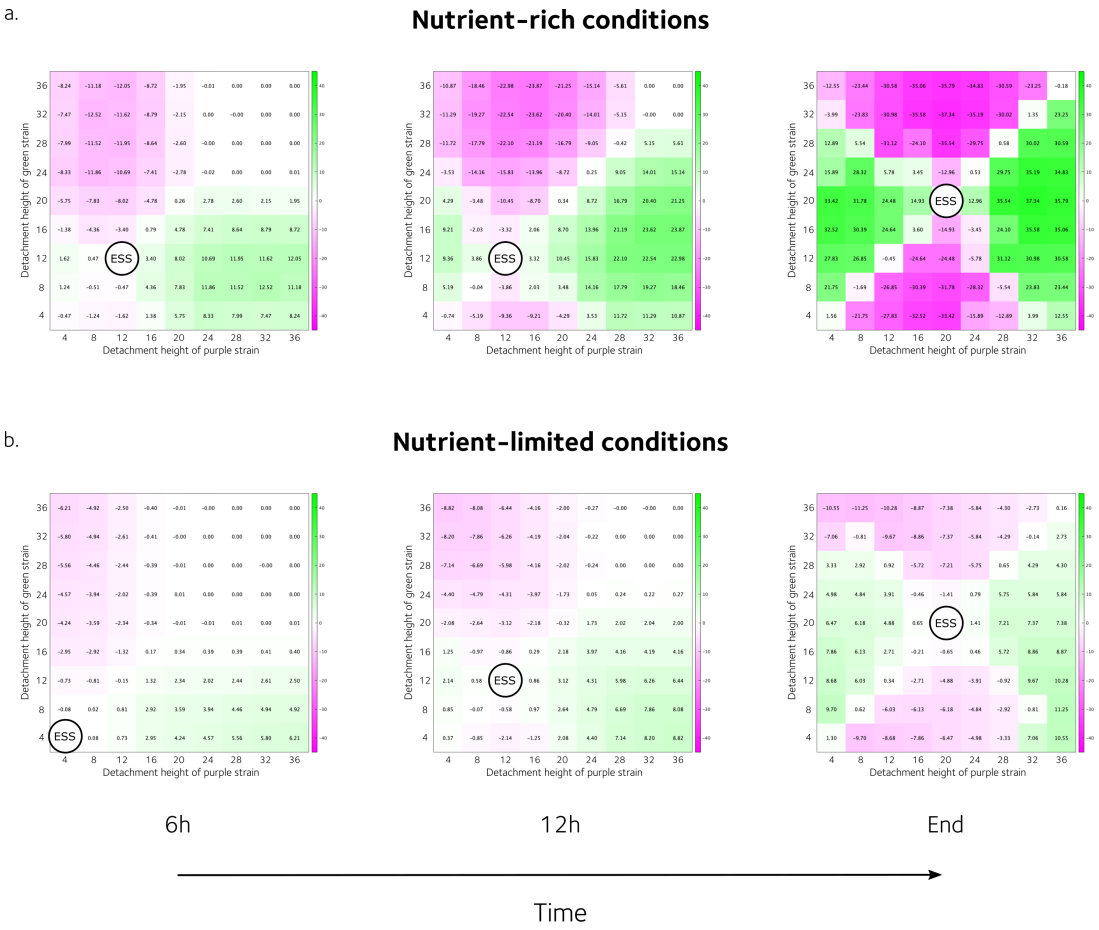

Figure B.8: Optimal detachment height in a 2-strain exploitative competition as a function of patch life-span — random initial configuration **a.** Nutrient-rich conditions. **b.** Nutrient-limited conditions. Evolutionary stable strategy height (ESS, white circle). n=3 simulation per case. Only the simulations on and above the black diagonal were run. The values were then mirrored for the bottom half as the cases are symmetrical to the ones above the diagonal.

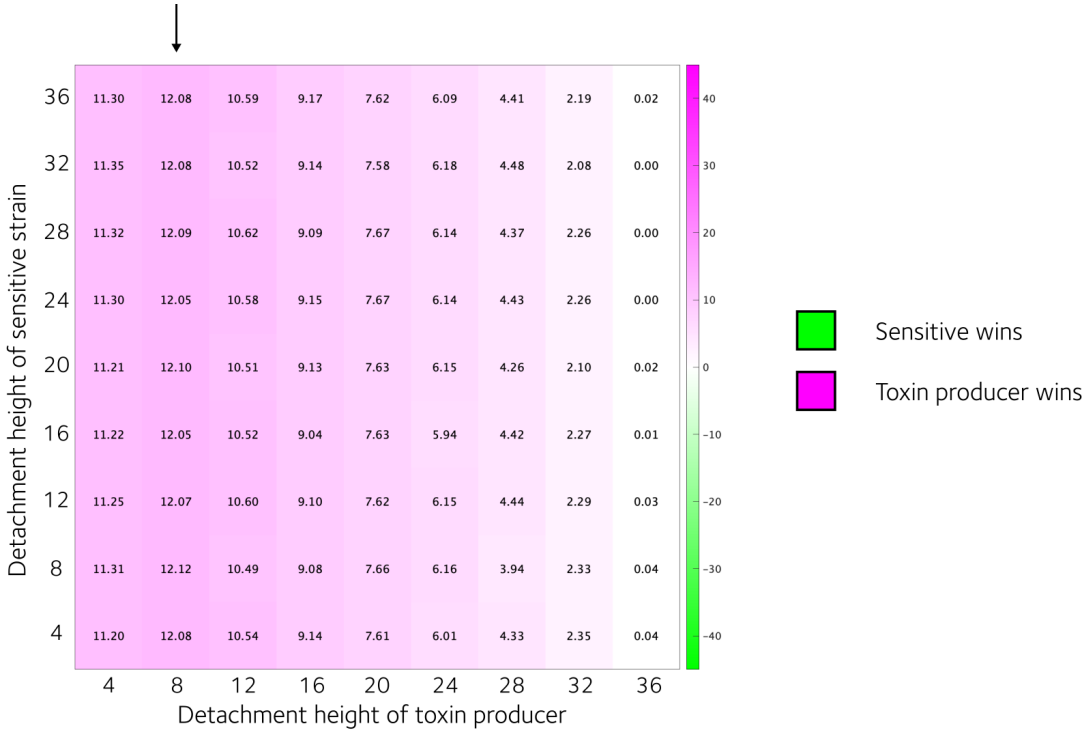

Figure B.9: Optimal strategy for a toxin producer in competition with a sensitive strain — nutrient-limited conditions & high toxin production. When toxins are produced abundantly, the optimal height for a toxin producer is its single strain optimum (i.e. 8 μm, black arrow). n=1 simulation per case.

Appendix C

Supplementary information for Chapter 4: "The Evolution and Ecology of Bacterial Warfare"

Supplemental Information

The Evolution and Ecology of Bacterial Warfare

Elisa T. Granato, Thomas A. Meiller-Legrand, and Kevin R. Foster

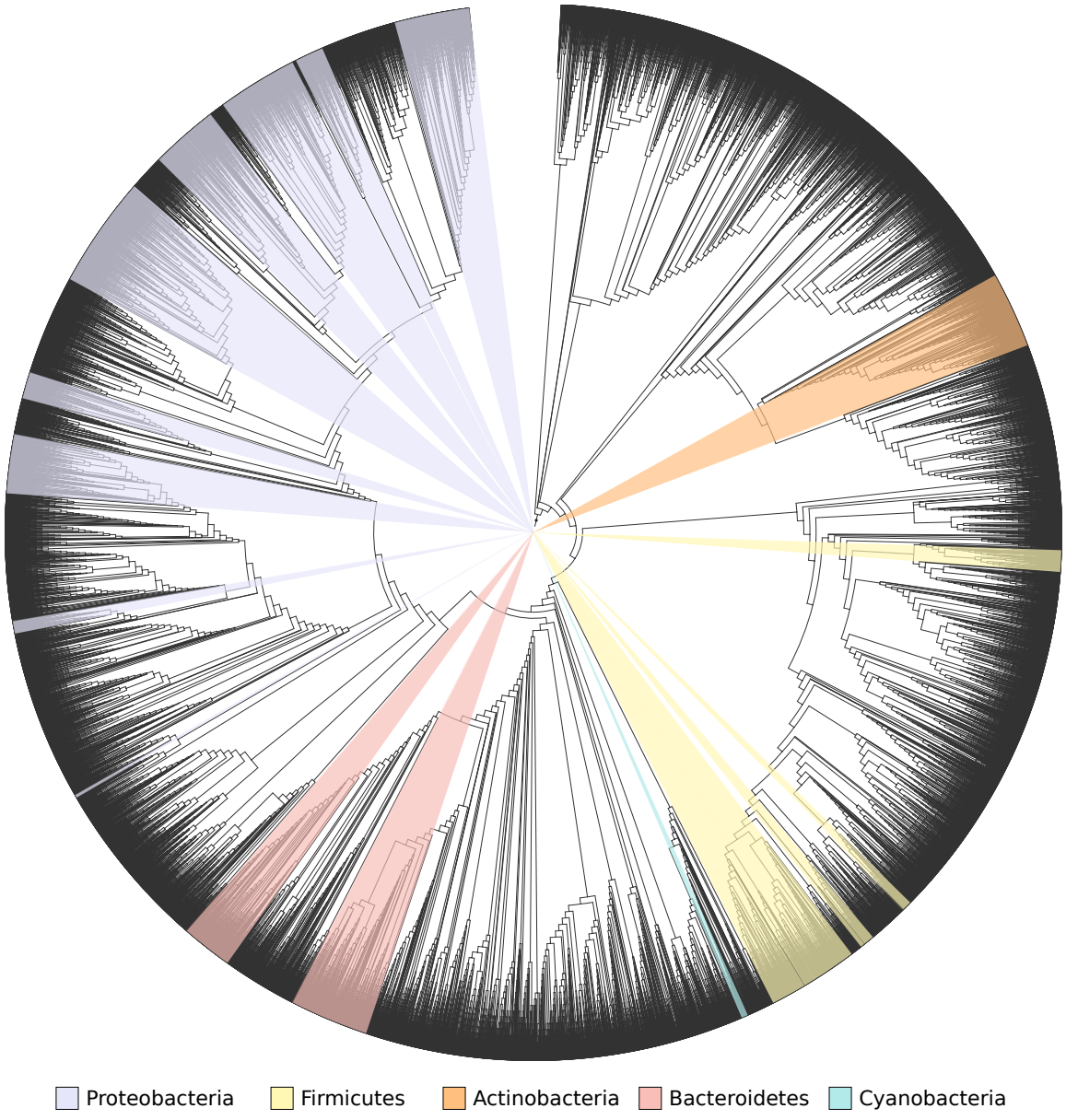
Proteobacteria
Firmicutes
Actinobacteria
Bacteroidetes
Cyanobacteria

Figure S1. The majority of sequenced bacterial families lack empirical data on weaponry. Refers to Figure 2.

The families to which the species displayed in Figure 2 belong are highlighted using the colours of the phyla to which they belong (blue, Proteobacteria; red, Bacteroidetes; yellow, Firmicutes; orange, Actinobacteria; turquoise, Cyanobacteria). Phylogenetic tree as built by Parks *et al.* [S1] and visualized with iTOL [S2] based on 94,759 genomes and including 152 families across the whole bacterial phylogeny. Note that many bacterial species are still missing from the figure, as they are not in DNA sequence databases. The cyanobacterial family where weapons have been studied contains only one species in the tree. To help it to be seen, we have manually widened the light blue colour bar above.

Table S1. Studies on bacterial weapon systems. Refers to Figure 2.

Phylum	Genus	Species	Gram stain	Weapon system									
				T4SS	T6SS	T7SS	CDI / Cdz	Nanotubes	OME	Small Molecules	Proteins	Tailocins	Phages
Proteobacteria - gamma	Acinetobacter	baumanii	-		[S3–S5]		[S6]						
Proteobacteria - gamma	Acinetobacter	baylyi	-		[S7,S8]		[S9]						
Proteobacteria - gamma	Acinetobacter	nosocomialis	-				[S6]						
Proteobacteria - gamma	Aeromonas	hydrophila	-		[S10]								
Proteobacteria - alpha	Agrobacterium	tumefaciens	-		[S11]					[S12]			
Firmicutes	Bacillus	amyloliquefaciens	+								[S13]		
Firmicutes	Bacillus	subtilis	+					[S14]		[S15,S16]			
Bacteroidetes	Bacteroides	fragilis	-		[S17–S19]						[S20]		
Bacteroidetes	Bacteroides	uniformis	-								[S21]		
Proteobacteria - beta	Bordetella	bronchiseptica	-										[S22]
Proteobacteria - beta	Burkholderia	dolosa	-				[S23]						
Proteobacteria - beta	Burkholderia	thailandensis	-		[S24–S26]		[S27]						
Proteobacteria - alpha	Caulobacter	crescentus	-				[S28]						
Proteobacteria - gamma	Citrobacter	rodentium	-		[S29]								
Firmicutes	Clostridium	difficile	+							[S30]			
Proteobacteria - gamma	Dickeya	dadantii	-		[S31]		[S32]						
Proteobacteria - gamma	Enterobacter	cloacae	-		[S33]		[S34]						
Firmicutes	Enterococcus	faecalis	+							[S35]	[S36]		[S37]
Proteobacteria - gamma	Erwinia	amylovora	-		[S39]								

Proteobacteria - gamma	Escherichia	coli	-		[S38]		[S32,S40]			[S41,S42]	[S43–S45]		[S46,S47]
Bacteroidetes	Flavobacterium	johnsoniae	-		[S17]								
Proteobacteria - gamma	Klebsiella	pneumoniae	-		[S48,S50]					[S49]			
Firmicutes	Lactobacillus	curvatus	+							[S51]			
Firmicutes	Lactobacillus	plantarum	+							[S52,S53]			
Firmicutes	Lactobacillus	salivarius	+							[S54]	[S55]		
Firmicutes	Lactobacillus	acidophilus	+							[S56]			
Firmicutes	Lactococcus	lactis	+										[S58]
Firmicutes	Listeria	monocytogenes	+							[S57]			
Proteobacteria - gamma	Moraxella	catarrhalis	-								[S61]		
Proteobacteria - delta	Myxococcus	xanthus	-						[S59,S60]	[S62,S63]			
Proteobacteria - gamma	Pantoea	agglomerans	-							[S64]			
Proteobacteria - gamma	Pantoea	ananatis	-		[S65]								
Proteobacteria - beta	Paraburkholderia	phymatum	-		[S66]								
Firmicutes	Pediococcus	acidilactici	+							[S67]			
Proteobacteria - gamma	Proteus	mirabilis	-		[S68,S69]								
Proteobacteria - gamma	Pseudoalteromonas	tunicata	-								[S70]		
Proteobacteria - gamma	Pseudomonas	aeruginosa	-		[S7,S17,S26,S71–S77]		[S78,S79]				[S80]	[S81]	[S82,S83]
Proteobacteria - gamma	Pseudomonas	chlororaphis	-									[S86]	
Proteobacteria - gamma	Pseudomonas	fluorescens	-		[S84,S85]							[S87]	
Proteobacteria - gamma	Pseudomonas	protegens	-		[S88,S89]								
Proteobacteria - gamma	Pseudomonas	putida	-		[S90]						[S91]		
Proteobacteria - gamma	Pseudomonas	syringae	-		[S92]		[S78]					[S93]	
Proteobacteria - gamma	Pseudomonas	taiwanensis	-		[S96]								
Proteobacteria - alpha	Rhizobium	leguminosarum	-							[S94]	[S95]		[S97]
Proteobacteria - gamma	Salmonella	typhimurium	-		[S98]						[S99]		[S100]
Proteobacteria - gamma	Serratia	marcescens	-		[S101–S104]								

Proteobacteria - gamma	Shigella	sonnei	-		[S105]								
Firmicutes	Staphylococcus	aureus	+			[S106]				[S107]			[S108]
Firmicutes	Staphylococcus	epidermidis	+							[S109]			
Firmicutes	Staphylococcus	hominis	+								[S110]		
Firmicutes	Staphylococcus	lugdunensis	+							[S111]			
Firmicutes	Streptococcus	intermedius	+			[S112]							
Firmicutes	Streptococcus	pneumoniae	+							[S113–S115]	[S116,S117]		
Actinobacteria	Streptomyces	coelicolor	+							[S118]			
Actinobacteria	Streptomyces	griseus	+							[S118]			
Actinobacteria	Streptomyces	sp. Mg1	+							[S119]			
Cyanobacteria	Synechococcus	sp. CC9605	-							[S120]			
Proteobacteria - gamma	Vibrio	alginolyticus	-		[S121]								
Proteobacteria - gamma	Vibrio	cholerae	-		[S8,S26,S122–S127]								
Proteobacteria - gamma	Vibrio	fischeri	-		[S128]								
Proteobacteria - gamma	Vibrio	parahaemolyticus	-		[S129–S131]								
Proteobacteria - gamma	Xanthomonas	citri	-	[S132]									
Proteobacteria - gamma	Xanthomonas	perforans	-								[S133]		
Proteobacteria - gamma	Xenorhabdus	bovienii	-									[S134]	
Proteobacteria - gamma	Xenorhabdus	nematophila	-									[S135]	

Supplemental References

S1. Parks, D.H., Chuvochina, M., Waite, D.W., Rinke, C., Skarshewski, A., Chaumeil, P., and Hugenholtz, P. (2018). A standardized bacterial taxonomy based on genome phylogeny substantially revises the tree of life. Nat. Biotechnol. *36*, 996–1004.

S2. Letunic, I., and Bork, P. (2016). Interactive tree of life (iTOL) v3: an online tool for the display and annotation of phylogenetic and other trees. Nucleic Acids Res. 44, W242–W245.

S3. Carruthers, M.D., Nicholson, P.A., Tracy, E.N., and Munson, R.S. (2013). *Acinetobacter baumannii* utilizes a type VI secretion system for bacterial competition. PLoS ONE *8*, e59388.

S4. Weber, B.S., Hennon, S.W., Wright, M.S., Scott, N.E., de Berardinis, V., Foster, L.J., Ayala, J.A., Adams, M.D., and Feldman, M.F. (2016). Genetic dissection of the type VI secretion system in *Acinetobacter* and identification of a novel peptidoglycan hydrolase, TagX, required for its biogenesis. mBio *7*, e01253-16.

S5. Repizo, G.D., Gagné, S., Foucault-Grunenwald, M.-L., Borges, V., Charpentier, X., Limansky, A.S., Gomes, J.P., Viale, A.M., and Salcedo, S.P. (2015). Differential role of the T6SS in *Acinetobacter baumannii* virulence. PLoS ONE *10*, e0138265.

S6. Harding, C.M., Pulido, M.R., Di Venanzio, G., Kinsella, R.L., Webb, A.I., Scott, N.E., Pachón, J., and Feldman, M.F. (2017). Pathogenic *Acinetobacter* species have a functional type I secretion system and contact-dependent inhibition systems. J. Biol. Chem. *292*, 9075–9087.

S7. Basler, M., Ho, B.T., and Mekalanos, J.J. (2013). Tit-for-tat: type VI secretion system counterattack during bacterial cell-cell interactions. Cell *152*, 884–894.

S8. Shneider, M.M., Buth, S.A., Ho, B.T., Basler, M., Mekalanos, J.J., and Leiman, P.G. (2013). PAAR-repeat proteins sharpen and diversify the type VI secretion system spike. Nature *500*, 350–353.

S9. De Gregorio, E., Esposito, E.P., Zarrilli, R., and Di Nocera, P.P. (2018). Contact-dependent growth inhibition proteins in *Acinetobacter baylyi* ADP1. Curr. Microbiol. *75*, 1434–1440.

S10. Wong, M.J.Q., Liang, X., Smart, M., Tang, L., Moore, R., Ingalls, B., and Dong, T.G. (2016). Microbial herd protection mediated by antagonistic interaction in polymicrobial communities. Appl. Environ. Microbiol. *82*, 6881–6888.

S11. Ma, L.-S., Hachani, A., Lin, J.-S., Filloux, A., and Lai, E.-M. (2014). *Agrobacterium tumefaciens* deploys a superfamily of type VI secretion DNase effectors as weapons for interbacterial competition in planta. Cell Host Microbe *16*, 94–104.

S12. Cooksey, D.A., and Moore, L.W. (1982). Biological control of crown gall with an Agrocin mutant of *Agrobacterium radiobacter*. Phytopathology *72*, 919–921.

S13. Scholz, R., Vater, J., Budiharjo, A., Wang, Z., He, Y., Dietel, K., Schwecke, T., Herfort, S., Lasch, P., and Borriss, R. (2014). Amylocyclicin, a novel circular bacteriocin produced by *Bacillus amyloliquefaciens* FZB42. J. Bacteriol. *196*, 1842–1852.

S14. Stempler, O., Baidya, A.K., Bhattacharya, S., Malli Mohan, G.B., Tzipilevich, E., Sinai, L., Mamou, G., and Ben-Yehuda, S. (2017). Interspecies nutrient extraction and toxin delivery between bacteria. Nat. Commun. *8*, 315.

S15. Straight, P.D., Willey, J.M., and Kolter, R. (2006). Interactions between *Streptomyces coelicolor* and *Bacillus subtilis*: role of surfactants in raising aerial structures. J. Bacteriol. *188*, 4918–4925.

S16. Bais, H.P. (2004). Biocontrol of *Bacillus subtilis* against infection of *Arabidopsis* roots by *Pseudomonas syringae* is facilitated by biofilm formation and surfactin production. Plant Physiol. *134*, 307–319.

S17. Russell, A.B., Wexler, A.G., Harding, B.N., Whitney, J.C., Bohn, A.J., Goo, Y.A., Tran, B.Q., Barry, N.A., Zheng, H., Peterson, S.B., *et al.* (2014). A type VI secretion-related pathway in Bacteroidetes mediates interbacterial antagonism. Cell Host Microbe *16*, 227–236.

S18. Verster, A.J., Ross, B.D., Radey, M.C., Bao, Y., Goodman, A.L., Mougous, J.D., and Borenstein, E. (2017). The landscape of type VI secretion across human gut microbiomes reveals its role in community composition. Cell Host Microbe *22*, 411-419.

S19. Chatzidaki-Livanis, M., Geva-Zatorsky, N., and Comstock, L.E. (2016). *Bacteroides fragilis* type VI secretion systems use novel effector and immunity proteins to antagonize human gut Bacteroidales species. Proc. Natl. Acad. Sci. USA *113*, 3627–3632.

S20. Chatzidaki-Livanis, M., Coyne, M.J., Roelofs, K.G., Gentyala, R.R., Caldwell, J.M., and Comstock, L.E. (2017). Gut symbiont *Bacteroides fragilis* secretes a eukaryotic-like ubiquitin protein that mediates intraspecies antagonism. mBio *8*, e01902-17.

S21. Roelofs, K.G., Coyne, M.J., Gentyala, R.R., Chatzidaki-Livanis, M., and Comstock, L.E. (2016). *Bacteroidales* secreted antimicrobial proteins target surface molecules necessary for gut colonization and mediate competition *in vivo*. mBio *7*, e01055-16.

S22. Joo, J., Gunny, M., Cases, M., Hudson, P., Albert, R., and Harvill, E. (2006). Bacteriophage-mediated competition in *Bordetella* bacteria. Proc. Biol. Sci. *273*, 1843–1848.

S23. Perault, A.I., and Cotter, P.A. (2018). Three distinct contact-dependent growth inhibition systems mediate interbacterial competition by the cystic fibrosis pathogen *Burkholderia dolosa*. J. Bacteriol. *200*, e00428-18.

S24. Schwarz, S., West, T.E., Boyer, F., Chiang, W.-C., Carl, M.A., Hood, R.D., Rohmer, L., Tolker-Nielsen, T., Skerrett, S.J., and Mougous, J.D. (2010). *Burkholderia* type VI secretion systems have distinct roles in eukaryotic and bacterial cell interactions. PLoS Pathog. *6*, e1001068.

S25. Russell, A.B., Singh, P., Brittnacher, M., Bui, N.K., Hood, R.D., Carl, M.A., Agnello, D.M., Schwarz, S., Goodlett, D.R., Vollmer, W., *et al.* (2012). A widespread bacterial type VI secretion effector superfamily identified using a heuristic approach. Cell Host Microbe *11*, 538–549.

S26. Russell, A.B., LeRoux, M., Hathazi, K., Agnello, D.M., Ishikawa, T., Wiggins, P.A., Wai, S.N., and Mougous, J.D. (2013). Diverse type VI secretion phospholipases are functionally plastic antibacterial effectors. Nature *496*, 508–512.

S27. Nikolakakis, K., Amber, S., Wilbur, J.S., Diner, E.J., Aoki, S.K., Poole, S.J., Tuanyok, A., Keim, P.S., Peacock, S., Hayes, C.S., *et al.* (2012). The toxin/immunity network of *Burkholderia pseudomallei* contact-dependent growth inhibition (CDI) systems. Mol. Microbiol. *84*, 516–529.

S28. García-Bayona, L., Guo, M.S., and Laub, M.T. (2017). Contact-dependent killing by *Caulobacter crescentus* via cell surface-associated, glycine zipper proteins. eLife *6*, e24869.

S29. Gueguen, E., and Cascales, E. (2013). Promoter swapping unveils the role of the *Citrobacter rodentium* CTS1 type VI secretion system in interbacterial competition. Appl. Environ. Microbiol. *79*, 32–38.

S30. Passmore, I.J., Letertre, M.P.M., Preston, M.D., Bianconi, I., Harrison, M.A., Nasher, F., Kaur, H., Hong, H.A., Baines, S.D., Cutting, S.M., *et al.* (2018). Para-cresol production by *Clostridium difficile* affects microbial diversity and membrane integrity of Gram-negative bacteria. PLoS Pathog. *14*, e1007191.

S31. Koskiniemi, S., Lamoureux, J.G., Nikolakakis, K.C., t'Kint de Roodenbeke, C., Kaplan, M.D., Low, D.A., and Hayes, C.S. (2013). Rhs proteins from diverse bacteria mediate intercellular competition. Proc. Natl. Acad. Sci. USA *110*, 7032–7037.

S32. Aoki, S.K., Diner, E.J., t'Kint de Roodenbeke, C., Burgess, B.R., Poole, S.J., Braaten, B.A., Jones, A.M., Webb, J.S., Hayes, C.S., Cotter, P.A., *et al.* (2010). A widespread family of polymorphic contact-dependent toxin delivery systems in bacteria. Nature *468*, 439–442.

S33. Whitney, J.C., Beck, C.M., Goo, Y.A., Russell, A.B., Harding, B.N., De Leon, J.A., Cunningham, D.A., Tran, B.Q., Low, D.A., Goodlett, D.R., *et al.* (2014). Genetically distinct pathways guide effector export through the type VI secretion system. Mol. Microbiol. *92*, 529–542.

S34. Beck, C.M., Morse, R.P., Cunningham, D.A., Iniguez, A., Low, D.A., Goulding, C.W., and Hayes, C.S. (2014). CdiA from *Enterobacter cloacae* delivers a toxic ribosomal RNase into target bacteria. Structure *22*, 707–718.

S35. Gilmore, M.S., Rauch, M., Ramsey, M.M., Himes, P.R., Varahan, S., Manson, J.M., Lebreton, F., and Hancock, L.E. (2015). Pheromone killing of multidrug-resistant *Enterococcus faecalis* V583 by native commensal strains. Proc. Natl. Acad. Sci. USA *112*, 7273–7278.

S36. Kommineni, S., Bretl, D.J., Lam, V., Chakraborty, R., Hayward, M., Simpson, P., Cao, Y., Bousounis, P., Kristich, C.J., and Salzman, N.H. (2015). Bacteriocin production augments niche competition by enterococci in the mammalian gastrointestinal tract. Nature *526*, 719–722.

S37. Duerkop, B.A., Clements, C.V., Rollins, D., Rodrigues, J.L.M., and Hooper, L.V. (2012). A composite bacteriophage alters colonization by an intestinal commensal bacterium. Proc. Natl. Acad. Sci. USA *109*, 17621–17626.

S38. Flaugnatti, N., Le, T.T.H., Canaan, S., Aschtgen, M.-S., Nguyen, V.S., Blangy, S., Kellenberger, C., Roussel, A., Cambillau, C., Cascales, E., *et al.* (2016). A phospholipase A $_1$ antibacterial type VI secretion effector interacts directly with the C-terminal domain of the VgrG spike protein for delivery. Mol. Microbiol. *99*, 1099–1118.

S39. Tian, Y., Zhao, Y., Shi, L., Cui, Z., Hu, B., and Zhao, Y. (2017). Type VI Secretion systems of *Erwinia amylovora* contribute to bacterial competition, virulence, and exopolysaccharide production. Phytopathology *107*, 654–661.

S40. Aoki, S.K. (2005). Contact-dependent inhibition of growth in *Escherichia coli*. Science *309*, 1245–1248.

S41. Sassone-Corsi, M., Nuccio, S.-P., Liu, H., Hernandez, D., Vu, C.T., Takahashi, A.A., Edwards, R.A., and Raffatellu, M. (2016). Microcins mediate competition among Enterobacteriaceae in the inflamed gut. Nature *540*, 280–283.

S42. Eberhart, L.J., Ochoa, J.N., Besser, T.E., and Call, D.R. (2014). Microcin MccPDI reduces the prevalence of susceptible *Escherichia coli* in neonatal calves. J. Appl. Microbiol. *117*, 340–346.

S43. Gordon, D.M., and Riley, M.A. (1999). A theoretical and empirical investigation of the invasion dynamics of colicinogeny. Microbiology *145*, 655–661.

S44. Chao, L., and Levin, B.R. (1981). Structured habitats and the evolution of anticompetitor toxins in bacteria. Proc. Natl. Acad. Sci. USA *78*, 6324–6328.

S45. Majeed, H., Gillor, O., Kerr, B., and Riley, M.A. (2011). Competitive interactions in *Escherichia coli* populations: the role of bacteriocins. ISME J. *5*, 71–81.

S46. Brown, S.P., Le Chat, L., De Paepe, M., and Taddei, F. (2006). Ecology of microbial invasions: amplification allows virus carriers to invade more rapidly when rare. Curr. Biol. *16*, 2048–2052.

S47. Gama, J.A., Reis, A.M., Domingues, I., Mendes-Soares, H., Matos, A.M., and Dionisio, F. (2013). Temperate bacterial viruses as double-edged swords in bacterial warfare. PLoS ONE *8*, e59043.

S48. Hsieh, P.-F., Lu, Y.-R., Lin, T.-L., Lai, L.-Y., and Wang, J.-T. (2019). *Klebsiella pneumoniae* type VI secretion system contributes to bacterial competition, cell invasion, type-1 fimbriae expression, and in vivo colonization. J. Infect. Dis. *219*, 637–647.

S49. De Lorenzo, V., Martínez, J.L., and Asensio, C. (1984). Microcin-mediated interactions between *Klebsiella pneumoniae* and *Escherichia coli* strains. J. Gen. Microbiol. *130*, 391–400.

S50. Liu, L., Ye, M., Li, X., Li, J., Deng, Z., Yao, Y.-F., and Ou, H.-Y. (2017). Identification and characterization of an antibacterial type VI secretion system in the carbapenem-resistant strain *Klebsiella pneumoniae* HS11286. Front. Cell. Infect. Microbiol. *7*, 442.

S51. Vogel, R.F., Pohle, B.S., Tichaczek, P.S., and Hammes, W.P. (1993). The competitive advantage of *Lactobacillus curvatus* LTH 1174 in sausage fermentations is caused by formation of curvacin A. Syst. Appl. Microbiol. *16*, 457–462.

S52. Leal, M.V., Baras, M., Ruiz-Barba, J.L., Floriano, B., and Jiménez-Díaz, R. (1998). Bacteriocin production and competitiveness of *Lactobacillus plantarum* LPCO10 in olive juice broth, a culture medium obtained from olives. Int. J. Food Microbiol. *43*, 129–134.

S53. Ruiz-Barba, J.L., Cathcart, D.P., Warner, P.J., and Jimenez-Diaz, R. (1994). Use of *Lactobacillus plantarum* LPCO10, a bacteriocin producer, as a starter culture in Spanish-style green olive fermentations. Appl. Environ. Microbiol. *60*, 2059–2064.

S54. Corr, S.C., Li, Y., Riedel, C.U., O'Toole, P.W., Hill, C., and Gahan, C.G.M. (2007). Bacteriocin production as a mechanism for the antiinfective activity of *Lactobacillus salivarius* UCC118. Proc. Natl. Acad. Sci. USA *104*, 7617–7621.

S55. Riboulet-Bisson, E., Sturme, M.H.J., Jeffery, I.B., O'Donnell, M.M., Neville, B.A., Forde, B.M., Claesson, M.J., Harris, H., Gardiner, G.E., Casey, P.G., *et al.* (2012). Effect of *Lactobacillus salivarius* bacteriocin Abp118 on the mouse and pig intestinal microbiota. PLoS ONE *7*, e31113.

S56. Kanatani, K., Tahara, T., Yoshida, K., Miura, H., Sakamoto, M., and Oshimura, M. (1992). Plasmid-associated bacteriocin production by and immunity of *Lactobacillus acidophilus* TK8912. Biosci. Biotechnol. Biochem. *56*, 648–651.

S57. Quereda, J.J., Dussurget, O., Nahori, M.-A., Ghozlane, A., Volant, S., Dillies, M.-A., Regnault, B., Kennedy, S., Mondot, S., Villoing, B., *et al.* (2016). Bacteriocin from epidemic *Listeria* strains alters the host intestinal microbiota to favor infection. Proc. Natl. Acad. Sci. USA *113*, 5706–5711.

S58. Alexeeva, S., Guerra Martínez, J.A., Spus, M., and Smid, E.J. (2018). Spontaneously induced prophages are abundant in a naturally evolved bacterial starter culture and deliver competitive advantage to the host. BMC Microbiology *18*, 120.

S59. Dey, A., Vassallo, C.N., Conklin, A.C., Pathak, D.T., Troselj, V., and Wall, D. (2016). Sibling rivalry in *Myxococcus xanthus* is mediated by kin recognition and a polyploid prophage. J. Bacteriol. *198*, 994–1004.

S60. Vassallo, C.N., Cao, P., Conklin, A., Finkelstein, H., Hayes, C.S., and Wall, D. (2017). Infectious polymorphic toxins delivered by outer membrane exchange discriminate kin in myxobacteria. eLife *6*, e29397.

S61. Attia, A.S., Sedillo, J.L., Hoopman, T.C., Liu, W., Liu, L., Brautigam, C.A., and Hansen, E.J. (2009). Identification of a bacteriocin and its cognate immunity factor expressed by *Moraxella catarrhalis.* BMC Microbiol. *9*, 207.

S62. Xiao, Y., Wei, X., Ebright, R., and Wall, D. (2011). Antibiotic production by myxobacteria plays a role in predation. J. Bacteriol. *193*, 4626–4633.

S63. Xiao, Y., Gerth, K., Müller, R., and Wall, D. (2012). *Myxobacterium*-produced antibiotic TA (Myxovirescin) inhibits type II signal peptidase. Antimicrob. Agents Chemother. *56*, 2014–2021.

S64. Giddens, S.R., Houliston, G.J., and Mahanty, H.K. (2003). The influence of antibiotic production and pre-emptive colonization on the population dynamics of *Pantoea agglomerans* (*Erwinia herbicola*) Eh1087 and *Erwinia amylovora* in planta. Environ. Microbiol. *5*, 1016–1021.

S65. Shyntum, D.Y., Theron, J., Venter, S.N., Moleleki, L.N., Toth, I.K., and Coutinho, T.A. (2015). *Pantoea ananatis* utilizes a type VI secretion system for pathogenesis and bacterial competition. Mol. Plant Microbe Interact. *28*, 420–431.

S66. de Campos, S.B., Lardi, M., Gandolfi, A., Eberl, L., and Pessi, G. (2017). Mutations in two *Paraburkholderia phymatum* type VI secretion systems cause reduced fitness in interbacterial competition. Front. Microbiol. *8*, 2473.

S67. Foegeding, P.M., Thomas, A.B., Pilkington, D.H., and Klaenhammer, T.R. (1992). Enhanced control of *Listeria monocytogenes* by in situ-produced pediocin during dry fermented sausage production. Appl. Environ. Microbiol. *58*, 884–890.

S68. Alteri, C.J., Himpsl, S.D., Pickens, S.R., Lindner, J.R., Zora, J.S., Miller, J.E., Arno, P.D., Straight, S.W., and Mobley, H.L.T. (2013). Multicellular bacteria deploy the type VI secretion system to preemptively strike neighboring cells. PLoS Pathog. *9*, e1003608.

S69. Wenren, L.M., Sullivan, N.L., Cardarelli, L., Septer, A.N., and Gibbs, K.A. (2013). Two independent pathways for self-recognition in *Proteus mirabilis* are linked by type VI-dependent export. mBio *4*, e00374-13.

S70. Rao, D., Webb, J.S., and Kjelleberg, S. (2005). Competitive interactions in mixed-species biofilms containing the marine bacterium *Pseudoalteromonas tunicata*. Appl. Environ. Microbiol. *71*, 1729–1736.

S71. Hood, R.D., Singh, P., Hsu, F., Güvener, T., Carl, M.A., Trinidad, R.R.S., Silverman, J.M., Ohlson, B.B., Hicks, K.G., Plemel, R.L., *et al.* (2010). A type VI secretion system of *Pseudomonas aeruginosa* targets a toxin to bacteria. Cell Host Microbe *7*, 25–37.

S72. Russell, A.B., Hood, R.D., Bui, N.K., LeRoux, M., Vollmer, W., and Mougous, J.D. (2011). Type VI secretion delivers bacteriolytic effectors to target cells. Nature *475*, 343–347.

S73. Ge, X., Wei, W., Li, G., Sun, M., Li, H., Wu, J., and Hu, F. (2017). Isolated *Pseudomonas aeruginosa* strain VIH2 and antagonistic properties against *Ralstonia solanacearum*. Microb. Pathog. *111*, 519–526.

S74. LeRoux, M., De Leon, J.A., Kuwada, N.J., Russell, A.B., Pinto-Santini, D., Hood, R.D., Agnello, D.M., Robertson, S.M., Wiggins, P.A., and Mougous, J.D. (2012). Quantitative single-cell characterization of bacterial interactions reveals type VI secretion is a double-edged sword. Proc. Natl. Acad. Sci. USA *109*, 19804–19809.

S75. Hachani, A., Allsopp, L.P., Oduko, Y., and Filloux, A. (2014). The VgrG proteins are "à la Carte" delivery systems for bacterial type VI effectors. J. Biol. Chem. *289*, 17872–17884.

S76. Jiang, F., Waterfield, N.R., Yang, J., Yang, G., and Jin, Q. (2014). A *Pseudomonas aeruginosa* type VI secretion phospholipase D effector targets both prokaryotic and eukaryotic cells. Cell Host Microbe *15*, 600–610.

S77. LaCourse, K.D., Peterson, S.B., Kulasekara, H.D., Radey, M.C., Kim, J., and Mougous, J.D. (2018). Conditional toxicity and synergy drive diversity among antibacterial effectors. Nat. Microbiol. *3*, 440–446.

S78. Mercy, C., Ize, B., Salcedo, S.P., de Bentzmann, S., and Bigot, S. (2016). Functional characterization of *Pseudomonas* contact dependent growth inhibition (CDI) systems. PLoS ONE *11*, e0147435.

S79. Melvin, J.A., Gaston, J.R., Phillips, S.N., Springer, M.J., Marshall, C.W., Shanks, R.M.Q., and Bomberger, J.M. (2017). *Pseudomonas aeruginosa* contact-dependent growth inhibition plays dual role in host-pathogen interactions. mSphere *2*, e00336-17.

S80. Inglis, R.F., Gardner, A., Cornelis, P., and Buckling, A. (2009). Spite and virulence in the bacterium *Pseudomonas aeruginosa*. Proc. Natl. Acad. Sci. USA *106*, 5703–5707.

S81. Heo, Y.-J., Chung, I.-Y., Choi, K.B., and Cho, Y.-H. (2007). R-type pyocin is required for competitive growth advantage between *Pseudomonas aeruginosa* strains. J. Microbiol. Biotechnol. *17*, 180–185.

S82. Burns, N., James, C.E., and Harrison, E. (2015). Polylysogeny magnifies competitiveness of a bacterial pathogen *in vivo*. Evol. Appl. *8*, 346–351.

S83. Davies, E.V., James, C.E., Kukavica-Ibrulj, I., Levesque, R.C., Brockhurst, M.A., and Winstanley, C. (2016). Temperate phages enhance pathogen fitness in chronic lung infection. ISME J. *10*, 2553–2555.

S84. Decoin, V., Barbey, C., Bergeau, D., Latour, X., Feuilloley, M.G.J., Orange, N., and Merieau, A. (2014). A type VI secretion system is involved in *Pseudomonas fluorescens* bacterial competition. PLoS ONE *9*, e89411.

S85. Decoin, V., Gallique, M., Barbey, C., Le Mauff, F., Poc, C.D., Feuilloley, M.G., Orange, N., and Merieau, A. (2015). A *Pseudomonas fluorescens* type 6 secretion system is related to mucoidy, motility and bacterial competition. BMC Microbiol. *15*, 72.

S86. Dorosky, R.J., Yu, J.M., Pierson, L.S., and Pierson, E.A. (2017). *Pseudomonas chlororaphis* produces two distinct R-tailocins that contribute to bacterial competition in biofilms and on roots. Appl. Environ. Microbiol. *83*, e00706-17.

S87. Fischer, S., Godino, A., Quesada, J.M., Cordero, P., Jofre, E., Mori, G., and Espinosa-Urgel, M. (2012). Characterization of a phage-like pyocin from the plant growth-promoting rhizobacterium *Pseudomonas fluorescens* SF4c. Microbiology *158*, 1493–1503.

S88. Whitney, J.C., Chou, S., Russell, A.B., Biboy, J., Gardiner, T.E., Ferrin, M.A., Brittnacher, M., Vollmer, W., and Mougous, J.D. (2013). Identification, structure, and function of a novel type VI secretion peptidoglycan glycoside hydrolase effector-immunity pair. J. Biol. Chem. *288*, 26616–26624.

S89. Tang, J.Y., Bullen, N.P., Ahmad, S., and Whitney, J.C. (2018). Diverse NADase effector families mediate interbacterial antagonism via the type VI secretion system. J. Biol. Chem. *293*, 1504–1514.

S90. Bernal, P., Allsopp, L.P., Filloux, A., and Llamas, M.A. (2017). The *Pseudomonas putida* T6SS is a plant warden against phytopathogens. ISME J. *11*, 972–987.

S91. Parret, A.H.A., Schoofs, G., Proost, P., and De Mot, R. (2003). Plant lectin-like bacteriocin from a rhizosphere-colonizing *Pseudomonas* isolate. J. Bacteriol. *185*, 897–908.

S92. Haapalainen, M., Mosorin, H., Dorati, F., Wu, R.-F., Roine, E., Taira, S., Nissinen, R., Mattinen, L., Jackson, R., Pirhonen, M., *et al.* (2012). Hcp2, a secreted protein of the phytopathogen *Pseudomonas syringae* pv. Tomato DC3000, is required for fitness for competition against bacteria and yeasts. J. Bacteriol. *194*, 4810–4822.

S93. Hockett, K.L., Renner, T., and Baltrus, D.A. (2015). Independent Co-option of a tailed bacteriophage into a killing complex in *Pseudomonas*. mBio *6*, e00452-15.

S94. Triplett, E.W., and Barta, T.M. (1987). Trifolitoxin production and nodulation are necessary for the expression of superior nodulation competitiveness by *Rhizobium leguminosarum* bv. trifolii Strain T24 on clover. Plant Physiol. *85*, 335–342.

S95. Oresnik, I.J., Twelker, S., and Hynes, M.F. (1999). Cloning and characterization of a *Rhizobium leguminosarum* gene encoding a bacteriocin with similarities to RTX toxins. Appl. Environ. Microbiol. *65*, 2833–2840.

S96. Chen, W.-J., Kuo, T.-Y., Hsieh, F.-C., Chen, P.-Y., Wang, C.-S., Shih, Y.-L., Lai, Y.-M., Liu, J.-R., Yang, Y.-L., and Shih, M.-C. (2016). Involvement of type VI secretion system in secretion of iron chelator pyoverdine in *Pseudomonas taiwanensis.* Sci. Rep. *6*, 32950.

S97. Schwinghamer, E.A., and Brockwell, J. (1978). Competitve advantage of bacteriocin- and phage-producing strains of *Rhizobium trifolii* in mixed cultures. Soil Biol. Biochem. *10*, 383–387.

S98. Sana, T.G., Flaugnatti, N., Lugo, K.A., Lam, L.H., Jacobson, A., Baylot, V., Durand, E., Journet, L., Cascales, E., and Monack, D.M. (2016). *Salmonella* Typhimurium utilizes a T6SS-mediated antibacterial weapon to establish in the host gut. Proc. Natl. Acad. Sci. USA *113*, E5044–E5051.

S99. Nedialkova, L.P., Denzler, R., Koeppel, M.B., Diehl, M., Ring, D., Wille, T., Gerlach, R.G., and Stecher, B. (2014). Inflammation fuels colicin Ib-dependent competition of *Salmonella* serovar Typhimurium and *E. coli* in enterobacterial blooms. PLoS Pathog. *10*, e1003844.

S100. Bossi, L., Fuentes, J.A., Mora, G., and Figueroa-Bossi, N. (2003). Prophage contribution to bacterial population dynamics. J. Bacteriol. *185*, 6467–6471.

S101. Murdoch, S.L., Trunk, K., English, G., Fritsch, M.J., Pourkarimi, E., and Coulthurst, S.J. (2011). The opportunistic pathogen *Serratia marcescens* utilizes type VI secretion to target bacterial competitors. J. Bacteriol. *193*, 6057–6069.

S102. Alcoforado Diniz, J., and Coulthurst, S.J. (2015). Intraspecies competition in *Serratia marcescens* is mediated by type VI-secreted Rhs effectors and a conserved effector-associated accessory protein. J. Bacteriol. *197*, 2350–2360.

S103. Mariano, G., Monlezun, L., and Coulthurst, S.J. (2018). Dual role for DsbA in attacking and targeted bacterial cells during type VI secretion system-mediated competition. Cell Rep. *22*, 774–785.

S104. English, G., Trunk, K., Rao, V.A., Srikannathasan, V., Hunter, W.N., and Coulthurst, S.J. (2012). New secreted toxins and immunity proteins encoded within the type VI secretion system gene cluster of *Serratia marcescens*. Mol. Microbiol. *86*, 921–936.

S105. Anderson, M.C., Vonaesch, P., Saffarian, A., Marteyn, B.S., and Sansonetti, P.J. (2017). *Shigella sonnei* encodes a functional T6SS used for interbacterial competition and niche occupancy. Cell Host Microbe *21*, 769–776.

S106. Cao, Z., Casabona, M.G., Kneuper, H., Chalmers, J.D., and Palmer, T. (2017). The type VII secretion system of *Staphylococcus aureus* secretes a nuclease toxin that targets competitor bacteria. Nat. Microbiol. *2*, 16183.

S107. Kawada-Matsuo, M., Shammi, F., Oogai, Y., Nakamura, N., Sugai, M., and Komatsuzawa, H. (2016). C55 bacteriocin produced by ETB-plasmid positive *Staphylococcus aureus* strains is a key factor for competition with *S. aureus* strains. Microbiol. Immunol. *60*, 139–147.

S108. Haaber, J., Leisner, J.J., Cohn, M.T., Catalan-Moreno, A., Nielsen, J.B., Westh, H., Penadés, J.R., and Ingmer, H. (2016). Bacterial viruses enable their host to acquire antibiotic resistance genes from neighbouring cells. Nat. Commun. *7*, 13333.

S109. Janek, D., Zipperer, A., Kulik, A., Krismer, B., and Peschel, A. (2016). High frequency and diversity of antimicrobial activities produced by nasal *Staphylococcus* strains against bacterial competitors. PLoS Pathog. *12*, e1005812.

S110. Nakatsuji, T., Chen, T.H., Narala, S., Chun, K.A., Two, A.M., Yun, T., Shafiq, F., Kotol, P.F., Bouslimani, A., Melnik, A.V., *et al.* (2017). Antimicrobials from human skin commensal bacteria protect against *Staphylococcus aureus* and are deficient in atopic dermatitis. Sci. Transl. Med. *9*, eaah4680.

S111. Zipperer, A., Konnerth, M.C., Laux, C., Berscheid, A., Janek, D., Weidenmaier, C., Burian, M., Schilling, N.A., Slavetinsky, C., Marschal, M., *et al.* (2016). Human commensals producing a novel antibiotic impair pathogen colonization. Nature *535*, 511–516.

S112. Whitney, J.C., Peterson, S.B., Kim, J., Pazos, M., Verster, A.J., Radey, M.C., Kulasekara, H.D., Ching, M.Q., Bullen, N.P., Bryant, D., *et al.* (2017). A broadly distributed toxin family mediates contact-dependent antagonism between gram-positive bacteria. eLife *6*, e26938.

S113. Regev-Yochay, G., Trzcinski, K., Thompson, C.M., Malley, R., and Lipsitch, M. (2006). Interference between *Streptococcus pneumoniae* and *Staphylococcus aureus*: in vitro hydrogen peroxide-mediated killing by *Streptococcus pneumoniae*. J. Bacteriol. *188*, 4996–5001.

S114. Selva, L., Viana, D., Regev-Yochay, G., Trzcinski, K., Corpa, J.M., Lasa, I., Novick, R.P., and Penades, J.R. (2009). Killing niche competitors by remote-control bacteriophage induction. Proc. Natl. Acad. Sci. USA *106*, 1234–1238.

S115. Maricic, N., Anderson, E.S., Opipari, A.E., Yu, E.A., and Dawid, S. (2016). Characterization of a multipeptide lantibiotic locus in *Streptococcus pneumoniae*. mBio *7*, e01656-15.

S116. Dawid, S., Roche, A.M., and Weiser, J.N. (2007). The blp bacteriocins of *Streptococcus pneumoniae* mediate intraspecies competition both in vitro and in vivo. Infect. Immun. *75*, 443–451.

S117. Valente, C., Dawid, S., Pinto, F.R., Hinds, J., Simões, A.S., Gould, K.A., Mendes, L.A., de Lencastre, H., and Sá-Leão, R. (2016). The *blp* Locus of *Streptococcus pneumoniae* plays a limited role in the selection of strains that can cocolonize the human nasopharynx. Appl. Environ. Microbiol. *82*, 5206–5215.

S118. Wiener, P. (1996). Experimental studies on the ecological role of antibiotic production in bacteria. Evol. Ecol. *10*, 405–421.

S119. Stubbendieck, R.M., and Straight, P.D. (2015). Escape from lethal bacterial competition through coupled activation of antibiotic resistance and a mobilized subpopulation. PLoS Genet. *11*, e1005722.

S120. Paz-Yepes, J., Brahamsha, B., and Palenik, B. (2013). Role of a microcin-C-like biosynthetic gene cluster in allelopathic interactions in marine *Synechococcus*. Proc. Natl. Acad. Sci. USA *110*, 12030–12035.

S121. Salomon, D., Klimko, J.A., Trudgian, D.C., Kinch, L.N., Grishin, N.V., Mirzaei, H., and Orth, K. (2015). Type VI secretion system toxins horizontally shared between marine bacteria. PLoS Pathog. *11*, e1005128.

S122. MacIntyre, D.L., Miyata, S.T., Kitaoka, M., and Pukatzki, S. (2010). The *Vibrio cholerae* type VI secretion system displays antimicrobial properties. Proc. Natl. Acad. Sci. USA *107*, 19520–19524.

S123. Zhao, W., Caro, F., Robins, W., and Mekalanos, J.J. (2018). Antagonism toward the intestinal microbiota and its effect on *Vibrio cholerae* virulence. Science *359*, 210–213.

S124. Unterweger, D., Miyata, S.T., Bachmann, V., Brooks, T.M., Mullins, T., Kostiuk, B., Provenzano, D., and Pukatzki, S. (2014). The *Vibrio cholerae* type VI secretion system employs diverse effector modules for intraspecific competition. Nat. Commun. *5*, 3549.

S125. Dong, T.G., Ho, B.T., Yoder-Himes, D.R., and Mekalanos, J.J. (2013). Identification of T6SS-dependent effector and immunity proteins by Tn-seq in *Vibrio cholerae*. Proc. Natl. Acad. Sci. USA *110*, 2623–2628.

S126. Zheng, J., Ho, B., and Mekalanos, J.J. (2011). Genetic analysis of anti-amoebae and anti-bacterial activities of the type VI secretion system in *Vibrio cholerae*. PLoS ONE *6*, e23876.

S127. Ishikawa, T., Sabharwal, D., Bröms, J., Milton, D.L., Sjöstedt, A., Uhlin, B.E., and Wai, S.N. (2012). Pathoadaptive conditional regulation of the type VI secretion system in *Vibrio cholerae* O1 strains. Infect. Immun. *80*, 575–584.

S128. Speare, L., Cecere, A.G., Guckes, K.R., Smith, S., Wollenberg, M.S., Mandel, M.J., Miyashiro, T., and Septer, A.N. (2018). Bacterial symbionts use a type VI secretion system to eliminate competitors in their natural host. Proc. Natl. Acad. Sci. USA *115*, E8528–E8537.

S129. Salomon, D., Gonzalez, H., Updegraff, B.L., and Orth, K. (2013). *Vibrio parahaemolyticus* type VI secretion system 1 is activated in marine conditions to target bacteria, and is differentially regulated from system 2. PLoS ONE *8*, e61086.

S130. Salomon, D., Klimko, J.A., and Orth, K. (2014). H-NS regulates the *Vibrio parahaemolyticus* type VI secretion system 1. Microbiology *160*, 1867–1873.

S131. Salomon, D., Kinch, L.N., Trudgian, D.C., Guo, X., Klimko, J.A., Grishin, N.V., Mirzaei, H., and Orth, K. (2014). Marker for type VI secretion system effectors. Proc. Natl. Acad. Sci. USA *111*, 9271–9276.

S132. Souza, D.P., Oka, G.U., Alvarez-Martinez, C.E., Bisson-Filho, A.W., Dunger, G., Hobeika, L., Cavalcante, N.S., Alegria, M.C., Barbosa, L.R.S., Salinas, R.K., *et al.* (2015). Bacterial killing via a type IV secretion system. Nat. Commun. *6*, 6453.

S133. Hert, A.P., Roberts, P.D., Momol, M.T., Minsavage, G.V., Tudor-Nelson, S.M., and Jones, J.B. (2005). Relative importance of bacteriocin-like genes in antagonism of *Xanthomonas perforans* Tomato race 3 to *Xanthomonas euvesicatoria* Tomato race 1 strains. Appl. Environ. Microbiol. *71*, 3581–3588.

S134. Ciezki, K., Murfin, K., Goodrich-Blair, H., Stock, S.P., and Forst, S. (2017). R-type bacteriocins in related strains of *Xenorhabdus bovienii*: Xenorhabdicin tail fiber modularity and contribution to competitiveness. FEMS Microbiol. Lett. *364*, fnw235.

S135. Morales-Soto, N., and Forst, S.A. (2011). The xnp1 P2-like tail synthesis gene cluster encodes xenorhabdicin and is required for interspecies competition. J. Bacteriol. *193*, 3624–3632.

Appendix D

Droplet Printing Reveals the Importance of Micron-Scale Structure for Bacterial Ecology

nature COMMUNICATIONS

ARTICLE

https://doi.org/10.1038/s41467-021-20996-w OPEN

Droplet printing reveals the importance of micron-scale structure for bacterial ecology

Ravinash Krishna Kumar[1], Thomas A. Meiller-Legrand[2,3], Alessandro Alcinesio[1], Diego Gonzalez[3,5], Despoina A. I. Mavridou[4], Oliver J. Meacock[2,3,6], William P. J. Smith[2,3], Linna Zhou[1], Wook Kim[3,7], Gökçe Su Pulcu[1], Hagan Bayley[1✉] & Kevin R. Foster[2,3✉]

Bacteria often live in diverse communities where the spatial arrangement of strains and species is considered critical for their ecology. However, a test of this hypothesis requires manipulation at the fine scales at which spatial structure naturally occurs. Here we develop a droplet-based printing method to arrange bacterial genotypes across a sub-millimetre array. We print strains of the gut bacterium *Escherichia coli* that naturally compete with one another using protein toxins. Our experiments reveal that toxin-producing strains largely eliminate susceptible non-producers when genotypes are well-mixed. However, printing strains side-by-side creates an ecological refuge where susceptible strains can persist in large numbers. Moving to competitions between toxin producers reveals that spatial structure can make the difference between one strain winning and mutual destruction. Finally, we print different potential barriers between competing strains to understand how ecological refuges form, which shows that cells closest to a toxin producer mop up the toxin and protect their clonemates. Our work provides a method to generate customised bacterial communities with defined spatial distributions, and reveals that micron-scale changes in these distributions can drive major shifts in ecology.

[1] Department of Chemistry, University of Oxford, Oxford, UK. [2] Department of Biochemistry, University of Oxford, Oxford, UK. [3] Department of Zoology, University of Oxford, Oxford, UK. [4] Department of Molecular Biosciences, University of Texas at Austin, Austin, TX, USA. [5] Present address: Laboratoire de Microbiologie, Institut de Biologie, Université de Neuchâtel, Neuchâtel, Switzerland. [6] Present address: Department of Physics and Astronomy, University of Sheffield, Sheffield, UK. [7] Present address: Department of Biological Sciences, Bayer School of Natural & Environmental Sciences, Duquesne University, Pittsburgh, PA, USA. ✉email: hagan.bayley@chem.ox.ac.uk; kevin.foster@zoo.ox.ac.uk

Bacteria commonly exert strong effects on the growth and survival of surrounding cells via mechanisms that include nutrient competition, quorum sensing and toxin production[1–4]. Consequently, the position of different strains and species in space is thought to be critical for the ecology of bacterial communities, and indeed how they affect us[5–11]. In particular, the way in which different strains of bacteria are arranged when a community first develops is expected to be a key predictor of which strains dominate and, more generally, whether the community thrives or perishes[12–21]. When strains and species grow apart in distinct patches, for example, this is expected to limit the impacts of competitive mechanisms, thereby promoting both coexistence and productivity.

The importance of spatial structure is broadly supported by comparisons of liquid with solid-surface (agar) culture, and agar-based manipulations on the millimetre-to-centimetre scale (Fig. 1b)[22–27]. However, natural spatial structure often occurs at much finer scales, with data from the mammalian microbiome suggesting that the micron-to-millimetre scale is particularly important[6,11,28]. For example, while there appears to be significant genotypic mixing in the gut microbiome[29], the dental and tongue microbiome is more structured, with patches of bacteria dominated by one genotype reaching tens to hundreds of microns in scale[8,9,30]. Moreover, there is evidence that solute gradients within bacterial communities can limit the distance at which cells affect each other to micron scales[31–33], raising the possibility that

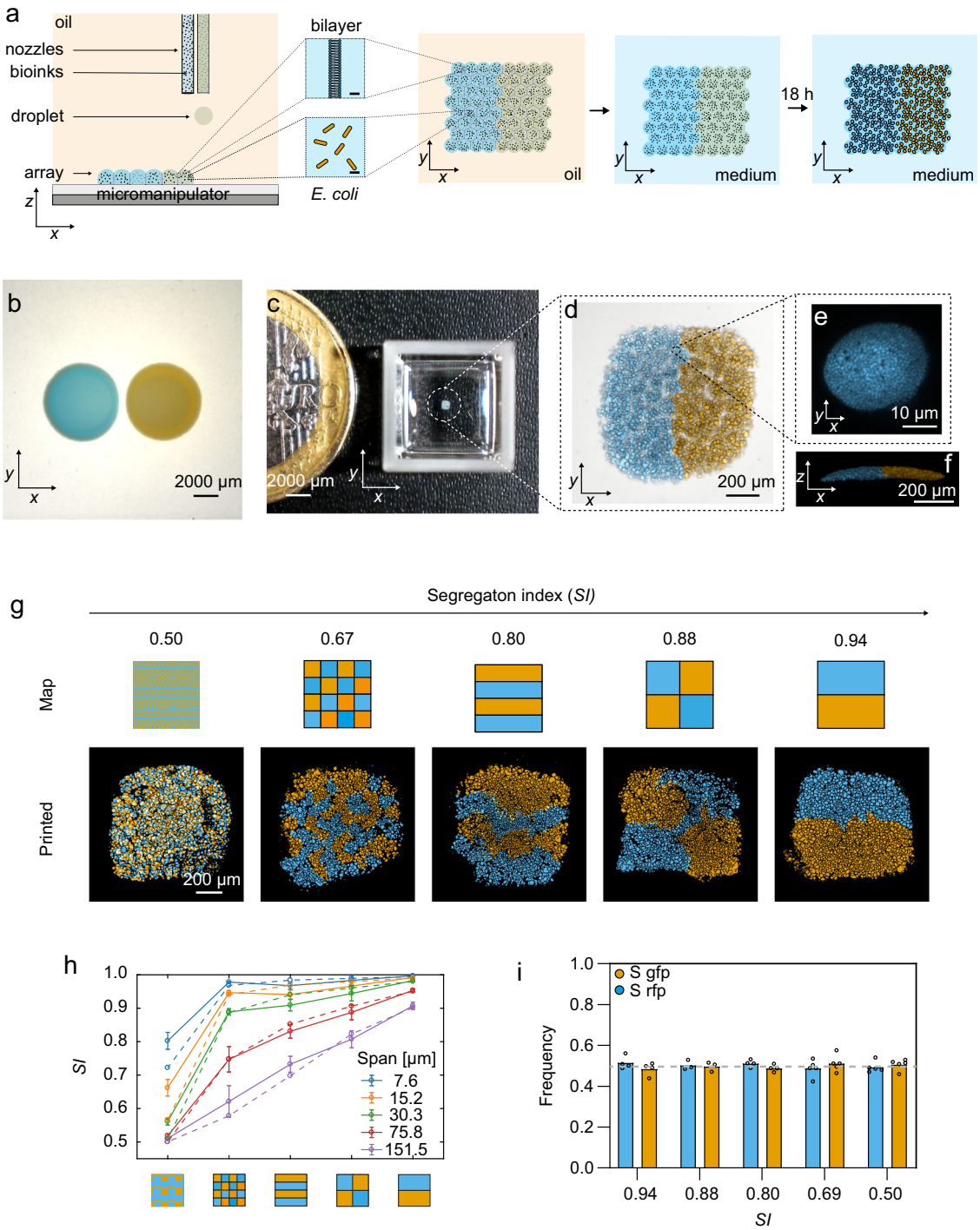

Fig. 1 Droplet printing generates viable bacterial communities with defined micron-scale patterning. a A schematic of the fabrication of printed bacterial communities by droplet printing (depicted in the *x*, *z* and *x*, *y* dimensions), transfer to LB medium and growth. **b** A composite (brightfield and fluorescence) stereomicroscope image of two side-by-side spotted colonies of susceptible (S) gfp and S rfp strains grown for 24 h at 37 °C from starting cell densities of 10^8 cells mL^{-1}. **c** A photograph of a printed array (after 18 h of growth and transfer to M9 medium) with a 1-euro coin for size comparison. Images in **b** and **c** are taken at the same magnification. **d** A higher magnification, composite (transmitted light and fluorescence) confocal microscope image of a 7 × 8 × 1 (*x*, *y*, *z* droplets) printed array containing S gfp and S rfp strains segregated to opposite sides of the structure. **e** A confocal fluorescence microscopy image of an S rfp microcolony in the *x*, *y* planes ($n = 4$ biologically independent experiments). **f** A 3D rendering of z-stacked confocal microscopy images of the same printed community as in **d** ($n = 4$ biologically independent experiments). **g** Segmented fluorescence images of printed communities (7 × 8 × 1 (*x*, *y*, *z* droplets)) of S gfp and S rfp strains at graded degrees of genetic mixing accompanied by the corresponding printing map and the calculated segregation indices (*SI*) at a local neighbourhood of 100 μm (see 'Methods'). The local neighbourhood is the spatial scale on which genetic mixing is measured. In **b**–**g**, S gfp and S rfp strains are false-coloured orange and sky blue, respectively. **h** A plot showing the calculated *SI* of printed arrays (smooth lines) at different sizes of local neighbourhoods ('spans') (7.6–151.5 μm) compared to the *SI* of the printing maps (dashed lines). Data points are the mean of $n = 9$ printed arrays, and error bars are the standard deviation. **i** A bar chart showing the frequency of S gfp and S rfp strains in arrays printed at different *SI* values. Each data point is a biologically independent replicate and the height of the bars are the mean frequencies of the strains. The grey line shows the initial starting frequency (0.5 for both genotypes). A Kruskal–Wallis test found a non-significant difference between the median frequencies of S gfp at different *SI* values ($P = 0.2736$; see Supplementary Table 1 for statistical tests). In **i**, the term 'frequency' (*f*) of a genotype *a* in a printed array containing genotypes *a* and *b* after 18 h of competition is defined as $f = A_a/(A_a + A_b)$, where *A* is the total cross-sectional area that a genotype occupies in the printed array.

differences in the arrangement of genotypes at these scales will have impacts.

While fine-scale spatial structure is hypothesised to be important for the form and function of microbial communities, direct tests are needed. A key barrier is a requirement for a technology that can manipulate the patterning of interacting bacteria at the relevant spatial scales. A range of printing technologies exists to position and pattern microbes[34–39]. However, the typical focus of this work has been the production of biomaterials, such as bacterial sensors (e.g., bacteria embedded in a 3D hydrogel), rather than ensuring that bacteria can grow and interact as a community. Moreover, current printing methods typically have a resolution at the millimetre scale rather than the micrometre scale at which natural communities appear often to be structured. Here, we present a high-resolution droplet printing method that allows us to position interacting microbes in specific patterns in submillimetre arrays. With this, we are able to manipulate and study the ecology of microbial communities patterned at micron scales (Fig. 1). Our experiments reveal that changing the arrangement of bacterial genotypes across these fine scales can be critical for ecological outcomes.

Results

A new method to print patterned microbial communities. Our method works by piezo injection of tailored 'bioinks' comprising bacterial cells (*E. coli*, ≈10^8 cells mL^{-1}), molten agarose (1.5% w/v) and lysogeny broth (LB) medium into an oil/phospholipid solution at 37 °C. The method generates 110-μm-diameter droplets (≈70 cells per droplet), which are deposited into 2D patterns by line-by-line printing (Fig. 1a). The droplets are initially surrounded by monolayers of phospholipid, which form bilayers on contact with one another, thereby creating a stabilised, support-free structure[40,41] (Fig. 1a). The resulting array is then gelled, and the lipid bilayers removed by the addition of an oil (silicone oil AR20, which causes the lipid to precipitate) to create a final printed community of bacteria in agarose suspended in LB medium ('Methods') (Fig. 1a, c–f). Within the printed community, bacteria grew from single-cell dispersions (with starting 2D centre-to-centre distances of 18 ± 2 μm) into 3D microcolonies (with median diameters of 15 (10–21) μm) over 18 h of growth (see Supplementary Fig. 1 and Supplementary Methods 1 for further characterisation of printed arrays). To validate the method, we printed two fluorescently labelled strains of *E. coli*. This demonstrated the ability to print specific patterns and, with them, to vary the amount of genetic mixing (defined by a segregation index (*SI*)[16], see 'Methods' and Supplementary Fig. 2) at the scale of the arrays (Fig. 1g). Importantly, the calculated *SI* of our printed arrays matched well with the theoretical *SI* of the respective printing maps (Fig. 1h), and the imposed patterns did not impact the frequencies of strains that differ only in the fluorophore that they carry (Fig. 1i) (Supplementary Fig. 2 and Supplementary Methods 1.2). With this method, therefore, we can systematically alter the spatial arrangement of bacterial strains across naturally relevant scales to study how they interact and grow.

Competition between toxinogenic and susceptible cells. We next sought to test whether this spatial structure is important for the ecology of interacting bacteria. To do this, we studied a common ecological interaction in the mammalian gut: interference competition between strains of *E. coli* that produce protein toxins known as colicins[24,42–45]. While colicin production can be critical for survival, there is diversity in the types of colicins carried by *E. coli* strains, and many strains carry none at all—suggesting that colicin release is not always beneficial[44] (Supplementary Methods 2.1). We began by performing two-way competitions between susceptible non-colicin-producing strains (S) and a range of colicin-producing strains (P) in printed communities at different *SI* values (Fig. 2) (see Table 1 for strains used). Theory suggests that genetic mixing can favour colicin producers, by giving them more access to susceptible cells. Conversely, increasing spatial structure has the potential to isolate producer genotypes from susceptible genotypes, which might protect susceptible genotypes if the competition is restricted to the boundaries between genotypes (Fig. 2b, c)[46–48]. These predictions are borne out in experiments with bacteriocins performed at large spatial scales[23,49]. However, it was far from clear whether the micron-scale spatial structure would have similar effects in our experiments. Colicins are released from cells (they do not remain attached), will easily diffuse through agar[26,49] and are highly toxic, killing with single-hit kinetics[50,51]. These features of colicin biology mean they are able to diffuse and kill across the millimetre-to -centimetre scale, which might overwhelm any structure at the micron scale.

In spite of the potentially long-range activity of colicins, we found that altering spatial structure across the micron scale had significant effects on the outcome of competition between the bacteria. For all but one of the colicin types (E8), the introduction of fine-scale spatial structure enabled a distinct patch of the susceptible strains to persist (Fig. 2d–h). The strength of this effect reflects the relative ability of each colicin strain to kill susceptible strains[49,52] (Fig. 2a and Supplementary Fig. 3d–f). As might be expected, the more potent killers were less affected by

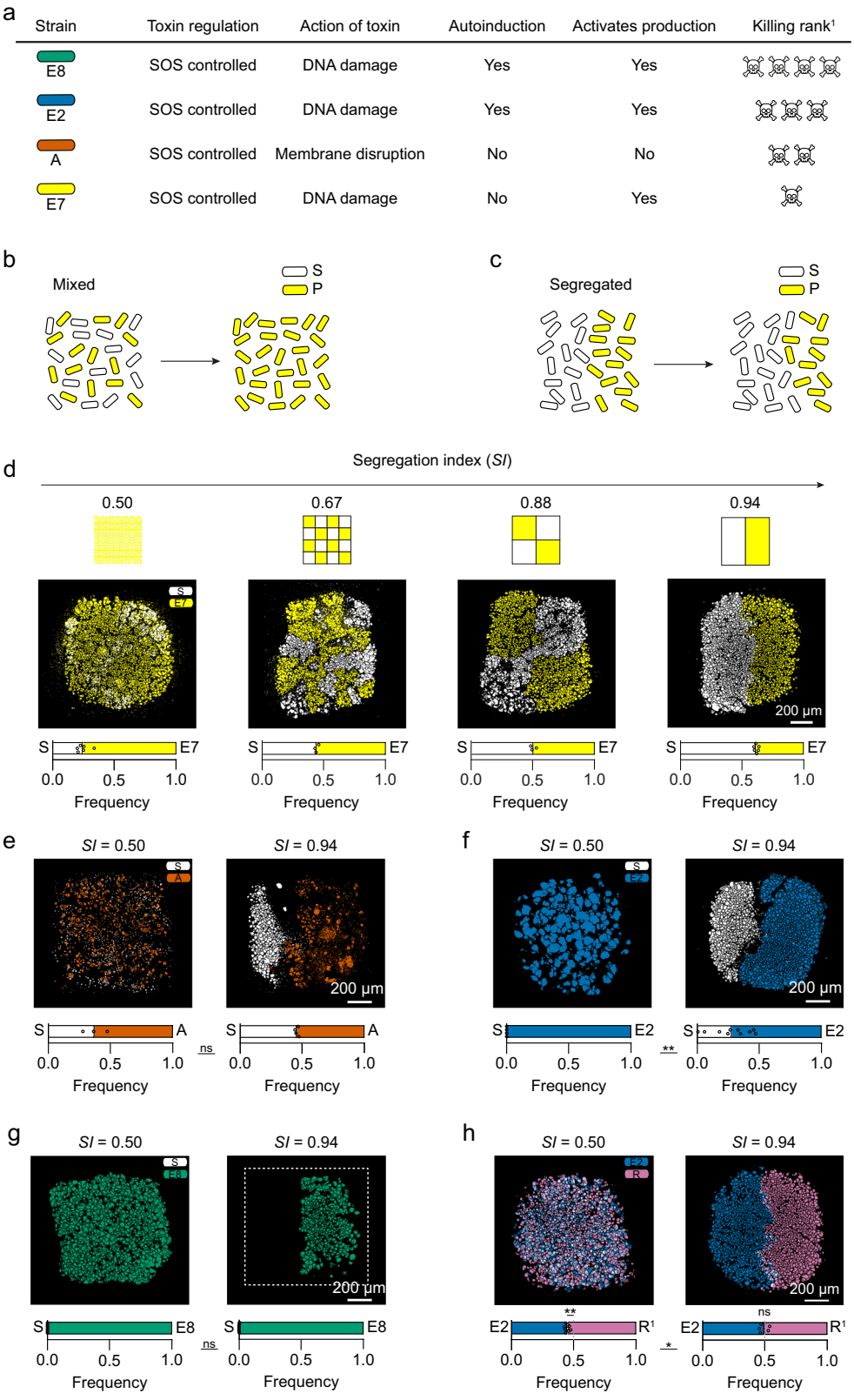

spatial structure, with the colicin E8 producer killing off the susceptible cells irrespective of whether there was structure (Fig. 2g). E8 is known to be both a potent colicin and one that is produced at high levels due to autoinduction, whereby producing cells promote toxin production in clonemates (Supplementary Fig. 3e). For all the other strains, we found that spatial structure creates an ecological refuge[53] for susceptible cells. Even though the refuge is only a few hundred microns across, it allowed susceptible cells to better survive competition with toxin-producing strains for two of the combinations. For E7, this effect was so strong that the susceptible strain was able to outgrow the colicin producer when printed side by side (Fig. 2d, $f_S = 0.65 \pm$

Fig. 2 Micron-scale structure shapes competition between susceptible and colicin-producing strains by creating ecological refuges. a The characteristics of each colicin-producing strain used in this study. [1]The 'killing rank' ranks the ability of each of the colicin-producing strain to kill colicin-susceptible strains, see refs. [49,52] and data therein. **b**, **c** A schematic hypothesis, of how susceptible and colicin-producer frequencies change over time, in a genetically mixed spatial structure ($SI = 0.50$) (**b**), and in a genetically segregated spatial structure ($SI = 0.94$) (**c**), if susceptible growth rates outweigh the cost of toxin production. **d**, Segmented fluorescence images of S cells (white) and E7 cells (yellow) in communities printed at an initial SI of 0.50 ($n = 6$), 0.67 ($n = 3$), 0.88 ($n = 3$) and 0.94 ($n = 6$) with accompanying printing maps. A Kruskal Wallis test showed a statistically significant relationship between the change in frequencies of S with SI (Kruskal–Wallis statistic: 15.63, $P < 0.001$, see Supplementary Table 2 for the statistical test). **e**–**g** Segmented fluorescence images of S cells (white) and A cells (vermillion) ($n = 3$ and $n = 4$ for $SI =$ 0.50 and 0.94, respectively) (**e**), and E2 cells (blue) ($n = 4$ and $n = 10$ for $SI = 0.50$ and 0.94, respectively) (**f**), and E8 cells (bluish-green) ($n = 7$ and $n = 7$ for $SI = 0.50$ and 0.94, respectively) (**g**), in communities printed at an initial $SI = 0.50$ and 0.94. **h** Segmented fluorescence images of E2 cells (blue) and R^1 cells (reddish-purple) in communities printed at an initial SI of 0.50 ($n = 9$) and 0.94 ($n = 6$). In **d**–**h**, each fluorescently segmented image was taken after 18 h of competition. Below each fluorescently segmented imaged is a stacked bar chart of the frequencies of strains in the array. Each data point represents a biologically independent replicate; the mean frequencies of each strain are where the bars meet. In **e**–**h**, unpaired Mann–Whitney tests were performed to assess the statistical significance of the changes in frequencies of competing strains at different SI values. For **e**, $P = 0.6286$; for **f**, $P = 0.0020$; for **g**, $P = 0.4462$; for **h**, $P = 0.0336$ (see Supplementary Tables 3 for statistical tests). In **h**, one-sample t and Wilcoxon tests showed a statistically significant ($P = 0.0039$) and non-significant ($P > 0.6250$) difference between the median frequencies of E2 and R^1 at $SI = 0.50$ and 0.94, respectively (see Supplementary Tables 3 for statistical tests).

Table 1 Strains used in this study.

Strain and genotype	Abbreviation	Toxin	Resistance to colicins	Colour code
BZB1011	S	None	No	
BZB1011 ΔbtuB	R^1	None	Yes—colicin A, E7, E2, E8	
BZB1011 immE2	R^2	None	Yes—colicin E2	
BZB1011 pColA	A	Colicin A	No	
BZB1011 pColE7	E7	Colicin E7	No	
BZB1011 pColE2	E2	Colicin E2	No	
BZB1011 immE2 pColE2	E2*	Colicin E2	No	
BZB1011 pColE8	E8	Colicin E8	No	

Each colicin-producing strain is immune to its cognate toxin. For BZB1011 (S), the orange and sky blue colour codes are used to represent S cells expressing sfGFP and mRFP1, respectively, in Figs. 1 and 4. The white colour code represents S cells in Figs. 2 and 3.

0.02 at $SI = 0.94$). Counts of colony-forming units confirmed that the imaged susceptible cells in the printed arrays were viable, despite the presence of the toxin producer (Supplementary Fig. 3i). Exploring the case of E7 in more detail revealed a graded response to spatial structure, where progressively decreasing spatial structure (decreasing SI) led to a progressive increase in the abundance of the E7 colicin producer (Fig. 2d). At high genotypic mixing, the outcome of the competition was reversed, where now the toxin producer outcompeted the susceptible strain (Fig. 2d, $f_S = 0.24 \pm 0.05$ at $SI = 0.50$).

We also found an effect of spatial structure when a colicin producer strain competes with a colicin-resistant strain (R^1) rather than a susceptible strain (Fig. 2h). The colicin producer has a lower growth rate due to the costs of colicin production (Supplementary Fig 3g–h). However, this growth disadvantage only translates to an ecological disadvantage in the absence of spatial structure, i.e., when the two strains are well mixed ($f_{E2} = 0.46 \pm 0.02$ at $SI = 0.50$). When growing side-by-side in a structured community, the colicin producer reaches the same abundance as the resistant strain, despite its slower growth rate. We saw the same effect of spatial structure for another strain combination (S and R^1) that also lacks any toxin-mediated competition (Supplementary Fig. 4c). In these experiments, the micron-scale segregation of the two strains shifts competition to occur more within strains than between strains. As a result, the negative effects of inter-strain competition on a slower-growing strain are weakened. While our focus is interference competition (via toxins), we find that exploitative competition (mediated by differences in growth rate) is also affected by the introduction of spatial structure in the printed arrays.

Competition between toxinogenic strains. We have shown that the arrangement of bacteria at the submillimetre scale is important for the outcome of both interference and exploitative competition. Moreover, as predicted by both ecological and evolutionary theory, our results suggest that the key effect of printing strains side by side—as opposed to well mixed—is to weaken interactions (Fig. 2b, c)[23,54,55]. We next explored the importance of positioning for competition between pairs of toxin-producing strains, which are each immune to their own toxin but able to kill the other (Fig. 3). At first, these appeared to follow the same pattern as the previous (producer vs susceptible) experiments. In one (E2 and E7), we saw the same refuge effect with spatial structure, where the strain (E7) that is eliminated under mixed conditions can persist when printed side by side with the more dominant strain (E2) (Fig. 3a). The dominance of E2 is expected because a higher proportion of E2 cells make colicins than E7 cells due to autoinduction[56,57]. In another case, one strain (A) eliminated the other (E2) irrespective of spatial structure (Fig. 3b). Here, the potency of colicin A cells is expected because E2 is a DNase that activates the SOS response, which activates colicin A expression. By contrast, A does not activate E2 expression because colicin A targets membrane integrity rather than DNA (Fig. 2a and Supplementary Fig. 3f)[26,52,58]. However, a third combination (E2 and E8) had a surprising outcome (Fig. 3c). Here, without spatial structure, the dominant strain E8 eliminated E2 as though E2 were simply a susceptible strain. By contrast, with spatial structure ($SI = 0.94$), both strains were almost completely eliminated, something not seen when these strains grow side-by-side at larger distances on agar plates[49].

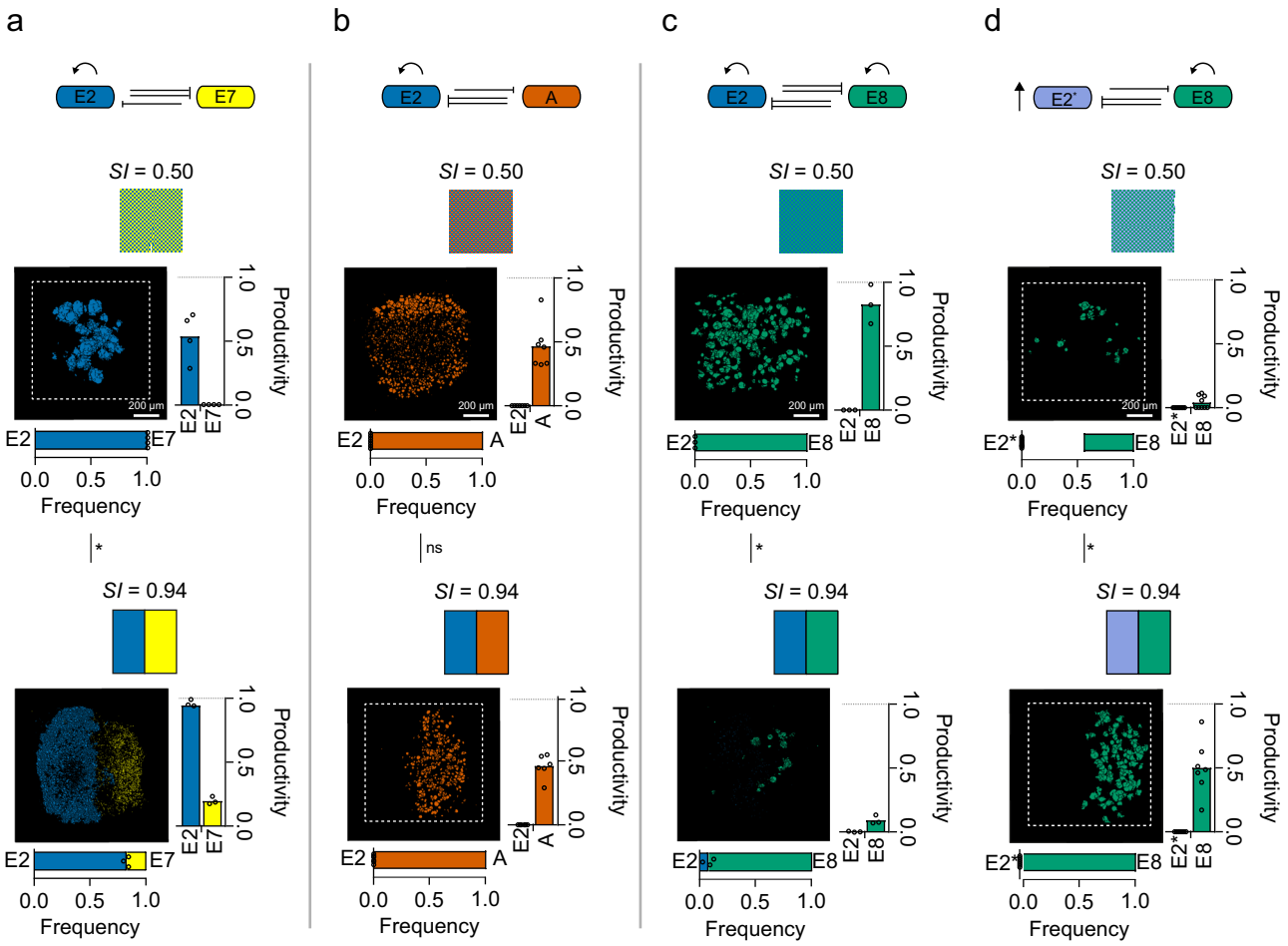

Fig. 3 Micron-scale structure shapes competition between colicin-producing strains and can drive mutual destruction. a–d Competition schematics followed by the corresponding segmented fluorescence images of E2 cells (blue) and E7 cells (yellow) ($n = 4$ and $n = 3$ for $SI = 0.50$ and 0.94, respectively) (**a**), E2 cells and A cells (vermillion) ($n = 7$ and $n = 6$ for $SI = 0.50$ and 0.94, respectively) (**b**), E2 cells and E8 cells (bluish-green) ($n = 3$ and $n = 3$ for $SI = 0.50$ and 0.94, respectively) (**c**) and E2* cells (bluish-grey) and E8 cells ($n = 9$ and $n = 7$ for $SI = 0.50$ and 0.94, respectively) (**d**) in genetically mixed ($SI = 0.50$) and fully segregated ($SI = 0.94$) printed communities after 18 h of competition. In the bacterial warfare schematics, the curly arrows represent autoinduction, the single- inhibition arrows represent lower aggression, the double-inhibition arrows represent higher aggression and the vertical arrow represents a faster growth rate. Above each segmented fluorescence image is the corresponding printing map. Below each segmented fluorescence image is a stacked bar chart of the frequencies of strains in each printed array after 18 h of competition. Each data point is a biologically independent replicate, and the mean frequencies of each strain are denoted where the bars meet. The mean frequency of E8 in E2* vs E8 at $SI = 0.50$ (**d**) is shown as the length of the bar and the data points denote the frequencies of E2*. To the right of each segmented fluorescence image is a bar chart of the productivities of strains in printed arrays. Each data point is a biologically independent replicate and the mean productivities of each strain are denoted by the heights of the bars. In **a**–**d**, unpaired Mann–Whitney tests were performed to assess the statistical significance in the changes in frequencies of competing strains at different SI values. For **a**, $P = 0.0286$; for **b**, $P > 0.9999$; for **c**, $P = 0.0286$; for **d**, $P = 0.0337$ (see Supplementary Tables 4 for statistical tests). In **a**–**d**, the term 'productivity' (p) of a genotype a in a printed array after 18 h of competition is defined as $p = A_a/A_S$, where A_S is the total cross-sectional area that a susceptible genotype occupies after 18 h of competition (at the same starting density and spatial pattern as genotype a), but without interference competition.

We next sought to understand how spatial structure could enhance competition, and moreover do it to the extent that both populations collapse. We hypothesised that the answer lay in the fact that both of these strains exhibit autoinduction of colicin production. Similar to the effects of quorum sensing, this density-dependent regulation occurs because the import of a clonemate's DNA-damaging colicin increases a cell's probability of colicin release (Supplementary Fig. 3e). Autoinduction can have strong effects on competition between colicin strains[49]. In our experiments, we hypothesised that spatial structure provided E2 cells with enough refuge to reach a sufficient cell density to activate collective colicin production through autoinduction, thereby allowing them to inhibit E8 cells more strongly. To explore this, we studied competitions between E8 and an E2 strain engineered to lack autoinduction in colicin production (E2*, see 'Methods') (Fig. 3d). As predicted, this greatly reduced the impact of E2 on E8 in the presence of spatial structure. Moreover, the effects of the spatial structure were reversed, with mutual destruction of the two competitors now occurring under mixed conditions without spatial structure. This ability of the engineered E2* strain to eliminate E8 under mixed conditions is likely to stem from the relatively high growth rate of E2* (Supplementary Fig. 3g, h), which allows it to rapidly establish itself in mixed arrays. In sum, the impact of the spatial structure depends on whether E2 does, or does not, perform autoinduction. Moreover, in both cases, we see a strong effect where the printed pattern determines whether one strain thrives or both are largely eliminated.

Three-genotype printing explains how 'microrefuges' form. The impacts of autoinduction demonstrate that fine-scale structure can have surprising and complex effects on bacterial interactions. Nevertheless, one effect that is commonly seen is that spatial structure creates a refuge, with subordinate strains better able to persist with spatial structure than without it. We sought, therefore, to understand the mechanistic basis of this refuge effect, using prints of three different types of bioinks to explore the interface between a colicin E2 producer and a susceptible strain (Fig. 4a). Printing cell-free agarose between an E2 strain and a susceptible strain removed the refuge effect, suggesting that the distribution of colicins was not limited by diffusion across the printed array (Fig. 4e). This result implied that the susceptible cells closest to the E2 producer were somehow interrupting the diffusion of colicins across the array. We hypothesised that this could occur if susceptible cells bind and thereby 'mop up' colicin molecules as they pass[59]. To explore this, we engineered a colicin-resistant strain that lacks the BtuB receptor for colicin E2 (Table 1, Fig. 4b and Supplementary Fig. 4a) (see Supplementary Methods 2.2). As predicted by our model, the refuge effect was eliminated even though there were cells growing next to the colicin producer (Fig. 4f). However, the BtuB mutation also makes the cells resistant to colicin (Supplementary Fig. 4b), such that the lack of protection could be linked in some way to the lack of cell death from E2 activity. To exclude this possibility, we engineered a strain that carries BtuB, but which is resistant to colicins via cytoplasmic expression of the E2 immunity protein (Table 1, Fig. 4b and Supplementary Fig. 4a). This strain was not affected by the colicin of the E2 producer (Supplementary Fig. 4b) but did provide protection (Fig. 4g). We conclude, therefore, that binding of diffusing colicins by intoxicated cells is critical to the refuge effect. More generally, these experiments highlight the importance of processes that counteract the effects of diffusion at these scales, whether it be by binding, importing, or digesting solutes.

Discussion

The ecological interactions within microbial communities are central to their properties and impacts[5,7]. However, the fine spatial scales at which microbes position and interact are a challenge for experimental microbiology. Here we have presented a method for arranging microbial genotypes in defined 2D arrays with micron-scale resolution. This method allowed us to establish a causal link between the arrangement of bacterial strains at these fine scales and ecological outcomes. We find that spatial structure impacts the outcome of both interference and exploitative competition. Moreover, the fine-scale structure can shift the outcome of competition from one strain dominating to another, and it can be the difference between one strain thriving and mutual destruction. A key principle that emerges across our experiments is that spatial segregation is often protective and limits the effects of one strain on the other. We show that for colicin E2, this is explained by the ability of susceptible cells to bind the toxin rather than by diffusion limitation. The extent of such refuge effects—and whether coexistence is stable or transitory—is likely to depend on a number of factors that we have not explored here. These factors include the length of the time that strains grow together, the turnover in nutrients and the initial frequencies of strains, which are all interesting targets for future work.

We find that one cannot simply translate results on the effect of spatial structure from coarse to fine scales. The outcomes we see in our arrays can be very different to those seen at larger scales. In particular, the conditions under which we observe mutual destruction (Fig. 3c) correspond to conditions that allow coexistence at a larger scale[49]. Nevertheless, many of our other findings mirror the conclusions from experiments at larger spatial scales[23,60] where spatial segregation is well known to limit competition and promote coexistence. Our work, therefore, demonstrates that space still matters when one considers patterning at the fine scales that appear more typical in nature. Our findings also fit well with a large body of work on bacterial biofilms, which emphasises how both the binding and breakdown of solutes can generate strong gradients over small spatial scales, even when diffusion is not itself limiting[32,33,61–64]. The commonness of these micron-scale solute gradients suggests that the effects we have documented here will be important across many species and ecological interactions. The manipulation of fine-scale spatial structure, therefore, has significant potential for both understanding and controlling microbial communities.

Methods

Preparing aqueous phases. Phosphate-buffered saline (PBS) (1×, pH 7.4, Gibco) was used as purchased. Lysogeny broth Miller (LB-Miller) medium was prepared by adding 10 g of tryptone (BD Difco™), 5 g of yeast extract (BD Difco™) and 10 g of sodium chloride (Fischer) to 1 L of Milli-Q® water and autoclaving. 5× M9 medium (Sigma-Aldrich) without a carbon source (12.8 g L^{-1} $Na_2HPO_4.7H_2O$, 3 g L^{-1} KH_2PO_4, 0.5 g L^{-1} NaCl, 1 g L^{-1} NH_4Cl, 2 mM $MgSO_4$ and 0.1 mM $CaCl_2$) was dissolved in Milli-Q® water, autoclaved and filtered through 0.22-µm polyethersulfone membrane (Millex-GP Syringe Filter Unit). LB-Miller agar solutions (molten) were prepared by combining LB-Miller medium with agar (final concentration of 1.5% w/v) (BD Difco™) and autoclaving. 2.0% w/v of ultra-low-gelling-temperature (ULGT) agarose (Sigma-Aldrich) was prepared by dissolving 100 mg in 5 mL of LB-Miller medium and autoclaving. The hydrogel was kept molten by keeping the solution in a static incubator at 37 °C. Molten solutions were only used for a week. Antibiotics were dissolved in Milli-Q® water, filter-sterilised (0.22-µm polyethersulfone membrane) and frozen (−20 °C) as stock solutions at 100 mg mL^{-1} for ampicillin and 30 mg mL^{-1} for kanamycin (Sigma-Aldrich).

Preparing lipid/oil solutions. Lipids were purchased from Avanti® Polar Lipids in powder form and stored at −80 °C. Undecane and silicone oil AR20 (Sigma-Aldrich) were filtered before use through 0.22-µm filters (Corning®) under vacuum. An optimised lipid/oil solution was prepared for printing[65]. Lipid films were prepared by bringing ampoules to room temperature and dissolving in anhydrous chloroform (Sigma-Aldrich) to make a chloroform/lipid solution at lipid concentrations of 25 mg mL^{-1}. Chloroform/lipid stock solutions were used immediately. Using glass syringes (Hamilton®), 45 µL and 20 µL of lipid stock solutions 1,2-diphytanoyl-sn-glycero-3-phosphocholine (DPhPC) and 1-palmitoyl-2-oleoyl-sn-glycero-3-phosphocholine (POPC), respectively, were transferred into a 7-mL, isopropanol-cleaned, Teflon-capped glass vial (Supleco®). The lipid/chloroform solution was evaporated under a slow stream of nitrogen while rotating by hand to produce an even lipid film. The film was dried under vacuum for 24 h, then stored under house nitrogen at −80 °C until use. When required for printing, films were left at room temperate for 30 min, then 2 mL of a pre-mixed solution of undecane and silicone oil AR20 (35:65 by volume) was added to the film, followed by sonication (Branson 2800 ultrasonic bath 230 V) for 1 h. The total concentration of lipids was 1 mM with a molar ratio of DPhPC:POPC of 2:1. Lipid films were kept for a maximum of 2 months.

Construction of recombinant DNA. Plasmid and primers used in this study are listed in Supplementary Tables 15 and 17, respectively. All PCRs were performed using KOD Hot Start DNA polymerase (Novagen®), following standard protocols. Plasmids were assembled using one-step isothermal assembly (NEBuilder® HiFi DNA Assembly Master Mix M5520AA). All constructs were sequenced to verify whether sequences were correct (Source BioScience). The plasmids pGRG25-P*max*:*sfgfp*, pGRG25-P*max*:*mrfp1* and pGRG25-Pmax:*immE2* plasmids were provided from Mavridou et al.[49]. The plasmids coding for the fluorescent proteins YPet (pBC11-P*ybaJ*:*ypet*) and mNeonGreen (pBC43-P*ybaJ*:*blFP-Y3*) were provided by Olivier Cunrath. The plasmid coding for the IPTG-inducible expression of ImmE2 (pC001-P*trc*:*immE2*[66]) was provided by Nick Housden and Colin Kleanthous. The generation of the plasmid from which ImmE2 is constitutively expressed (pTML9-P*max*:*immE2*) was assembled from the pBC22-P*ybaj*:*bfp* backbone (a plasmid identical in sequence to the plasmids encoding the YPet and mNeonGreen fluorescent proteins but expressing BFP) using the primers TML-P57 and TML-P58, the ImmE2 coding sequence from pC001-P*trc*:*immE2* using the primers TML-P61 and TML-P62 and the promoter and RBS driving the expression of superfolder GFP in pGRG25-P*max*:*sfgfp* using TML-P59 and TML-P60. All the primers used in this study were generated using SnapGene®.

Construction of bacterial strains. Bacterial strains used in this study are outlined in Table 1 and Supplementary Table 16. *E. coli* BZB1011 and BZB1011 pCol genotypes were provided from references[49,67]. Chromosomally labelled (*Tn7* insertion) sfGFP and mRFP1 BZB1011 strains and BZB1011 pCol genotypes were

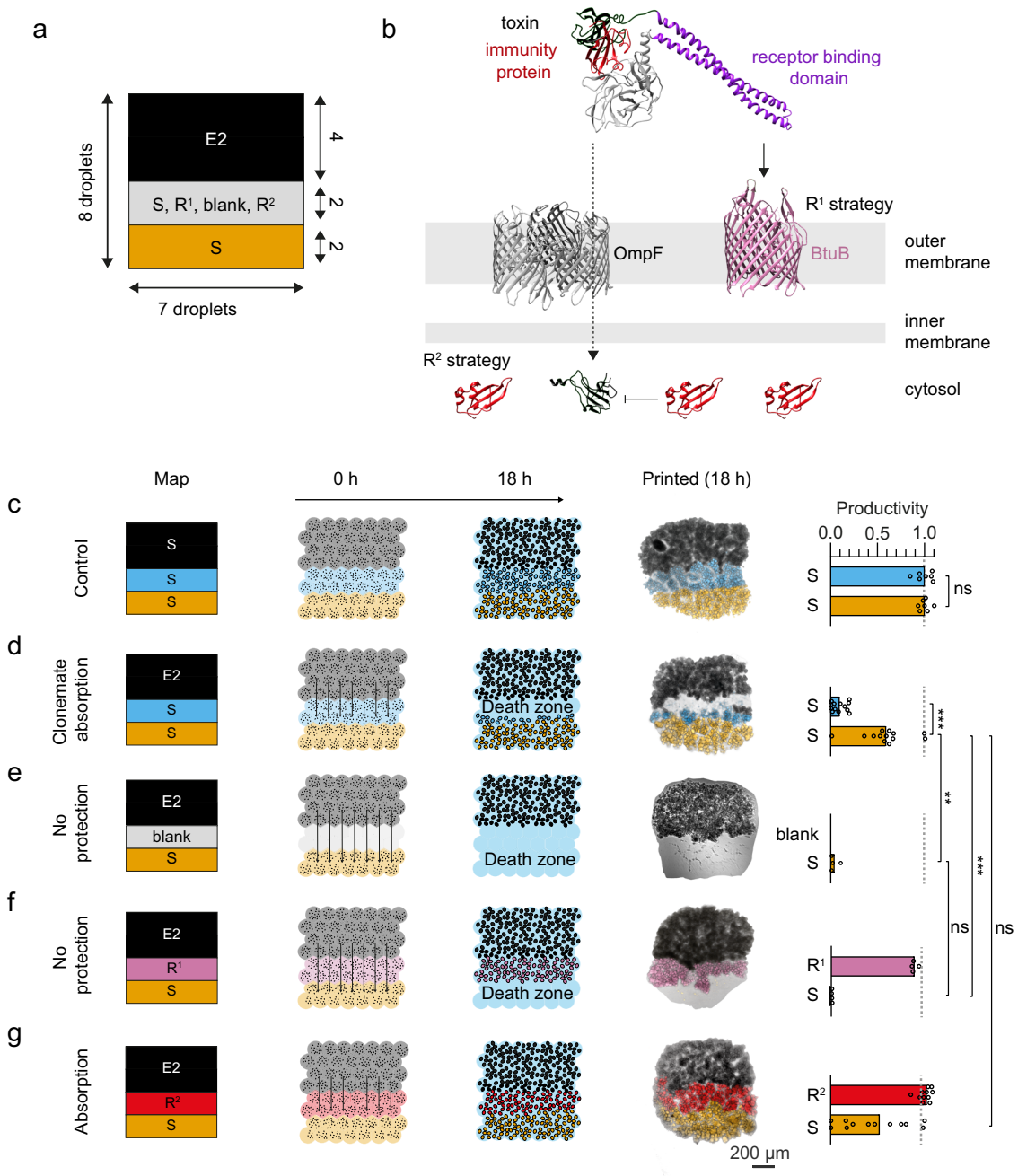

Fig. 4 Susceptible cells protect clonemates by binding incoming toxin. a Schematic of the printing map used for testing clonemate absorption. The producer strip (E2) consists of 7 × 4 × 1 droplets (black), the changeable strip consists of 7 × 2 × 1 droplet (grey) and the sensitive strip consists of 7 × 2 × 1 droplets (orange) in the *x*, *y* and *z* dimensions, respectively. **b** A schematic of the two resistance strategies used for creating R^1 and R^2. R^1 is resistant to colicins because of deletion of the BtuB receptor (which normally binds colicins). R^2 is resistant to colicins through constitutive expression of the cognate immunity protein, which binds and inactivates the toxin when it enters the cytosol. **c**–**g** Printing maps, competition schematics, composite bright-field and fluorescence microscopy images and bar charts of printed communities comprising three bioinks. **c** The control printed arrays containing three S strains ($n = 7$). A Wilcoxon test showed that the median productivities of S-skyblue (S rfp) and S-orange (S gfp) were non-significantly different ($P > 0.9999$, see Supplementary Table 5 for the statistical test). **d** Printed arrays containing E2 cells (black) and two S strains ($n = 13$). A Wilcoxon test showed that the median productivities of S-skyblue and S-orange were significantly different ($P = 0.0002$, see Supplementary Table 6 for the statistical test). **e** Printed arrays containing E2 cells, a strip of agarose not containing bacteria and S cells ($n = 4$). Mann–Whitney tests showed the median productivities of S-orange in **e** and **d**, and **e** and **f** were significantly ($P = 0.0029$) and non-significantly ($P = 0.1143$) different, respectively (see Supplementary Tables 7 for the statistical test). **f** Printed arrays containing E2 cells, R^1 cells (reddish-purple) and S cells ($n = 4$). A Mann–Whitney test showed that the median productivities of S-orange in **d** and **f** were significantly different ($P = 0.008$, see Supplementary Table 8). **g** Printed arrays containing E2 cells, R^2 cells (red) and S cells ($n = 12$). A Mann–Whitney test showed that the median productivities of S-orange in **d** and **g** were non-significantly different ($P = 0.604$, see Supplementary Table 9). In **d**–**g**, arrows on schematics represent the predicted colicin reach during the competition experiments (not to scale). In the bar charts, each data point is a biologically independent replicate and the height of the bars are mean productivity values. In **c**–**g**, the term 'productivity' (p) of a genotype a in a printed array after 18 h of competition is defined as $p = A_a/A_S$, where A_S is the total cross-sectional area that a susceptible genotype occupies after 18 h of competition (at the same starting density and spatial pattern as genotype a), but without interference competition.

provided from Mavridou et al.[49]. The BZB1011 *ΔbtuB sfgfp::Tn7* or *mrfp1::Tn7* strains were created by using the method described by Cianfanelli et al.[68]. Briefly, the regions (700 base pairs) upstream and downstream of the *btuB* gene were amplified by PCR and joined together in the pFOK plasmid using the NEB® HiFi DNA Assembly Master Mix. In all, 5 µL of the reaction was then transformed into chemically competent *E. coli* Jke201 (recovery in 1 mL of LB-Miller medium + 100 µM diamino pumilic acid (DAP) and selected on LB-Miller agar plates (1.5% w/v) supplemented with 100 µM DAP and 50 µg mL^{-1} kanamycin). Transformants were screened by colony PCR (GoTaq G2 polymerase) and sequencing (Source Bioscience) using the primers oOPC-614 and oOPC-615. Three clones carrying the correct plasmid (pTML8) were then conjugated with BZB1011 *sfgfp::Tn7* and BZB1011 *mrfp1::Tn7*. Trans-conjugants for which a second recombination event had occurred were then counter-selected. Clones were finally verified by colony PCR and sequencing (by using the primers TML-P9 and TML-P10) for deletion of the *btuB* gene. The BZB1011 *immE2::Tn7* pColE2 pBC11-P*ybaJ:ypet* or pBC43-P*ybaJ:blFP-Y3* genotypes were generated by transforming competent BZB1011 *immE2::Tn7* pColE2 cells (from Mavridou et al.[49]) with the respective plasmids, and by selecting for transformants on LB-Miller agar plates (1.5% w/v) supplemented with 30 µg mL^{-1} of kanamycin. The BZB1011 *mrfp1::Tn7* pC001-P*trc:immE2* and BZB1011 *mrfp1::Tn7* pTML-9-P*max:immE2* genotypes were generated by transforming competent BZB1011 *mrfp1::Tn7* with either pC001-P*trc:immE2* or pTML-9-P*max*:immE2, and selecting for transformants on LB-Miller agar plates (1.5% w/v) supplemented with 100 µg mL^{-1} of ampicillin.

Competent cell preparation and transformation. The strain for transformation was inoculated in LB-Miller medium overnight. The next day, the optical density at 600 nm (OD_{600}) of the overnight culture was measured using a spectrophotometer (Thermo Scientific, Genesys 10 S UV-VIS). The overnight culture was then inoculated into 50 mL of LB-Miller medium to a final OD_{600} of 0.05, and then incubated at 37 °C (shaking at 225 rpm) until the OD_{600} reached ≈0.4. Next, the cultures were split into centrifuge tubes (25 mL in each) and centrifuged at 4 °C for 10 min at 1734 g. Following this, the supernatants were discarded, and each pellet was gently resuspended in 12.5 mL of 4 °C 100 mM $CaCl_2$ + 15% v/v glycerol solutions. After the addition of these solutions, cultures were left on ice for 45 min. After this, cultures were again centrifuged at 4 °C for 10 min at 1734 × *g*. Centrifuged pellets were recombined pairwise by resuspending one of the pellets in 5 mL of ice-cold 100 mM $CaCl_2$ + 15% v/v glycerol solution, and using this resuspension, the second pellet was resuspended. Following this, 200 µL of competent bacteria were aliquoted into 1.5-mL centrifuge tubes and directly frozen at −80 °C.

To transform competent cells, 100 µL of competent cells were thawed on ice. Once thawed, DNA (≈100 ng for plasmids or 5 µL of Gibson assembly reaction mixtures) was added to the cells. The cells were then kept on ice for 30 min. Following this, the cells were heat-shocked by transferring the tube containing the cells and DNA into a 42 °C water bath for 45 s and then transferring the tube back on ice for 2 min. The cells were then recovered by adding 900 µL of LB-Miller medium and incubating for an hour at 37 °C (shaking at 225 rpm). After one hour of recovery, 100 µL of the cultures were plated on selective LB-Miller agar (1.5% w/v). The remaining 900 µL were centrifuged for 1 min at 8000 × *g*, followed by discarding of the supernatant and resuspension of the pellet in 100 µL of LB-Miller medium. The final 100 µL were then plated on the corresponding selective LB-Miller agar (1.5% w/v). Both plates were then incubated overnight at 37 °C in a static incubator and checked for transformants the following day.

Growth curves and analysis. Overnight cultures of the strains tested were normalised to an OD_{700} (optical density taken at 700 nm)[69] of 0.2 in PBS and washed twice. About 10 µL of normalised cultures were added to the wells (containing 190 µL of LB-Miller medium) of a flat-bottom transparent 96-well plate (excluding the two first and two last columns, which were filled with 200 µL of sterile Milli-Q® water), bringing the initial OD_{700} to 0.01. The layout of the plate was randomised using the CRUK PlateLayout tool (https://github.com/crukci-bioinformatics/PlateLayout) for each biologically independent replicate ($n = 3$). Three wells were left uninoculated to calculate background OD_{700}. The plate was then incubated at 37 °C (shaking at 400 rpm, double orbital) in a plate reader (BMG Labtech Omega) for 24 h, measuring OD_{700} every 5 min.

Doubling times were calculated from the growth curves using a custom Python script. In brief, data were imported in Python dataframes, sorted and the mean of the technical replicates calculated. The mean of the biologically independent replicates was then calculated. The data were then plotted, and the doubling times calculated using the data points between OD 0.2 and 0.7 (exponential phase) and a custom script (https://doi.org/10.5281/zenodo.4328623). Lag-phase duration was calculated using DMFit 3.5 (https://www.combase.cc/index.php/en/8-category-en-gb/21-tools)[70]. Plate reader data were formatted to be used by DMFit using a custom Python script.

Growth inhibition assay. The resistance of BZB1011 *sfgfp::Tn7 ΔbtuB*, BZB1011 *mrfp1::Tn7 ΔbtuB*, BZB1011 *mrfp1::Tn7* pC001-P*trc:immE2* and BZB1011 *mrfp1::Tn7* pTML-9-P*max:immE2* strains to colicin E2 was assessed using a growth inhibition assay adapted from White et al.[71]. Each strain to be tested and BZB1011 pColE2 were inoculated in 3 mL of LB-Miller medium and incubated overnight at 37 °C (shaking at 225 rpm). The following day, the overnight cultures were diluted in LB-Miller medium to an OD_{600} of 0.05 and incubated at 37 °C (shaking at 225 rpm) until they reached an OD_{600} between 0.6 and 0.7. In all, 200 µL of the cultures were then added to molten soft LB-Miller agar (0.75% w/v) kept at 56 °C and poured over LB-Miller agar plates (1.5% w/v). After the plates had dried, 2 µL of serially diluted E2 overnight culture was spotted on the plates. Plates were then incubated at 37 °C (static) overnight and imaged to check for inhibition zones or lack of inhibition zones (which determined resistance).

Preparation of bioinks. Genotypes were cultured directly from glycerol stocks (50% v/v glycerol) in 4 mL of LB-Miller medium for 15 h (shaking at 250 rpm). From the overnight cultures, 20 µL of each was added to 2 mL of fresh LB-Miller medium and cultured for 3 h (shaking at 250 rpm). Cultures were then normalised to 10^9 cells mL^{-1} by centrifugation at 8000 × *g* for 5 min and resuspended in 100 µL of fresh LB-Miller medium. Centrifugation, removal of the supernatant and addition of fresh LB medium (100 µL) were repeated twice to remove any colicin in the supernatant. If 1:1 competitions were investigated at an *SI* of 0.50, the two normalised bacteria cultures were combined at a 1:1 ratio (50 + 50 µL). At any other *SI* (that required two or three nozzles for printing), a bioink was created per culture. To create the bioinks, 150 µL of molten 2.0% w/v ULGT agarose in LB-Miller medium (37 °C), 30 µL of LB-Miller medium and 20 µL of normalised culture were combined in PCR tubes and mixed by gently pipetting back and forward using a 200-µL pipette to homogenise the solution for printing. Pipette tips (Corning® 1–200 µL Filtered IsoTip™) and PCR tubes were maintained at 37 °C before homogenising the bioink.

Printing bacterial droplet networks containing bacteria. The functioning of the 3D droplet printer is outlined in our previous work[41]. In brief, a custom-built piezoelectric transducer (±130 V) transmits controlled pressure impulses to a chamber filled with Milli-Q® water. The chamber is connected to a glass nozzle (with a tip diameter of ≈150 µm) from which the aqueous printing solution is ejected (Supplementary Fig. 8). To prevent mixing of the printing solution with the water inside the chamber and nozzle, an undecane oil plug of ≈5 µL was used to separate the two solutions. A quartz cuvette (Starna Scientific Ltd) with dimensions of 20 × 10 × 10 mm (length, width and height) was filled with 1 mL of lipid/oil solution and mounted on the micromanipulator. An IR heater (Beurer Ltd., 150 W) was used to equilibrate the temperature of the nozzles and the quartz cuvette (from a fixed distance) to approximately 37 °C over 30 min. After equilibration, the bioink was loaded into the nozzle, and the tip was immersed into the lipid/oil solution contained in the quartz cuvette, which was positioned on a digitally controlled micromanipulator (PatchStar micromanipulator, Scientifica, 20-nm resolution). The micromanipulator movements and the piezo actuation were synchronised using a custom-made software developed in LabVIEW (National Instruments™). Printing was monitored using a side-on stereomicroscope (Nikon® SMZ745T) and videos and pictures were acquired using a digital camera (Thorlabs DCC1645C) mounted on the microscope. For creating patterns at *SI* = 0.67, 0.80, 0.88 and 0.94, a second nozzle was used simultaneously to the first. The second nozzle was normalised to the offset of the first nozzle so that the pattern could be printed line-by-line. For three bioinks, the two smaller strips were printed first using two nozzles followed by replacing the first nozzle with a new nozzle containing the third bioink for printing the larger strip. The third nozzle was aligned with a control droplet to complete the pattern.

Creating printed arrays containing bacteria from printed droplet networks. Once droplet networks were printed, the structures were left for 15 mins at 37 °C to allow the droplets to reach their equilibrium contact angles. Following equilibration, networks were moved to the fridge (4 °C) for 1 min 30 s to partially gel the ULGT agarose. Next, networks were moved from the fridge to ambient temperature (22 °C) and washed with silicone oil AR20 by initially removing 500 µL of the lipid/oil solution and then adding 600 µL of silicone oil AR20. Then, 600 µL of the diluted lipid/oil solution were removed followed by addition of 600 µL of silicone oil AR20. This was repeated two more times. The silicone oil washing step was performed to precipitate the lipids so that the tessellated droplets of partially gelled ULGT agarose could connect with each other. After washing, the networks were left for 5 min at ambient temperature to allow complete breaking of all bilayers and consequent connection of partially gelled ULGT agarose droplets. After 5 min, the networks were moved to the fridge for 45 min to create a gelled block of LB-Miller ULGT agarose containing patterned bacteria (printed arrays). After 45 min, each printed array was moved to individual containers filled with 600 µL of LB-Miller media (Nunc™, Lab-Tek™ II Chamber Slide™ System (8 wells)) by hydrating the array in 0.5 µL of LB-Miller medium (using a 0.5-µL Hamilton® syringe), followed by picking up the LB-Miller droplet containing the printed array (using a cut pipette tip (20 µL)) and pipetting the printed array into the container. Sterile 20-µL pipette tips were cut using a sterile scalpel (No. 21 Swann-Morton®). Printed arrays were encapsulated in LB-Miller medium and subsequently transferred into chambers by using a Leica® EZ4 Stereomicroscope with a ×16 eyepiece.

Bacterial competition experiments within printed arrays and imaging of results. For competition experiments, printed arrays in LB-Miller media were

incubated at 37 °C for 18 h. After 18 h, printed arrays were washed with M9 medium to remove excess bacteria that grew out into solution from the printed arrays during the competition experiment. Within each compartment containing a printed array, 400 µL of LB-Miller medium were removed and 200 µL of M9 medium were added. Following this, 200 µL of the medium were removed and another 200 µL of M9 medium were added to further wash and remove the bacteria. Finally, printed arrays were picked up using a cut pipette tip (20 µL) and transferred into individual containers containing 400 µL of M9 media (Nunc™, Lab-Tek™ II Chambered Coverglass (eight wells)). Printed arrays were left in M9 media for 10 h to allow the exchange of LB medium with M9 medium, required for imaging. Printed arrays were imaged using a Leica® SP5 confocal microscope using a HC PL Fluotar ×10/0.30 objective (0.3 numerical aperture), at excitation wavelengths of 405 nm and 546 nm and emission cut-offs at 420–520 nm and 625 nm, respectively (exciting superfolder GFP, mRFP1, YPet and mNeonGreen), a *z*-step of 2.73 µm and scanning speed of 400 Hz.

Colony-forming units of printed arrays. Printed arrays were washed and transferred to 400 µL of M9 medium after 8 h of competition. This time point was chosen because space in the printed arrays was saturated with *E. coli* within 8 h. Next, printed arrays were moved to individual 1-mL centrifuge tubes containing 200 µL of M9 medium and melted at 55 °C for 1 min in a thermomixer (Eppendorf ThermoMixer® C) shaking at 1000 rpm. Following this melting, the *E. coli*-containing solutions were serially diluted by 10,000-fold (100 µL in 900 µL of M9 medium). Following this, 10,000× diluted solutions were plated by beads on 1.5% w/v LB-Miller agar plates and then left to grow for 24 h at 37 °C in a static incubator. After 24 h, colonies were counted using a Zeiss PlanApo Z ×0.5 objective on an AxioZoom.V16 Zeiss microscope. Genotypes were recognised by fluorescence.

Flow cytometry of printed arrays. Printed arrays were washed and transferred to 400 µL of M9 medium after 18 h of competition. Next, printed arrays were moved to individual 1-mL centrifuge tubes containing 200 µL of M9 medium and melted. The cell suspensions were diluted a further tenfold in M9 medium. Diluted cell suspensions were analysed on a BD Accuri C6 Flow Cytometer (Version 1.0.264.21) using 10,000 and 8000 as thresholds for the forward and side scatter parameters, respectively. For each experimental condition, 20,000 events were quantified per sample. A custom-written script was written on Rstusdio (Version 1.3.959) to analyse data. The population of bacteria was gated by considering only the events within the core of the cell population in order to minimise count biases (Supplementary Fig. 7c). This was calculated from the forward and side scatter dimensions. Cells that had a fluorescence intensity above $2^{9.5}$ were assigned as BZB1011 *sfgfp*::*Tn7*. Cells below this were assigned as BZB1011 *mrfp1*::*Tn7* (Supplementary Fig. 7d). Counts shown in Supplementary Fig. 2c are based on the first 3000 cells that met the selection criteria, which were used to calculate the frequencies of BZB1011 *sfgfp*::*Tn7* and BZB1011 *mrfp1*::*Tn7*. Contour plots were visualised using FlowJo 10.7.0 (Tree Star, Inc.).

Microcolony quantification by image analysis. 2D segmentation: 3D confocal images of printed arrays were projected into 2D using an average intensity projection (using FIJI[72] software). The resulting 2D images were then segmented using a combination of ridge detection[73], morphological watershed[74] and intensity thresholding. This generated binary images of microcolonies. Each binary image was then used as a mask to extract each microcolony's position, orientation, length and width, as well as its brightness in the two fluorescence channels. Image segmentation and analysis were performed using MATLAB® (MathWorks®) (R2017a) with a custom-written user interface (FAST: https://doi.org/10.5281/zenodo.4323627).

Print isolation: Some images of prints contained small pieces of detached debris and regions from other prints. To automatically remove these from downstream analyses, the size of each print was estimated and used to exclude these external microcolonies. In the first step of this process, the approximate centre of the print $(\overline{x},\overline{y})$ was found by averaging the x and y coordinates of all microcolonies in the image. The average distance of each microcolony from $(\overline{x},\overline{y})$ was then calculated as $\overline{r}$. The approximate side length of the print L was then found as

$$L = \frac{6\overline{r}}{\left(\sqrt{2}+\log\left(1+\sqrt{2}\right)\right)}. \quad (1)$$

This was used to set a radial distance threshold on the detected microcolony positions, allowing the main print to be isolated from unrelated microcolonies. $(\overline{x},\overline{y})$ was then recalculated excluding these microcolonies, providing a more accurate measure of the centre of the print.

Print registration: The above approximation of L assumes that prints are perfectly square. To obtain a more accurate measure of the size of the rectangular prints, they were first registered to the x–y coordinate system. This required finding an angle θ through which each print could be rotated to bring it into alignment with all other prints. The first stage of this process involved finding the convex hull of the print, and then measuring the distance between each point on the hull and $(\overline{x},\overline{y})$. These values were then resampled onto a regularly spaced series of N polar angles φ_n measured from $(\overline{x},\overline{y})$. The mean was then subtracted from the resulting series of values, resulting in a function $d(\varphi)$ that was positive at values of φ where the outer boundary of the print was further-than-average away from the centre and negative at values of φ where it was closer than average.

$d(\varphi)$ has peaks at values of φ corresponding to each of the four corners of the print interleaved with troughs at values of φ corresponding to the sides. Furthermore, $d(\varphi)$ is circular, with $d(\varphi_1) = d(\varphi_{N+1})$. θ could therefore be found from the phase of the Discrete Fourier Transform (DFT) on $d(\varphi)$ with wavenumber $k = 4$. Explicitly,

$$\theta = \frac{1}{4}\left(\pi - \arg\left(\sum_{n=0}^{N-1} d(\varphi_n)\cdot e^{-\frac{i8\pi}{N}n}\right)\right). \quad (2)$$

The position of each microcolony was then rotated about $(\overline{x},\overline{y})$ by θ, and the size of the print in each direction estimated as the difference between the minimum and maximum x and y coordinates of the registered microcolonies.

Microcolony neighbour–neighbour distance estimation: Delaunay triangulation[75] was applied to the positions of all microcolonies in the print. Microcolonies directly connected in the resulting triangulation were assigned as neighbours. Microcolonies forming the outer boundary of the print were therefore excluded when calculating the radial neighbour–neighbour distance profile.

3D segmentation: 3D segmentation of confocal microcolony data was performed using a generalisation of the algorithm used during 2D segmentation. Specifically, a rough segmentation of the initial array of voxel intensities $I(x, y, z)$ was first generated by applying a simple intensity threshold, allowing the bright microcolony-containing regions to be separated from the dark background. However, variations in background intensity and intermediate intensities of voxels between closely packed microcolonies prevented this approach from reliably isolating individual microcolonies within these regions.

To separate these closely packed microcolonies, we located 3D ridge-like features (e.g., blobs, sheets or tubes) that were dark relative to nearby microcolonies[76,77]. Initially, $I(x, y, z)$ was convolved with a Gaussian kernel $G(x, y, z, \sigma)$ of spatial scale σ to isolate features at that scale:

$$\widetilde{I}(x,y,z,\sigma) = I(x,y,z) * G(x,y,z,\sigma) \quad (3)$$

The second-order derivatives of $\widetilde{I}$ ($\widetilde{I}_{xx}$, $\widetilde{I}_{xy}$, etc.) were next used to construct the Hessian H of the image at each voxel:

$$H(x,y,z,\sigma) = \begin{bmatrix} \widetilde{I}_{xx} & \widetilde{I}_{xy} & \widetilde{I}_{xz} \\ \widetilde{I}_{yx} & \widetilde{I}_{yy} & \widetilde{I}_{yz} \\ \widetilde{I}_{zx} & \widetilde{I}_{zy} & \widetilde{I}_{zz} \end{bmatrix} \quad (4)$$

H contains information on the 3D features of scale σ present within the image around position (x, y, z). These features can be classified by finding the eigenvalues λ_1, λ_2 and λ_3 of H, where $|\lambda_1| \geq |\lambda_2| \geq |\lambda_3|$[76,77]. However, as we were not concerned with the specific type of feature separating microcolonies, we generated a binary segmentation of the image simply by finding all voxels for which λ_1 was above a threshold value. This fine-grained mask was then combined with the initial rough segmentation using a voxelwise AND filter, generating the final segmentation.

Calculating segregation indices. We used a *SI* to measure genetic mixing within printed arrays, and to quantify printing fidelity. *SI* was computed for printed-colony micrographs as follows:

1. Segmentation: Each micrograph pixel was assigned a genetic identity ('A', 'B' or 'None') by comparing its two fluorescence channel intensities, thresholded separately using Otsu's method[78]. Pixels in which both channels exceeded the intensity threshold were classified as containing neither cell type ('None').
2. Local *SI*: We computed a local segregation index s_i for each A- or B-type pixel i, by comparing its genetic identity with those of neighbouring pixels. For a square neighbourhood of size h, $s_i(h)$ is defined as

$$s_i(h) = \frac{1}{N_i(h)}\sum_{j=1}^{N_i(h)} g_i(j), \quad g_i(j) = \begin{cases} 1, & \text{pixels } i \text{ and } j \text{ are kin} \\ 0, & \text{otherwise} \end{cases} \quad (5)$$

   where $N_i(h)$ is the number of A- or B-type pixels within h rows or columns of focal pixel i. Thus, $s_i(h)$ is the fraction of i's neighbours that share its genotype. Note: for ease of image processing, here we are considering square neighbourhoods instead of the circular ones used previously[19,71].
3. Global *SI*: We defined the global segregation index *SI* for a community micrograph as the arithmetic mean of local segregation indices for each of M focal pixels:

$$SI(h) = \frac{1}{M}\sum_{i=1}^{M} s_i(h). \quad (6)$$

$SI(h)$ varies in value from 0.5 (high genetic mixing on spatial scale h) to 1.0 (no genetic mixing).

To assess printing fidelity, we generated reference images representing the idealised community structure (Supplementary Fig. 2e) and compared the resulting

SI(h) values with those measured for printed communities (Fig. 1h). This comparison revealed a good fit between measured and reference *SI*(h) values for a range of spatial scales (Fig. 1h; $h = 5$, 10, 20, 50, 100 px, equivalent to 7.6, 15.2, 30.3, 75.8, 151.5 µm), confirming that community printing is capable of modulating genetic mixing. Image processing and *SI* calculations were carried out using MATLAB® (MathWork®) (R2017a) and code is available at https://zenodo.org/record/4354822#.X9zArJP7RPU.

Definitions and calculations. The term 'frequency' (f) of a genotype, a, in a printed array containing genotype a and b after 18 h of competition is defined as

$$f = \frac{A_a}{(A_a + A_b)} \quad (7)$$

A is the total cross-sectional area that a genotype occupies in the printed array. A is calculated by segmentation of z-projected (by average intensity) confocal microscopy images of the printed array. f is used in Figs. 1, 2, and 3. In Supplementary Fig. 2a, A = total volume occupied by a strain, number of cells and number of CFUs for 3D segmentation, flow cytometry and CFU, respectively.

The term 'productivity' (p) of a genotype, a, in a printed array after 18 h of competition is defined as

$$p = \frac{A_a}{A_S} \quad (8)$$

A_s is the total cross-sectional area that a susceptible genotype occupies after 18 h of competition (at the same starting density and spatial pattern as genotype a), but without interference competition. For competition between two genotypes (Fig. 3), this would be the total cross-sectional area occupied by a susceptible strain at the given *SI*, competing against another susceptible strain. For competition between three genotypes (Fig. 4), this would be the total cross-sectional area occupied by a susceptible genotype in the strip (Fig. 4c), competing against the other two susceptible genotypes in the other strips.

Data availability

Raw datasets, including image-processing data and micrographs, generated and/or analysed during this study, are available in the figshare repository https://doi.org/10.6084/m9.figshare.13379579[79]. Source data are provided with this paper.

Code availability

Code used for 3D segmentation and subsequent analysis of z-projected and z-stacked confocal images is available at https://doi.org/10.5281/zenodo.4153224. The FAST tracking package, along with instructions on its use, is available at https://mackdurham.group.shef.ac.uk/FAST_DokuWiki/dokuwiki. Our written code for calculations of segregation indices is available at https://doi.org/10.5281/zenodo.4354822. The CRUK PlateLayout tool used to randomise cultures in 96-well plates is available at https://github.com/crukci-bioinformatics/PlateLayout. Doubling times and lag phases were analysed from liquid culture growth curves using a custom-written script (https://doi.org/10.5281/zenodo.4328623) and DMFit 3.5 (https://www.combase.cc/index.php/en/8-category-en-gb/21-tools), respectively.

Received: 4 November 2020; Accepted: 6 January 2021;
Published online: 08 February 2021

References

1. West, S. A., Diggle, S. P., Buckling, A., Gardner, A. & Griffin, A. S. The social lives of microbes. *Annu. Rev. Ecol. Evol. Syst.* **38**, 53–77 (2007).
2. Little, A. E. F., Robinson, C. J., Peterson, S. B., Raffa, K. F. & Handelsman, J. Rules of engagement: interspecies interactions that regulate microbial communities. *Annu. Rev. Microbiol.* **62**, 375–401 (2008).
3. Waters, C. M. & Bassler, B. L. Quorum sensing: cell-to-cell communication in bacteria. *Annu. Rev. Cell Dev. Biol.* **21**, 319–346 (2005).
4. Hibbing, M. E., Fuqua, C., Parsek, M. R. & Peterson, S. B. Bacterial competition: surviving and thriving in the microbial jungle. *Nat. Rev. Microbiol.* **8**, 15–25 (2009).
5. Nadell, C. D., Drescher, K. & Foster, K. R. Spatial structure, cooperation and competition in biofilms. *Nat. Rev. Microbiol.* **14**, 589–600 (2016).
6. Donaldson, G. P., Lee, S. M. & Mazmanian, S. K. Gut biogeography of the bacterial microbiota. *Nat. Rev. Microbiol.* **14**, 20–32 (2016).
7. Stacy, A., McNally, L., Darch, S. E., Brown, S. P. & Whiteley, M. The biogeography of polymicrobial infection. *Nat. Rev. Microbiol.* **14**, 93–105 (2016).
8. Mark Welch, J. L., Rossetti, B. J., Rieken, C. W., Dewhirst, F. E. & Borisy, G. G. Biogeography of a human oral microbiome at the micron scale. *Proc. Natl Acad. Sci. USA* **113**, 791–800 (2016).
9. Wilbert, S. A., Mark Welch, J. L. & Borisy, G. G. Spatial ecology of the human tongue dorsum microbiome. *Cell. Rep.* **30**, 4003–4015.e3 (2020).
10. Tropini, C., Earle, K. A., Huang, K. C. & Sonnenburg, J. L. The gut microbiome: connecting spatial organization to function. *Cell Host Microbe* **21**, 433–442 (2017).
11. Cordero, O. X. & Datta, M. S. Microbial interactions and community assembly at microscales. *Curr. Opin. Microbiol.* **31**, 227–234 (2016).
12. Kreft, J. U. Biofilms promote altruism. *Microbiology* **150**, 2751–2760 (2004).
13. Xavier, J. B. & Foster, K. R. Cooperation and conflict in microbial biofilms. *Proc. Natl Acad. Sci. USA* **104**, 876–881 (2007).
14. Nadell, C. D., Xavier, J. B., Levin, S. A. & Foster, K. R. The evolution of quorum sensing in bacterial biofilms. *PLoS Biol.* **6**, e14 (2008).
15. Nadell, C. D. et al. Cutting through the complexity of cell collectives. *Proc. R. Soc. Lond., B, Biol. Sci.* **280**, 20122770 (2013).
16. Nadell, C. D., Foster, K. R. & Xavier, J. B. Emergence of spatial structure in cell groups and the evolution of cooperation. *PLoS Comput. Biol.* **6**, e1000716 (2010).
17. Borenstein, D. B., Meir, Y., Shaevitz, J. W. & Wingreen, N. S. Non-local interaction via diffusible resource prevents coexistence of cooperators and cheaters in a lattice model. *PLoS ONE* **8**, e63304 (2013).
18. Mitri, S., Xavier, J. B. & Foster, K. R. Social evolution in multispecies biofilms. *Proc. Natl Acad. Sci. USA* **108**, 10839–10846 (2011).
19. Estrela, S. & Brown, S. P. Metabolic and demographic feedbacks shape the emergent spatial structure and function of microbial communities. *PLoS Comput. Biol.* **9**, e1003398 (2013).
20. Momeni, B., Brileya, K. A., Fields, M. W. & Shou, W. Strong inter-population cooperation leads to partner intermixing in microbial communities. *eLife* **2**, e00230 (2013).
21. Momeni, B., Waite, A. J. & Shou, W. Spatial self-organization favors heterotypic cooperation over cheating. *eLife* **2**, e00960 (2013).
22. Chao, L. & Levin, B. R. Structured habitats and the evolution of anticompetitor toxins in bacteria. *Proc. Natl Acad. Sci. USA* **78**, 6324–6328 (1981).
23. Kerr, B., Riley, M. A., Feldman, M. W. & Bohannan, B. J. M. Local dispersal promotes biodiversity in a real-life game of rock-paper-scissors. *Nature* **418**, 171–174 (2002).
24. Majeed, H., Gillor, O., Kerr, B. & Riley, M. A. Competitive interactions in *Escherichia coli* populations: the role of bacteriocins. *ISME J.* **5**, 71–81 (2011).
25. Pande, S. et al. Privatization of cooperative benefits stabilizes mutualistic cross-feeding interactions in spatially structured environments. *ISME J.* **10**, 1413–1423 (2016).
26. Gonzalez, D., Sabnis, A., Foster, K. R. & Mavridou, D. A. I. Costs and benefits of provocation in bacterial warfare. *Proc. Natl Acad. Sci. USA* **115**, 7593–7598 (2018).
27. Kim, W., Racimo, F., Schluter, J., Levy, S. B. & Foster, K. R. Importance of positioning for microbial evolution. *Proc. Natl Acad. Sci. USA* **111**, 1639–1647 (2014).
28. Walker, A. W. et al. The species composition of the human intestinal microbiota differs between particle-associated and liquid phase communities. *Environ. Microbiol.* **10**, 3275–3283 (2008).
29. Mark Welch, J. L., Hasegawa, Y., McNulty, N. P., Gordon, J. I. & Borisy, G. G. Spatial organization of a model 15-member human gut microbiota established in gnotobiotic mice. *Proc. Natl Acad. Sci. USA* **114**, E9105–E9114 (2017).
30. Kim, D. et al. Spatial mapping of polymicrobial communities reveals a precise biogeography associated with human dental caries. *Proc. Natl Acad. Sci. USA* **117**, 12375–12386 (2020).
31. Kim, H. J., Boedicker, J. Q., Choi, J. W. & Ismagilov, R. F. Defined spatial structure stabilizes a synthetic multispecies bacterial community. *Proc. Natl Acad. Sci. USA* **105**, 18188–18193 (2008).
32. Dal Co, A., van Vliet, S. & Ackermann, M. Emergent microscale gradients give rise to metabolic cross-feeding and antibiotic tolerance in clonal bacterial populations. *Philos. Trans. R. Soc. B* **374**, 20190080 (2019).
33. Dal Co, A., van Vliet, S., Kiviet, D. J., Schlegel, S. & Ackermann, M. Short-range interactions govern the dynamics and functions of microbial communities. *Nat. Ecol. Evol.* **4**, 366–375 (2020).
34. Merrin, J., Leibler, S. & Chuang, J. S. Printing multistrain bacterial patterns with a piezoelectric inkjet printer. *PLoS ONE* **2**, e663–e667 (2007).
35. Connell, J. L., Ritschdorff, E. T., Whiteley, M. & Shear, J. B. 3D printing of microscopic bacterial communities. *Proc. Natl Acad. Sci. USA* **110**, 18380–18385 (2013).
36. Lehner, B. A. E., Schmieden, D. T. & Meyer, A. S. A straightforward approach for 3D bacterial printing. *ACS Synth. Biol.* **6**, 1124–1130 (2017).
37. Liu, X. et al. 3D printing of living responsive materials and devices. *Adv. Mater.* **30**, 1704821 (2017).
38. Schaffner, M., Rühs, P. A., Coulter, F., Kilcher, S. & Studart, A. R. 3D printing of bacteria into functional complex materials. *Sci. Adv.* **3**, eaao6804 (2017).
39. Gupta, S. et al. Investigating the dynamics of microbial consortia in spatially structured environments. *Nat. Commun.* **11**, 2418 (2020).
40. Holden, M. A., Needham, D. & Bayley, H. Functional bionetworks from nanoliter water droplets. *J. Am. Chem. Soc.* **129**, 8650–8655 (2007).
41. Villar, G., Graham, A. D. & Bayley, H. A tissue-like printed material. *Science* **340**, 48–52 (2013).

42. Gordon, D. M., Riley, M. A. & Pinou, T. Temporal changes in the frequency of colicinogeny in *Escherichia coli* from house mice. *Microbiology* **144**, 2233–2240 (1998).
43. Riley, M. A. & Gordon, D. M. The ecological role of bacteriocins in bacterial competition. *Trends Microbiol.* **7**, 129–133 (1999).
44. Riley, M. A. & Chavan, M. A. *Bacteriocins* (Springer Berlin Heidelberg, 2007).
45. Granato, E. T. & Foster, K. R. The evolution of mass cell suicide in bacterial warfare. *Curr. Biol.* **30**, 2836–2843 (2020).
46. Gardner, A. & West, S. A. Spite and the scale of competition. *J. Evolution Biol.* **17**, 1195–1203 (2004).
47. Gardner, A., West, S. A. & Buckling, A. Bacteriocins, spite and virulence. *Proc. R. Soc. Lond., B, Biol. Sci.* **271**, 1529–1535 (2004).
48. Bucci, V., Nadell, C. D. & Xavier, J. B. The evolution of bacteriocin production in bacterial biofilms. *Am. Nat.* **178**, E162–E173 (2011).
49. Mavridou, D. A. I., Gonzalez, D., Kim, W., West, S. A. & Foster, K. R. Bacteria use collective behavior to generate diverse combat strategies. *Curr. Biol.* **28**, 345–355 (2018).
50. Timmis, K. & Hedges, A. J. The killing of sensitive cells by colicin D. *Biochim. Biophys. Acta* **262**, 200–207 (1972).
51. Shannon, R. & Hedges, A. J. Kinetics of lethal adsorption of colicin E2 by *Escherichia coli*. *J. Bacteriol.* **93**, 1353–1359 (1967).
52. Ghazaryan, L., Giladi, I. & Gillor, O. The effects of colicin production rates on allelopathic interactions in *Escherichia coli* populations. *Microorganisms* **7**, 564 (2019).
53. Berryman, A. A. & Hawkins, B. A. The refuge as an integrating concept in ecology and evolution. *Oikos* **115**, 192–196 (2006).
54. Durrett, R. & Levin, S. Allelopathy in spatially distributed populations. *J. Theor. Biol.* **185**, 165–171 (1997).
55. Coyte, K. Z., Schluter, J. & Foster, K. R. The ecology of the microbiome: networks, competition, and stability. *Science* **350**, 663–666 (2015).
56. Pugsley, A. P. Autoinduced synthesis of colicin E2. *Mol. Gen. Genet.* **190**, 379–383 (1983).
57. Ghazaryan, L., Soares, M. I. M. & Gillor, O. Auto-regulation of DNA degrading bacteriocins: molecular and ecological aspects. *Antonie van. Leeuwenhoek* **105**, 823–834 (2014).
58. Cascales, E. et al. Colicin biology. *Microbiol. Mol. Biol. R.* **71**, 158–229 (2007).
59. Inglis, R. F., Hall, A. R. & Buckling, A. The role of 'soaking' in spiteful toxin production in *Pseudomonas aeruginosa*. *Biol. Lett.* **9**, 20120569 (2012).
60. Rendueles, O., Amherd, M. & Velicer, G. J. Positively frequency-dependent interference competition maintains diversity and pervades a natural population of cooperative microbes. *Curr. Biol.* **25**, 1673–1681 (2015).
61. Xu, K. D., Stewart, P. S., Xia, F., Huang, C. T. & McFeters, G. A. Spatial physiological heterogeneity in *Pseudomonas aeruginosa* biofilm is determined by oxygen availability. *Appl. Environ. Microbiol.* **64**, 4035–4039 (1998).
62. Walters, M. C., Roe, F., Bugnicourt, A., Franklin, M. J. & Stewart, P. S. Contributions of Antibiotic penetration, oxygen limitation, and low metabolic activity to tolerance of *Pseudomonas aeruginosa* biofilms to ciprofloxacin and tobramycin. *Antimicrob. Agents Chemother.* **47**, 317–323 (2003).
63. Stewart, P. S. & Franklin, M. J. Physiological heterogeneity in biofilms. *Nat. Rev. Micro* **6**, 199–210 (2008).
64. Nadell, C. D., Xavier, J. B. & Foster, K. R. The sociobiology of biofilms. *FEMS Microbiol. Rev.* **33**, 206–224 (2009).
65. Alcinesio, A. et al. Controlled packing and single-droplet resolution of 3D-printed functional synthetic tissues. *Nat. Commun.* **11**, 2105 (2020).
66. Li, W. et al. Dual recognition and the role of specificity-determining residues in colicin E9 DNase-immunity protein interactions. *Biochemistry* **37**, 11771–11779 (1998).
67. Ghazaryan, L., Tonoyan, L., Ashhab, A. A., Soares, M. I. M. & Gillor, O. The role of stress in colicin regulation. *Arch. Microbiol.* **196**, 753–764 (2014).
68. Cianfanelli, F. R., Cunrath, O. & Bumann, D. Efficient dual-negative selection for bacterial genome editing. *BMC Microbiol.* **20**, 129 (2020).
69. Hecht, A., Endy, D., Salit, M. & Munson, M. S. When wavelengths collide: bias in cell abundance measurements due to expressed fluorescent proteins. *ACS Synth. Biol.* **5**, 1024–1027 (2016).
70. Baranyi, J. & Roberts, T. A. A dynamic approach to predicting bacterial growth in food. *Int. J. Food Microbiol.* **23**, 277–294 (1994).
71. White, P. et al. Exploitation of an iron transporter for bacterial protein antibiotic import. *Proc. Natl Acad. Sci. USA* **114**, 12051–12056 (2017).
72. Schindelin, J. et al. Fiji: an open-source platform for biological-image analysis. *Nat. Methods* **9**, 676–682 (2012).
73. Lindeberg, T. Edge detection and ridge detection with automatic scale selection. *Int. J. Comput. Vis.* **30**, 117–156 (1998).
74. Meyer, F. Topographic distance and watershed lines. *Signal Process.* **38**, 113–125 (1994).
75. Berg, de, M, Kreveld, van, M, Overmars, M. & Schwarzkopf, O. *Computational Geometry*. Ch. 9 (Springer, Berlin, Heidelberg, 1997).
76. Sato, Y. et al. Three-dimensional multi-scale line filter for segmentation and visualization of curvilinear structures in medical images. *Med. Image Anal.* **2**, 143–168 (1998).
77. Jin, J., Yang, L., Zhang, X. & Ding, M. Vascular tree segmentation in medical images using Hessian-based multiscale filtering and level set method. *Comput. Math Methods Med.* **2013**, 502013 (2013).
78. Otsu, N. A threshold selection method from gray-level histograms. *IEEE T. Syst. Man. Cy-S* **9**, 62–66 (1979).
79. Krishna Kumar, R. et al. Image processing data, micrographs, and confocal microscopy images of printed arrays containing *E. coli*. Figshare, https://doi.org/10.6084/m9.figshare.13379579 (2020).

Acknowledgements

This research was supported by a European Research Council Advanced Grant SYNTISU, which supports R.K.K., L.Z., G.S.P. and H.B., and by a European Research Council Advanced Grant 787932 and a Wellcome Trust Investigator award 209397/Z/17/Z to K.R.F. and W.P.J.S. T.A.M.-L. and A.A. acknowledge funding from the University of Oxford, and the EPSRC & BBSRC Centre for Doctoral Training in Synthetic Biology (grant EP/L016494/1), and A.A. also acknowledges funding from a Clarendon Fund Scholarship. O.J.M. acknowledges funding from the EPSRC Life Sciences Interface Centre for Doctoral Training (grant EP/F500394/1). D.G. acknowledges funding from the Swiss National Science Foundation Postdoc Mobility Fellowships P2LAP3_155109 and P300PA_167703. D.A.I.M. acknowledges funding from the MRC Career Development Award MR/M009505/1. The authors thank the electronic and mechanical workshops in the Physical and Theoretical Chemistry Department for aid in the design and construction of the piezo drivers, Olivier Cunrath, Nicholas Housden and Colin Kleanthous for plasmids, Connor Sharp and Daniel Unterweger for useful discussions and Elisa Granato for spotting and imaging colonies for Fig. 1b.

Author contributions

R.K.K., D.G., W.K., G.S.P., H.B. and K.R.F. conceived and designed experiments. R.K.K. and K.R.F. wrote the paper, with comments from other authors. R.K.K., T.A.M.-L. and A.A. performed experiments. O.J.M. and W.P.J.S. wrote custom software for image analysis of printed arrays and calculation of segregation indices, respectively. D.A.I.M. and D.G. designed and generated the colicin toolbox. L.Z. designed and built the high-power piezo driver.

Competing interests

The authors declare no competing interests.

Additional information

Supplementary information The online version contains supplementary material available at https://doi.org/10.1038/s41467-021-20996-w.

Correspondence and requests for materials should be addressed to H.B. or K.R.F.

Peer review information *Nature Communications* thanks the anonymous reviewer(s) for their contribution to the peer review of this work.

Reprints and permission information is available at http://www.nature.com/reprints

Publisher's note Springer Nature remains neutral with regard to jurisdictional claims in published maps and institutional affiliations.

Open Access This article is licensed under a Creative Commons Attribution 4.0 International License, which permits use, sharing, adaptation, distribution and reproduction in any medium or format, as long as you give appropriate credit to the original author(s) and the source, provide a link to the Creative Commons license, and indicate if changes were made. The images or other third party material in this article are included in the article's Creative Commons license, unless indicated otherwise in a credit line to the material. If material is not included in the article's Creative Commons license and your intended use is not permitted by statutory regulation or exceeds the permitted use, you will need to obtain permission directly from the copyright holder. To view a copy of this license, visit http://creativecommons.org/licenses/by/4.0/.

© The Author(s) 2021